A FRAMEWORK FOR TECHNOLOGY EXPLORATION OF AVIATION ENVIRONMENTAL MITIGATION STRATEGIES

A Thesis
Presented to
The Academic Faculty

by

Matthew J. LeVine

In Partial Fulfillment
of the Requirements for the Degree
Doctor of Philosophy in the
The Daniel Guggenheim School of Aerospace Engineering

Georgia Institute of Technology
December 2015

A FRAMEWORK FOR TECHNOLOGY EXPLORATION OF AVIATION ENVIRONMENTAL MITIGATION STRATEGIES

Approved by:

Professor Dimitri Mavris, Advisor
Regents Professor and Boeing
Professor of Advanced Aerospace
Systems Analysis at the Daniel
Guggenheim School of Aerospace
Engineering
Director of the Aerospace Systems
Design Laboratory
Georgia Institute of Technology

Dr. Michelle Kirby
Senior Research Engineer
Civil Aviation Division Chief
Aerospace Systems Design Laboratory
Georgia Institute of Technology

Professor Brian German
The Daniel Guggenheim School of
Aerospace Engineering
Associate Director of the Aerospace
Systems Design Laboratory
Georgia Institute of Technology

Professor John-Paul Clarke
The Daniel Guggenheim School of
Aerospace Engineering
Director of the Air Transportation
Laboratory
Georgia Institute of Technology

Dr. José Bernardo
Software Engineer
Propulsor Technology Inc.

Date Approved: November 16, 2015

ACKNOWLEDGEMENTS

I would like to thank my advisor, Dr. Mavris, for all of the opportunities that he has placed before me during my time at the Aerospace Systems Design Laboratory. While I learned a lot in his classes, most of the lessons that I will take forward came in the form of one-on-one discussions in his office about life as an academic or conversations in the hallways at conferences. These lessons are invaluable and will likely shape my academic career for years to come. I owe a special thanks to Dr. Michelle Kirby, who hired me when I was an undergraduate. She saw something in me early, and she gradually entrusted me with more and more responsibility over the course of several years. She taught me a lot about academic research and managing projects, and I hope to carry those skills into my future research pursuits. I would like to thank Dr. José Bernardo, who was my partner in crime on this research for years. Much of the research presented in this thesis was built on the foundation of his own dissertation. He often made me think outside the box thanks to his insatiable curiosity, and he provided me with the best example of how to be a successful doctoral candidate. I also would like to thank Dr. Brian German and Dr. John-Paul Clarke for serving on my thesis committee and providing valuable feedback and insight.

A number of past and present research staff at the Aerospace Systems Design Laboratory contributed their expertise and advice to this research over the past few years. I would like to thank Chris Perullo, Dr. Holger Pfaender, Dr. Taewoo Nam, Dr. Graham Burdette, Dr. Brian Kestner, Dr. John Salmon, Dr. Jimmy Tai, Dr. Jeff Schutte, Dr. Hernando Jimenez, Dr. Paul Brett, and Ben Havrilesko. The combined knowledge from all of these experts helped me piece together the large number of moving parts included in this dissertation. I also would like to acknowledge a number

of students that contributed to various parts of the model development, data collection and analysis included in this thesis: Sean Samuel, Stephanie MacLeod, Abhay Kaul, Lynn Huynh, Amelia Wilson, Olivier Kiehl, Emmanuel Lacouture, Clark Kjorlaug, and Robert Moss. I also want to acknowledge my neighbors in the lab and fellow musketeers, Imon Chakraborty and Mohammed Hassan, who have experienced much of the trials and tribulations of the PhD process in parallel with me.

I want to thank the Federal Aviation Administration for funding this research, first under the Partnership for AiR Transportation Noise and Emissions Research (PARTNER) and eventually under the Aviation Sustainability Center (ASCENT). I would like to thank the Office of Environment and Energy, and specifically Joe DiPardo, the FAA program manager for this project. I would also like to thank David Senzig, from the John A. Volpe National Transportation Systems Center, and Fabio Grandi from the FAA Office of Environment and Energy. Each provided me with much insight on standard procedures and methods which greatly informed some of the developments in this work.

I must thank my grandparents, Morrie and Marilyn, for their continued financial and emotional support. I hope that I have made you proud and that I can continue to give you reasons to kvell over me for years to come. I would also like to thank my siblings, Stacy, Robyn, Scott, Andrea, and Leslie, for the confidence you have instilled in me and all of the lessons I have learned from your examples. You may not understand exactly what I do, but that doesn't stop you from bragging about me to anyone who will listen.

I am eternally grateful to my parents, Mitch and Ellie, for their lifelong support. Dad, you instilled a thirst for knowledge in me from a very young age, and always emphasized being well-rounded. You never pushed me towards any career path, and you let me choose my own way. I pride myself on the breadth of my interests, and you have always made me feel proud of my accomplishments regardless of the discipline. I

know that you always wanted one of your kids to be a doctor in the LeVine tradition, and now you've got one (albeit a doctor of philosophy). Mom, you have always been the rock of our family. You have nourished, protected, and fought for all of your ducklings. The list of things you have done to enable my success would be longer than this dissertation, and nothing I can say within this acknowledgment will truly do you justice. I love you very much, and I owe everything to you.

Finally, I would like to thank Andrea Knezevic. You have been my closest companion throughout this whole process, celebrating the highest of highs with me and comforting me through the lowest of lows. No one else really understands who I am and what I have been through on a day to day basis. You not only helped me get through this experience the past five years, but you allowed me to live a better life than any graduate student could ever imagine. You have elevated my consciousness and shaped me as a human being, and for that I am forever grateful.

TABLE OF CONTENTS

LIST OF TABLES

LIST OF FIGURES

SUMMARY

Many aviation forecasts agree that global passenger demand will continue to increase steadily over the next few decades. The increasing difficulty of balancing environmental impacts with these operations is a major obstacle to the sustainable growth of the aviation industry. These environmental impacts include, but are not limited to, community noise exposure, local air quality around the airport terminal-area, and climate effects. Organizational bodies such as the Joint Planning and Development Office (JPDO) in the United States and the International Air Transport Association (IATA) have stressed the importance of new aircraft-level technologies as the enabler for sustainable growth, but detailed fleet-level models like the Aviation Environmental Design Tool (AEDT) feature complicated setups and prohibitively long run times for enumerating multiple technology scenarios. The goal of this thesis was to develop a framework for modeling relevant environmental performance metrics and objectively simulating the future environmental impacts of aviation given the evolution of the fleet, the development of new technologies, and the expansion of airports. The research focuses on how to evaluate fleet-level impacts of vehicle-level technologies with enough computational speed to enable scenario analysis. By exchanging fidelity for computational speed, a screening-level framework for assessing aviation's environmental impacts can be developed to observe new insights on fleet-level trends and inform environmental mitigation strategies.

This was accomplished by developing per class average "generic-vehicle" models that can reduce the fleet to a few representative aircraft models for predicting fleet results with reasonable accuracy. The method for Generating Emissions and Noise, Evaluating Residuals and using Inverse method for Choosing the best Alternatives

(GENERICA) expands a previous generic vehicle formulation to additionally match DNL contours across a subset of airports. Discriminant analysis was leveraged to assign aircraft to groups that reduced the variance per class. Designs of experiments, surrogate models, Monte Carlo simulations, and "desirability" scores were combined to set the vehicle design parameters and reduce the mean relative error across the subset of airports. Results show these vehicle models more accurately represented contours at busy airports operating a wide variety of aircraft as compared to a traditional representative-in-class approach. Additionally, a rapid method for assessing population exposure counts was developed and incorporated into the noise tool, and the generic vehicles demonstrated accuracy with respect to population exposure counts for the actual fleet in the baseline year.

To demonstrate the capabilities enabled by these generic vehicles, a few technology scenarios and replacement schedules were defined. The generic vehicles were used as virtual test-beds for quantifying aircraft-level performance improvements. Existing system-wide fleet performance tools were integrated to simultaneously assess savings in fuel burn and noise contours for each technology scenario relative to a Business-as-Usual scenario. The technology scenarios demonstrated significant improvements in fuel efficiency and reductions in population exposure over time, with the replacement schedule for the single aisle vehicles proving most critical for each. Finally, the rapid noise tool was leveraged to explore placements of new runways at ten capacity constrained airports. Contour areas and population exposure counts from a continuous space of possible new runway locations were evaluated for 2030 flight schedules at these airports. The configurations for minimal contour area proved quite different than configurations for minimal population exposure. Fleet-level integration of the best runways showed additional reductions in population exposure counts for each technology scenario despite increases in contour areas.

CHAPTER I

INTRODUCTION

Despite powerful market shocks the aviation sector has recorded robust growth in recent history, and experts from industry and government alike expect this trend to continue in the coming years. The Boeing Company recently raised its 20-year forecast for commercial jet demand by 3.8% due to market indicators which show that "air traffic outstrips global economic growth" and that "passenger traffic has been very resilient," thus requiring an increase in production of vehicles to replace an aging fleet [1]. Airlines have also demonstrated their confidence in the industry over the long term, as indicated by the large number of purchases announced at the 2013 Paris Air Show, including "signed orders and purchase commitments... for 466 planes" from Airbus and a "tally of 442 planes" for Boeing [2]. Between Boeing and Airbus there are now 24 planes rolling off assembly lines per week; the number stood at 11 a decade ago [3]. That rate of growth is expected to continue climbing as airlines move to replace older "gas-guzzling" aircraft in the wake of higher fuel costs. Moreover, the FAA predicts that passenger enplanements will increase 92.3% by 2040, or approximately 2.3% annually [4]. All of these projections, however, are demand-based forecasts that assume national and international air transportation systems will be able to support the increasing size of the fleet and a corresponding increase in the volume of flights.

While airport capacity limits and air traffic deconfliction are important issues that must be resolved to accommodate this future demand, these are not the only constraints on the sustainable growth of the aviation industry. In fact, a Government Accounting Office survey of the 50 busiest airports in the year 2000 revealed that the

1

increasing difficulty of balancing environmental concerns with airport operations was one of the primary obstacles to completing new runway projects, which is in turn the most effective method for increasing airport capacity [5]. In fact, the Joint Planning and Development Office's (JPDO) 2007 Concept of Operations projected that based on current operational trends, environmental impacts will be the primary constraint on the capacity and flexibility of the Next Generation Air Transportation System (NextGen) unless these impacts are managed and mitigated. The latter document suggests the following strategies for mitigating environmental impacts:

> "New technology, procedures, and policies in NextGen minimize impacts on community noise and local air quality and mitigate water quality impacts, energy use, and climate effects. NextGen environmental compatibility is achieved through a combination of improvements in aircraft design, aircraft performance and operational procedures, land use around airports, and policies and incentives to accelerate technology introduction into the fleet. Intelligent flight planning and improved flight management capabilities enable the optimization of route selection, landing, and approach procedures based on a range of data including noise, emissions, and fuel burn, thus enhancing the ability to reduce environmental effects on the ground and in the airspace. Reinvigorated R&D and refined technology implementation strategies balancing near-term technology development and maturity needs with long-term cutting-edge research help aircraft keep pace with changing environmental requirements [6]."

The Concept of Operations assumes that technologies focused on improving aircraft performance with respect to noise, fuel burn, and emissions will be developed and integrated into the fleet at a rate that, combined with more efficient

2

flight management, will mitigate increasing demand on the aviation infrastructure. Policymakers would then be able to enact more aggressive regulations to ensure reductions in community noise, climate effects, and emissions that affect local air and water quality are achieved. Enacting these aggressive regulations would also serve to alleviate community concerns about land use and runway development, which would in turn allow airports and the air transportation system to increase its capacity.

While the Concept of Operations is an initiative by the United States, the international community has come to similar conclusions concerning the necessary methods for achieving reductions in environmental impacts of aviation. An example of this conclusion is represented in the International Air Transport Association (IATA) schematic roadmap for CO_2 emission reduction displayed in Figure 1 [7].
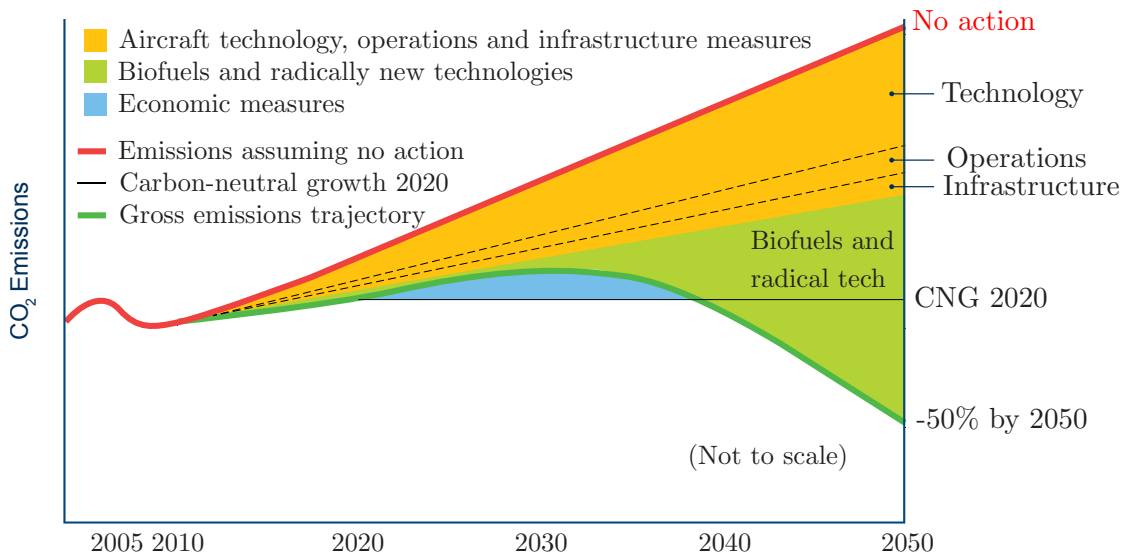
Figure 1: IATA Schematic CO_2 Emissions Reduction Roadmap [7]

This schematic reflects IATA's four-pillar strategy to help achieve the aviation industry's ambitious emission reduction goals. The four pillars are as follows:

- Investment in new technology (more efficient airframe, engines and equipment, sustainable biofuels, new energy sources)

- Efficient operations (drive for maximum efficiency and minimum weight)

- Effective infrastructure (improve air routes, air traffic management and airport procedures)

- Positive economic measures (carbon offsets, global emissions trading)

Both of these entities agree that new technologies are the most significant enabler of sustainable growth for the aviation industry. However, to properly assess the capability of a future fleet of aircraft to achieve certain goals and thresholds of environmental impact, a framework must be developed that can objectively analyze the impact of technologies and the influence of evolving airport infrastructures.

In an effort to reflect on JPDO and IATA's proposals for mitigating the environmental impacts of aviation, Chapter 1 focuses on three areas related to this problem:

1. Environmental policy-making in the context of aviation

2. Technology development programs designed to protect the environment while enabling sustained aviation growth

3. Airport development and land use planning to improve capacity constraints at major airports

Exploring each of these areas helps to motivate the objective of this research by providing some context and identifying current limitations and capability gaps.

1.1 Environmental Policy

The purpose of environmental policy-making is to develop laws and regulations that allow for sustainable growth of the industry while simultaneously protecting the health and well-being of the local, national, or global community. In the area of civil aviation

environmental protection, these regulations set limits on harmful pollutants that are produced by aircraft, which includes emissions from the combustion of hydrocarbons as well as unwanted and disruptive noise. While each country establishes its own laws and regulations through their respective regulatory bodies, civil aviation is by its nature a global enterprise and requires a global initiative to mitigate the impacts of increasing aviation demand. For this reason, the United Nations (UN) created the International Civil Aviation Organization (ICAO) in 1945 to govern standards for aviation worldwide. ICAO's environmental efforts were originally divided between the Committee on Aircraft Engine Emissions and the Committee on Aircraft Noise, but these committees were simultaneously superseded in 1983 by the formation of the Committee on Aviation Environmental Protection (CAEP). As of 2013, CAEP consists of 23 member nations and 16 observers representing other nations and organizational bodies that have an interest in its work, such as the International Coordinating Council of Aerospace Industries Associations (ICCAIA), the International Air Transport Association (IATA), and the United Nations Framework Convention on Climate Change (UNFCCC) [8]. The committee was established "for the purpose of assisting in the further development of Standards, Recommended Practices and Procedures (SARPs) and/or guidance material on aircraft noise and engine emissions" [9]. CAEP meetings take place every three years, and in the past have alternated focus between new noise standards and new emissions standards. At CAEP/6 in 2004, however, participants recognized that effective mitigation strategies require a better understanding of the interdependencies between noise and emissions and their overall impacts. This led to the identification of the following three goals [10]:

1. To limit or reduce the impact of aviation greenhouse gas (GHG) emissions on the global climate

2. To limit or reduce the impact of aviation emissions on local air quality

3. To limit or reduce the number of people affected by significant aircraft noise

The latter goals have led to ongoing development of analytical tools and databases that can account for these interdependencies and help to define effective mitigation strategies that meet these three goals simultaneously. In the United States, the FAA Office of Environment and Energy (AEE) worked with the US Department of Transportation (USDOT) Volpe National Transportation Systems Center (Volpe Center), the ATAC Corporation, Metron Aviation, and CSSI Inc. to develop the next generation of airport analysis tool, known as the Aviation Environmental Design Tool (AEDT) [11]. AEDT is a software system that is designed to dynamically model aircraft performance in space and time to compute fuel burn, emissions, and noise. Full flight gate-to-gate analyses are possible for study sizes ranging from a single flight at an airport to scenarios at the regional, national, and global levels. AEDT replaces the traditional public-use aviation environmental tools, such as the Integrated Noise Model (INM) and the Emissions and Dispersion Modeling System (EDMS). AEDT incorporates procedures and performance calculations that are similar to these legacy tools, leveraging extensive system databases covering airports, airspace, and fleet information that span the global nature of the aviation industry. The coefficients in these databases are very specifically defined with respect to the standards and algorithms on which AEDT is built. A diagram of the AEDT system structure with all of its capabilities is shown in Figure 2 [11].

While CAEP establishes global standards for evaluating the environmental impact of each aircraft-engine combination, the responsibility of establishing laws and enforcing them still lies with the member nations. In the United States, The National Environmental Policy Act of 1969 (NEPA) requires each Federal agency to disclose to the interested public a clear, accurate description of potential environmental

www.manaraa.com
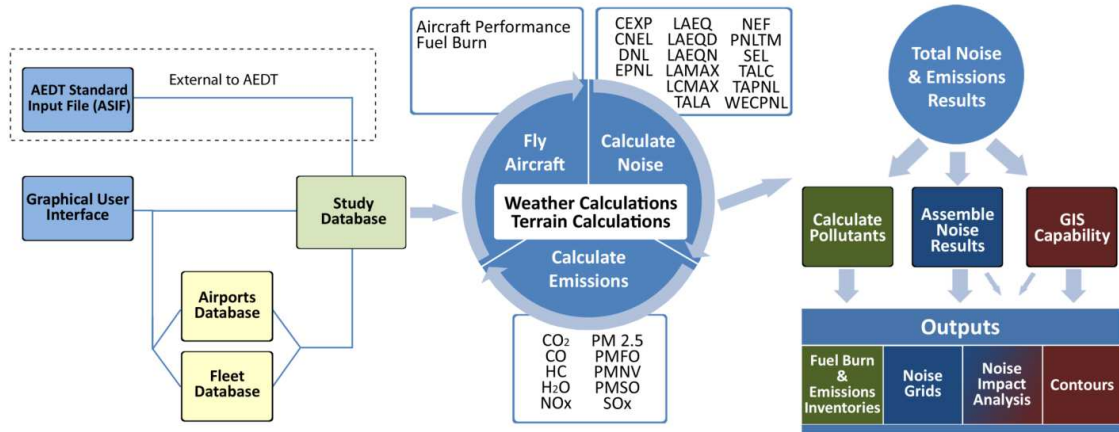
Figure 2: AEDT System Structure [11]

impacts that may result from proposed Federal actions. Additionally, these agencies must explore reasonable alternatives to those actions and produce comparisons with respect to these environmental impacts. Through NEPA, Congress directed federal agencies to incorporate environmental factors in their planning and decision making processes [12]. The Environmental Protection Agency (EPA) is the primary U.S. government entity in charge of establishing aircraft and aircraft engine emissions standards "for any air pollutant that could reasonably endanger public health and welfare," as directed by the Clean Air Act (CAA) of 1970 [13]. The CAA requires the EPA to set national ambient air quality standards for the following six pollutants: nitrogen oxides (NO_x), sulfur oxides (SO_x), carbon monoxide (CO), ozone (O_3), particulate matter (PM), and lead (Pb) [14]. When establishing aircraft engine emissions standards, the EPA must consult with the Department of Transportation (DOT) to ensure these regulations align with current and future aircraft technology capabilities with appropriate consideration to compliance cost as well as any potential negative impacts on aircraft safety. Once these standards are agreed upon, the DOT delegates responsibility for enforcing these standards to the Federal Aviation

7

Administration (FAA). The FAA ensures compliance with these regulations by reviewing and approving certification test plans, procedures, test reports, and engine emissions certification levels. The EPA aligns its goals with certification standards that are developed by ICAO under CAEP [13].

Similarly in 1970, the United States Congress directed issues concerning noise beyond aviation to the Environmental Protection Agency (EPA). Congress charged the EPA with conducting studies regarding the "effects of noise on public health and welfare," which was achieved through the EPA's Office of Noise Abatement and Control (ONAC) [15]. Part of this study concluded that transportation and aviation noise had negatively impacted the property values of over 44 million people, which led to the establishment of noise emission standards via the Noise Control Act of 1972 [16]. The document, among other achievements, codified the measurements for the impact of community noise, established through metrics generally referred to as equivalent (or equivalency) sound metrics [17]. These are referred to as equivalency metrics because they "average the intensity [of sound] over a given period of time [18]." Different government agencies, however, disagree about the noise-level threshold which corresponds to significant noise exposure. Additionally, the metrics used for aircraft and engine certification are different from those used to determine population exposed to significant noise.

Determining the interdependencies between noise and emissions can become convoluted given the variety of noise metrics and the different emissions species from hydrocarbon combustion. Given the United States' member status in CAEP, the EPA and the FAA generally align their goals with that of ICAO. Thus, the metrics should support the three goals concerning greenhouse gas emissions, local air quality, and significant noise exposure. These metrics will be discussed in detail in Chapter 2.

1.2 Technology Development

The challenge of maintaining and improving mobility in the face of increasingly congested airspace while simultaneously addressing aviation's environmental footprint is the main driving force for new technology development in aviation. This has led to strategic aviation technology programs in the United States, Europe, and other countries with emerging aeronautics industries. These programs are often supported by governments and structured in partnerships between industry and research establishments [7]. In Europe, the Clean Sky JTI (Joint Technology Initiative) was born in 2008 and represents a unique Public-Private Partnership between the European Commission and industry. This initiative is made up of six Integrated Technology Demonstrators (ITDs), including active wing technologies and new aircraft configurations, lightweight and efficient cores, and novel engine designs, just to name a few [19]. This initiative, combined with the Single European Sky ATM Research (SESAR) for developing advances in air-traffic management, is funded under the European Union's Framework Program to meet the goals outlined by the Advisory Council for Aeronautical Research in Europe (ACARE) in their Strategic Research Agendas [7, 20, 21]. Some of the short-term environmental goals of these agendas, combined with the more long-term goals defined in the Strategic Research and Innovation Agenda (SRIA), are outlined in the Vision 2020/Flightpath 2050 goal set in Table 1 below [22, 23]:

Table 1: Vision 2020/Flightpath 2050 Environmental Goals

Goals	Technology Benefits Relative to a Year 2000 Reference Aircraft	
	Vision 2020	Flightpath 2050
CO_2 reduction per passenger km	-50%	-75%
NO_x reduction	-80%	-90%
$EPNL_{dB}$ noise reduction	-50%	-65%

In Table 1, $EPNL_{dB}$ stands for Effective Perceived Noise Level in decibels, which is a metric that takes into account the duration of the signal and the presence of pure tones to better approximate the human response to unwanted noise [24]. It should be noted that a 50% reduction in perceived noise is equivalent to a reduction of 10-dB according to the conventions of a decibel scale and human perception of sound. The focus of these technology programs is to identify promising technologies and advance their maturity levels such that their benefits can be realized within the time-frame specified [7].

In the United States, aviation technology research goals are established by the National Aeronautics and Space Administration (NASA). NASA defines its goals with respect to current aircraft at generation N, with a 3-tiered goal structure referred to as N+1, N+2, and N+3 generations. The goals for each of these generations are defined in Table 2 [25].

Table 2: NASA N+ Goals

Goals	N+1 = 2015	N+2 = 2020	N+3 = 2025
Reference Configuration	Single Aisle	Large Twin Aisle	Single Aisle
	Technology Benefits		
Cumulative Noise	−32 dB	−42 dB	−52 dB
LTO NO_x emissions	−60%	−75%	−80%
Aircraft Fuel Burn	−33%	−50%	−60%

In Table 2, cumulative noise refers to the sum of $EPNL_{dB}$ values at three locations around the runway that are used for aircraft noise certification (flyover, lateral, and approach) [26]. LTO NO_x refers to NO_x emissions during the Landing-Takeoff cycle, which generally comprises emissions below an airfield equivalent altitude of 3,000 ft, including taxi-in and -out, take-off, climb-out, and approach-landing [27]. The

N+1 goals are pursued primarily by the FAA's Continuous Lower Energy Emissions and Noise (CLEEN) technology program, with support from NASA. The CLEEN program is a NextGen effort to accelerate development and commercial deployment of environmentally promising aircraft technologies and sustainable alternative fuels [28]. Because of the short time-frame, this program tends to focus on technologies that can either be retrofitted to existing aircraft in the fleet or quickly integrated into the manufacturing of the next generation of conventional configuration aircraft. The N+2 goals are pursued primarily by NASA's Environmentally Responsible Aviation (ERA) project. This project explores and documents the feasibility, benefits, and technical risk of vehicle concepts and enabling technologies to reduce aviation's impact on the environment [29]. Because of the increasingly aggressive goals of the N+2 generation, ERA tends to focus on more advanced technologies with particular emphasis on unconventional aircraft configurations such as the hybrid wing body (HWB) due to promising reductions in fuel burn, emissions, and noise [30]. The N+3 goals are pursued via NASA's Subsonic Fixed Wing (SFW) program, with a focus on low-maturity technologies as well as advanced analysis techniques [31]. Like their European counterparts, these programs are designed to advance the maturity levels of promising technologies. The technology advancement goals for each program are defined in terms of Technology Readiness Levels (TRLs), a systematic metric/measurement system that supports assessments of the maturity of a particular technology and the consistent comparison of maturity between different types of technology [32]. The values range from lowest maturity at TRL 1 to highest maturity at TRL 9, as demonstrated in Figure 3 [33].

The CLEEN program focuses on advancing technologies from TRL levels of 3-4, corresponding to a proof-of-concept or a demonstration in a laboratory environment, to TRL levels of 6-7, corresponding to a developmental stage and a demonstration in a relevant environment [28, 32]. The ERA program similarly aims at advancing
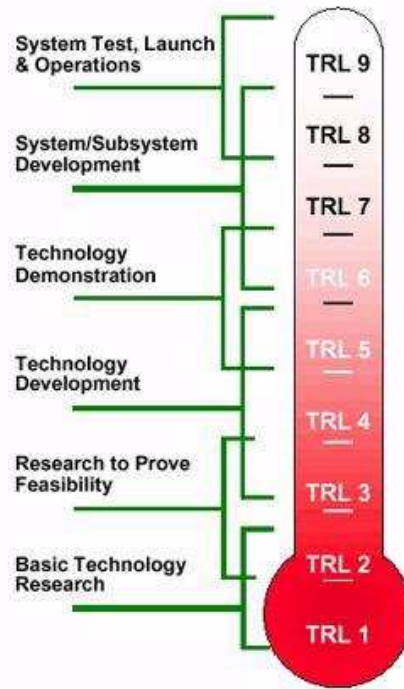
Figure 3: NASA Technology Readiness Level (TRL) Meter [33]

technologies to a systems integration level (TRL level of at least 6), while the SFW program focuses on achieving lower maturity TRL levels between 2-4 with the goal of infusing these technologies into the fleet much further in the future [34].

These program goals are stated with respect to various reference vehicles with vehicle-level metrics. The European goals do not cite a specific vehicle, instead referring to single aircraft technology benefits over year 2000 technology [7]. NASA's N+1 and N+3 goals are referenced against a single-aisle reference vehicle, specifically a Boeing B737-800 aircraft with CFM56-7B engines, whereas the N+2 goals are referenced against a large twin-aisle reference vehicle, specifically a Boeing B777-200 aircraft with GE90 engines [25]. While these aircraft represent the current state-of-the-art, proper assessment of fleet-wide improvements due to technology infusion requires aggregating the technology impact on each currently in-production aircraft according to forecast schedules of operations [30]. The previously mentioned reference vehicles do not fully represent the diversity of the fleet, thus achieving the

12

specific goals outlined by NASA and ACARE may not yield the system-level results anticipated. In reality, the fleet is made up of several thousand aircraft, with hundreds of unique airframe-engine combinations. Typical fleet-level analyses, such as the inventory studies conducted by the John A. Volpe National Transportation Systems Center using AEDT, rely on extensive databases that catalog the performance of every aircraft-engine combination in the fleet and link this performance to operational schedules [35]. These databases are validated against manufacturer provided data, but this type of information is unavailable for future vehicles infused with future technologies that are currently at low TRL levels, and thus projections rely on assumptions of improved performance that are not connected to specific technologies. Simultaneous quantification of these technology impacts and the interdependencies of the environmental metrics at the fleet level would require modeling technologies at the vehicle-level for every unique aircraft-engine combination and then aggregating to the fleet level, but this would be time-consuming and computationally expensive.

A common approach when forecasting the impact of future technology vehicles is to simplify the fleet into "generic vehicles" that represent the performance of various classes of aircraft. An example of this is included in the World Fleet Modeling chapter of the IATA Technology Roadmap 2013, where average vehicles with generic technologies are defined for each of the CAEP/8 defined seat classes [7]. The performance of these generic vehicles are simulated in a vehicle design tool capable of modeling impacts of future technologies. However, seat classes are defined based on internal seat configurations rather than vehicle performance, and thus a single airframe-engine combination may be classified in multiple classes despite the fact that the vehicle's performance changes very little due to these different seating configurations. Furthermore, these generic vehicles are designed to average the fuel-burn and emissions within each class without any consideration for noise, making it difficult to gauge the impact of technologies on fuel-burn, emissions, and

13

noise simultaneously.

This work proposes an average generic vehicle approach with classification based on vehicle performance rather than seating configurations. The fleet is categorized based on the performance of each aircraft-engine combination with respect to the metrics defined in Chapter 2. The method for defining these average generic vehicles also becomes more complicated when trying to include noise due to the airport-dependent nature of the noise metrics. A novel method for finding average generic vehicles that include average noise will be formulated in Chapter 3.

1.3 Airport Development and Land Use Planning

As mentioned previously, new runways present the most extensive capacity change that can occur at an airport. The capacity effect of new runways depend most on (a) orientation and dependence in relation to other runways (i.e., parallel, converging, intersecting), and (b) expected runway use (i.e., arrivals, departures, or mixed mode). With a new runway project, there may be a need for convincing evidence that the benefit of the capacity improvement is justified because it may have adverse environmental effects [36]. The FAA requires an Environmental Assessment (EA) to unconditionally approve an Airport Layout Plan (ALP) depicting a proposed runway to determine if the project will have significant impact on noise, air quality, water quality, or historical artifacts [12]. If the environmental impact is determined to be significant, an Environmental Impact Study (EIS) must be prepared and made available to the public [37]. Community opposition due to concerns about aviation noise and other environmental impacts can arise during the public outreach required by federal law when federally-funded airport expansion projects are proposed and can contribute to project delays at some airports, with the median time for completion of a new runway increasing from 10-years to 14-years as a result of these delays [38].

14

Currently, aircraft noise is the single most significant local objection to airport expansion and construction [39]. As the national aerospace system becomes increasingly capacity-constrained it will be ever more important to remove the limits introduced by community noise impacts. The federal government often provides some funding for local abatement, such as sound insulation and land-purchases to reduce future concerns, but local government decisions that allow communities to expand land use into these noise-sensitive areas erode these noise reduction gains, according to a 2004 FAA report to Congress [40]. The United States General Accounting Office (GAO) predicts that future increases in air traffic and changes in aircraft flight paths could lead to more noise complaints from the community [39]. A balanced approach is necessary to mitigate these complaints in the face of increasing traffic, with operational procedures providing the greatest near-term benefits, and reductions in source noise (airframes and engines) being required in the long-term for further reductions. Continuing policy efforts to encourage appropriate land use will be required throughout [40].

Although noise is the primary environmental constraint on airport operations and expansion, many airports either put local air quality concerns on equal footing with noise or anticipate they will be on equal footing soon. Emissions of nitrogen oxides (NOx), carbon monoxide (CO), unburned hydrocarbons (UHC) and particulate matter (PM) from a variety of airport sources contribute to local air quality deterioration, resulting in human health and welfare impacts [40]. Although some airports may be required to mitigate emission increases arising from projects covered by NEPA and the CAA, a GAO study in 2003 indicated that most emission reduction actions are done voluntarily. However, aviation industry representatives as well as federal and state officials testified before the House of Representatives that new air quality standards, combined with the boost in emissions expected from increases in air travel, could cause airports to be subject to more emission control requirements

in the future [41]. This may put another damper on attempts to expand airports and build new runways.

In 2003, the FAA convened a team to begin the Future Airport Capacity Task (FACT). The team was led by the FAA's Airports organization (ARP) and included representatives from the Air Traffic Organization (ATO) and the MITRE Corporation's Center for Advanced Aviation System Development (CAASD). FACT1 was an assessment of the future capacity of the nation's airports and metropolitan areas, FACT2 was a follow-up study in 2007; the FACT3 study was published in January of 2015. The goal of the FACT studies was to determine which airports and metropolitan areas have the greatest need for additional capacity. Each FACT study included detailed analysis of 56 commercial service airports selected from a larger set of 291 commercial service airports based on potential capacity issues [42]. The FACT3 analysis includes current aircraft fleet mix projections, updated NextGen planning, and modeling of gate and surface constraints on airport capacity [43]. This study found that while NextGen provided incremental benefits, the demand growth at many airports projects to outpace these increases in capacity. The study identified 10 airports (listed in Table 3) that could potentially be capacity constrained by 2030 if not earlier. Of these 10 airports, only Philadelphia International Airport (PHL) has a plan for building a new runway that could potentially alleviate airport capacity by 2030.

Table 3: FACT3 Capacity Constrained Airports

Airport	Code	2011	2020	2030
Hartsfield-Jackson Atlanta International Airport	ATL	✗	✗	✗
Charlotte Douglas International Airport	CLT			✗
Newark Liberty International Airport	EWR	✗	✗	✗
George Bush Intercontinental Airport	IAH			✗
John F. Kennedy International Airport	JFK	✗	✗	✗
McCarran International Airport	LAS			✗
LaGuardia Airport	LGA	✗	✗	✗
Philadelphia International Airport	PHL	✗	✗	✗[1]
Pheonix Sky Harbor International Airport	PHX			✗
San Francisco International Airport	SFO		✗[2]	✗

[1] New runway planned may mitigate delays by 2030

[2] NextGen implementation may mitigate delays in 2020

This analysis focused solely on capacity constraints and delays, and did not take into account future noise restrictions or emission control requirements. This may be due to the confidence that JPDO initiatives will advance technologies and operating procedures enough that these environmental constraints will never be realized. Runway placements and orientations would most likely be limited due to surrounding populations and noise-sensitive areas. To avoid these areas, departure and approach flight tracks with sharp turns may be employed; this creates a penalty in terminal area fuel burn and emissions. Advanced technologies for fuel burn and emission reduction may be able to mitigate these penalties. Alternatively, noise reduction technologies may allow for the construction of new runways without requiring these sharp turning flight tracks for noise abatement. A method for rapidly evaluating community noise exposure for different runway/airport configurations in conjunction with a fleet of technology-infused aircraft will be discussed in more detail in Chapter 4.

1.4   Summary of Motivation

The final goal of this research is to outline a framework for evaluating the future state of aviation and its relative impacts on the environment. Since this type of analysis concerns future technologies that are still under development, the framework must hinge on modeling and simulation. Thus, the objective of this research is as follows:

Research Objective: *To develop a framework for modeling relevant environmental performance metrics and objectively simulating the future environmental impacts of aviation given the evolution of the fleet, the development of new technologies, and the expansion of airports.*

This framework should be flexible enough to evaluate multiple scenarios against each other such that promising mitigation strategies can be down-selected and explored in detail. Given the computational expense typically associated with high fidelity modeling and simulation, this methodology should leverage lower fidelity methods. By exchanging fidelity for computational speed, more scenarios can be evaluated. In this way, the framework will serve as a screening capability, and the most promising scenarios could be re-evaluated using more computationally demanding high fidelity models. Thus, the overarching hypothesis for this research is as follows:

Overarching Hypothesis: *By exchanging fidelity for computational speed, a screening-level framework for assessing aviation's environmental impacts can be developed to observe new insights on fleet-level trends and inform environmental mitigation strategies.*

An overview of this framework is displayed in Figure 4. Fidelity is reduced

18

by simplifying the fleet to a handful of per class average generic vehicles that are optimized to match the fleet-level aggregate results of a diverse fleet for a given baseline schedule of operations. This simplification reduces the combinatorial nature of the fleet-level problem, which becomes even more complicated when exploring multiple technology scenarios. The generic vehicles can serve as virtual testbeds for modeling technology infusion, and the performance of these technology vehicles can be linked to a model of fleet evolution to conduct bottom-up integrated fleet-level analysis of multiple environmental metrics simultaneously. Flight schedules from these simulations can also be extracted to rapidly explore multiple runway locations. If these explorations can be linked to a simple method for quantifying population distribution around an airport, the contour areas and population exposure counts for every possible runway location can be quickly compared and the ideal locations can be identified.
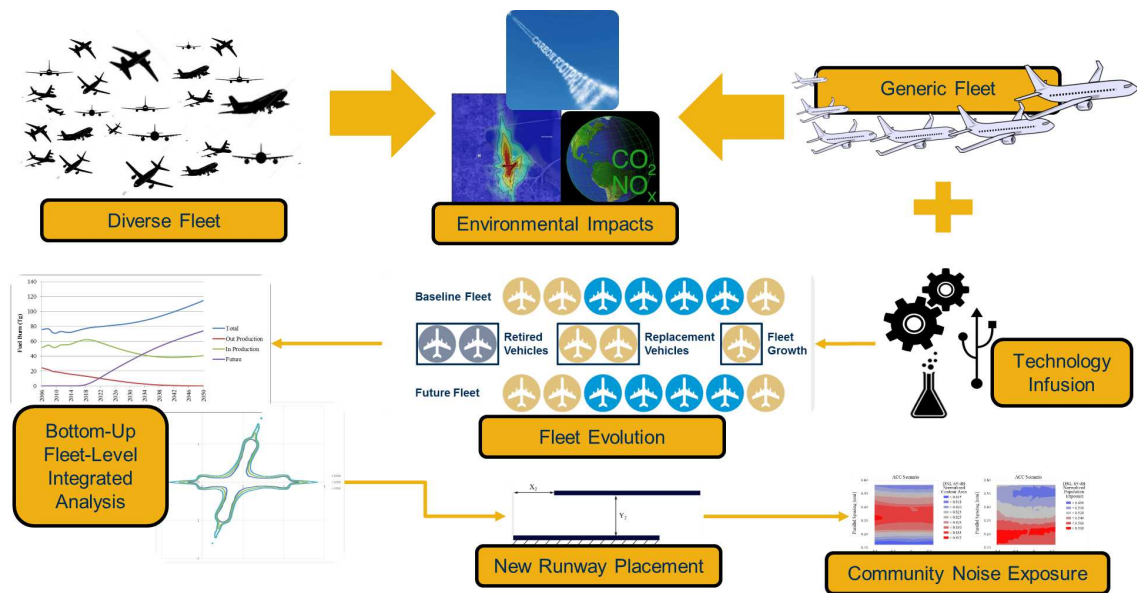
Figure 4: Overview of Proposed Framework

Chapter 2 establishes the relevant environmental impact metrics. Background is provided on existing methods for fleet-level analysis and capability gaps are

identified. These capability gaps and technical challenges lead to research questions and hypothesis statements. In Chapter 3, approaches for addressing these technical challenges are formulated. These approaches center on exchanging fidelity for computational speed, including a method for defining performance-based average generic vehicles that include average noise as well as a method for incorporating population counts into an existing rapid noise tool. Chapter 4 demonstrates the implementation of these methods in an effort to answer the research questions and support the hypothesis statements. Chapter 5 demonstrates some examples of fleet-level capabilities that leverage the average generic vehicle and population methods. These capabilities include fleet-level analysis under various technology and replacement scenarios as well as a low-fidelity environmental assessment of new runway locations. Chapter 6 summarizes the contributions of this work and outlines potential future work that builds upon the methods and analysis presented in this research.

CHAPTER II

BACKGROUND AND TECHNICAL CHALLENGES

Chapter 1 introduced the overarching research objective and an overview of the proposed framework. This chapter begins with literature review on the relevant metrics for quantifying the environmental impacts of aviation. Once these metrics are established, a review of previous work on fleet-level modeling is included, with particular focus on Becker's generic vehicle methodology [44]. Additionally, a rapid airport-level noise tool developed by Bernardo and current best practices for quantifying population exposure are reviewed. The modeling and simulation requirements associated with integrating the fleet-level analysis for each of the environmental impact metrics are formulated.

The generic vehicle methodology hinges on reducing the diversity of the fleet to a few representative classes, and thus the actual aircraft in the fleet should be intelligently assigned to a small subset of classes. The drawback of traditional seat capacity based groupings is discussed, which motivates the need for a more rigorous multiclass classification method. It is proposed that class assignments should be made with the goal of reducing in-class variability with respect to the relevant metrics, and this can be accomplished through the use of statistical techniques. The exclusion of community noise exposure from Becker's formulation represents a capability gap, and the airport-dependent nature of the noise metrics necessitates a modification of Becker's approach centered on accuracy at *each* airport as opposed to just cumulative metrics across all airports. In order to trace the influence of different sources of operational complexity on the generic vehicle designs, a series of validation tests of sequentially increasing complexity is suggested. Given that the

www.manaraa.com

generic vehicles must balance accuracy for multiple metrics simultaneously, these tests must be formulated as multiobjective optimization problems that can identify a set of Pareto optimal aircraft for each class rather than a single optimal solution. The inability to rapidly compute population exposure counts is identified as another capability gap. An approach that conforms to Bernardo's rapid noise computation method is proposed to address this gap.

2.1 Review of Prior Work

Chapter 1 cited a few goals by various US and European technology programs, but a variety of different metrics were included in these goals. A decomposition of the CAEP goals helps to define the relevant environmental impact metrics, and previous methods for quantifying these metrics are reviewed.

2.1.1 Environmental Impact Metrics

As discussed in Chapter 1, the need to capture the interdependencies between noise and emissions and their overall impacts led CAEP to delineate three specific goals. Each of these goals are discussed in more detail and a final list of relevant environmental performance metrics are selected.

2.1.1.1 Greenhouse Gas (GHG) Emissions

GHGs are gases that trap heat in the atmosphere via the cycle demonstrated in Figure 5. While some incoming solar radiation is reflected by the Earth's atmosphere, some of it is able to penetrate and warm the Earth's surface, where it is converted to heat and emitted as infrared radiation. Some of this infrared radiation escapes the Earth's atmosphere, but as the concentration of GHGs increases so does the amount

22

of radiation absorbed and re-emitted, leading to increased surface and tropospheric temperatures [45].
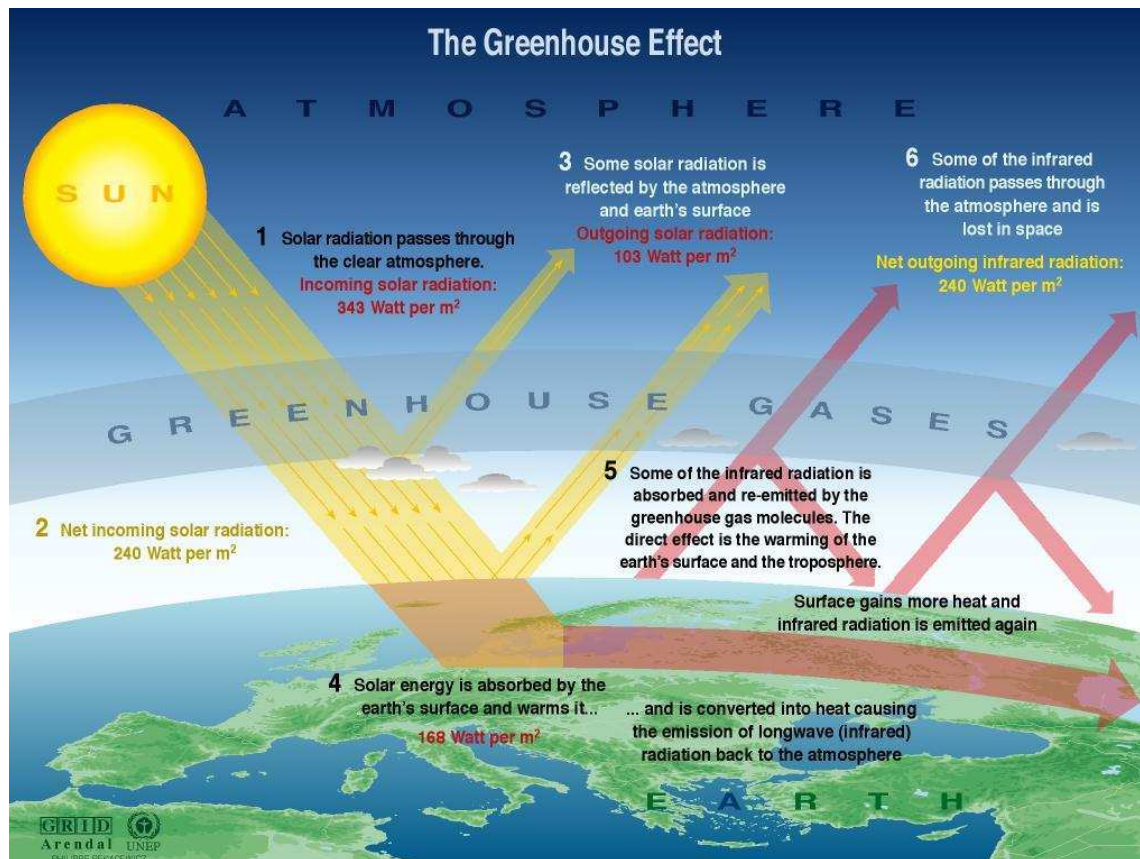
Figure 5: The Greenhouse Effect [45]

GHGs species' contributions to changes in the Earth's energy budget are quantified in terms of radiative forcing (RF), a measure of the change in energy flux (typically in Watts per meter squared) due to changes in these GHGs. Positive RF leads to surface warming, whereas negative RF leads to surface cooling. The Intergovernmental Panel on Climate Change (IPCC) Working Group I's list of major greenhouse gases and their relative contributions to RF relative to levels in the year 1750 is shown in Figure 6 [46].

The "well-mixed" species feature uniform distributions throughout the atmosphere, regardless of the location of the emission source due to longer

23

Radiative forcing by emissions and drivers

Emitted compound		Resulting atmospheric drivers	Radiative forcing	Level of confidence
Anthropogenic — Well-mixed greenhouse gases	CO_2	CO_2	1.68 [1.33 to 2.03]	VH
	CH_4	CO_2 H_2O^{str} O_3 CH_4	0.97 [0.74 to 1.20]	H
	Halo-carbons	O_3 CFCs HCFCs	0.18 [0.01 to 0.35]	H
	N_2O	N_2O	0.17 [0.13 to 0.21]	VH
Anthropogenic — Short lived gases and aerosols	CO	CO_2 CH_4 O_3	0.23 [0.16 to 0.30]	M
	NMVOC	CO_2 CH_4 O_3	0.10 [0.05 to 0.15]	M
	NO_x	Nitrate CH_4 O_3	-0.15 [-0.34 to 0.03]	M
	Aerosols and precursors (Mineral dust, SO_2, NH_3, Organic carbon and Black carbon)	Mineral dust Sulphate Nitrate Organic carbon Black carbon	-0.27 [-0.77 to 0.23]	H
		Cloud adjustments due to aerosols	-0.55 [-1.33 to -0.06]	L
		Albedo change due to land use	-0.15 [-0.25 to -0.05]	M
Natural		Changes in solar irradiance	0.05 [0.00 to 0.10]	M
Total anthropogenic RF relative to 1750		2011	2.29 [1.13 to 3.33]	H
		1980	1.25 [0.64 to 1.86]	H
		1950	0.57 [0.29 to 0.85]	M

Figure 6: Radiative Forcing Relative to 1750 in $\frac{W}{m^2}$ [46]

atmospheric residence times, whereas the concentrations of "short-lived gases" tend to vary by location. Figure 6 shows that CO_2 is the primary anthropogenic species contributing to a net positive RF. For this reason it is often used as a reference when comparing relative influences of GHGs. The two most important characteristics of a GHG in terms of climate impact are how well the gas absorbs energy (preventing it from immediately escaping to space), and how long the gas stays in the atmosphere [47]. The Global Warming Potential (GWP) for a gas is a measure of the total energy that a gas absorbs over a particular period of time (usually 100 years), compared to carbon dioxide [48]. As a reference, CO_2 has a GWP of 1, with an atmospheric lifetime of 50-200 years. Methane (CH_4), by comparison, has a GWP of 21, but only has an atmospheric lifetime of 12 years. Nitrous oxide (N_2O) has a GWP of 310 with an

atmospheric lifetime of 120 years, but the relative concentrations in the atmosphere are much smaller than that of CO_2 [47]. Thus, CO_2 is the GHG that accounts for the greatest impact to current and historical warming trends [49].

CO_2 emissions typically demonstrate direct correlations with the amount of fuel burned by an aircraft because CO_2 is a direct product of hydrocarbon fuel combustion, as evidenced by the following simplified global kinetic mechanism [50]:

$$C_xH_y + \left(x + \frac{y}{4}\right)O_2 \rightarrow xCO_2 + \frac{y}{2}H_2O \tag{1}$$
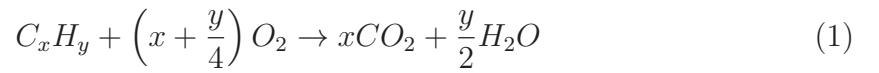
Therefore, an aircraft that reduces the amount of fuel required to complete a mission will likely demonstrate a reduction in CO_2 emissions as well. Equation (1) only lists the products of ideal combustion, but in reality there are often many other species that are produced due to some incomplete combustion. The relative concentrations of these products also change depending on the operating regime. A list of typical aircraft engine combustion products and relative concentrations is shown in Table 4 [51].

In Table 4, ppmv is parts per million by volume, such that one μl of the gas in 1 liter of air is equal to 1 ppmv. The term ppmw refers to parts per million by weight (ppbw is parts per billion by weight), and ppmC refers to parts per million by carbon. The unit ppmC is calculated by multiplying the concentration of the compound in ppmv by the number of carbon atoms in that compound. This unit is typically used for reporting ambient hydrocarbons because the number of carbon atoms is a very crude indicator of the total reactivity of a group of hydrocarbon compounds [52]. Comparing the low-power and high-power concentrations in Table 4 shows that combustion is less efficient at the idle power setting as this represents an off-design condition typically corresponding to landing procedures. Thus, the concentrations of CO_2 and H_2O are lower while the concentrations of CO, total hydrocarbons (such as CH_4), and partially oxidized hydrocarbons are higher.

Table 4: Engine Combustion Products and Typical Concentrations

Type	Species	Approximate Concentrations	
		Low-power (idle)	High-power
Air	N_2	77%	77%
	O_2	17.3-19%	13-16.3%
	Ar	0.9%	0.9%
Complete Combustion Products	H_2O	1.4-2.4%	3-5%
	CO_2	1.4-2.4%	3-5%
Incomplete Combustion Products	CO	50-2000 ppmv	1-50 ppmv
	Total HCs	50-1000 ppmC	1-20 ppmC
	Part. Ox. HCs	25-500 ppmC	1-20 ppmC
	H_2	5-50 ppmv	5-100 ppmv
	Soot	0.5-25 ppmw	0.5-50 ppmw
Nonhydrocarbon Fuel Components	SO_2, SO_3	1-5 ppmw	1-10 ppmw
	Metals, Metal Oxides	5-20 ppbw	5-20 ppbw
Oxides of Nitrogen	NO, NO_2	5-50 ppmv	50-500 ppmv

Cross-referencing Table 4 with Figure 6, it becomes clear that tracking CO_2 will be the most significant indicator of aviation's contribution to the well-mixed GHG emissions. While methane is also a significant contributor to RF amongst the well-mixed gases, the relative concentrations of CH_4 emissions are small, especially during the higher-power cruise phase of flight that accounts for the majority of an aircraft mission.

Of the short-lived gases listed in Figure 6, the most significant species with respect to aircraft engine emissions are the nitrogen oxides (NO_x), which includes nitric oxide (NO) and nitrogen dioxide (NO_2). These emissions are produced when air passes through high temperature and high pressure combustion, as is common in the combustors of jet engines. The nitrogen and oxygen concentrations in the air combine to form these NO_x gases, with these concentrations increasing when the engines operate at high-power [53]. NO_x gases have competing effects with respect to RF. These emissions in the upper troposphere act as an indirect GHG by causing a short-term increase of ozone (O_3) which is an important greenhouse gas. This increase

26

in O_3 is a result of the following chemical mechanism [54]:

$$OH + CO \rightarrow HO_2 + CO_2 \tag{2}$$

$$HO_2 + NO \rightarrow NO_2 + OH \tag{3}$$

$$NO_2 + hv \rightarrow NO + O(^3P) \tag{4}$$

$$O(^3P) + O_2 \rightarrow O_3 \tag{5}$$

Where:

hv = photon from sunlight

$O(^3P)$ = Oxygen atom in ground state

This short term increase is caused by nitric oxide (NO) gases competing for hydroperoxyl (HO_2) radicals, a species that typically eliminates atmospheric O_3. With less HO_2 radicals to eliminate O_3, the level of O_3 increases and, consequently, so does the amount of energy retained by the atmosphere. Additionally, the reaction represented in Equation (3) produces nitrogen dioxide (NO_2), which in turn participates in net photochemical O_3 production via Equations (4) and (5). On a longer scale, emissions of NO_x lead to reduced levels of methane (CH_4), which is the second-most significant GHG after CO_2 [49]. This relationship occurs due to the increase in hydroxyl (OH) radicals via Equation (3). CH_4 is one of the main reactants for the OH radical, which is the primary oxidant in the troposphere. Hence, CH_4 controls the abundance of OH in the troposphere. Oxidation of CH_4 leads to O_3 production due to the increasing production of carbon monoxide molecules that in turn react with the OH radicals in Equation (2). In addition, oxidation of CH_4 in the

27

presence of sufficient concentrations of NO_x leads to further production of OH and, hence, acts as an amplifier of HO_x species [55]. Therefore, NO_x emissions in the upper troposphere contribute both to negative RF mechanisms through its destruction of atmospheric methane as well as positive RF via its contribution to O_3 production. In the stratosphere, NO_x emissions actually serve to deplete O_3 by the following chemical mechanism [56]:

$$O_3 + NO \rightarrow NO_2 + O_2 \tag{6}$$

$$NO_2 + O \rightarrow NO + O_2 \tag{7}$$

$$NO_2 + O_3 \rightarrow NO + 2O_2 \tag{8}$$

Both Equations (6) and (8) represent O_3 sinks. These reactions are more common in the stratosphere because of the larger concentrations of O_3, as demonstrated in Figure 7 [57]. The peak in O_3 concentration in the stratosphere, commonly referred to as the "ozone layer", reflects much of the incoming solar radiation. Depletion of the stratospheric O_3 thus increases the amount of incoming radiation, leading to net positive RF. Commercial aircraft typically operate in the upper troposphere and lower stratosphere, but the future commercial fleet may feature commercial supersonic jets that operate at higher stratospheric altitudes. Therefore, an increase in supersonic flights would increase the positive RF from aircraft engine NO_x emissions.

The combination of all of these reactions make it difficult to ascertain the exact impact of NO_x emissions on RF and climate change, which is why the level of confidence in the impact of these emissions is listed as medium in Figure 6. The potential impact, however, suggests a need to track NO_x emissions, especially during a high-altitude cruise.

In addition to the above species, a substantial part of the aviation climate impact may be due to aviation induced cloudiness including contrail cirrus, changes in
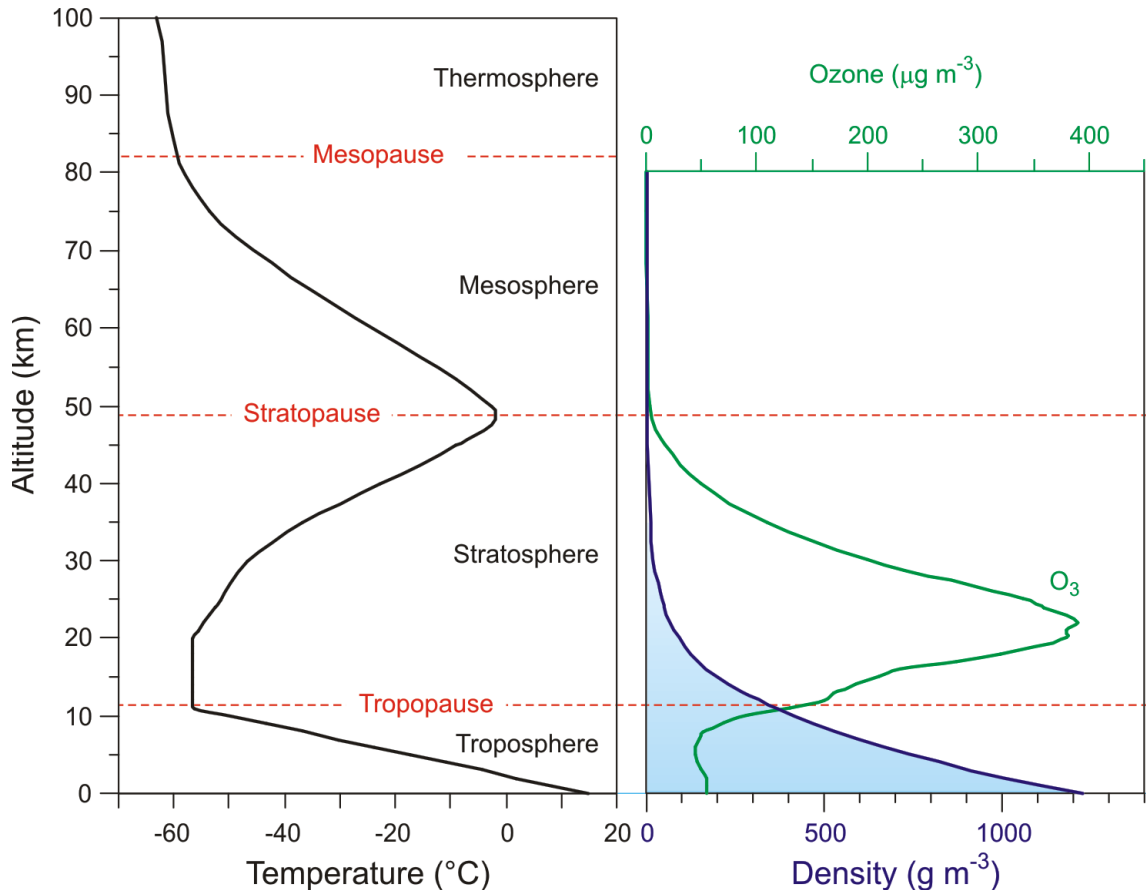
Figure 7: Ozone Concentration by Altitude [57]

cirrus properties, and cirrus occurrences due to soot emissions [58]. These contrail formations form under favorable meteorological conditions and sometimes depend on concentrations of soot particles in the upper-troposphere [59]. This implies that contrail formation will vary regionally and seasonally, which greatly increases the uncertainty related to its impact on the climate. Given this uncertainty, the inclusion of contrails was scoped from this research, but as modeling of contrails improves and the impacts are better understood they should be included in future problem formulations connecting aviation activities to changes in radiative forcing.

Therefore, the primary metrics for quantifying aviation's contribution to GHG emissions should be the aggregate CO_2 and aggregate NO_x emissions by all aircraft; this should include emissions for the entirety of every flight. Currently an aircraft

CO_2 emission standard does not exist [60]. In October 2013, ICAO reached a preliminary agreement to develop global rules by the end of the decade that would control airline emissions, partially as a compromise to the European Union's stance on levying carbon fees on airlines operating in European airspace [61]. For the near term, fuel burn can be used as a surrogate measure of carbon dioxide emissions until a CO_2 emission standard is defined, as these values are directly related [60]. This is consistent with the NASA N+ goals from Table 2, which do not cite any targets with respect to CO_2 specifically but rather express goals with respect to aircraft fuel burn. Because CO_2 is a well-mixed species, the metric of interest is total mission fuel burn, which is dominated by fuel burn during the cruise segment. Tracking terminal area fuel burn should be considered as well since this serves as a good indicator of vehicle performance during the more transient phases of the mission, including takeoff, climb-out and approach-landing conditions when engines are operating near idle. Thus, the metrics that shall be used for quantifying aviation's contribution to GHG emissions for this study are total mission fuel burn and total mission NO_x emissions. It should be noted that ICAO does not currently define a standard for NO_x emissions in the upper atmosphere because these emissions are difficult to measure directly for certification tests [62]. However, experiments have been performed to investigate the relationship between the engine emission index of NO_x, the compressor outlet temperature, and the engine pressure ratio. These experiments have led to regression equations that can be used to estimate total NO_x emissions given knowledge of the latter engine specifications [63].

2.1.1.2   Local Air Quality

While there is much uncertainty about the net impacts of NO_x emissions in the upper atmosphere, the contribution of these emissions on the ground and in the terminal area
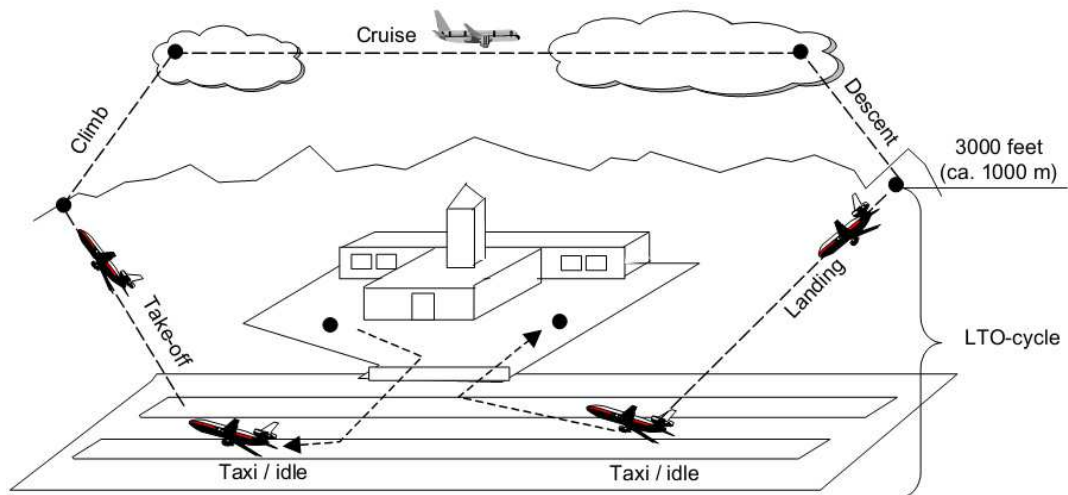
Figure 8: Landing-Takeoff (LTO) Cycle Definition [65]

to reduction in local air quality is much better understood [64]. ICAO has established and regularly updates emissions standards for terminal-area nitrogen oxides (NO_x). More specifically, these standards are defined for the Landing-Takeoff (LTO) cycle, which is represented pictorially in Figure 8 [65]. When CAEP proposes new changes to existing standards, the changes are usually cited with respect to a reference engine with an overall pressure ratio (OPR) of 30, but due to the direct relationship between NO_x and OPR, CAEP defines standard curves as a function of OPR. An example of CAEP/6 (2004) and CAEP/8 (2010) standards for higher thrust engines is shown in Figure 9 [62]. Currently, the EPA has adopted these international standards with the CAEP/8 standards officially enacted for any engine introduced after January 1, 2014 [62]. Previously manufactured engines are held to the CAEP/6 standard. The adoption of these standards explains why NASA defines its local air-quality goals with respect to LTO NO_x, as seen in Table 2.

When NO_x and volatile organic compounds (VOCs) in the terminal-area react in the presence of sunlight, they form photochemical smog, a significant form of air pollution. Children, people with lung diseases such as asthma, and people who work or exercise outside are particularly susceptible to adverse effects of smog, such as
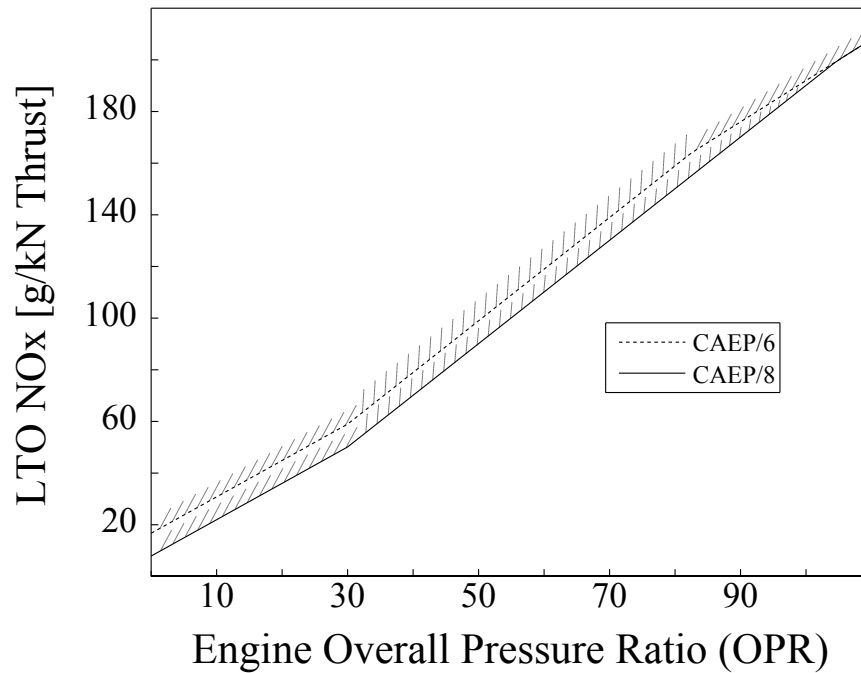
Figure 9: CAEP LTO NO$_x$ Emissions Standards

damage to lung tissue and reduction in lung function [66]. Additionally, when nitrogen dioxide (NO$_2$) reacts with atmospheric moisture, the following chemical mechanism contributes to increasing occurrences of acid rain [67]:

$$2NO_2 + H_2O \rightarrow HNO_2 + HNO_3 \tag{9}$$

$$3HNO_2 \rightarrow HNO_3 + 2NO + H_2O \tag{10}$$

$$4NO + 3O_2 + 2H_2O \rightarrow 4HNO_3 \tag{11}$$
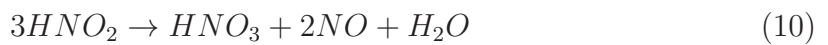
Equation (9) shows how nitrogen dioxide reacts with water to form nitrous acid (HNO$_2$) and nitric acid (HNO$_3$). The nitrous acid further decomposes as shown in Equation (10), which generates more nitric oxide and water molecules to react with atmospheric oxygen to further increase nitric acid levels, as shown in Equation (11). Nitric acid increases the acidity in rainwater, which can degrade the pH balance of

32

soil, cause a decline in local plant and animal life and even damage infrastructure built from stone.

While particulate matter, carbon monoxide, and other minor species also contribute to degradation of local air-quality, national and international agencies focus attention on terminal area NO_x as evidenced by its inclusion in both the ACARE goals in Table 1 and the NASA N+ goals in Table 2. This is because considerable progress has been made in the past few decades in reducing unburned hydrocarbons and carbon monoxide emissions. Much of these reductions are due to improvements in combustor efficiencies, as the latter species are products of incomplete combustion that are more prevalent during off-design low-power engine operation, but NO_x emissions have proven more difficult to control considering their increased concentration during high-power engine operation. Therefore, LTO NO_x shall be the metric for quantifying aviation's impact on local air-quality. In order to gain transparency for these emissions and how they correspond to each phase of an aircraft mission, the LTO cycle shall be disaggregated into departure and approach emissions (each including runway taxiing).

2.1.1.3 Community Exposure to Significant Aircraft Noise

Fuel burn and emissions are easily quantified and compared with units of mass or concentration, but measuring noise can be complicated due to its spatial and temporal variations. As a result, many different noise metrics exist. In the ACARE and NASA N+ goals in Tables 1 and 2, respectively, targeted improvements in noise are stated with respect to Effective Perceived Noise Level in decibels ($EPNL_{dB}$). The goals choose this perception-corrected metric because it is commonly used by agencies (including the FAA) for engine certification. $EPNL_{dB}$ is derived from the Tone-corrected Perceived Noise-Level (PNLT) metric that uses a complicated

formula for adjusting noise values by calculating a correction factor as a function of sound-pressure-levels (SPL) in each of the $1/3^{\text{rd}}$-octave frequency bands between 80-Hz and 10-kHz. These tone-correction factors are dependent on the frequency of the tone and its excess over the level of noise present in the adjacent $1/3^{\text{rd}}$-octave frequency bands, approximately capturing the presence of piercing pure tones that can be perceived as a greater nuisance. PNLT is measured in units of TPN$_{dB}$ [68]. EPNL$_{dB}$ expands upon PNLT by correcting for duration as follows [69]:

$$D = 10 \log_{10} \left[\sum_{k=0}^{2d} \left(10^{\frac{PNLT(k)}{10}} \right) \right] - PNLT_{max} - 13 \qquad (12)$$

$$EPNL_{dB} = PNLT_{max} + D \qquad (13)$$

Where:

$PNLT_{max}$ = max Tone-corrected Perceived Noise Level of the PNLT time history

D = duration correction factor

d = time interval during which the level exceeds $PNLT_{max} - 10$-TPN$_{dB}$

k = index of the time step

As mentioned in Chapter 1, the NASA N+ goals in Table 2 specifically target reductions in cumulative EPNL$_{dB}$, which refers to three locations around the runway that are used by the FAA for engine noise certification. These locations are depicted in Figure 10 [70]. The community and sideline reference points characterize departure noise, whereas the approach reference point characterizes noise during approach procedures. The community reference point (also referred to as flyover, takeoff, centerline, or cutback location) is located along the extended runway centerline at a distance of 21,325 ft (6,500 m) from the start of the takeoff roll [26]. The

sideline reference point has a fixed lateral distance of 1,476 ft (450 m) from the runway centerline, but the longitudinal location is determined by the maximum noise observed along the sideline reference axis and varies with each aircraft [26]. This peak typically occurs after the aircraft has lifted off and once lateral attenuation has diminished [70]. The approach reference point is located on the extended runway centerline at a distance of 6,562 ft (2,000 m) from the runway threshold [26]. The cumulative $EPNL_{dB}$ is the sum of the $EPNL_{dB}$ measurements at each of these locations, which is commonly used by industry as well as the NASA N+ goals [70].
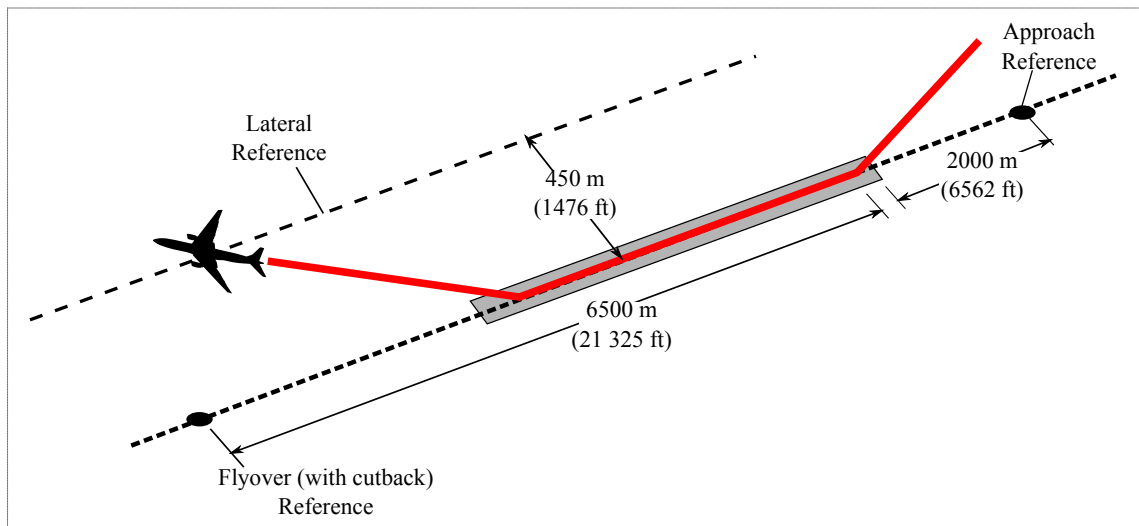
Figure 10: EPNL Certification Reference Points [70]

These reference points provide a standard for monitoring noise from new aircraft-engine combinations and allows the FAA to define thresholds that must be met by new aircraft. The FAA uses standards for these reference points in a similar manner as the LTO NO_x standard described earlier, with acceptable cumulative $EPNL_{dB}$ levels typically being dependent on maximum aircraft weight and number of engines. The FAA defines different "stages" of noise compliance for classifying aircraft according to these certification measurements, which allows them to compare and contrast noise-levels for various aircraft and prioritize which vehicles need to be

phased out of the fleet first [26]. These certification measurements, however, do not provide any indication of population exposure or annoyance due to aircraft noise, and thus another noise metric is required.

As mentioned in Chapter 1, the Noise Control Act of 1972 codified the measurements for community noise impacts via equivalency metrics. The primary equivalency metrics used for assessing noise exposure due to aviation are the Sound Exposure Level (SEL) and the Day Night Level (DNL). The SEL is an equivalency exposure metric that represents a single event by expressing, in decibels, the sound exposure level as if the entire event occurred in one second of time. The entire pressure signal is integrated with respect to time over the duration of the event and the decibel level is then calculated using a reference time of unity, as follows [71]:

$$SEL_{dB} = 10 \log_{10} \left[\frac{1}{t_2 - t_1} \int_{t_1}^{t_2} \frac{P_A^2(t)\, \mathrm{d}t}{P_0^2 t_0} \right] \tag{14}$$

Where:

$P_A^2(t)$ = A-weighted pressure squared, as a function of time

P_0 = Reference sound pressure (20 μPa)

t_0 = Reference time (1 second)

t_1 = Time at the beginning of the event

t_2 = Time at the end of the event

In Equation (14), the term A-weighted refers to a spectral weighting scheme that represents how humans perceive noise at different frequencies by emphasizing sound components in the frequency range where most speech information resides. This yields higher levels in the mid-frequency (2000 to 6000 Hz) range and lower

levels in both low frequency and high frequency ranges [11]. Decibel measures using A-weighting are commonly referenced with the units dBA. A semi-logarithmic frequency plot of A-weighting is shown in Figure 11. A-weighting tends to be used when evaluating impact of airport noise on the human population.
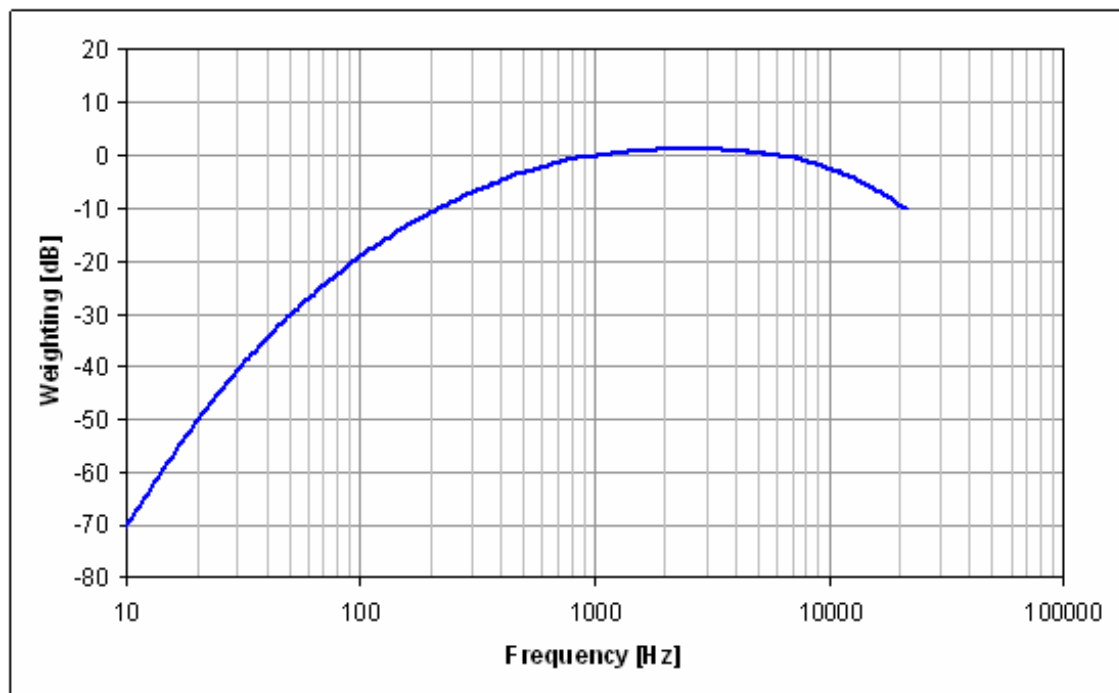
Figure 11: A-Weighted Adjustment Curve [11]

Given a grid of points defined around an airport runway, the SEL values for any single event (such as a takeoff or landing) can be calculated at each grid point. The procedure for calculating these SEL values is outlined in the Society of Automotive Engineers Aerospace Information Report 1845 (SAE-AIR-1845) [71]. This document explicitly defines reference conditions and the manner in which aircraft trajectories and velocities shall be calculated. Once this aircraft performance is determined, SEL noise values at each grid point are calculated using the referenced Noise-Power-Distance (NPD) data sets. The NPD data for a fixed-wing aircraft consists of a set of decibel levels for various combinations of aircraft engine power

37

states and slant distances from observer to aircraft. This NPD data contains source noise from the entire aircraft, including airframe, engines, high-lift devices, etc. An underlying assumption is that the NPD data represents an aircraft proceeding along a straight flight path of infinite length and parallel to the ground at a reference velocity of 160 kts and standard day atmospheric conditions. Separate NPD-curves are defined for approach and departure procedures to represent the differences between these two operating states. Standard curves are defined for the following reference distances: 200, 400, 630, 1000, 2000, 4000, 6300, 10000, 16000, and 25000 feet [72]. A notional plot of approach and departure SEL-NPDs is displayed in Figure 12. Sometimes these NPD curves are plotted on logarithmic plots with distance on the x-axis and SEL decibels on the y-axis, with different series corresponding to different thrust levels. However, the information conveyed is the same. It should be noted that similar NPDs can be defined for other noise metrics (such as EPNL), but the SEL-NPDs are the standard set of curves used for assessing community noise exposure.

The SEL grids are calculated by measuring the distance from the aircraft (approximated as a point source) to each grid location for each segment. Given the distance to the location and the engine power level, noise is interpolated from the NPD data set. Linear interpolations are used between tabulated power-settings, whereas logarithmic interpolation is used between tabulated distances. Corrections are made to account for extra ground attenuation and shielding by both the airframe and separate jet engine exhaust flows, the combination of which is commonly referred to as lateral attenuation. Since the NPD data corresponds to a reference velocity of 160 kts, a duration correction due to a difference from the ground speed implicit in this basic noise data must be made as well [73]. These segments are then logarithmically summed up and averaged over the duration of the entire event [71]. By plotting contours of equal SEL values, the aircraft noise signature can be defined and understood spatially, as is demonstrated in the notional SEL contour plots in
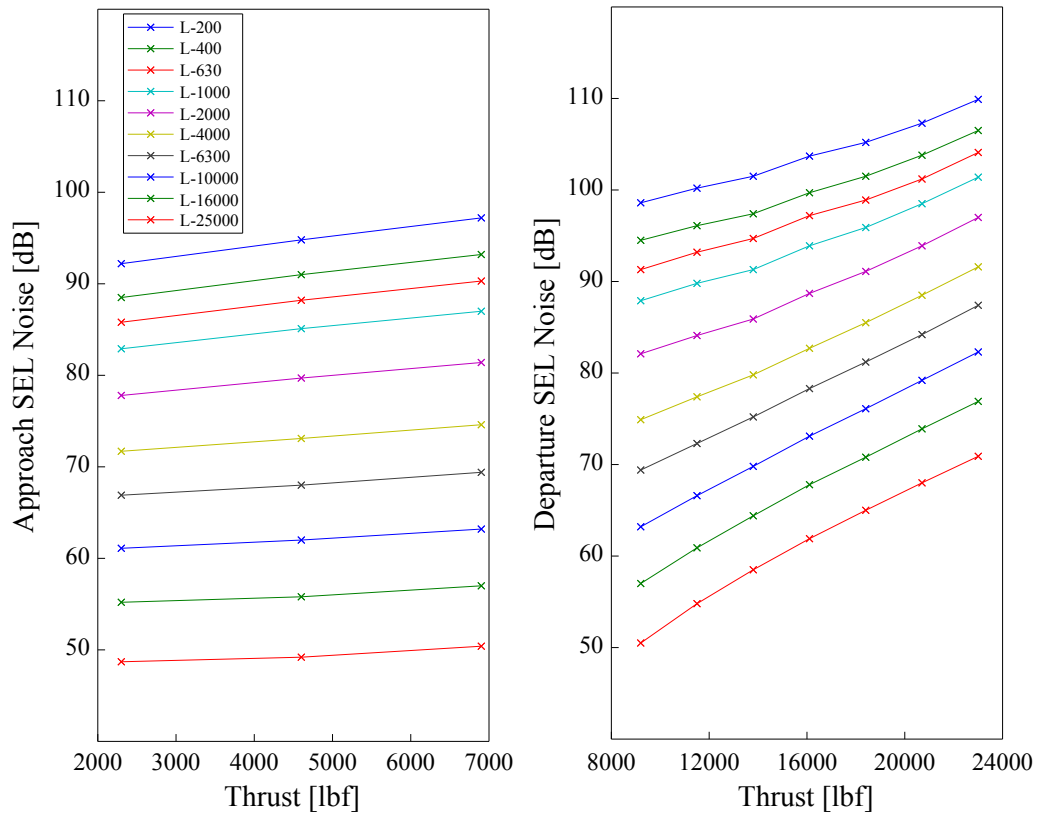
Figure 12: Notional Noise-Power-Distance (NPD) Data

Figure 13.

The plot on the left results from a notional approach procedure with the runway threshold defined at the origin, whereas the plot on the right results from a notional departure procedure with the brake-release point at the origin. As can be seen, the different contour levels resemble photographic scalings of each other, with higher decibel SEL contours corresponding to smaller contour areas. The shapes of these contours approximate how the aircraft noise radiates away from the axis of the flight path as the aircraft moves from left-to-right along the x-axis for each event. The decrease in SEL levels demonstrates how the noise attenuates as it radiates from the aircraft. The SEL maximum contour width (perpendicular to the runway axis) is characterized primarily by the maximum takeoff thrust on the runway, whereas The SEL maximum contour length (along the runway axis) is characterized by the aircraft
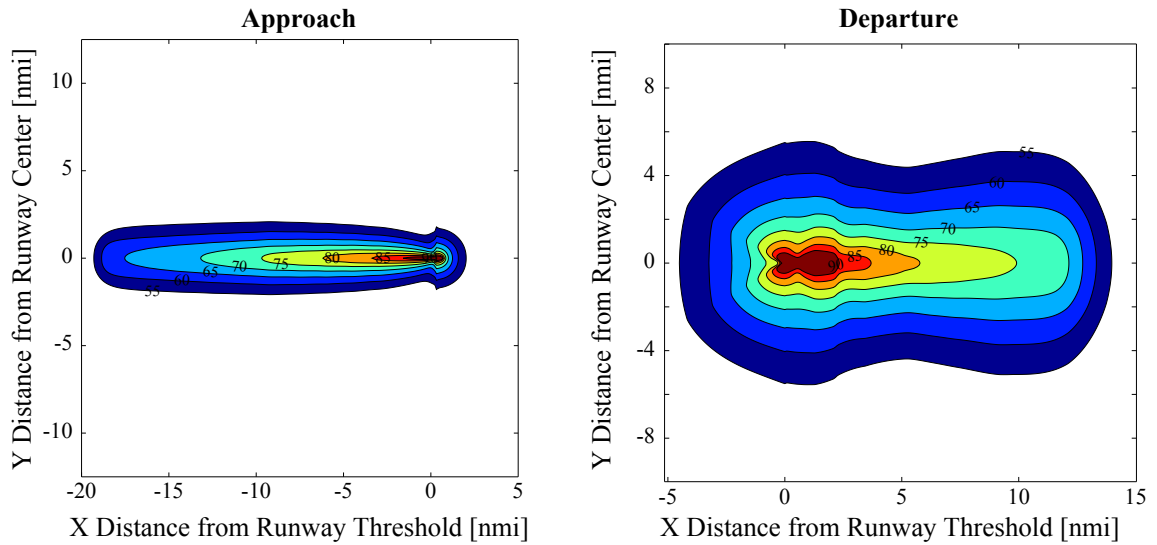
Figure 13: Notional Approach and Departure SEL Contours

climb-out trajectory and thrust profile.

It should be noted that the choice of spacing between the grid points determines the extent to which fluctuations of SEL noise are taken into account. Consequently, the quality of the noise contours will depend on the choice of the grid spacing, especially in such zones where sharp changes occur in the noise contours. Interpolation errors on the noise contours are minimized by a close grid spacing, but this increases on the other hand the computation time as the SEL noise then has to be calculated in a large number of grid points. Comparative studies have shown that a maximum value of about 0.16 nmi for a fixed, even grid spacing constitutes a good compromise between accuracy (standard deviation less than 0.5 dB for low and medium noise contours) of the interpolated noise contours and the computation time spent [73]. For the purposes of this work, a slightly finer resolution of 0.08 nmi spacing in each direction shall be used.

The DNL is a closely related airport-level equivalency-exposure-metric that attempts to characterize the soundscape of an environment over the course of an entire day. DNL serves as a measure of average sound level over a period of 24-hours, obtained from the accumulation of all events (i.e. approach and departure operations)

40

with the addition of 10 decibels to events that occur between 10pm and 7am. This penalty is applied because aircraft noise at night is often perceived as more intrusive due to the fact that nighttime ambient noise is less than daytime ambient noise, and several negative effects of noise are related to sleep disturbance. This cumulative metric is airport specific and requires knowledge of the volume of operations as well as the distribution of vehicles. The calculation of DNL values requires aggregating SEL noise as follows [71]:

$$DNL_{dB} = 10 \log_{10} \left[\sum_{i=1}^{n} \left(N_i * 10^{\frac{SEL_i}{10}} \right) + \sum_{j=1}^{m} \left(N_j * 10^{\frac{SEL_j+10}{10}} \right) \right] - 49.4 \qquad (15)$$

Where:

DNL = Day-Night Average Noise Level at grid point (dB)

SEL_i = Sound Exposure Level at gridpoint of the ith daytime flight

N_i = Number of operations of the ith daytime flight

n = Total number of aircraft with daytime flights

SEL_j = Sound Exposure Level at gridpoint of the jth nighttime flight

N_j = Number of operations of the jth daytime flight

m = Total number of aircraft with daytime flights

The constant term in Equation (15) is derived from averaging the sound pressure over the total number of seconds in a day. The American National Standards Institute (ANSI), the U.S. National Research Council (NRC), and several other federal agencies and administrations recommend DNL for assessment of

41

environmental noise [74]. This recommendation is based on years of attitudinal survey studies, beginning with the seminal work by Schultz in 1978 that detailed the percent of population annoyed as a function of DNL in decibels as shown in Figure 14 [75].
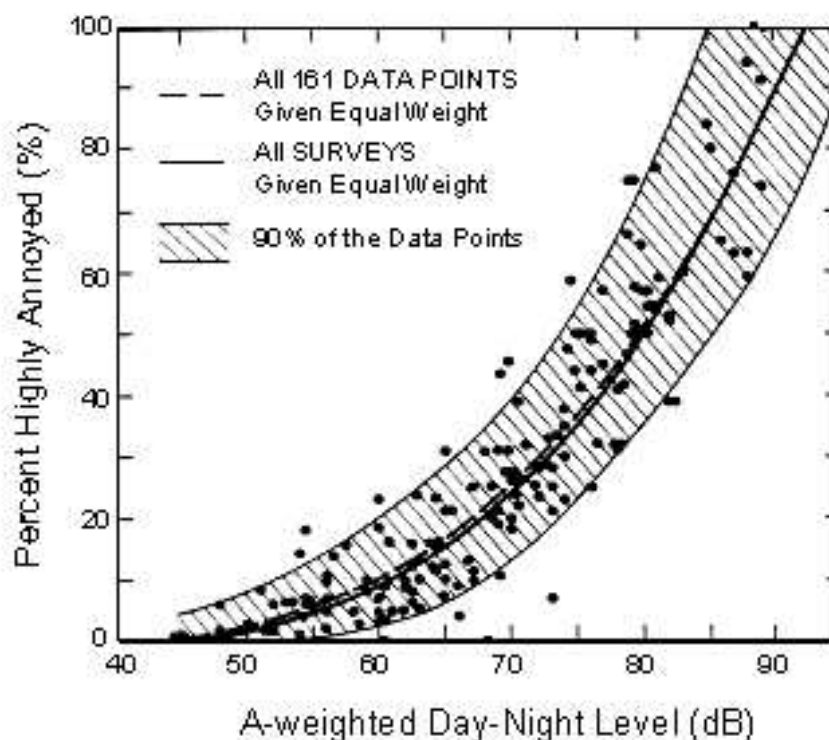
Figure 14: Percentage of Population Highly Annoyed versus DNL [75]

Currently, the FAA states goals for noise mitigation in terms of reducing the number of people exposed to significant noise, where significant noise is defined as aircraft noise above a DNL of 65-decibels [76]. For example, in calendar year 2012, the FAA aimed at decreasing the amount of population exposed to DNL 65-dB to less than 386,000. The FAA regularly sets targets by analyzing the historical rate of change of noise exposure versus long-term projections of air traffic demand. According to the National Environmental Policy Act (NEPA), areas exposed to DNL levels of 65-dB or greater are entitled to federal aid in terms of

42

elements of the Noise Compatibility Plan (NCP), such as sound insulation for homes [77]. The population exposed to this level of noise is calculated by performing a Federal Aviation Regulation (FAR) Part 150 study, which refers to a part of Title 14 of the U.S Code of Federal Regulations (CFR). A FAR Part 150 study is a noise-compatibility/land-use study designed to identify and evaluate measures to mitigate the impact of aircraft noise in the vicinity of airports [74]. These studies define contours of equal DNL noise exposure (particularly DNL 65-dB) and superimpose these contours over population density maps from Census data, as demonstrated by the example 2011 noise contour map for Cleveland-Hopkins airport in Figure 15 [78].
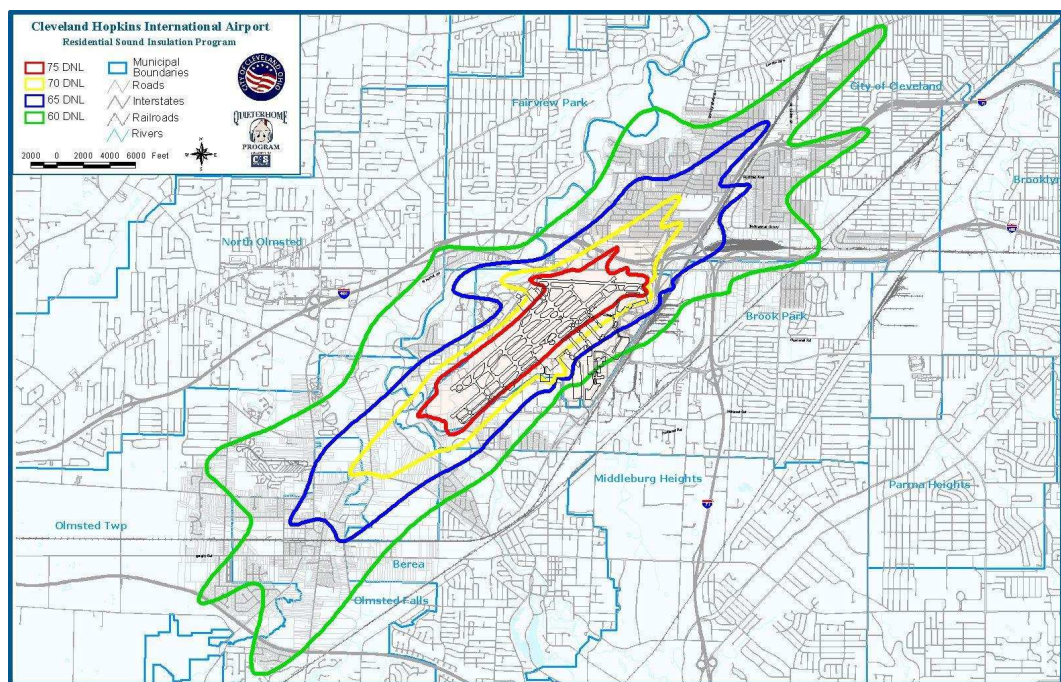
Figure 15: Example FAR Part 150 DNL Contour Map [78]

Given the observed relationship between annoyance and DNL-levels as well as the ability to calculate spatial noise exposure cross-referenced with population density, the DNL metric is better than the certification $EPNL_{dB}$ metric for quantifying significant

noise exposure. The true metric of interest is the count of population exposed to this significant noise, but the areas and shapes covered by the DNL contour will serve as valuable intermediate metrics that capture the contributions of the fleet, operations, and airport configurations. Despite the fact that the FAA only considers significant noise to be DNL levels of 65-dB or greater, many other U.S. agencies set the significant noise exposure threshold at DNL 55-dB [74]. Therefore, it is useful to use both the DNL 65-dB and 55-dB contour areas and shapes as the relevant noise metrics, with the latter representing a potentially more stringent future metric.

The complexity of airport geometries and infrastructures lead to irregularly shaped DNL contours such that the maximum contour lengths and widths do not provide enough information about the contour shape. Each airport features unique numbers of runways and runway locations that determine the shape of the airport noise signature. Bernardo reviewed multiple shape metrics and determined that Detour and Spin provide a good reference for shape comparisons [79]. Detour is defined as the perimeter of the convex hull of the shape, while Spin is defined as the average of the square Euclidean distance between all interior points and the centroid [80]. Notional diagrams of these shape metrics are displayed in Figure 16. To define shape indices that range from 0 to 1, each of these shape metrics are normalized with respect to the measure for a circle of equal area.

$$\text{Detour} = \text{Perimeter}_{\text{ConvexHull}}$$

$$\text{Spin} = \frac{d_1^2 + d_2^2 + ... + d_n^2}{\# \text{ of points}}$$
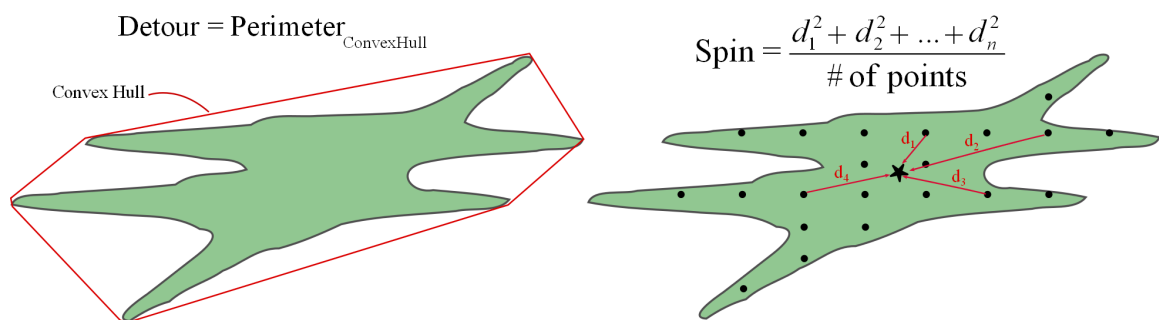
Figure 16: Detour (left) and Spin (right) Shape Metrics [79]

Finally, overlaying these DNL contours on spatially distributed population data around an airport allow for the calculation of population counts exposed to significant noise. For the US, the source for population data is the US Census Bureau, which reports population counts by Census-blocks (smallest polygonal unit), block groups (aggregated blocks), and tracts (aggregated block groups) as shown in the hierarchy in Figure 17 [81].
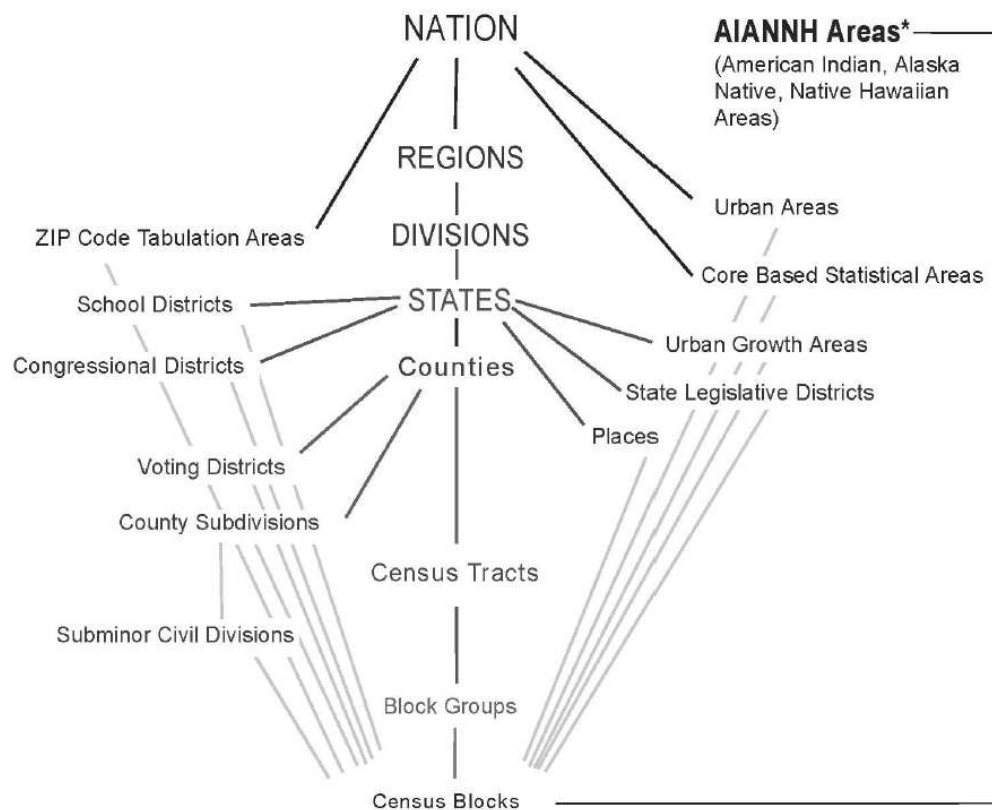
Figure 17: Standard Hierarchy of Census Geographic Entities [81]

At the finest resolution (block level), a uniform population distribution is often assumed, or the population values may be an attribute assigned to the block (polygon) centroids. Similarly, population values for block groups and tracts are reported at the centroids of the block group and tract polygons. For exposure and risk analyses, these centroids often serve as "receptor" points for calculating exposure or dosage

45

from some agent (such as cumulative airport/aircraft noise). The Census Bureau links this population and housing unit counts to spatial information through the Topologically Integrated Geographic Encoding and Referencing (TIGER) products, which includes shapefiles and geodatabases for use with ArcGIS® [82]. An example of this spatial data can be seen in Figure 18, which displays the Census-blocks for the state of Georgia. As can be seen the resolution is very fine, with Georgia containing 291,086 Census-blocks and population counts ranging from 0 to 3,228 people per Census-block. By visualizing the data spatially, an area of interest can be defined with a buffer from a given location. In Figure 18, for example, a Latitude-Longitude point is defined to mark Hartsfield-Jackson airport, and a 50 nautical mile radius is defined around this point. Each state Census-block contains a large magnitude of data, so in this way the data can be filtered by spatial relevance.
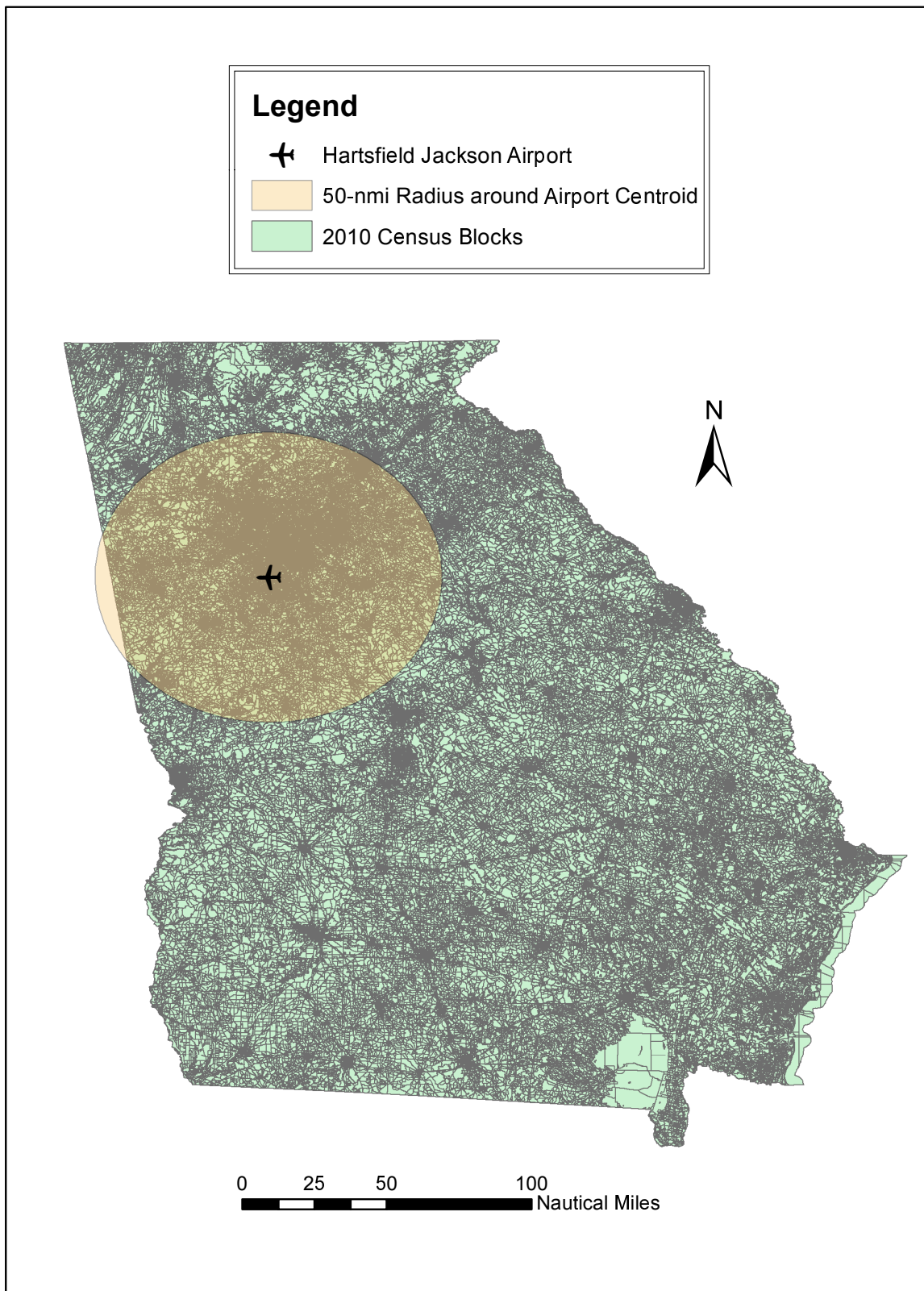
Figure 18: State of Georgia Census Blocks

The final list of environmental impact metrics considered for this research are included below in Tables 5 and 6. For each of the CAEP goals, the vehicle-level and fleet-level metrics are listed.

Table 5: Environmental Impact Metrics: Vehicle-Level

CAEP Goal	Metric
GHGs	Total Mission Fuel Burn [kg] Total Mission NO_x Emissions [g]
Local Air Quality[1]	Terminal Area Departure NO_x Emissions [g] Terminal Area Approach NO_x Emissions [g]
Noise Exposure[2]	SEL Contour Areas [nmi^2] SEL Contour Maximum Widths [nmi] SEL Contour Maximum Lengths [nmi]

[1] Also track terminal area fuel burn (below 3,000-ft)

[2] Track multiple SEL decibel levels

Table 6: Environmental Impact Metrics: Fleet-Level

CAEP Goal	Metric
GHGs	Aggregate Fuel Burn [kg] Aggregate NO_x Emissions [g]
Local Air Quality[1]	Aggregate Departure NO_x Emissions [g] Aggregate Approach NO_x Emissions [g]
Noise Exposure[2]	DNL Contour Areas [nmi^2] DNL Contour Shapes: Detour Index[3] DNL Contour Shapes: Spin Index[3] Population Exposure Counts

[1] Also track aggregate terminal area fuel burn (below 3,000-ft)

[2] DNL 65-dB and DNL 55-dB

[3] Normalized on a 0-1 scale

Aggregate fuel burn and NO_x emissions can be calculated by linking vehicle-level performance to operational frequencies. This formulation is relatively simple, as it

essentially represents a weighted sum of the vehicle level performance metrics as summarized by Equation (16):

$$Y = \sum_{i=1}^{Num_{AC}} \left(\sum_{x} n_{i,x} y_i(x) \right) \tag{16}$$

Where:

Y = Fleet-level aggregation of fuel-burn or NO_x emissions

i = Unique aircraft index

Num_{AC} = Total number of unique aircraft in the fleet

x = Unique mission lengths

$n_{i,x}$ = Number of operations by aircraft i at mission length x

$y_i(x)$ = Performance of aircraft i as a function of mission length x

This formulation lends itself to very rapid calculations, especially if the performance of aircraft as a function of mission length $y_i(x)$ is reduced to a second order regression. These calculations can be performed by sampling from these regressions and multiplying by the flight frequency. This formulation does not work for noise, however, because noise is inherently an airport-level metric. Noise contour areas and population exposure depend on vehicle-level noise footprints, operational distributions and volumes at each airport, runway configurations at these airports, and the distribution of population around the airport. Fleet-level noise is characterized by accumulating contour areas and population exposure counts across all of the airports. However, many of the airports do not feature significant volume of operations or are isolated from local communities. Given the computational expense of noise calculations, noise studies often identify a subset of relevant airports with

significant noise exposure to make the problem more manageable. The subset of airports to be used for this research are the MAGENTA 95 airports which account for the majority of the national counts of population exposed to significant noise [83]. This subset is consistent with the airport set used by Bernardo in developing his Generic Airport categories, and thus the airport runway configurations and baseline schedules were conveniently available [79]. The methods outlined in this work are applicable regardless of the subset of airports, although the inclusion of international airports with different operational volumes and distributions may lead to different results for the generic vehicle approach.

2.1.2 Review of Surrogate Methods for Fleet-Level Analysis

Fleet simplifications are often used for fleet-level studies. For example, Purdue University has and continues to develop their Fleet-Level Environmental Evaluation Tool (FLEET) to investigate how fleet-level environmental impacts will evolve over time [84]. This tool centers on an aircraft allocation model that represents airline operations and decision-making rather than focusing on specific technologies or technology packages. To manage the number of aircraft types used by the airline, current (and potential future) aircraft are aggregated into six classes based on seat capacity. To represent different technology "ages" within these classes, each class is further segregated into categories of representative-in-class, best-in-class, new-in-class, and future-in-class. Representative-in-class aircraft are those that had the highest number of operations in 2005 within each seat class and are typically older aircraft. The best-in-class aircraft are those that had the most recent service entry date within each seat class as of 2005 and, thus, incorporate more recent technological advances. A list of the classes with their corresponding representative-in-class and best-in-class aircraft is shown in Table 7 [84].

Table 7: Purdue FLEET Aircraft Classes

Class	Seats	Representative-in-class	Best-in-class
Class 1	20-50	Canadair RJ200/RJ440	Embraer ERJ145
Class 2	51-99	Canadair RJ700	Embraer 170
Class 3	100-149	Boeing 737-300	Boeing 737-700
Class 4	150-199	Boeing 757-200	Boeing 737-800
Class 5	200-299	Boeing 767-300	Airbus A330-200
Class 6	300+	Boeing 747-400	Boeing 777-200ER

The new-in-class aircraft are either aircraft currently under development that will enter service in the future or concept aircraft that incorporate technology improvements expected in the future. Likewise, the future-in-class aircraft are those aircraft expected to include another generation of technology improvements and therefore expected to enter in service a date further in the future. The airline model operates only these aircraft as a representative fleet mix [84]. While this method does provide a useful example of ways to simplify the fleet, by using fixed new-in-class and future-in-class vehicles, this model is limited in its ability to explore a variety of future technology scenarios.

In an effort to address this limitation, Becker introduced "generic vehicle" concepts for modeling and simulating aggregate fleet fuel burn and NO_x emissions [44]. The goal of these generic vehicles were to reduce a complex and diverse fleet to a subset of physics-based vehicle-level models that could match the aggregate metrics of the full fleet when linked to the same operational schedules as shown in Equation (16). Traditionally, vehicles have been grouped by internal seat layouts and seating capacity into seat classes, such as the CAEP/8 seat classes listed in Table 8.

Under this approach a single airframe type can be classified into multiple seat classes depending on the internal seat layout. For example, Figure 19 shows the same vehicle with the same fuselage under two different seating layouts for two different airlines. One airline fits 178 seats into the fuselage, classifying the aircraft as a Seat Class 5 vehicle. The other airline increases the seat-pitch between rows, which only

www.manaraa.com

Table 8: CAEP/8 Seat-Class Definitions

Seat Class ID	Passenger Capacity	Type of Aircraft/Layout[1]
SC1[2]	1-20	General Aviation
SC2	21-50	Regional Jet
SC3	51-100	Regional Jet
SC4	101-150	Single Aisle
SC5	151-210	Single Aisle
SC6	211-300	Small Twin Aisle
SC7	301-400	Large Twin Aisle
SC8	401-500	Large Quad
SC9	501-600	Large Quad

[1] Most common type of aircraft associated with each seat-class

[2] SC1 not included in this study due to few operations at relevant airports

allows for 150 seats, classifying the same aircraft as a Seat Class 4 vehicle.

178 seats = SC5

150 seats = SC4
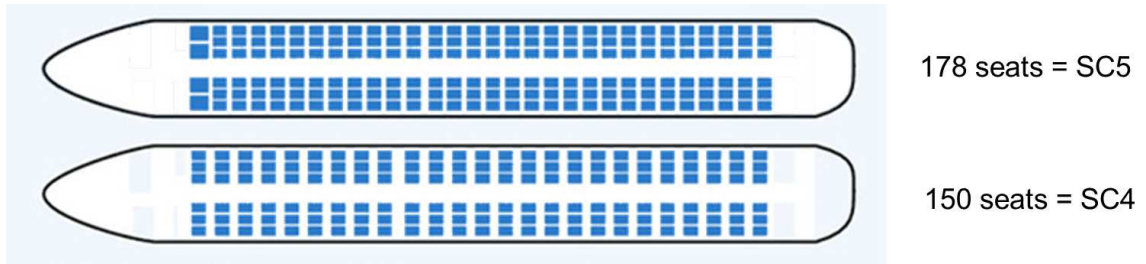
Figure 19: Multiple Seat-Class Configurations for Same Vehicle

SeatGuru® provides extensive lists of vehicles and seating configurations. A few examples of aircraft that fall into multiple seat classes depending on how airlines configure the internal seat layout include [85]:

- The Embraer ERJ-190 may range from 94 to 114 passengers (spans SC3-SC4).

- The Airbus A321 may range from 185-220 passengers (spans SC5-SC6).

- The Boeing 767-300ER may range from 218-350 passengers (spans SC6-SC7).

The performance of the aircraft itself, however, does not typically vary greatly due to this internal layout. Becker instead proposed grouping vehicles on multiple metrics

to create a better distinction between groups. He defines "capability groups" which take into account the maximum payload and the maximum range of each airframe [44]. Becker used these metrics to identify four groups:

- Regional Jet (RJ)

- Single Aisle (SA)

- Small Twin Aisle (STA)

- Large Twin Aisle (LTA)

Given these groups, Becker explored three methods for surrogating the fleet. The first method used a best-in-class representation similar to that used in the Purdue FLEET model, but this yielded significant errors at the fleet-level with respect to a set of reference operations and increased error with respect to variable schedules of operations. The second method employed a parametric correction factor applied to these best-in-class vehicles, which significantly improved results for both the reference operations and variable operations. These correction factors, however, were defined for a fixed technology condition, and thus proved incapable of accurately capturing impacts of technology infusion. The third method utilized an average vehicle approach, which filters settings for vehicle design parameters in order to reduce the error of aggregate results. This method was inspired by a similar approach used by the Environmental Protection Agency (EPA) for conducting an analysis of annual automobile emissions data in the context of corporate average fuel economy regulations [86]. Becker enumerated the following steps for this average vehicle approach:

1. Conduct effect screening to determine which input parameters are in fact the most influential on the relevant fleet-level metrics.

2. Calculate a target representing the aggregate performance of the fleet for each metric of interest using Equation (16).

3. Vary the key input parameters from effect screening around the reference vehicle to generate engine cycle and airframe geometry combinations for design space exploration.

4. Conduct thorough design space exploration to identify the best option for an averaged vehicle that hits the aggregate targets calculated for the entire fleet for each environmental metric.

The problem of matching aggregate targets can equivalently be described as attempting to minimize error with respect to these targets. Given the linear nature of Equation (16), minimizing error within each class minimizes the combined fleet-level error. Relative error is used to compare multiple metrics on different scales and avoid biasing the generic vehicles toward accuracy in any one metric over the others, but the method doesn't favor over-predicting or under-predicting and instead focuses on minimizing the magnitude of this relative error. The resulting physics-based models can then be used for modeling technology infusion at the component or subsystem level such that the interdependencies and compatibilities for multiple technologies can be quantified and propagated to aircraft system-level performance. These technology-infused models can then be used in conjunction with forecasts and fleet-evolution models to objectively project the future environmental impacts under various technology scenarios.

This method provided better accuracy for a set of reference operations and acceptable accuracy for variable operations and technology infusion. The maximum relative error among the metrics (total-mission fuel burn, terminal-area fuel burn, total-mission NO_x emissions, and terminal-area NO_x emissions) for each of Becker's method is summarized in Table 9 [44].

Table 9: Maximum Errors from Becker's Experimental Results

Experiment	Surrogate Fleet Method		
	Best-in-class	Parametric Correction Factor	Average Vehicle
Reference Operations	51.00%	0.71%	0.96%
Variable Operations	52.73%	0.87%	2.42%
Technology Implementation		110.91%	3.73%

Becker's work demonstrated that the average vehicle approach can match aggregate fleet data within a reasonable level of accuracy for the baseline reference fleet, a fleet with variations in operations, and a fleet with technology infusion. A similar approach was used in the World Fleet Modeling chapter of the IATA Technology Roadmap 2013 previously mentioned in Chapter 1 [7].

2.1.3 Review of Rapid Airport-Level Noise Computation Model

Bernardo developed and validated the Airport Noise Grid Integration Method (ANGIM) for rapid computation of noise grids and contours to enable scenario analysis. This method simplifies and accelerates the process used in the Integrated Noise Model (INM) by pre-calculating the vehicle-level SEL-grids under the simplifying assumptions of standard sea-level atmospheric conditions and straight-in, straight-out ground tracks. These assumptions allow the vehicle-level SEL grids to be precalculated and stored in local memory such that they can be called using simple table lookup routines. In this way, ANGIM serves as a screening level capability that complements detailed models like INM or AEDT [79]. ANGIM is an example of a method that exchanges fidelity for computational speed, and thus it can serve as an integral piece of the proposed framework.

ANGIM uses a schedule of operations on each runway at an airport to logarithmically sum the vehicle-level SEL grids to runway-level DNL grids. These

runway-level grids are then translated and rotated with respect to the runway configurations. ANGIM finally overlays the properly oriented runway-level grids, interpolates them to account for inexact grid-meshing, and sums these grids logarithmically to approximate an airport-level DNL grid. Contours of equal DNL decibel values can be defined from these airport-level DNL grids, and ANGIM is capable of calculating the areas of these contours as well as a series of shape-metrics such as the previously mentioned Detour Index and Spin Index. This method is diagrammed in Figure 20. It should be noted that in the absence of specific runway utilization information, ANGIM assumes that each runway features cross-flow operations (i.e. runway operates evenly in each direction over the course of the day) and that operations by each aircraft in the flight-schedule are evenly divided over all available runways.
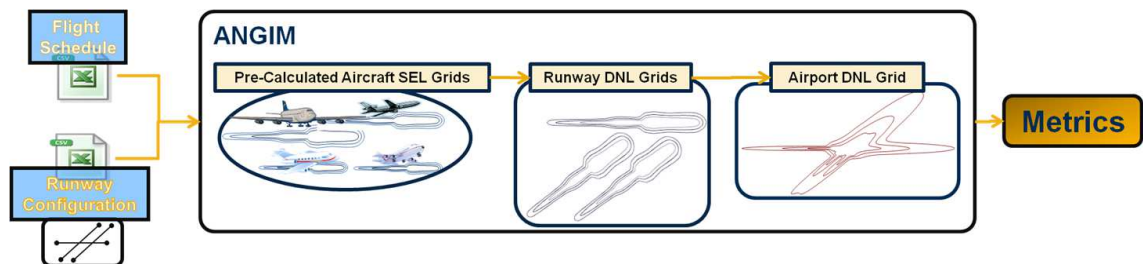
Figure 20: Airport Noise Grid Integration Method (ANGIM) [79]

2.2   *Formulation of Modeling and Simulation Requirements*

The framework proposed in this work hinges on modeling and simulation at both the fleet- and vehicle-level, but fidelity and speed must be balanced such that many alternatives can be explored while still enabling meaningful and traceable analysis. Thus, requirements must be derived for both fleet-level and vehicle-level modeling and simulation tools to ensure this balance is appropriate.

56

2.2.1 Requirements for a Fleet-Level Model

Much like the legacy tools that preceded it, AEDT is designed to perform official inventory analyses such as FAR Part 150 studies. For this reason, it includes many layers of complexity such as detailed weather and terrain models. While these layers are necessary for official inventories, the complicated setups and computational expense associated with them inhibits the ability to use AEDT for a screening-level scenario analysis that isolates the sensitivities of aircraft performance improvements. In order to perform this screening-level analysis, a fleet-level tool must be designed to reflect the structure of AEDT (shown in Figure 2 in Chapter 1) but reduce it to a more simplified formulation.

Becker outlines the requirements for fleet-level modeling and simulation of fuel burn and NO_x emissions [44]. Inputs to the model include aircraft performance results derived from vehicle-level modeling and simulation tools, along with operational schedules that represent the frequency of flights by each vehicle type at each mission length. This formulation is relatively simple, as it essentially represents a weighted sum of the vehicle level performance metrics. This formulation does not work for noise, however, because noise is inherently an airport-level metric as is evident from the discussion of noise metrics. Noise contour areas and population exposure depend on the operational distributions and volumes at each airport, the runway configurations at these airports, and the distribution of population around the airport. Thus, a unique set of requirements must be defined for a noise modeling tool, and this tool must focus on airport-level analysis.

Dikshit and Crossley define the following five requirements for a generic airport noise modeling tool [87]:

1. *Single-valued:* Provides a single point of comparison.

2. *Rapidly Computable:* To enable evaluation of a multitude of scenarios.

3. *Simple Formulation:* To avoid resource allocation problems.

4. *Correlated:* Compares favorably to a detailed model for validation.

5. *Flexible:* Able to incorporate and evaluate impacts of new technologies and/or aircraft.

The generic fleet-level model proposed by the authors focused on a single-metric, the DNL 65-dB contour area. The model approximated the area around the airport with a regression dependent on the number of operations and the aircraft $EPNL_{dB}$ certification measurements. This model, however, did not capture any spatial details about the noise. Bernardo critiques these requirements and proposes slight modifications to them. Bernardo accepts the notion that the model should be rapid, correlated with an industry standard or detailed model, and flexible enough to incorporate new technologies and aircraft. However, he rejects the simplicity of the regression model, instead replacing it with a requirement for automation and comparatively short setup times relative to a detailed model. Bernardo additionally rejects the single-valued metric requirement and the sole use of the DNL 65-dB contour area. A simple regression for contour area cannot properly capture the number of people exposed to significant noise due to its lack of spatial data. Bernardo's six requirements for a generic fleet-level noise model are as follows [79]:

1. Easily incorporates new and technology-modified aircraft

2. Computational speed with respect to detailed models

3. Acceptable accuracy with respect to detailed models

4. Simple-to-manage inputs

5. Full automation

6. Contour area and shape information captured

The latter methods and requirements, however, are limited to fleet-level noise. Given the three CAEP goals defined in Chapter 1 and the corresponding metrics, it naturally follows that the fleet-level tool must be able to evaluate total mission metrics (such as total fuel burn and NO_x emissions) as well as terminal area metrics (such as LTO NO_x emissions and DNL contours) while adhering to current best practices. In the past, fleet-level analyses of aviation's contributions to each of these metrics were divided amongst many different tools. The consequence of these decoupled analyses was an inability to capture the interdependencies of fuel burn, emissions, and noise. Thus, an appropriate fleet-level environmental impact tool shall:

1. Measure total mission and terminal area metrics for fuel burn and NO_x emissions.

2. Measure DNL contour area and shape information.

3. Capture interdependencies between all of the metrics.

4. Adhere to current standards and best practices.

5. Incorporate existing aircraft with industry validated data where available.

6. Easily incorporate new and technology modified aircraft.

7. Demonstrate computational speed with respect to detailed models.

8. Demonstrate acceptable accuracy with respect to detailed models.

9. Feature simple-to-manage inputs.

10. Leverage automation as much as possible.

A notional formulation of a screening-level tool for fleet-level analysis that meets these requirements is diagrammed in Figure 21. The formulation hinges on linking the operational schedules between simple fuel burn and NO_x calculations as

www.manaraa.com

represented in Equation (16) and the airport-level formulation for computing noise contours and eventually population exposure.
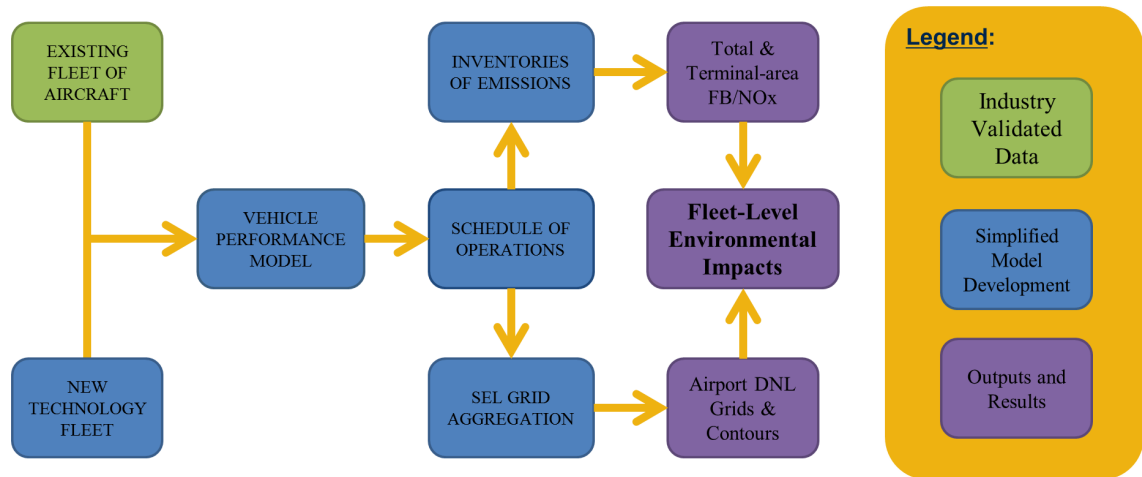
Figure 21: Notional Diagram of Integrated Fleet-Level Environment

2.2.2 Requirements for a Vehicle-Level Model

The integrated tool suite in Figure 21 captures fleet-level responses that depend on operational schedules and fleet mixes, but it is limited in its capabilities to objectively assess the impacts of technology infusion and the evolution of the fleet. Most technology development is focused on aircraft-level system and subsystem improvements. Thus, an alternative modeling and simulation environment is required in order to assess vehicle-level technology impacts.

Many of the requirements for the vehicle-level model should match the requirements established for the fleet-level tool in the previous section. The model must focus on the same type of metrics as the fleet-level tool and capture interdependencies between these metrics. The noise analysis must focus on the SEL metric as opposed to the DNL metric, as the latter is an airport-level metric whereas the former is a vehicle-level metric. This model should be validated against industry data when available, and should feature manageable setup procedures with

www.manaraa.com

an emphasis on automation. The most important requirement for the vehicle-level tool is to fill in the gaps that can't be accomplished with the fleet-level tool and to interface with said fleet-level tool. Thus, the vehicle-level model shall:

1. Model component-level performance using as much physics-based formulations as possible.

2. Model system- and subsystem-level impacts from technology infusion.

3. Model interactions and compatibilities for technology packages with multiple technology concepts infused simultaneously.

4. Generate an integrated analysis of aircraft performance, exhaust emissions, and source noise.

5. Employ a simple formulation with automation for exploring multiple technology scenarios on multiple vehicle types.

6. Be traceable, validated, and endorsed by industry and government agencies.

7. Interface with the fleet-level tool suite.

By capturing the technology impacts at the subsystem level the model will be able to more objectively evaluate the impacts of technology at the aircraft system level, including any potential incompatibilities from multiple technologies infused simultaneously on the same aircraft.

2.3   Technical Challenges

The previously developed generic vehicles only focused on aggregate fuel burn and emissions metrics. Fleet-level accuracy is important for noise as well, because the true measure of noise impact is the number of people exposed to significant noise.

To determine this, noise impacts must be aggregated to define DNL 65-dB contours, and these contours must be superimposed over population maps in a Geographical Information System (GIS) such as Esri's ArcGIS® framework. If the airport-level DNL 65-dB contour is inaccurate, these counts of people exposed to significant noise can be misleading.

One objective of this study is to add the complexities of noise calculations for defining these generic vehicles. If the vehicles in the fleet can be binned into categories and reduced to a handful of per class average generic vehicles that can match aggregate fleet results for fuel burn, emissions, *and noise* with reasonably accuracy, this would reduce run-times considerably while still providing a screening-level fidelity for an objective fleet-level evaluation of various technology packages. This is especially critical for noise analysis due to the computational expense of the grid-based noise methods. These generic vehicles can be used as replacement aircraft in future years to approximate fuel burn, emissions, and noise under the uncertainty of future fleet composition. Additionally, these generic vehicles can serve as virtual test beds to estimate the fleet-level impacts of various technology infusion scenarios, capturing the interdependencies of noise and emissions.

Expanding the generic vehicles to include noise introduces a few additional technical challenges beyond Becker's approach. The fleet classification problem must be revisited and reformulated in a manner designed to reduce in-class variance for multiple metrics simultaneously. Validation with respect to fleet-level targets must be reformulated as airport-level targets, but the operational complexities that are unique to each airport may confound this validation. Additionally, the true noise metric of population exposure to significant noise must somehow be incorporated into the noise analysis for proper validation of the accuracy of the generic vehicles.

2.3.1 Fleet Classification

While Becker's capability groups classified vehicles into groups that fly similar route types, they do not take into account the actual performance of these aircraft with respect to the environmental metrics of interest. This leads to the following research question:

RQ 1: What parameters should be used to classify aircraft into generic vehicle groups?

Given that the end goal is to define vehicles that match aggregate metrics for the combined fleet, the classification scheme should delineate groups based on the corresponding vehicle-level performance metrics from Table 5 that map to these fleet-level metrics. To reduce the variability of vehicle performance per group, this study proposes classifying aircraft into "vehicle classes" which are defined by both the payload-range capability as well as the vehicle-level performance with respect to the environmental metrics discussed previously. The first hypothesis proposes that this type of classification scheme will result in a better generic fleet than the traditional seat-class groupings:

Hypothesis 1: A per-class average generic fleet of vehicles defined by vehicle-class groupings based on similarities in the environmental performance metrics will feature superior fleet-level accuracy compared to a per-class average generic fleet of vehicles defined by traditional seat-class groupings.

The justification for this hypothesis can be derived from simple probability theory and statistics. Suppose that for a given metric, the relative error of the best average generic vehicle within a class relative to the target metrics across a subset of airports

can be represented by a univariate normal distribution, $\epsilon_i \sim N\left(\mu_{\epsilon_i}, \sigma^2_{\epsilon_i}\right)$. The ideal generic vehicle will reduce the mean error within the group to approximately zero, but the variance is a function of the variance in performance across the subset of airports. Probability theory then suggests that under the assumption of independence between each group, the aggregated performance of the generic fleet is also normally distributed with the mean being the sum of the individual group means and the square of the standard deviation being equal to the sum of the squares of the standard deviations of each group, as shown in Equation (17) [88].

$$\sum \epsilon_i \sim N\left(\sum \mu_{\epsilon_i}, \sum \sigma^2_{\epsilon_i}\right) \tag{17}$$

Where:

ϵ_i = Normally distributed error for i^{th} vehicle class

μ_{ϵ_i} = Mean error for i^{th} vehicle class

$\sigma^2_{\epsilon_i}$ = Variance of error for i^{th} vehicle class

Equation (17) is only true under the assumption of independence, as this leads to a correlation of zero and allows for the omission of covariance terms. It should also be noted that separate normally distributed random variables can be uncorrelated without being independent, in which case Equation (17) would not hold. However, given that each per-class generic vehicle will only be used to represent vehicles within its own group, it is reasonable to assume that the error distributions for each generic vehicle class is independent of the error for the other vehicle classes. Given this assumption, it can clearly be seen that a grouping that reduces the variance within each class should lead to a reduction in the overall variance at the fleet level.

64

In reality, this abstract justification is overly simplified for a number of reasons. First, the generic vehicles will actually be represented by multivariate error distributions as opposed to a single univariate error distribution, and the metrics for each error distribution *within a class* are likely correlated with each other. Second, the variance of the vehicle-level performance is not necessarily representative of the actual variance within each group, as the aggregate performance will actually be weighted by the frequency of operations by each constituent vehicle. Third, the relative error may not actually be normally distributed for each metric. In order to objectively test this hypothesis, the generic vehicle tests introduced in this research will be performed in parallel for the proposed vehicle-class groupings as well as the traditional seat-class groupings.

Equation (17) suggests that the fleet-level variance would likely benefit from more groups with less deviations from the mean in each group, the extreme being n groups corresponding to n unique aircraft in the fleet. For this extreme, each of the n groups feature one unique aircraft and thus zero variance. This is computationally inefficient, however, and was the impetus for the overarching hypothesis of exchanging fidelity for speed. A generic fleet of m groups, where $m < n$, will reduce computation time but will increase the deviations from the mean. The seat class formulation features eight classes (excluding SC1), and to ensure that better fleet-level results for the vehicle-class formulation are not confounded by the resolution of the classes a number less than eight should be chosen. For this work, Becker's vehicle classes have been modified from four to six classes to reflect the structure of current research and development programs by the major aircraft manufacturers [89]:

1. Regional Jet (RJ)

2. Small Single Aisle (SSA)[1]

---

[1]Becker's Single Aisle (SA) class was split into the SSA and LSA classes primarily due to distinctions in noise contour lengths for different single aisle stretch-variants.

3. Large Single Aisle (LSA)

4. Small Twin Aisle (STA)

5. Large Twin Aisle (LTA)

6. Very Large Aircraft (VLA)[2]

Assigning vehicles to these vehicle-class groups to reduce the variance in the performance metrics requires the implementation of supervised multiclass classification algorithms. There are generally a few approaches to the classification problem, with each typically attempting to map training data to the assignment of a class label through mathematical or statistical techniques [90]. Regardless of which approach is used, the vehicle-level performance metrics should be used as training data, and the method should be able to assign aircraft into one of these six classes.

2.3.2 Fleet-Level Characterization

Fuel burn and NO_x emission metrics are very simply mapped from vehicle-level performance to fleet-level aggregations due to the fact that they are mass-based metrics. Noise, however, depends on instantaneous sound pressure levels that spread out spatially and must be integrated over the duration of events. This spatio-temporal dependence means that the noise metric depends on the local airport configurations and operational schedules, and thus cannot be mapped to fleet-level aggregations with simple linear summations of vehicle-level performance as is possible for the mass-based metrics. This motivates the following research question:

RQ 2: *Given that noise is an airport-level metric, how can it be incorporated into the average-generic vehicle formulation?*

---

[2]Becker did not include this class in his formulation. This class features larger four-engine aircraft.

Research Question 2 implies that Becker's formulation requires a modification to incorporate noise. The importance of accuracy in contour areas and shapes at each airport for accurate population exposure counts further implies that this formulation should not simply be centered around aggregated fleet results but rather should focus on accuracy at *each* airport. This airport-level characterization was suggested in Equation (17) which defined the accuracy of a generic vehicle model across a subset of airports, where the errors for each metric at each airport sample in the subset are combined into a *distribution* of errors.

Becker has already demonstrated that an average generic vehicle approach provides better fleet-level accuracy than a traditional representative vehicle approach for fuel burn and NO_x emissions, and the linear equations for these metrics suggest that the method should work similarly for an airport-level formulation. The second hypothesis proposes that this also holds for the DNL noise contours:

Hypothesis 2: *A fleet of average generic vehicles will more accurately approximate the DNL 65-dB noise contours across a subset of airports as compared to a traditional representative-in-class approach.*

The complexities of the noise calculations prevent this hypothesis from being accepted strictly from mathematical arguments, and thus experimentation is required. This hypothesis shall be tested in a similar manner as Becker's previous formulation. The cumulative noise contour areas from both the representative-in-class approach and the average generic vehicle approach shall be quantified and compared against a set of airport-level targets using actual vehicles. The representative-in-class vehicles shall be defined using traditional seat-class[3] designations and choosing the vehicle in

---

[3]For the purposes of this study, seat class refers specifically to the CAEP/8 definitions as listed in Table 8 [60].

each seat class with greatest prevalence in the operational schedules. As mentioned in the previous section, the generic vehicle approach will be repeated for both seat-class and the proposed vehicle-class groupings. The accuracy of each approach will be evaluated with respect to *each* airport in addition to the cumulative results across the entire subset.

2.3.3   Airport Operational Complexities

Once the vehicle classes and the target airports are established, a series of validation tests must be defined for benchmarking the best average generic vehicle designs. The airport-level characterization requires these tests to account for different factors that contribute to the variability of the airport-level results, with target aggregate metrics generated from the combination of vehicle-level performance of the constituent vehicles linked to frequency weightings from the baseline operational schedules *at each airport*. These airport-level results depend on many different operational complexities, which motivates the following research question:

RQ 3: Given the unique operations and mission specifications associated with each airport, can the generic vehicles still balance accuracy across a subset of airports?

For this work the stochasticity of atmospheric conditions and airport-specific diverging ground tracks have been removed to enable rapid noise calculations. However, each airport still features unique operational distributions, trip-length distributions, operational volumes, and infrastructures. The fuel burn and NO_x emissions relationships to these operational complexities can be readily understood from simple examination of Equation (16) which is a linear equation that is weighted by operational frequencies. As mentioned previously, vehicle-level performance for

these metrics typically vary quadratically with mission range. Furthermore, the fuel burn and NO_x emissions do not depend on the airport infrastructures (assuming standard day atmospheric conditions and no diverging ground tracks). It can be reasoned that the airport-level error for these metrics can be minimized by matching the vehicle-level performance of each average generic vehicle to a weighted average of the actual vehicle operations at each airport.

For the noise contours, the relationship to these operational complexities is not as clear. This is due to the spatial nature of noise propagation and attenuation which features unique SEL contour sizes and shapes for each vehicle in the fleet. Each unique stage-length mission is modeled using a different takeoff weight. This modifies the climb-out trajectory which impacts the lengths of the SEL contours. The noise metrics also use logarithmic summations, and thus the frequency of operations by each unique vehicle and each class type cannot be clearly mapped to the airport-level metric, especially given the spatial distribution of noise introduced by each unique airport runway layout. Determining how each of these operational complexities impacts the airport-level noise metrics requires investigation through simulation-based experiments. Of all of these complexities, however, the per class operational distributions capture the frequency-weighted variability *within* each class, and thus it is anticipated to be the most important factor for selecting the average generic vehicle input parameters. This leads to the following hypothesis:

Hypothesis 3: *If the operational distributions of each vehicle class across a subset of airports can be isolated from other operational complexities, the average generic vehicle that minimizes the mean error for the DNL noise contours across the subset of airports will also minimize the error at each airport when all of these operational complexities are reintroduced.*

Once again, the justification for this hypothesis can be derived from simple probability theory and Equation (17). By isolating the error distributions for each class (ϵ_i) and minimizing the mean error for each (μ_{ϵ_i}), the combined classes should also minimize the airport-level mean error. The additional operational complexities can be thought of as adding variance to the target metrics across the different airports. Given that the generic fleet will operate under the same trip-length distributions, operational volume, and airport infrastructures as the actual target fleet, it can be assumed that the variance of the generic fleet performance will expand to match the additional variance of the target metrics. Thus, the operational distributions of the constituent vehicles in each class at each airport should ultimately define the average generic vehicles. To test this hypothesis, a series of validation tests with sequentially increasing complexity shall be formulated in an effort to first decouple the mean and variances of the error distributions. Sequentially increasing the complexity of the validation tests enables traceability for each source of operational complexity.

One challenge for these generic vehicle tests is the need to optimize multiple metrics simultaneously, which suggests that there is not one solution but rather a series of Pareto optimal solutions [91]. Adding to this challenge is the fact that these metrics are measured on different scales, and thus the optimization problem must be formulated in a manner that maps multiple objectives to a single objective function without biasing the generic vehicles towards accuracy in one metric over another. This type of mapping is often referred to as *scalarization*, and typically makes use of value or *desirability* functions which convert the objective of minimizing each objective function to a goal of maximizing an *overall desirability* across all of the objectives simultaneously. This conversion allows for the use of conventional single-objective optimization routines for a multiple objective optimization problem.

70

2.3.4 Methods for Calculating Population Exposure

All airport-level noise analysis included in this research shall use ANGIM, but this method currently lacks a capability for calculating population exposure counts around the airport. Airport noise exposure studies typically use either Census-block centroids or specific population receptor points as defined by a user [72]. In common practice, Census data are intersected with buffers of influence (such as DNL contours) using two primary approaches to quantify population at risk [92]:

1. Tally the entire population (if the centroid is inside the buffer) or zero population (if the centroid is outside the buffer)

2. Use an area weighted population accounting approach (based on the ratio of the areas of the polygon included in and excluded from the buffer).

The homogeneous population distributions assumed by the area-weighted method, unfortunately, seldom occur in the real world [93]. However, analytical approaches that use Census polygon centroids to represent population are likely to produce results containing substantial errors [92]. By assuming the population is concentrated at these receptor points, DNL decibel levels need only to be calculated at these centroid points instead of calculating an entire grid of receptor points as is required for visualizing the DNL contours. This saves some computation time, but the drawback of this method is that there is a mismatch between the Census block centroids contained within a contour and the Census blocks actually intersected by the contour, as is demonstrated in Figure 22. Additionally, using this approach is overly discretized and does not allow a continuous reduction in the extent of a DNL contour to map to a continuous reduction in population exposure counts. It is preferable that the spatial representation features continuous variability.

Thus rather than using the discrete centroids, the area-weighted population approach should be utilized on Census-block data with the justification that the
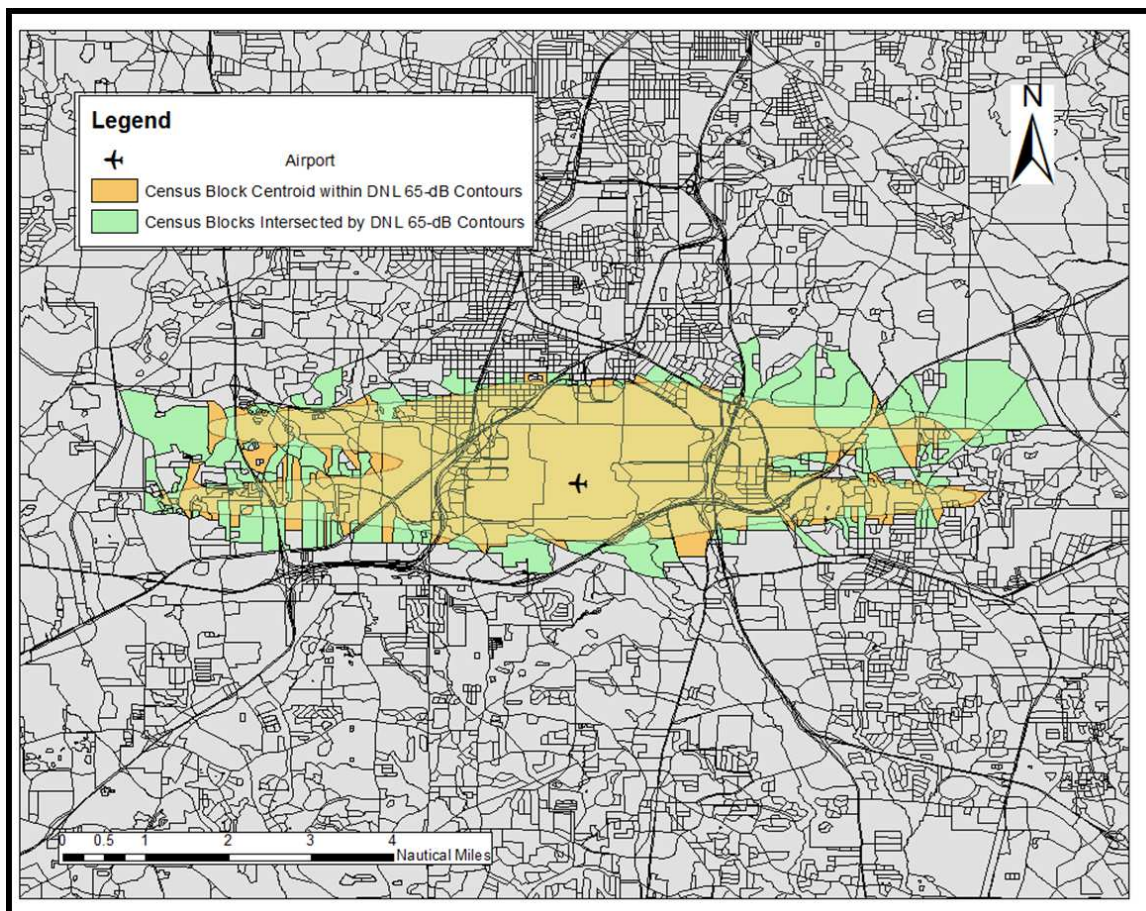
Figure 22: Drawbacks of Polygon Centroid Population Methods

high-resolution associated with this smallest areal unit of population data shall minimize the potential error associated with the assumption of uniform population distribution. More advanced techniques such as pycnophylactic interpolation or areal interpolation with the incorporation of ancillary data could be used, but given the complexity of these methods compared to the intended use of this Census-block data for a screening-level tool, the basic area-weighted approach benefits from its relative simplicity [93].

ANGIM has the ability to compute airport DNL grids as well as DNL contours for a given spatial reference setting the first primary runway brake-release point at the (0,0) grid point. These grids are currently set to a very fine grid-resolution of 0.08-nmi, and contours contain spatial data referenced to this brake-release point.

Thus if the brake-release point can be mapped to the actual geographical coordinates, the entire grid and the contours can also be mapped to geographical coordinates. Contour polygons can be defined in a GIS program such as ArcGIS®, and these contours can be overlaid with Census-block data to calculate population exposed to significant noise. However, it can be data intensive and time consuming to import contours for every potential scenario into ArcGIS® for performing these population exposure counts. One of the objectives of this research is to enable rapid noise computation models like ANGIM to include a screening-level analysis of population exposure counts. The generated contours from ANGIM must be linked to this Census block data in some other manner than calling a Geographical Information System every time a new scenario is calculated. This leads to the following research question:

RQ 4: How can assessment of community exposure to significant noise be accounted for in a rapid airport-level noise computation model?

The population method proposed in this work balances the computational benefits of the centroid method with the better assumption of uniform population distribution within the Census blocks. This shall be accomplished by mapping population data around airports to grid points corresponding to the resolution of noise analysis in ANGIM. The data can be exported from ArcGIS® through a one-time pre-processing and stored in ANGIM for rapid calculation of population exposure counts. This method will be discussed in more detail in Chapter 3.

2.4 Summary of Research Questions and Hypothesis Statements

Four research questions and three hypothesis statements were introduced in this chapter. They are repeated here for convenience with a brief summary of new formulations and methods that must be introduced to answer each research question:

RQ 1: What parameters should be used to classify aircraft into generic vehicle groups?

Hypothesis 1: A per-class average generic fleet of vehicles defined by vehicle-class groupings based on similarities in the environmental performance metrics will feature superior fleet-level accuracy compared to a per-class average generic fleet of vehicles defined by traditional seat-class groupings.

Research question 1 and the corresponding hypothesis statement suggest that classifying aircraft based on internal seat layouts introduces unnecessary per class variance with respect to each of the vehicle-level performance metrics. Instead, the vehicles should be classified using a multiclass classification method that leverages the vehicle-level performance metrics for class assignments with the goal of minimizing per class variance. Minimizing the variance within each class should lead to improved fleet-level accuracy for the combined generic fleet.

RQ 2: Given that noise is an airport-level metric, how can it be incorporated into the average-generic vehicle formulation?

Hypothesis 2: A fleet of average generic vehicles will more accurately approximate the DNL 65-dB noise contours across a subset of airports as compared

to a traditional representative-in-class approach.

Research question 2 and the corresponding hypothesis statement suggest that Becker's average generic vehicle methodology can be extended to capture fleet-level noise in addition to fuel burn and NO_x emissions. However, the airport-dependent nature of the noise metrics requires the fleet-level problem to be characterized differently than in Becker's original formulation. This modified characterization of the fleet-level problem shall focus on accuracy at *each* airport in addition to minimizing cumulative error.

RQ 3: *Given the unique operations and mission specifications associated with each airport, can the generic vehicles still balance accuracy across a subset of airports?*

Hypothesis 3: *If the operational distributions of each vehicle class across a subset of airports can be isolated from other operational complexities, the average generic vehicle that minimizes the mean error for the DNL noise contours across the subset of airports will also minimize the error at each airport when all of these operational complexities are reintroduced.*

Research question 3 and the corresponding hypothesis statement suggest a need for a series of validation tests with sequentially increasing operational complexity. In this manner, the influence of each level of complexity on noise computations across the subset of airports can be traced, but it is anticipated that the simplest formulation will suffice for optimizing the generic vehicle input parameter settings. This simpler formulation reduces the complexity of the multiobjective optimization problem for simultaneous accuracy in multiple metrics with potentially competing trends. Scalarization through the use of desirability functions allows for the use of

traditional single-objective optimization techniques on the multiobjective problem.

RQ 4: *How can assessment of community exposure to significant noise be accounted for in a rapid airport-level noise computation model?*

While Bernardo's rapid airport-level noise computation model provides a good compromise between fidelity and computational speed, in its current form it lacks a capability for rapidly computing community noise exposure in terms of population counts within the DNL contours. Area-weighted population accounting allows for the spatial representation of noise exposure to feature continuous variability, but importing georeferenced contour shapefiles into a Geographical Information System to calculate these area weightings is computationally inefficient. A method that maps population data to a grid of equal resolution to the noise computation model would allow for quick calculations of exposure counts while still allowing the continuous variability associated with area-weighted population accounting.

CHAPTER III

PROBLEM FORMULATION AND TECHNICAL APPROACH

Becker's methodology is posed as an equivalent optimization problem, but the computational expense introduced by including noise in the generic vehicle formulation requires a modification of his methodology. Exhaustive design space exploration for a high-fidelity vehicle-level model is impractical, and instead surrogate-based optimization techniques are proposed to exchange fidelity for computational speed.

Fleet classification into generic vehicle classes is accomplished through discriminant analysis, and the characterization of generic vehicle accuracy is reformulated as distributions of relative errors for each metric across a subset of airports. The distributions are characterized by the mean and the variance of these relative errors. Optimization of the generic vehicles is accomplished through a simplified test structure that decouples the mean and the variance such that the ideal generic vehicle matches the airport average for each target metric simultaneously. The generic vehicles can then be characterized by a single output for each metric, which allows for the construction of surrogate models mapping vehicle-level input parameters to airport-level metrics. Multiobjective optimization is accomplished by mapping each metric to desirability functions on a zero-to-one scale and combining these functions into an overall desirability score that is the geometric mean of the individual desirabilities. This overall desirability represents a single objective which enables the use of traditional optimization techniques.

Subsequent tests that reintroduce operational complexities no longer feature the

convenience of a single-output per metric, and thus the surrogate models can no longer be used. For these tests, only a subset of best generic vehicle alternatives from previous tests are carried forward and evaluated against each other using multicriteria decision making techniques. Finally, a grid-based method is introduced for pre-calculating population counts using Voronoi tessellation, intersections with 2010 Census block polygons, and area-weighted equations. This method requires a one-time pre-processing of population distributions at each airport to allow for instantaneous calculations of population exposure for any noise computations at these airports.

3.1 Modification of Average Generic Vehicle Methodology

The steps in Becker's methodology successfully identified input parameter settings for the best per class average generic vehicles, but his approach depended on design space exploration and enumeration of many alternatives. While Becker attempts to exhaustively explore the vehicle-level parameter design space to observe the impacts on each metric simultaneously, his approach could have been formulated as a mathematical optimization problem. The goal is to minimize the magnitude of the relative error with respect to targets generated from the actual fleet, as shown in Equation (18):

$$\underset{X_i}{\text{minimize}} \ f(X_i) = \eta_Y = \left| \frac{Y_{GV} - Y_{Target}}{Y_{Target}} \right| \tag{18}$$

Where:

X_i = Input parameter settings for i^{th} generic vehicle class

η_Y = Magnitude of relative error for metric Y with respect to targets

78

$$Y_{GV} = \text{Fleet-level aggregated metric for fleet of generic vehicles}$$

$$Y_{Target} = \text{Fleet-level aggregated target metric for actual fleet}$$

The input parameters in the physics-based model for each generic vehicle class (X_i) are selected in a manner that minimizes the fleet-level error for each metric. This optimization problem must be conducted for all of the metrics simultaneously, but each generic vehicle class can be optimized independently. For Becker's problem, computations of vehicle-level fuel burn and NO_x emissions for each alternative are computationally inexpensive which enables brute force exploration of the entire design space. The vehicle-level results for each alternative are very simply mapped to fleet-level results as a function of flight distances and number of operations, and thus the fitness of every alternative can quickly be determined and filtered to identify the input parameter settings that simultaneously balance fitness across all metrics.

The addition of noise analysis prohibits this brute force approach due to the increased computation time associated with noise grids. A modification of Becker's method is thus required that still enables exhaustive design space exploration with reasonable computation times, but also leverages optimization techniques. Conventional optimization algorithms often require many objective function calls per run. As modeling and simulation capabilities and the corresponding computational expenses have increased in recent years, there has been a recent push in academics and industry towards surrogate-based optimization (SBO) techniques. These SBO techniques replace direct optimization of expensive high-fidelity models with iterative refinement and reoptimization of a coarser low-fidelity model that is less computationally demanding [94]. The most popular surrogate models are polynomial response surfaces, kriging, support vector machines, space mapping, and artificial neural networks [95]. The optimal alternatives from the low-fidelity model can

79

always be verified in the high-fidelity model regardless of the choice of surrogate, but the use of the surrogate avoids the unnecessary expense associated with computing intermediate alternatives in the high fidelity model that fall between the initial guess and the final convergence of the optimizer.

These SBO techniques represent another method of exchanging fidelity for computational speed. To include noise in the generic vehicle methodology, Becker's approach should be modified to leverage these low-fidelity models. The steps for this modified methodology are as follows:

1. Calculate targets representing the aggregate performance per generic vehicle class for each environmental metric of interest.

2. Conduct effect screening to determine which input parameters are in fact the most influential on the relevant vehicle-level metrics.

3. Create designs of experiments from the *reduced* set of influential input parameter settings.

4. Evaluate the designs of experiments in the high-fidelity vehicle-level model and collect the metric performance for each alternative.

5. Create surrogate models that map these metrics to a fitness function leveraging multicriteria decision making techniques to identify alternatives that best match the metric targets.

6. Optimize the input parameter settings using the surrogate model.

7. Verify the optimized input parameter settings through evaluation in the high-fidelity model and comparison against fleet-level targets.

The first few steps are identical to Becker's methodology, but the use of surrogate models, multicriteria decision making, and optimization constitute new approaches

that are necessitated by the additional computational expense associated with noise analysis. This new methodology also differs from Becker's in the statistical approach to aircraft classification, the airport-level characterization of the problem, and the operational simplifications necessary to enable the surrogate-based optimization.

3.1.1 Multiclass Classification Method for Generic Vehicles

Previous methods for fleet classification have relied on one or two metrics (payload and range) to assign aircraft to groups. While these metrics can delineate aircraft that fly similar route types, this does not serve to minimize the performance variance within a group. To accomplish this, the classifications must be defined using a vector of the actual performance metrics.

There are a wide variety of multiclass classification methods in the literature. Some of these methods are extensions of more classical binary classification problems, including neural networks, decision trees, and k-nearest neighbors. In some cases, the multiclass problem can be converted into a set of binary classification problems with traditional methods like support vector machines. An example of a more traceable method designed specifically for the multiclass problem is hierarchical clustering. Hierarchical clustering techniques begin with every aircraft assumed to be its own cluster, and at each step the two closest clusters are joined, reducing the total number of clusters by one [90]. This method is highly dependent on its sequential nature, does not give any indication as to when to stop the groupings, and does not take advantage of heuristic understanding of what these groups should approximately look like.

For this work a technique referred to as linear discriminant analysis is suggested. Discriminant analysis is a method for predicting misclassifications among a priori groups of multivariate observations [96]. The method is built on linear algebra, principal component analysis, and multi-response permutation tests. The math for

discriminant analysis is complicated, but the basic steps for the context of the aircraft classification problem are as follows:

1. Collect performance metrics for every unique aircraft in the fleet and assign each to a class (a priori group).

2. For each aircraft, perform a "leave-one-out" cross-validation method where the aircraft is removed from the analysis, and must be allocated to a group as if it were a new observation.

3. Define a set of canonical axes that are linear combinations of the performance metrics that best distinguish the different a priori groups (minus the removed aircraft).

4. Calculate the Euclidean distance in the canonical space between the "new" observation and the centroids of each of the groups to determine the probability of classification in each group.

5. Repeat for every aircraft and determine which are correctly classified and which may be misclassified.

6. Reassign any misclassified aircraft to the appropriate group and repeat the process until there are no more misclassifications.

A notional canonical plot of the top two canonical variables is demonstrated in Figure 23. This example is for a representative problem included as part of the statistical software JMP$^{\text{TM}}$, but it visually demonstrates how discriminant analysis works. The example defines three groups using four descriptive variables. Canonical variables are constructed through linear combinations of the four variables with standardized coefficients for each. The standardized coefficients are used to offset differing scales among the variables [97]. The first canonical variable is the most

discriminating, meaning that the centroids between the different groups are spread out as much as possible in terms of variance. In this way, defining the canonical or discriminant variables amounts to finding principal component subspaces of the group centroids themselves [98].
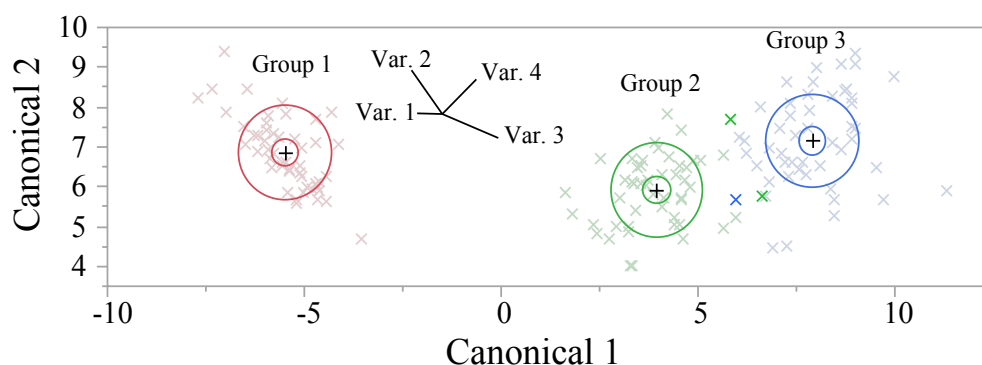
Standardized Scoring Coefficients

	Var. 1	Var. 2	Var. 3	Var. 4
Canonical 1	-0.426955	-0.521242	0.9472572	0.5751608
Canonical 2	0.0124075	0.7352613	-0.401038	0.5810399

Counts: Actual Rows by Predicted Columns

	Group 1	Group 2	Group 3
Group 1	50	0	0
Group 2	0	48	2
Group 3	0	1	49

Discriminant Scores

Row	Actual	Square Dist.	Probability	-Log(Prob)			Predicted	Prob(Pred)	Others
71	Group 2	8.66970	0.2532	1.373		*	Group 3	0.7468	
73	Group 2	4.87619	0.8155	0.204			Group 2	0.8155	Group 3: 0.18
78	Group 2	4.66698	0.6892	0.372			Group 2	0.6892	Group 3: 0.31
84	Group 2	8.43926	0.1434	1.942		*	Group 3	0.8566	
120	Group 3	8.19641	0.7792	0.249			Group 3	0.7792	Group 2: 0.22
124	Group 3	3.57858	0.9029	0.102			Group 3	0.9029	
127	Group 3	3.90184	0.8116	0.209			Group 3	0.8116	Group 2: 0.19
128	Group 3	3.31470	0.8658	0.144			Group 3	0.8658	Group 2: 0.13
130	Group 3	9.08495	0.8963	0.109			Group 3	0.8963	Group 2: 0.10
134	Group 3	7.23593	0.2706	1.307		*	Group 2	0.7294	
135	Group 3	15.83301	0.9340	0.068			Group 3	0.9340	
139	Group 3	4.09385	0.8075	0.214			Group 3	0.8075	Group 2 0.19

'*' indicates misclassified

Figure 23: Notional Canonical Plot for Discriminant Analysis

As can be seen, some of the color-coded groups are well defined by these two

83

canonical variables, but other groups overlap so closely that there is a greater possibility of misclassification. The small circles represent 95% confidence intervals for the group centroids, and the larger circles contain 50% of the members in each group. The closer these circles are to each other in the canonical plot, the poorer the distinction between the groups and the higher likelihood of misclassification. In the discriminant scores table, the probability of misclassification is reported as well as the most likely class assignment. If the probability of assignment to another class is greater than the probability of assignment to the a priori class, then that alternative becomes a candidate for reclassification. The discriminant analysis must be repeated after reclassification because these canonical variables and the resulting canonical plots change with each iteration.

This method was chosen due to the advantage of pre-defining the number of groups (the six vehicle classes) and the ability to leverage heuristic knowledge of competitive aircraft with similar physical and performance characteristics for the a priori assignments. The heuristics allow for a good starting guess such that the method converges in only a few iterations, and the method is built on traceable statistical analysis aimed at reducing in-class variance with respect to the performance metrics.

3.1.2   Airport-Level Characterization

The optimization problem posed in Equation (18) characterizes the fleet-level performance of the generic vehicles for each metric as a single aggregate value compared against a single aggregate target. Research question 2 and the corresponding hypothesis dictate a need for accuracy at *each* airport, which implies that generic vehicle performance cannot be characterized by single aggregate metric values but rather by distributions of metric values across a subset of airports. The

fitness of a particular generic vehicle model must be evaluated by comparing against target metrics at each airport. This can create difficulties when trying to implement optimization techniques which typically require a single objective function.

One common approach for evaluating model accuracy across multiple sample values is the use of root mean squared error (RMSE). When comparing two data sets (one set from theoretical prediction and the other from actual measurement), the RMSE of the pairwise differences of the two data sets can serve as a measure of how far on average the error is from zero [99]. In the context of the generic vehicle problem, RMSE across a subset of n airports is defined as follows:

$$RMSE = \sqrt{\frac{1}{n} \sum_{a=1}^{n} \left(Y_{GV,a} - Y_{Target,a}\right)^2} \qquad (19)$$

Where:

$Y_{GV,a}$ = Aggregated metric for fleet of generic vehicles at unique airport a

$Y_{Target,a}$ = Aggregated target metric for actual fleet at unique airport a

While RMSE represents a single value for optimization, it is a scale-dependent measure [100]. Given that the optimization problem actually includes multiple metrics each with different scales, it becomes difficult to compare RMSE between metrics or to formulate a multiobjective optimization problem that isn't biased towards a specific metric. Becker used relative error to avoid this bias, but for the airport-level formulation relative error must be defined on a per-airport basis. The distribution of relative error for each metric can then be characterized by the mean and variance of this relative error across the subset of airports as shown in Equation (20):

$$Y_{GV,a} = f\left(X_{RJ}, X_{SSA}, X_{LSA}, X_{STA}, X_{LTA}, X_{VLA}\right)$$

$$\eta_{a,Y} = \frac{Y_{GV,a} - Y_{Actual,a}}{Y_{Actual,a}}$$

$$\mu_Y = \frac{1}{n}\sum_{a=1}^{n}\eta_{a,Y} \tag{20}$$

$$\sigma_Y^2 = \frac{1}{n}\sum_{a=1}^{n}\left(\eta_{a,Y} - \mu_Y\right)^2$$

Where:

X_i = Input parameter settings for i^{th} generic vehicle class

$\eta_{a,Y}$ = Relative error for metric Y at unique airport a

μ_Y = Mean error for metric Y across subset of airports

σ_Y^2 = Variance of error for metric Y across subset of airports

This characterization measures the generic vehicle performance for each metric on a common scale, but each metric is represented by two measurements (mean and variance) instead of one. In principle, the RMSE for the relative errors, $\eta_{a,Y}$, could be used for optimization of a single value per metric, but the relative errors at smaller airports tend to be magnified relative to the larger airports due to smaller target values in the denominator. Thus, this approach would unnecessarily bias the optimization towards better accuracy at smaller airports.

Instead, a multi-tiered approach is proposed where first the variance and then the mean of these relative error distributions are minimized. The variance within a class shall be minimized through the previously discussed statistical classification of the actual fleet into performance-based vehicle classes. The mean error for each

86

metric across the subset of airports shall then be minimized by optimizing the input parameter settings for each generic vehicle model.

3.1.3 Method for Optimization of Average Generic Vehicles

Once the aircraft are assigned to the appropriate vehicle classes, a series of validation tests must be formulated to trace the different sources of operational variability. The test structure outlined in Table 10 sequentially adds more complexity such that the impact of each can be independently understood.

Table 10: Average Generic Vehicle Test Specifications

Test ID	Distributions	Mission Lengths	Operational Volumes[1]	Runway Layouts[2]
A	Isolated Classes	Most Common Stage-Lengths	2000 Ops per airport	Single Runway
B	Isolated Classes	Discretized Stage-Lengths	2000 Ops per airport	Single Runway
C	Combined Classes	Discretized Stage-Lengths	2000 Ops per airport	Single Runway
D	Combined Classes	Discretized Stage-Lengths	Actual Airport Volumes	Single Runway
E	Combined Classes	Discretized Stage-Lengths	Actual Airport Volumes	Actual Runways
F	Combined Classes	Discretized Stage-Lengths	Randomly Scaled Ops	Actual Runways

[1] Assumes 50% split between approach and departure operations
[2] Assumes uniform runway utilization with cross-flow

Test A is formulated to isolate the impact of the operational distributions of the constituent vehicles within each of the vehicle classes. Each vehicle class is tested

separately, so Test A actually comprises multiple tests. For each of the Test A class tests, it is assumed that all of the operations at each airport consist only of the relevant class being tested. The only source of variability in the target metrics from airport to airport is due to the percent distributions of each constituent vehicle within the class. The advantage of this formulation is that each of the generic vehicle alternatives is characterized by a single value for each metric. For a given metric, the quantity $Y_{GV,a}$ is identical for each unique airport a because the generic vehicle is allotted all of the scheduled flights, whereas the quantity $Y_{Target,a}$ is unique for each unique airport a. As a result, the relative error distributions for each metric calculated using Equation (20) feature identical variance for each generic vehicle alternative. The objective can now be simplified to minimizing the mean relative error for each metric.

A mean relative error of zero corresponds to the case when the generic vehicle performance matches the average target metric across the subset of airports (with respect to the Test A specifications). This ideal generic vehicle performance with respect to a given metric is represented in Equation (21):

$$Y_{GV,ideal} = \mu_{Target} = \frac{1}{n} \sum_{a=1}^{n} Y_{Target,a} \tag{21}$$

Where:

$Y_{GV,ideal}$ = Aggregated airport-level metric for ideal generic vehicle model

μ_{Target} = Average target metric for actual fleet across a subset of airports

$Y_{Target,a}$ = Aggregated target metric for actual fleet at unique airport a

This formulation makes the optimization problem much more tractable because the input parameter settings for each generic vehicle model can be mapped to a

88

single value per airport-level metric ($f(X_i) \rightarrow Y_{GV}$), enabling the use of surrogate models. There are many potential choices for surrogate models, but artificial feed-forward neural networks are suggested given the unknown functional forms relative to the input parameters. A neural network is a two-stage regression model typically represented by a network diagram as shown in Figure 24:
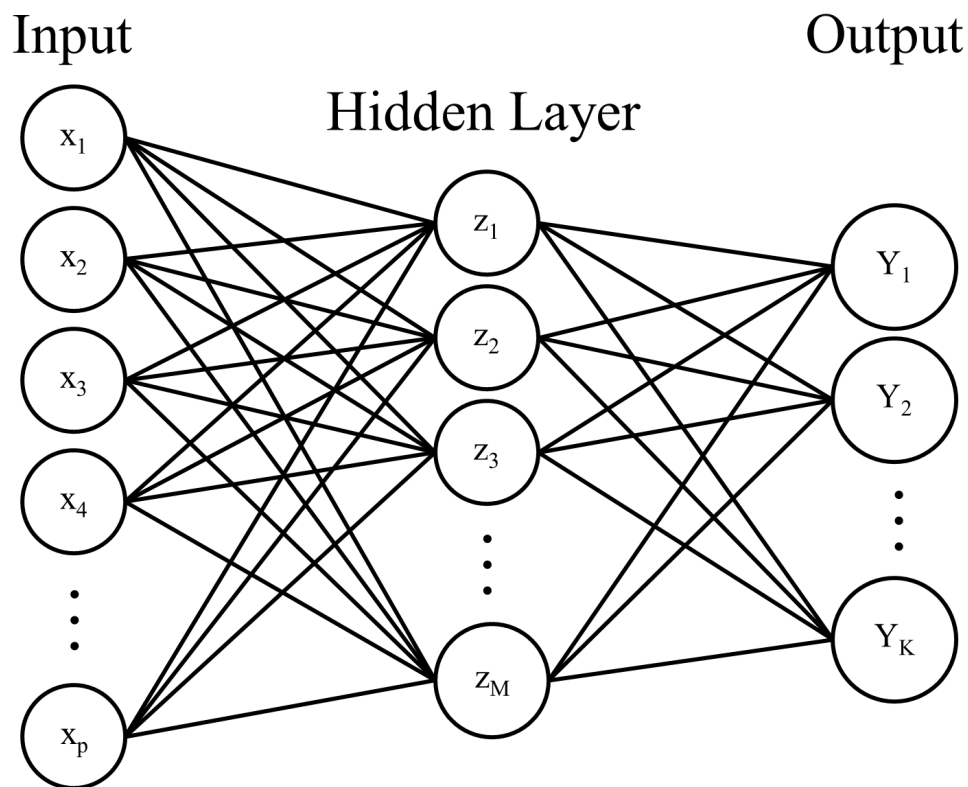
Figure 24: Diagram of Feed-Forward Neural Network

Derived hidden nodes, z_m, are created from linear combinations of the input parameters fed into an activation function, $\phi(v)$. The activation function is typically a sigmoid function ($\phi(v) = \frac{1}{1+e^{-v}}$), but other activation functions are possible. Then each metric, Y_k, is modeled as a function of linear combinations of the hidden nodes as shown in Equaation (22) [98].

89

$$z_m = \phi \left(\alpha_{0m} + \alpha_m^T X_i \right), \, m = 1, ..., M$$
$$Y_k = \beta_{0k} + \beta_k^T Z, \, k = 1, ..., K \tag{22}$$

Where:

z_m = Derived function for m^{th} hidden node

ϕ = Activation function (sigmoid)

α_m = Vector of linear weights applied to inputs for m^{th} hidden node

X_i = Vector of input parameter settings for i^{th} generic vehicle class

M = Total number of hidden nodes

Y_k = Output unit for k^{th} metric

β_k = Vector of linear weights applied to hidden nodes for k^{th} metric

Z = Vector of hidden nodes

K = Total number of metrics

The number of hidden nodes is flexible, but for model accuracy it is better to have too many than too few [98]. More hidden nodes, however, require more iterations for training the models, and they can also be more computationally expensive function calls when used with an optimizer. Thus, as always, fidelity and speed must be balanced. The unknown parameters in Equation (22) are the weights applied to the input parameters (α_m) and the weights applied to the hidden nodes (β_k). These unknowns are determined by sufficiently sampling the high-fidelity model, using a majority of the samples as training data and reserving some samples for validation. Sum of squared errors with respect to the actual outputs from the high-fidelity model

are used as a measure of fit with respect to both training and validation data, as is common for regression models.

The network diagram in Figure 24 shows the input parameters mapped to multiple metrics, and the ideal generic vehicle must satisfy Equation (21) for all of these metrics simultaneously. Given the different scales for the different metrics, scalarization is necessary. This can be accomplished by defining "desirability functions" for each metric such that each metric is mapped to a common scale. The ideal metric value from Equation (21) should map to a maximum desirability. The further the performance of the generic vehicle alternative strays from this ideal, the lower the desirability score. A notional example of a desirability function is shown in Figure 25:
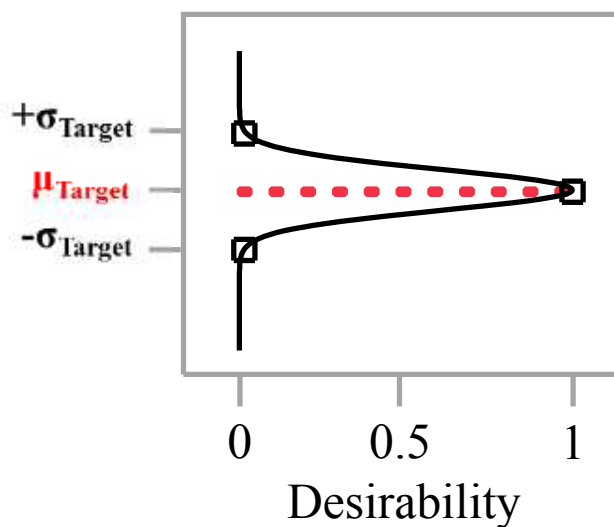
Figure 25: Notional Desirability Function for Generic Vehicle Target

The desirability function in Figure 25 resembles a Gaussian curve. The peak of the curve coincides with the mean of the target distribution, as defined in Equation (21), and maps to a maximum desirability score of one. In this example, the bounds of the desirability function are set by the standard deviations of the target metrics. In this manner, if the deviation of the generic vehicle performance from the ideal is greater than the standard deviation observed for the target metrics across the subset

of airports, the generic vehicle alternative is assigned a desirability score of zero. By formulating the desirability functions in this manner, each metric can be mapped to a common scale with each desirability function normalized by the existing variation across the subset of airports. This mapping assumes a uniform weighting for the importance of each metric, but practically other weightings could be explored by adjusting the bounds of each desirability function. Wider bounds implies a greater tolerance of error for a given metric, whereas narrower bounds implies a requirement for greater accuracy.

With each metric mapped to a common scale, the desirability scores can be combined to define a single-objective. An arithmetic mean of the individual desirability scores would provide a single-objective, but this formulation could potentially over-value a generic vehicle alternative that balances very bad accuracy in one metric with very good accuracy in another. Instead, an overall desirability score that is the geometric mean of the individual desirability scores is proposed. The geometric mean is less forgiving to generic vehicle alternatives that struggle for any one metric. Thus, the optimization problem can now be posed in terms of maximizing this overall desirability, as shown in Equation (23):

$$
\underset{X_i}{\text{maximize}} \quad D = \sqrt[k]{\prod_{j=1}^{k} d_j}
$$

$$
\text{such that} \quad \min BPR_i \leq BPR_{X_i} \leq \max BPR_i \tag{23}
$$

$$
\min OPR_i \leq OPR_{X_i} \leq \max OPR_i
$$

$$
\min Thrust_i \leq Thrust_{X_i} \leq \max Thrust_i
$$

Where:

X_i = Vector of input parameter settings for i^{th} generic vehicle class

92

$$d_j = \text{Desirability score for } j^{th} \text{ metric}$$

$$D = \text{Overall desirability score (geometric mean of metric desirabilities)}$$

$$BPR_i = \text{Vector of bypass ratio values in } i^{th} \text{ generic vehicle class}$$

$$OPR_i = \text{Vector of overall pressure ratio values in } i^{th} \text{ generic vehicle class}$$

$$Thrust_i = \text{Vector of sea-level static thrust values in } i^{th} \text{ generic vehicle class}$$

$$BPR_{X_i} = \text{Generic vehicle bypass ratio as } f(X_i)$$

$$OPR_{X_i} = \text{Generic vehicle overall pressure ratio as } f(X_i)$$

$$Thrust_{X_i} = \text{Generic vehicle sea-level static thrust as } f(X_i)$$

Equation (23) also subjects the input parameter settings to constraints on the final engine design. The purpose of these constraints is to ensure that the generic vehicle actually resembles the constituent vehicles within its class. If the optimizer were unconstrained, it could potentially find input parameter settings that match the target metrics but with infeasible engine designs. Technologies applied to this baseline generic vehicle with infeasible engines might lead to unrealistic or misleading levels of improvement. The constraints bound the OPR, BPR, and sea-level static thrust of the generic vehicle by the range of values observed for the constituent aircraft within the class.

The optimization problem shall be executed on the surrogate models, but results must be verified in the high-fidelity model. Even the most accurate surrogate model is still an approximation of the actual model, so the best input parameter settings from the optimization may not be as fit once verified in the high-fidelity model. Furthermore, the optimization is performed with respect to the Test A specifications, but the resulting generic vehicles must also be validated against each of the subsequent test specifications. Thus the goal of the optimization should not be to find a global

maximum of overall desirability for each generic vehicle class, but rather to populate a subset of fit alternatives for each class.

To accomplish this, Monte Carlo simulations should be used to broadly explore the design space and identify promising combinations of the input parameter settings. The surrogate models make these simulations computationally cheap such that the space can be explored at a high resolution. Thousands of input parameter settings can be instantaneously evaluated and ranked by overall desirability score. Only the top ranking alternatives need to be verified in the high-fidelity model, but it is anticipated that equally good or possibly better input parameter settings exist nearby in the design space. A focused design of experiments that slightly perturbs the input parameter settings around the top few alternatives from the Monte Carlo simulations on the surrogate models should be able to identify these potentially better alternatives.

3.1.4 Multicriteria Decision Making (MCDM)

Test A decouples the mean and the variance to enable the single-output formulation of the generic vehicle problem, but each of the successive tests does not feature this decoupling. Thus, the surrogate-based optimization approach can only be applied for Test A. Hypothesis 3 suggests that the best alternatives from Test A will still perform well for each of the subsequent tests, but for Tests B-F each alternative must be evaluated against each other which requires a comparison of error distributions for multiple metrics. Thus, a decision making technique is required that can evaluate multiple criteria each defined by distributions as opposed to single values.

In practice, any MCDM technique that meets this requirement can be used, but for this work Stochastic Multicriteria Acceptability Analysis (SMAA) was chosen. The technical approach does not hinge on this specific method, and thus only a brief

94

description is included here. A more detailed discussion of SMAA is included in Appendix A. Not only can this method accept distributions for each criterion, it also doesn't require preference information. Most MCDM techniques take preference information from a decision maker and evaluate alternatives with respect to these weightings. SMAA is described as an *inverse* multicriteria decision *aiding* technique, meaning the method provides descriptive measures for each alternative as opposed to simply ranking the alternatives. This is accomplished by evaluating multidimensional integrals with respect to the weight space and the criteria distributions to explore how each alternative may be ranked given different preferences for each metric, thus providing a decision maker with more detail and transparency.

The best alternatives from Test A and the perturbed design of experiments shall be evaluated against each other with respect to Test B specifications. A handful of the best alternatives from each generic vehicle class with respect to Test B shall be down-selected and carried forward for Tests C-F. These combined class tests shall compare full-factorial fleet combinations of the most fit alternatives from each class, once again using this SMAA formulation.

3.1.5 Summary of Approach to Generic Vehicles

Becker's original average generic vehicle methodology shall be modified to leverage surrogate-based optimization techniques. The performance variance within each generic vehicle class is minimized using discriminant analysis, and the generic vehicle optimization problem is characterized by minimizing the mean error across the subset of airports. Operational simplifications allow the vehicle-level input parameter settings for each generic vehicle class to be mapped to airport-level metrics, which enables the construction of surrogate models for each metric. Mappings of these output metrics to desirability functions reduces the multiobjective optimization

problem to a more tractable single-objective of maximizing the overall desirability score. Monte Carlo simulations on the surrogate models identify promising combinations of the input parameter settings for each generic vehicle class.

These best input parameter settings shall be verified in the high-fidelity vehicle-level model, and other fit alternatives are identified by slightly perturbing the input parameters. Only a subset can be carried forward because these subsequent tests introduce more operational complexities such that the surrogate models can no longer be used. For these more complex tests, an alternative multicriteria decision making technique shall be used to evaluate criteria characterized by distributions instead of single values. The best alternatives from each class shall be down-selected, and full-factorial combinations of these alternatives shall be explored to identify the best generic fleet.

3.2 Method for Rapid Computation of Community Noise Exposure

All of the preceding discussions on noise have focused on the DNL contour areas and shapes. As previously mentioned, the true noise metric of interest is the population exposed to this significant noise, which can be determined by overlaying these contours on maps of Census population densities. Assessing population exposure is one of the primary motivations for including Esri's ArcGIS® framework at the core of the AEDT system [11]. For a rapid airport-level noise computation tool like ANGIM, however, it is too cumbersome to import contours for every potential scenario into ArcGIS® for performing these population exposure counts.

Instead, a population grid method is proposed which exports Census block population to a grid conforming to the grid dimensions of the airport-level noise analysis. The reference grids are imported into ArcGIS® and geospatially aligned with a given airport runway endpoint. Each grid point is converted to a "Thiessen

polygon" via the Voronoi tessellation method [101]. The method of Voronoi tessellation generates polygons from a set of points that are mathematically defined by the perpendicular bisectors between all of the points. Each resulting polygon can be mapped to a single seed point, and the boundaries of these polygons are defined such that every point within the polygon has the smallest Euclidean distance with respect to that seed point as compared to any of the other seed points. A notional example of Voronoi tessellation for a seed of twenty points generating twenty polygons is shown in Figure 26.
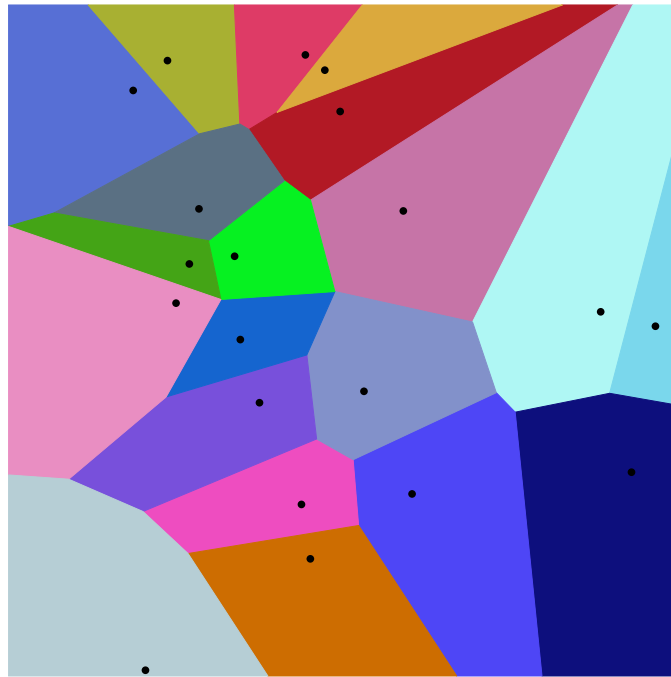
Figure 26: Notional Example of Voronoi Tessellation [102]

By using a grid of evenly spaced points conforming to the resolution of the noise analysis as the seed points for the Voronoi tessellation, the resulting Thiessen polygons are each a 0.08 nmi by 0.08 nmi square with the grid point at the center, as is notionally depicted in Figure 27. These square Thiessen polygons are intersected with the Census block polygon shapefiles. If a Census block boundary crosses a square Thiessen polygon, the latter is split into multiple polygons as is depicted

in Figure 27. The irregular shaped polygon in Figure 27 represents a 2010 Census block polygon, and the intersection of this polygon with one of the square Thiessen polygons is outlined.
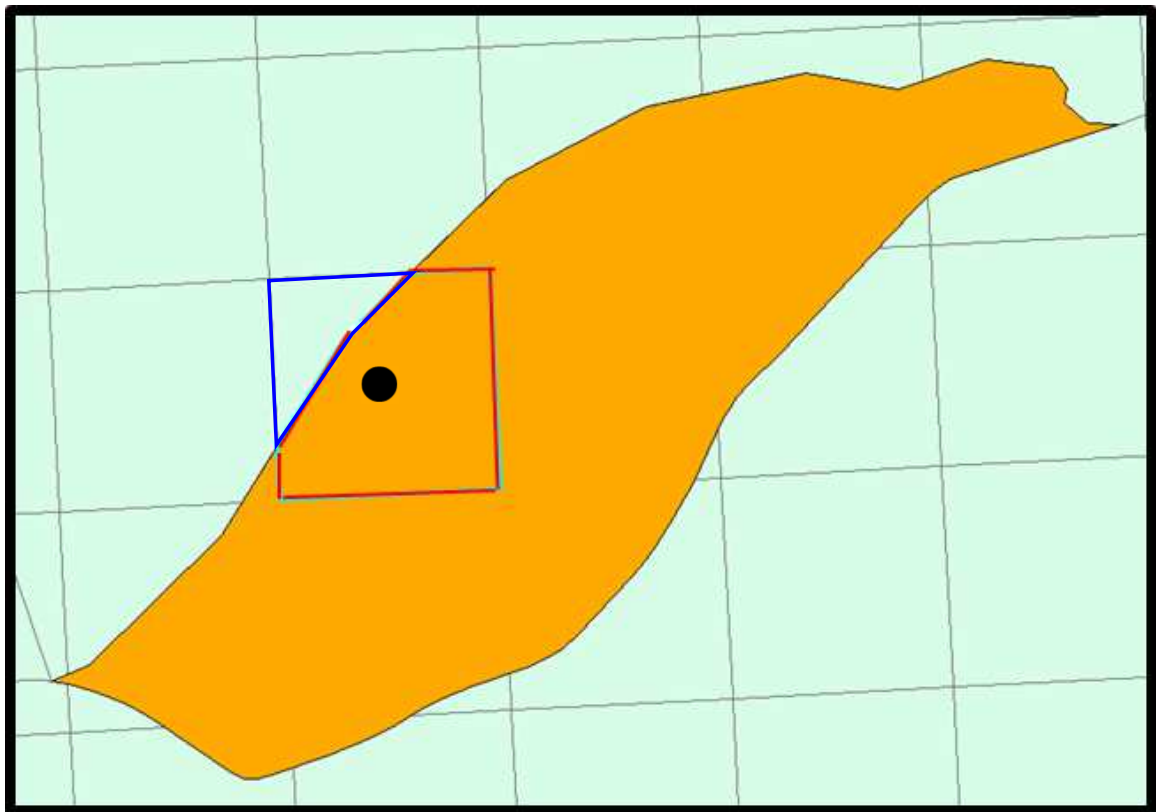
Figure 27: Intersection of Census Block and Thiessen Polygons

The population counts for the polygons resulting from the intersection operation can be calculated using the area-weighted formula in Equation (24):

$$Pop_{intersect} = \frac{Area_{intersect}}{Area_{block}} \cdot Pop_{block} \tag{24}$$

Where:

$Pop_{intersect}$ = Population count for polygon resulting from intersection

Pop_{block} = Population count joined to 2010 Census block polygon

$$Area_{intersect} = \text{Polygon area resulting from intersection}$$

$$Area_{block} = \text{2010 Census block polygon area}$$

Once the population counts are determined for each of these intersected polygons, the total population contained within the original square Thiessen polygons is summed and these counts are assigned to the original seed points. In this manner the 2010 Census block population counts are effectively discretized by the grid points from the noise analysis such that the total population counts surrounding the airport are conserved. This method takes advantage of the simpler computations associated with the centroid method but at a finer resolution with an assumption of uniform population distribution within a 2010 Census block polygon. Since the noise analysis is already calculating DNL decibel levels at each of these grid points, population exposure counts can be easily calculated by identifying which grid points are above a given noise threshold (typically DNL 65-dB but other decibel levels can be calculated as well) and summing the corresponding population at these grid points. In this manner, a continuous change in the size and shape of the noise contour maps to a continuous change in population exposure counts.

By conforming to the existing data structure in the noise model, these population grids enhance its capability to evaluate community noise exposure with minimal increase in run-time. To demonstrate the utility of pairing this method with the generic vehicle approach, population exposure counts for a 2010 baseline year shall be compared using the actual fleet of aircraft and then repeated using the final generic vehicle designs from the previous sequence of validation tests.

3.3 Summary of Technical Approach

While there is some flexibility in the techniques and models that can be used, the modified generic vehicle methodology hinges on statistical classification of the fleet, airport-level characterization of generic vehicle accuracy, and surrogate-based optimization. These surrogates enable cheaper exploitation of the input parameter settings for each generic vehicle class, which allows for more focused exploration in the high-fidelity models. This focused exploration populates a subset of fit alternatives, and multicriteria decision making evaluates these alternatives with respect to each of the validation test specifications. Once this best generic fleet is identified, their utility for airport-level noise analysis can be demonstrated and enhanced by adding a method for quantifying population exposure counts that conforms to the existing data structure in the rapid airport-level noise computation model.

CHAPTER IV

IMPLEMENTATION

With the technical approach for optimizing the generic vehicles established, the methodology was implemented by selecting modeling and simulation tools that meet the previously established requirements. Discriminant analysis was carried out to finalize the vehicle class assignments, which is visually shown to have less in-class variance than traditional seat-class groupings. A sensitivity analysis with respect to noise metrics was conducted on the physics-based vehicle-level model and cross-referenced against Becker's list of significant variables for fuel-burn and NO_x emissions to define a reduced subset of important variables. Space-filling designs of experiments were executed, and the results were used to train feed-forward neural networks for each metric. These surrogate models were incorporated in a prediction-profiler environment to enable Monte Carlo simulations. Desirability scores were calculated to identify good locations in the design space, and the performance with respect to these input parameter settings were verified in the physics-based vehicle-level model. Perturbed designs of experiments about these optimal locations were explored to identify slightly better alternatives, and SMAA was used to choose a subset of best alternatives for each class. Full-factorial combinations of these alternatives from each class were evaluated and a best generic fleet was defined for both the vehicle-class and seat-class based formulations.

Fleet-level results for each generic vehicle formulation were shown to be more accurate than a traditional representative-in-class approach, with the vehicle-class groupings proving slightly better than the seat-class groupings. The generic vehicles were then used in conjunction with pre-processed population grids at each airport.

These vehicles demonstrated good accuracy in population counts with respect to the actual fleet using the same population grid method, but at a much reduced computation time. Therefore, the generic vehicles and the population grids represent effective exchanges of fidelity for speed that enable the screening-level framework for assessing aviation's environmental impacts.

4.1 Selection of Modeling and Simulation Tools

The general requirements for modeling and simulation capabilities were outlined in Chapter 2. The types of analyses conducted in this study can be repeated with any set of tools that satisfy these requirements, but for the purposes of demonstration specific tools shall be selected. These tools are discussed briefly in this section.

4.1.1 Vehicle Performance Model and Schedule of Operations

The Aerospace Systems Design Laboratory (ASDL) at Georgia Tech has developed an in-house tool referred to as the "AEDT Tester." This tool uses the built-in AEDT algorithms and performance modules discussed previously to rapidly generate single-aircraft performance, fuel burn, emissions, and single-event SEL noise grids [103]. Vehicle coefficients can be extracted from the relevant databases and run through the AEDT Tester to capture the performance of existing vehicles. New vehicles can also be run through this tool provided that the relevant coefficients can be defined. The user can define unique operations, departure and arrival airport/runway locations, and atmospheric conditions to see how the performance of these vehicles change for different types of missions. The AEDT Tester does introduce some simplifications, such as an assumption of straight-in and straight-out ground tracks. However, the AEDT Tester does not incorporate the Geographical Information System (GIS) core that the full AEDT is built on, so inclusion of

location-specific information such as terrain and typical weather is not included.

4.1.2 Schedule of Operations and Airport-Level Computations

The AEDT Tester is still a vehicle-level tool for measuring environmental impacts of aviation. Thus, it cannot independently serve as a fleet-level model. The vehicle-level results from the AEDT Tester must be aggregated to generate airport-level results, which requires the inclusion of operational volumes and schedules that track the distribution of these operations between different vehicles as well as over different mission ranges. The source of this operational data may vary, but fleet-level tools often require simplification of the continuous range of mission trip lengths. One simplification for trip-length that is commonly associated with noise analysis is the use of a stage-length designation, as was common use for the Integrated Noise Model and currently in use for AEDT. Stage-length designations simplify mission trip lengths by discretizing them into nine bins. INM also defined a representative mission range per stage-length, as is demonstrated in Table 11 [72].

Table 11: Stage Length Designations

Stage Length	Min Distance [nmi]	Max Distance [nmi]	Representative Mission Range [nmi]
1	0	500	350
2	501	1000	850
3	1001	1500	1350
4	1501	2500	2200
5	2501	3500	3200
6	3501	4500	4200
7	4501	5500	5200
8	5501	6500	6200
9	6501	-	7200

To simplify the operations and to assure proper comparison of the impacts of

fuel burn, NO_x, and noise, the gate-to-gate flights shall also be discretized by stage-length. Fuel burn and NO_x measurements will be restricted to operations at the representative mission ranges listed in Table 11. With this simplified operations set, aggregate fuel burn and NO_x can be calculated using vehicle-level performance for each stage-length and simple spreadsheet calculations that link the performance to a schedule of operations. This can be done for both the total-mission and terminal-area metrics. DNL noise grids and contours, however, have an additional dependence on runway configuration and utilization. This contributes to the spatial nature of this metric, and thus an additional capability is required to aggregate noise.

Bernardo formulated ANGIM to satisfy all of his requirements for an airport-level noise model, and if the schedules used by ANGIM can simultaneously be linked to spreadsheet aggregations for fuel burn and NO_x, the additional requirements introduced in this work can also be met. Therefore, the airport-level tool for this work will actually be an integration of the AEDT Tester, ANGIM, and Excel spreadsheet aggregations for fuel burn and NO_x.

4.1.3 Physics-Based Vehicle-Level Model with Technology Infusion Capabilities

At the Georgia Institute of Technology, the issuance of the CAEP goals led to the development of the Environmental Design Space (EDS). EDS is a tool developed by Georgia Tech's Aerospace Systems Design Laboratory (ASDL) for the U.S. Federal Aviation Administration's Office of Environment and Energy (FAA/AEE) as part of a comprehensive suite of software tools that allows for a thorough assessment of the environmental effects of aviation [104]. EDS provides the capability to generate an integrated analysis of aircraft performance, source noise, and exhaust emissions at the aircraft level for potential future aircraft designs under different policy and technological scenarios. The integrated analysis enables the assessment

www.manaraa.com

of the interdependencies and associated trade-offs between aircraft performance, noise and emissions in a transparent and traceable manner. EDS employs mostly physics-based, integrated, multidisciplinary modeling and simulation that seamlessly combines core modules originally developed by NASA coupled with design rules and logic along with user-defined engine and airframe design parameters to create aircraft designs. The general EDS architecture is diagrammed in Figure 28 [105].
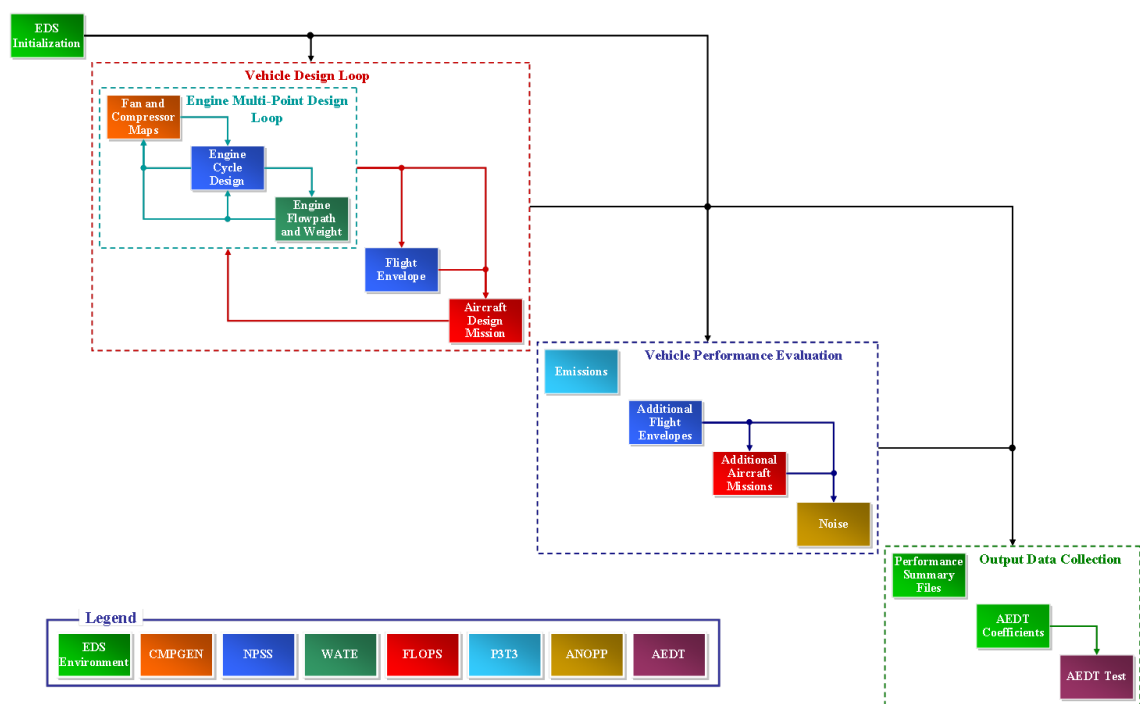

Figure 28: EDS Architecture

The EDS environment can be thought of as executed in four phases for a single vehicle. Phase 1 begins with the initialization steps, which establishes the different modes and options for running EDS and determines the settings of all the design variables. These design variables can include hundreds of different engine, aerodynamic, weight, and geometry settings. Phase 2 is the vehicle design phase which performs the necessary cycle analysis and then sizes the engine and airframe. The primary modules covering engine design include the Compressor Map

www.manaraa.com

Generation (CMPGEN) program for compressor map generation, the Numerical Propulsion System Simulation (NPSS) for thermodynamic cycle analysis, and the Weight Analysis of Turbine Engines (WATE) for engine flow path analysis and weight estimation [106, 107, 108, 109, 110, 111]. In this phase, there is first a design loop for the engine and then a design loop between the engine and airframe. The engine design loop first performs the thermodynamic cycle design with CMPGEN and NPSS at the aerodynamic design point; integrating a multi-point design methodology to ensure the engine meets thrust requirements at both top of climb (TOC) and take-off [112]. There are then iterations between the NPSS thermodynamic cycle and the WATE flow path analysis until the two analyses converge. After completion of the engine design loop, the vehicle design loop starts by running the thermodynamic cycle model in off-design mode throughout the flight envelope to generate an engine deck for the aircraft mission analysis. The aircraft mission analysis is performed in the Flight Optimization System (FLOPS) for a given mission, payload, thrust to weight ratio, and wing loading, scaling the engine deck thrust and the vehicle size to meet the targets [113]. If the engine deck thrust is scaled, the engine design loop is executed again with the new thrust targets. This loop is repeated until the engine does not scale in the aircraft mission analysis. The vehicle is fixed at the end of this phase.

Phase 3 is the vehicle performance evaluation phase. In this phase all desired performance evaluations are conducted including gaseous emissions, noise certification, takeoff and landing performance evaluations, and fuel burn for off-design points on a payload-range chart. Vehicle fuel burn performance for design and off-design conditions are executed in FLOPS, while emissions are estimated based on correlations derived from the P3-T3 method [114]. At the end of this phase, the aircraft engine state tables from NPSS and the certification trajectories generated from FLOPS are fed into the Aircraft Noise Prediction Program (ANOPP) to calculate certification $EPNL_{dB}$ values and NPD-curves for multiple noise metrics

[115, 116].

Phase 4 is the output data phase. Here all desired data is compiled into user-specified summary files. EDS includes an option to generate an AEDT Tester input file by matching the various performance tools to each of the required AEDT coefficients, which satisfies the requirement of an interface with the fleet-level tool. The methods for mapping EDS vehicles to the AEDT coefficients is described in detail in de Luis' PhD dissertation, although some modifications have been made to match improvements and changes to the AEDT detailed model [117]. In this way, the integrated fuel burn, NO_x, and noise performance generated by EDS can be evaluated in the integrated fleet-level tool suite in the same manner as any industry validated vehicle defined by the relevant coefficients. This allows for the use of the AEDT Tester as a common truth model for the existing fleet as well as future vehicles with technology infusion.

EDS models technology infusion using a series of additive or multiplicative factors at various levels of the analyses. These factors collectively encompass the technology design space defined by first formally collecting technology data in terms of its quantitative impacts and interactions with other potential technologies. The technology data is then formally recorded into a Technology Interaction Matrix (TIM) and Technology Compatibility Matrix (TCM) respectively. These matrices provide both traceability and transparency to the technology modeling and auditing process. Technology information may be gathered from publicly available literature, including peer reviewed publications, and subject matter experts, either at NASA or in industry. It is important to note that technology impacts are modeled at the component level and allowed to propagate through the EDS modeling and simulation environment in order to determine the system level benefits [118].

107

4.1.4 Integrated Airport-Level Environment with Specific Tools

The Environmental Design Space will be used to explore potential average generic vehicle designs. These vehicles will serve as technology testbeds to project the performance of future vehicles with advanced technologies, such as those currently being studied by the CLEEN and ERA programs. Given the selection of specific tools, the notional diagram in Figure 21 can now be updated with the specific tools used for this study as shown in Figure 29. This integrated environment will be used for optimization of the average generic vehicles.
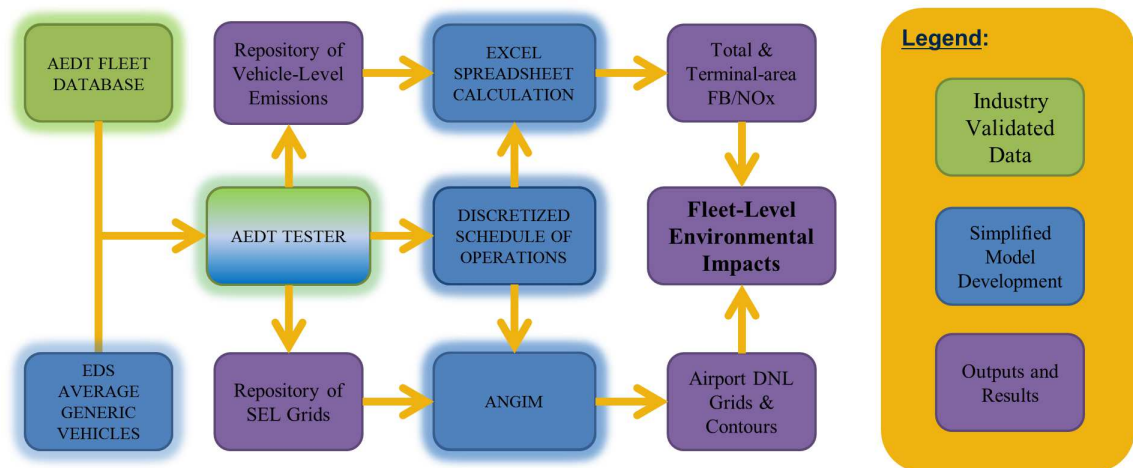

Figure 29: Integrated Airport-Level Environment with Specific Tools

4.2 Vehicle Classification through Discriminant Analysis

Before the current fleet of aircraft can be grouped into bins, some criteria must be established to determine which vehicles should be included in the study. The generic vehicle models are intended to serve as a representative replacement vehicle for future years when older vehicles are retired. Many of the vehicles that are currently out-of-production are being phased out because they are unreasonably loud or have very poor fuel economy relative to the current state-of-the-art vehicles. It is reasonable to assume that a new vehicle introduced in future years will have

performance more comparable to current in-production vehicles rather than the obsolete out-of-production vehicles, thus only in-production vehicles were included. This significantly reduced the fleet to the important and relevant aircraft. The vehicles must also have a significant number of operations and be significant contributors to aggregate fuel burn, emissions, and noise. This criteria eliminated most non-commercial aircraft such as general aviation aircraft, vehicles with fewer than 20 passengers, and turboprop aircraft.

Fuel burn and NO_x masses for total mission, terminal area departure, and terminal area approach for existing aircraft were calculated using the AEDT tester. For noise quantification the end goal requires that the combinations of generic vehicles should be able to match DNL contours for a given airport with a given schedule, but for the purposes of vehicle grouping the focus must remain on a vehicle-level metric such as the SEL contours. Measurements of SEL contours provide insight into the noise footprint of individual vehicles. Groupings focus on contours from SEL 70-dB to SEL 85-dB, as these SEL values at the vehicle level correlate well with the DNL 55-dB and 65-dB contours for a busy reference airport with 2,000 daily operations, as determined mathematically using Equation (15) in Chapter 2. In order to capture the size and extent of the contours, the metrics of interest are the contour areas, the maximum widths of the contours, and the maximum lengths.

With the fleet trimmed down to relevant in-production aircraft and given the metrics above, the performance of these vehicles can be compared and used for groupings. Different vehicles have different design ranges and thus to compare all of the vehicles on similar grounds, a short stage-length 1 mission of 350-nmi with the mission profile shown in Figure 30 was chosen. The mission represents a straight flight from an airport at sea-level static atmospheric conditions to another airport at sea-level static atmospheric conditions, cruising at 35,000 ft.
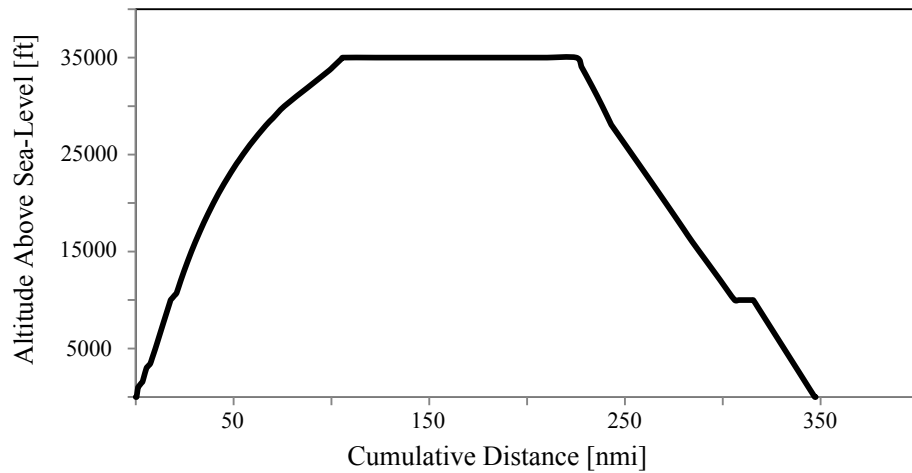
Figure 30: Common Stage-Length 1 Mission Profile

The performance metrics were collected for all of the aircraft in the fleet and used for discriminant analysis. Aircraft were assigned to groups based on heuristic knowledge and intuition. For example, the Airbus A320 and A321 vehicles should likely be classified in a group with its competitors, the Boeing B737-8 and B737-9 vehicles, based on similar geometries, passenger capacities, and mission profiles.

Once the a priori assignments were made and discriminant analysis was carried out, parallel plots were created to visually examine the remaining variability and determine if any of the groups needed to be disaggregated into two groups. A parallel plot, sometimes referred to as a parallel coordinate plot, is a common way of visualizing and analyzing high-dimensional and multivariate data. The visualization is closely related to time-series visualization, except that it applies to data where the vertical axes do not correspond to points in time. These axes represent each of the different metrics, and thus different trends and patterns can be identified by rearranging the order of the metrics. The vertices of each vertical line represent the minimum and maximum values for that metric amongst all of the alternatives, with the line representing a linear scale between these extremes. For example, if the line associated with an alternative crosses the vertical line for a metric at its midpoint, the value of the metric for that alternative is equal to the midpoint between the minimum

110

value and maximum value, or the minimum value plus 50% of the range. Lines that cluster close together represent alternatives with similar metric values, whereas lines that bound a larger area represent alternatives with greater variability with respect to the metric values.

For the parallel plots that follow, the various groups are plotted separately for increased visual clarity. It should be noted that the original vehicle-class groupings included both a Small Regional Jet (SRJ) and a Large Regional Jet (LRJ) class, but eventually the vehicles in the SRJ class were deemed out-of-production and not included in the generic vehicle exercise. Further research on market forecasts for regional jet aircraft showed that these smaller designs are in fact being phased out in favor of larger regional jet designs due to the projected increases in passenger demand for short-range flights [119, 120, 121, 122]. Therefore the SRJ vehicles were reclassified as out-of-production vehicles, and only the LRJ vehicles were carried forward. Henceforth, the LRJ class shall simply be referred to as the RJ class, which corresponds to the LRJ class in the parallel plots. The parallel plots for the vehicle classes are shown in Figure 31 whereas the equivalent parallel plots for the seat classes are shown in Figure 32. The aircraft are color-coded by their vehicle-class assignments to visually demonstrate that the seat classes include a broad range of vehicle types. While the metrics represented by the vertical lines are listed in groups in the figures to reduce the clutter on the horizontal axis, the vertical lines from left-to-right are as follows:

1. Maximum Range [nmi]

2. Maximum Payload [metric tons]

3. Total Mission Fuel-Burn [kg]

4. Departure Terminal-Area Fuel-Burn below 3,000-ft [kg]

5. Approach Terminal-Area Fuel-Burn below 3,000-ft [kg]

6. Total Mission NO_x Emissions [g]

7. Departure Terminal-Area NO_x Emissions below 3,000-ft [g]

8. Approach Terminal-Area NO_x Emissions below 3,000-ft [g]

9. Departure SEL 70-dB Contour Area [nmi^2]

10. Departure SEL 70-dB Contour Maximum Width [nmi]

11. Departure SEL 70-dB Contour Maximum Length [nmi]

12. Departure SEL 75-dB Contour Area [nmi^2]

13. Departure SEL 75-dB Contour Maximum Width [nmi]

14. Departure SEL 75-dB Contour Maximum Length [nmi]

15. Departure SEL 80-dB Contour Area [nmi^2]

16. Departure SEL 80-dB Contour Maximum Width [nmi]

17. Departure SEL 80-dB Contour Maximum Length [nmi]

18. Departure SEL 85-dB Contour Area [nmi^2]

19. Departure SEL 85-dB Contour Maximum Width [nmi]

20. Departure SEL 85-dB Contour Maximum Length [nmi]

21. Approach SEL 70-dB Contour Area [nmi^2]

22. Approach SEL 70-dB Contour Maximum Width [nmi]

23. Approach SEL 70-dB Contour Maximum Length [nmi]

24. Approach SEL 75-dB Contour Area [nmi^2]

25. Approach SEL 75-dB Contour Maximum Width [nmi]

26. Approach SEL 75-dB Contour Maximum Length [nmi]

27. Approach SEL 80-dB Contour Area [nmi^2]

28. Approach SEL 80-dB Contour Maximum Width [nmi]

29. Approach SEL 80-dB Contour Maximum Length [nmi]

30. Approach SEL 85-dB Contour Area [nmi^2]

31. Approach SEL 85-dB Contour Maximum Width [nmi]

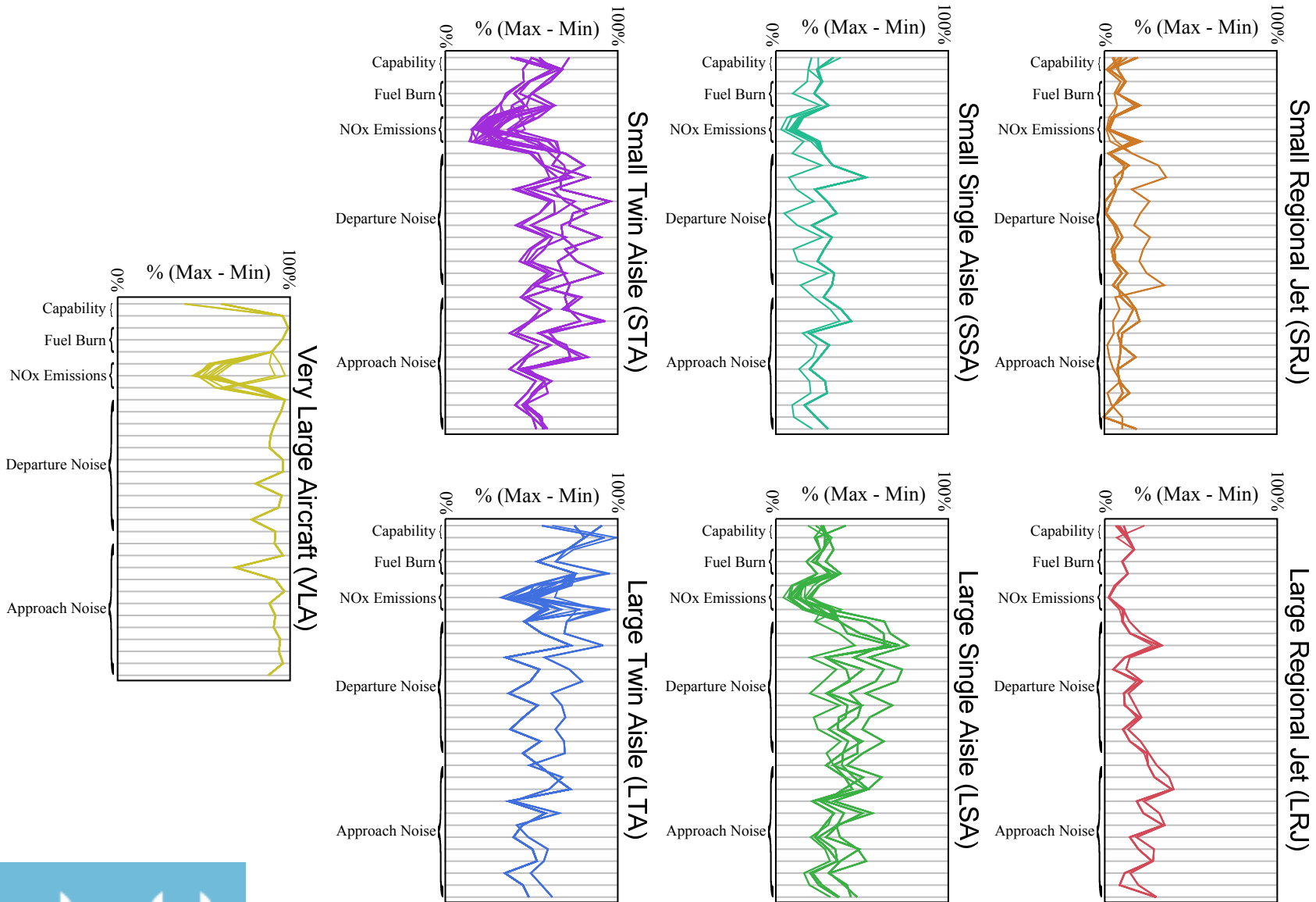32. Approach SEL 85-dB Contour Maximum Length [nmi]

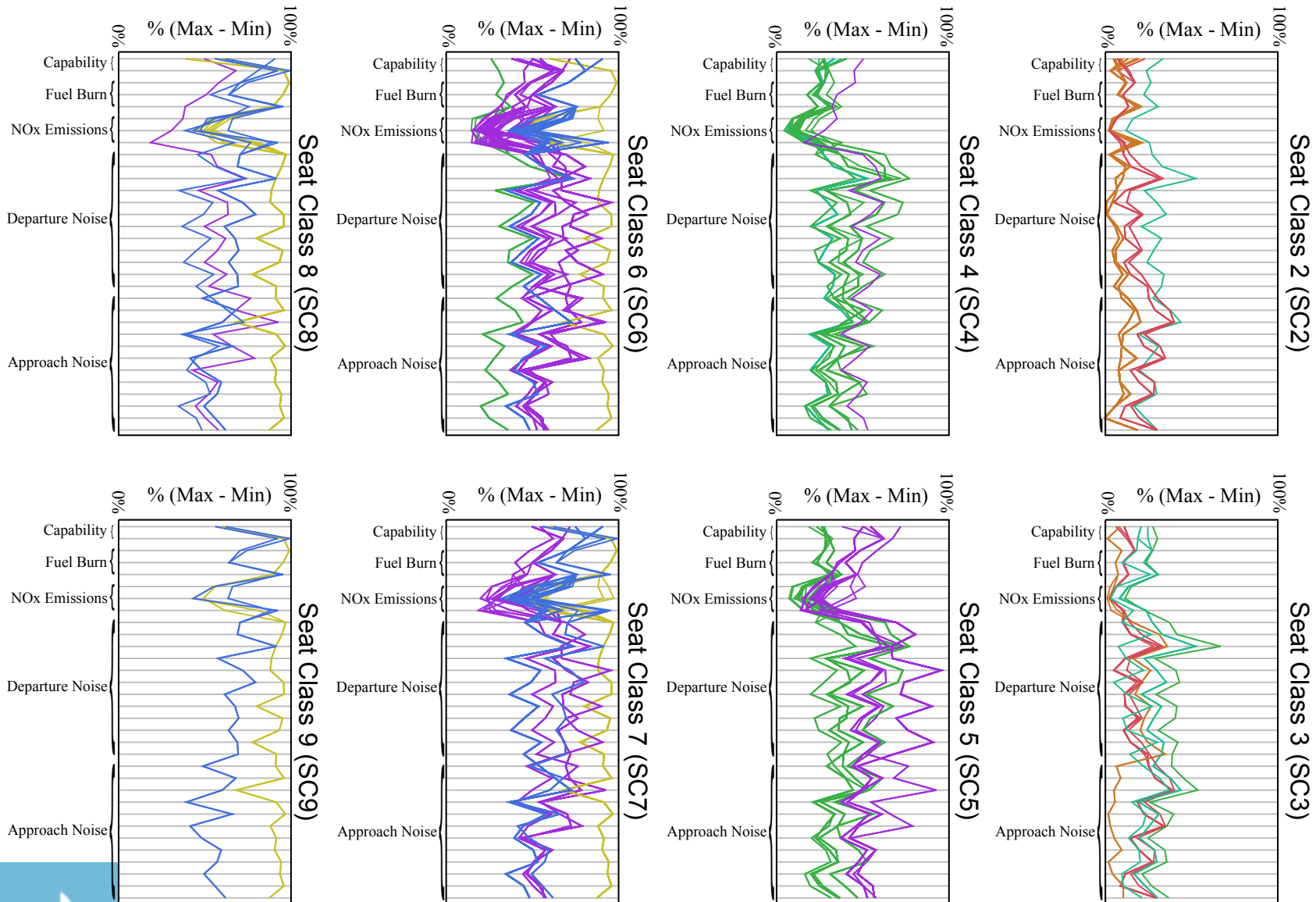Figure 31: Vehicle-Class Grouping Parallel Plots

114

Figure 32: Seat-Class Grouping Parallel Plots

115

A comparison of the parallel plots shows the advantage of grouping vehicles through discriminant analysis on the vector of performance metrics versus traditional seat-class groupings, as the latter feature much wider variability per class. This is demonstrated more specifically in Figure 33 by plotting the mission fuel burn and the departure noise contours corresponding to a stage-length 4 mission for aircraft in the fleet classified in Seat Class 6 (SC6).
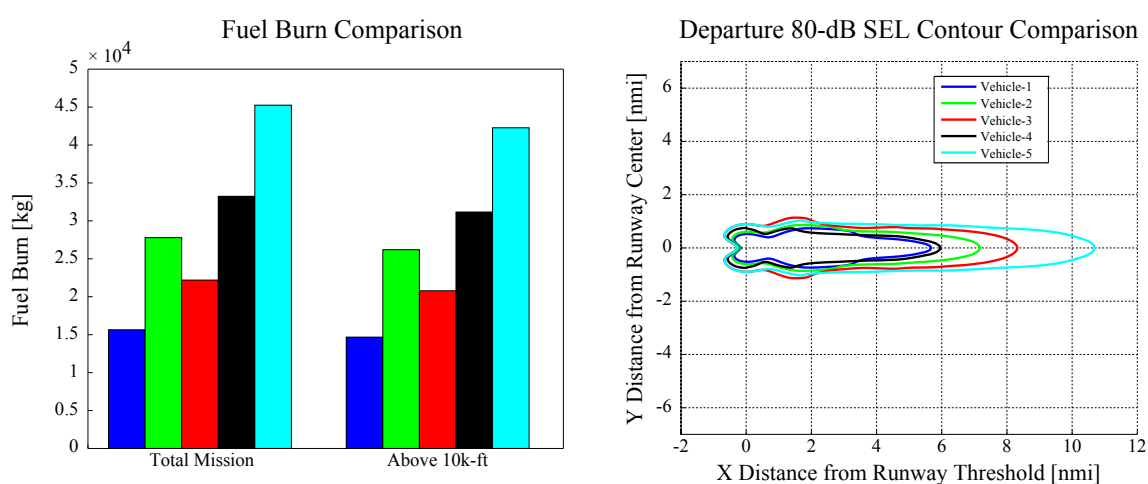

Figure 33: Stage-Length 4 Mission Comparison for Seat Class 6 Aircraft

Names of the specific vehicles are purposely removed to protect potentially sensitive data. All five of these vehicles have possible internal seat configurations that fall within the 210-300 passenger range, but the performance of these aircraft vary widely. Only vehicles 2 and 3, however, would be characterized as Small Twin Aisle (STA) vehicles. An average SC6 generic vehicle must balance the frequency weighted performance of all five of these vehicles, whereas an average STA generic vehicle would only have to balance the frequency weighted performance of vehicles with similar fuel burn and noise characteristics as vehicles 2 and 3.

The generic vehicle tests that follow were performed in parallel for both the vehicle classes and the seat classes. The generic vehicle engines must be bounded by the ranges of observed values of the constituent vehicles for each class. The engine

116

constraints for the vehicle classes and seat classes are shown in Tables 12 and 13, respectively.

Table 12: Vehicle Class Engine Constraints

Vehicle Class	SLS Thrust Uninstalled [lbf]		OPR		BPR	
	Min	Max	Min	Max	Min	Max
SRJ	7420	8350	17.2	19.06	4.72	5.23
LRJ	12670	13420	22.15	23.8	5.13	5.13
SSA	17400	27000	22.6	27.69	4.81	6.00
LSA	24200	32010	25.78	33.44	4.46	6.00
STA	48000	71110	23.4	35.8	4.2	5.2
LTA	74910	115530	32.2	42.24	5.7	8.6
VLA	56000	62000	28.37	34	4.2	5.1

Table 13: Seat Class Engine Constraints

Seat Class	SLS Thrust Uninstalled [lbf]		OPR		BPR	
	Min	Max	Min	Max	Min	Max
SC2	7420	8350	17.2	19.06	4.72	5.23
SC3	12670	25000	22.15	26.6	5.09	6.00
SC4	20600	50000	22.6	33.44	4.46	6.00
SC5	24200	68000	23.4	34.0	4.2	6.00
SC6	29990	97300	23.4	41.52	4.2	8.6
SC7	56000	115530	28.37	42.24	4.2	8.44
SC8	56000	115530	28.37	42.24	4.25	7.08
SC9	57160	115530	30.13	42.24	5.1	7.08

4.3 Input Parameter Reduction through Sensitivity Analysis

Becker also used EDS as his physics-based vehicle-level model, and he compiled an exhaustive list of parameters that significantly impacted fuel burn and NO_x emissions for both total mission and terminal area metrics [44]. A similar sensitivity

117

analysis was conducted on EDS to determine if any additional input parameters should be included when constructing surrogate models for noise.

4.3.1 Identifying Design Variables

Within the EDS architecture, ANOPP is the tool used to estimate source noise and calculate the resulting Noise-Power-Distance data necessary for quantifying the SEL grids. In order to identify the necessary design variables to include in the sensitivity analysis for noise metrics, a thorough examination of the ANOPP input file structure proved necessary. EDS has hundreds of possible input variables to choose from, but not all of these variables actually affect ANOPP inputs. Miscellaneous variables such as passenger compartment lengths or the number of passengers in first class or coach were defaulted. While airframe noise is considered a significant contributor to takeoff and landing noise, several of the aerodynamic and airframe related variables have redundant effects. For this reason, only a few of these variables were allowed to vary, including aspect ratio, sweeps on the wings and tails, thicknesses, flap ratios, and maximum lift coefficients at takeoff and landing.

The main contributors to departure noise are the engines due to the high thrust levels required, and thus the majority of the parameters included were engine-related variables. The ANOPP input files require the inclusion of engine cycle information generated by NPSS, and thus a majority of the cycle-design variables were included. ANOPP also has inputs for applying chevron geometries to the core and fan nozzles of the engines, which directly influence the noise responses, so these variables were included as well.

Broad variable ranges were initially defined for each of these input parameters, and a series of tests were conducted to tighten these ranges in manner that increased the success rate in EDS. Space-filling Latin hypercube designs of

experiments were constructed on these input parameters and run through the model. Noise-Power-Distance data for approach and departure at a few slant distances were parsed and characterized by their slopes and intercepts from linear regression. Additionally, each case was evaluated in the AEDT Tester to measure SEL contour areas in an effort to link the NPD trends with the contour trends.

4.3.2   Half-Normal Probability Plots

While many statistical tests were available, including analysis of variance, student t-tests, and half-normal probability plots, the latter was chosen for its visual clarity as well as its inclusion of both factor effects and interaction effects. A half-normal probability plot is a graphical tool that uses ordered estimate effects based on least squares estimation to help assess which factors are important and which are unimportant. A notional example of a half-normal plot is shown in Figure 34.
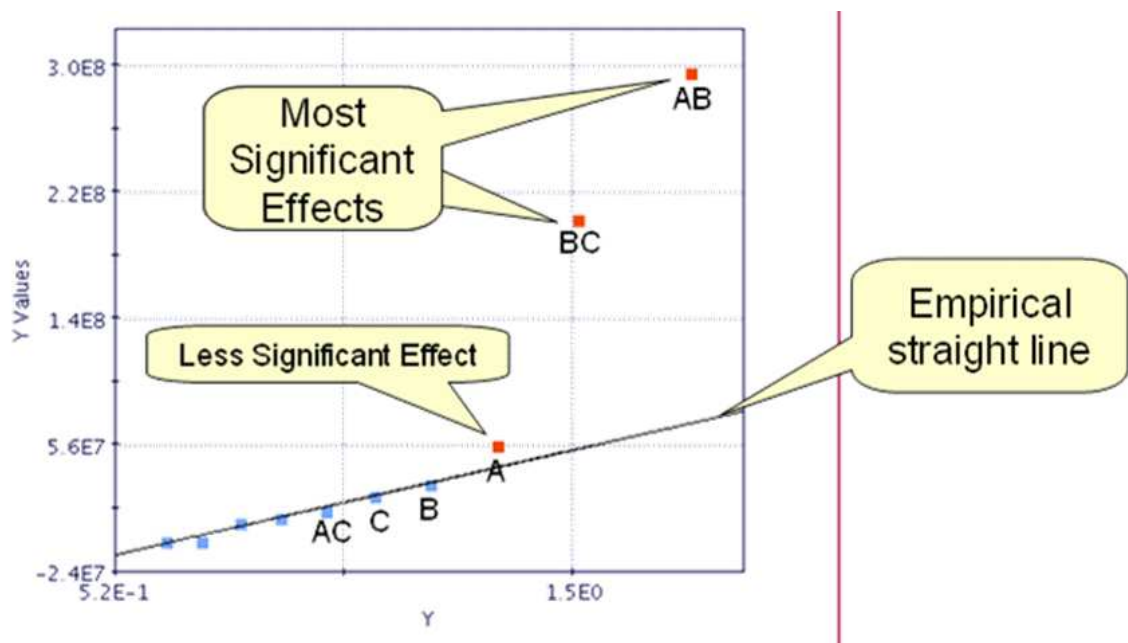

Figure 34: Notional Half-Normal Probability Plot

The horizontal axis represents statistical medians from a half-normal probability

distribution, while the vertical axis represents the ordered absolute value of the estimated effects for the main factors and interactions. For each factor, the distribution of errors from least-squared estimates is compared to a normal distribution. If the normal distribution is centered near zero, the factor is unimportant and will appear on an empirical straight line. If the normal distribution of errors is skewed and centered away from zero, the factor is important and will appear well off the empirical straight line. The further a point associated with a factor appears from this empirical straight line, the more dominant its effect. In this notional example, the interaction effect AB is the most dominant factor, followed by the BC interaction effect. The A factor has minor significance, while the B, C, and AC factors are insignificant. The plot is referred to as "half-normal" because the variables are ordered by the absolute value of the effect-size without consideration of whether the effect is positive or negative, thus representing the positive half of a normal distribution. The points are color-coded to distinguish whether the relationship is positive (i.e. direct relationship) or negative (i.e. inverse relationship).

4.3.3 Summary of Sensitivity Analysis

Many of these half-normal probability plots were generated for the various noise metrics tracked (NPD slopes, intercepts, contour areas), and the procedure was repeated for each vehicle class. Trends were mostly consistent between classes, and thus only a few qualitative tables of these observed trends are included here as examples. More detail is included in Reference [123].

The primary observation was that only a handful of variables significantly impacted noise, and these impacts tended to be consistent across different slant distances. These variables tended to have combined effects on the NPD linear regressions such that an increase in slope would be combined with a decrease in the

intercept, or vice versa. The impacts on the NPDs are thus characterized as "steep" or "flat" with respect to an increase in a design variable, as demonstrated for the Large Single Aisle EDS model in Table 14.

Table 14: NPD Sensitivities for Large Single Aisle EDS Model

| Variable Name	Physical Description	Impact on Approach Curves	Impact on Departure Curves
FLAPR	Area ratio of flaps to total wing area	Flat	Flat
SW	Wing area	Flat	Flat
TOC_Wratio	Mass-flow ratio of the top-of-climb to the aerodynamic design point	Steep	Steep
FPR	Fan pressure ratio	Steep	Steep
Ext_Ratio	Extraction ratio at aero design point	Flat	Flat
PER1	Ratio of core-nozzle perimeter with chevrons to core nozzle with no-chevron	Flat	Flat
Rating	NPSS thrust rating fraction for uprating or derating of an engine after design	Steep	Steep
T4max	Maximum allowable temperature at combustor exit/turbine inlet	Reduces Slope	Reduces Intercept
LPCPR	Low-pressure compressor pressure ratio at aero design point	Flat	Flat
HPCPR	High-pressure compressor pressure ratio at aero design point	Flat	Flat

Legend:
- Dominant
- Significant
- Minimal
- Insignificant

A steeper NPD implies that the noise levels are more sensitive to thrust setting. It should be noted that the airframe design variables like flap-ratio and wing-area lead to more flat NPDs, particularly for approach. This does not mean that the variable has a less significant impact on noise, but rather implies that the noise level is less dependent on thrust levels. By comparing the sensitivity analysis for the NPDs with the equivalent sensitivity analysis on contour areas for various SEL decibel values, a general relationship can be inferred. Steeper departure NPDs lead to larger contour areas, whereas more flat NPDs lead to smaller contour areas. The opposite is true for approach, where steeper NPDs lead to smaller contour areas, whereas more flat NPDs lead to larger contour areas. This is notionally demonstrated below Table 15.

Engine noise dominates airframe noise during departure because the engines are operating at highest performance levels during takeoff. Increasing fan-pressure-ratio (FPR) leads to higher turbulence levels, which increases broadband fan noise. This

Table 15: SEL Contour Sensitivities for Large Single Aisle EDS Model

Variable Name	Physical Description	Impact on 55dB Approach Contour Area	Impact on 65dB Approach Contour Area	Impact on 75dB Approach Contour Area	Impact on 55dB Departure Contour Area	Impact on 65dB Departure Contour Area	Impact on 75dB Departure Contour Area
FLAPR	Area ratio of flaps to total wing area	Increase	Increase	Increase	Increase	Increase	Decrease
SW	Wing area	Increase	Increase	Increase	Increase	Increase	Increase
TOC_Wratio	Mass-flow ratio of the top-of-climb to the aerodynamic design point	Decrease	Decrease	Increase	Increase	Increase	Increase
FPR	Fan pressure ratio	Decrease	Decrease	Increase	Increase	Increase	Increase
Ext_Ratio	Extraction ratio at aero design point	Increase	Increase	Increase	Decrease	Decrease	Decrease
PER1	Ratio of core-nozzle perimeter with chevrons to core nozzle with no-chevron	Increase	Increase	Increase	Decrease	Decrease	Decrease
Rating	NPSS thrust rating fraction for uprating or derating of an engine after design	Decrease	Decrease	Decrease	Decrease	Decrease	Increase
T4max	Maximum allowable temperature at combustor exit/turbine inlet	Decrease	Decrease	Decrease	Decrease	Decrease	Decrease
LPCPR	Low-pressure compressor pressure ratio at aero design point	Increase	Increase	Decrease	Decrease	Decrease	Decrease
HPCPR	High-pressure compressor pressure ratio at aero design point	Increase	Increase	Increase	Decrease	Decrease	Decrease
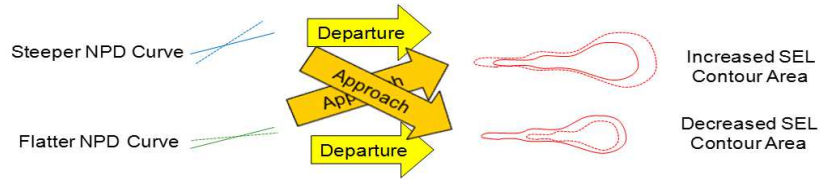
variable also contributes to higher jet noise by driving the fan-nozzle jet velocity higher. Therefore, an increase in FPR leads to steeper NPDs and increased contour areas. Mass-flow ratio of the top-of-climb to the aerodynamic design point (TOC_Wratio) is inversely proportional to bypass ratio, which is not a design variable in the EDS environment but rather a response that comes from the iterations of the engine multi-point design loop. Higher bypass ratios often drive larger fan diameters which leads to more fan noise, but this is countered by a reduction in jet noise from an increased buffer between the higher-velocity core flow and the ambient air, as well as improved mixing with the cooler fan-nozzle flow. Higher bypass ratios also can reduce the required jet-velocity to achieve a certain level of thrust, as the fan-nozzle increases the overall thrust by increasing its exiting mass-flow. Since jet noise tends to have a bigger impact than fan noise, the net effect of increased bypass ratio is typically lower overall noise. Therefore, increases in TOC_Wratio drive smaller bypass ratios, leading to steeper NPDs and larger noise contours. Extraction ratio (Ext_Ratio) is directly proportional to bypass ratio, so increases in this design variable drive larger bypass ratios, leading to more flat NPDs and smaller noise contours. Chevron geometries

122

($PER1$) are designed specifically to reduce noise, and increasing $PER1$ leads to more flat NPDs and smaller noise contours. The chevrons increase mixing between the core-nozzle stream and the fan-nozzle stream, which decreases low-frequency noise sources, but may result in significant high-frequency noise generation.

For approach, it was observed that flap ratios ($FLAPR$) and wing areas (SW) both contribute to more flat NPDs, which results in larger contour areas and thus louder approach noise. During approach the flaps and other high-lift devices are deployed in order to increase lift and decrease stall velocity, and the high deflection angle of these flaps introduces a significant amount of drag. Aerodynamic noise is closely associated with drag creation mechanisms because of the introduction of turbulent flow, which contributes to broadband noise. Additionally, vortices created by the flap-edge can introduce significant low-frequency noise. Similarly, increasing the wing area increases the areas of the deflected flaps, as flap ratio is defined with respect to the given wing area. The increase in wing area also leads to some confounding because of the impact on the duration of the entire approach procedure, keeping in mind that SEL is an integration of the entire noise event. Engine variable impacts are not dominant during approach because the engines are operating at near idle conditions. This is especially true for the Constant Descent Angle (CDA) approach procedures assumed in EDS, as no powered pull-up maneuvers are executed (which would generate additional engine noise). Still, these engine design variables, such as FPR and TOC_Wratio, do show some significance for approach. This significance can likely be explained by the fan operating at off-design conditions, which can result in noise characterized by multiple tonal components.

The inclusion of these few significant variables for the noise analysis with Becker's list of important variables for fuel burn and NO_x emissions makes for a more manageable list of input parameters. A reduced set of input parameters allows for construction of higher resolution space-filling designs of experiments.

123

Better resolution for these design of experiments allow the neural network-based surrogate models to capture more detail, which helps to increase the power of the surrogate-based optimization techniques.

4.4 Optimization and Selection of Generic Vehicles

With the aircraft classified into classes and the vehicle-level models reduced to a manageable subset of input parameters, the generic vehicle method described in Chapter 3 can be implemented. The combination of airport-level targets, surrogate-based optimization, perturbed design space exploration on the vehicle-level design tool, and inverse multi-criteria decision-making techniques form what shall heretofore be referred to as the method for Generating Emissions and Noise, Evaluating Residuals, and using Inverse methods for Choosing the best Alternatives, or the GENERICA method. This method is diagrammed in Figure 35.
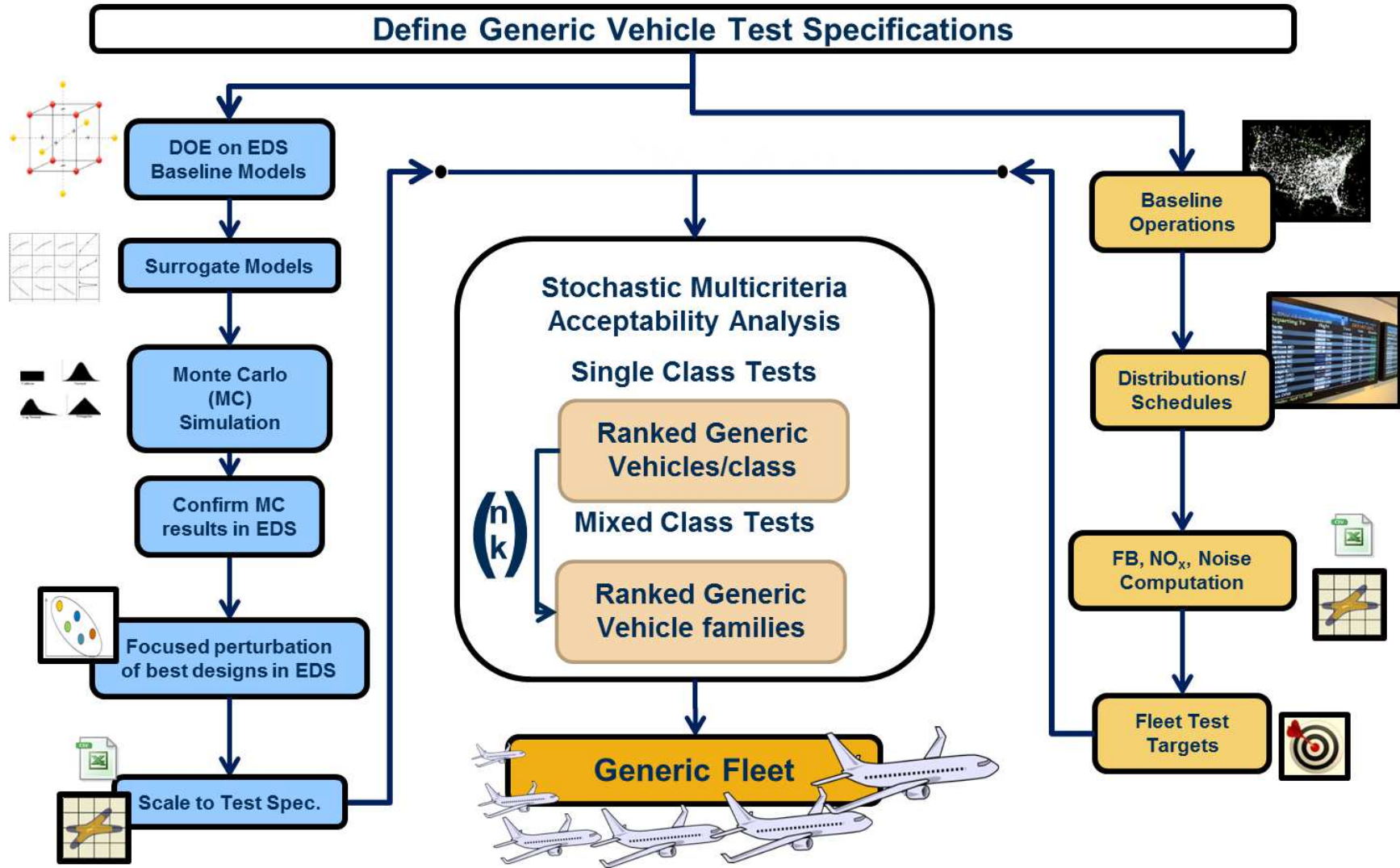
Figure 35: GENERICA Method

The test structure from Table 10 in Chapter 3 was executed sequentially. Targets for each airport were generated from the baseline schedules using the actual aircraft according to each test specification. The generic vehicle alternatives were assigned similar schedules, and the relative errors for each metric at each airport were quantified. These distribution of errors were used in conjunction with Stochastic Multicriteria Acceptability Analysis to provide information about the fitness of each alternative and choose which alternatives to carry forward to the next test.

4.4.1 Isolated Class Tests

As discussed in Chapter 3, Test A was formulated such that the EDS vehicles are characterized by a single value per metric. The performance of each potential EDS generic vehicle was aggregated in a manner consistent with the Test A specifications and relative errors were calculated at each airport, resulting in error distributions for each metric. This is notionally diagrammed in Figure 36.
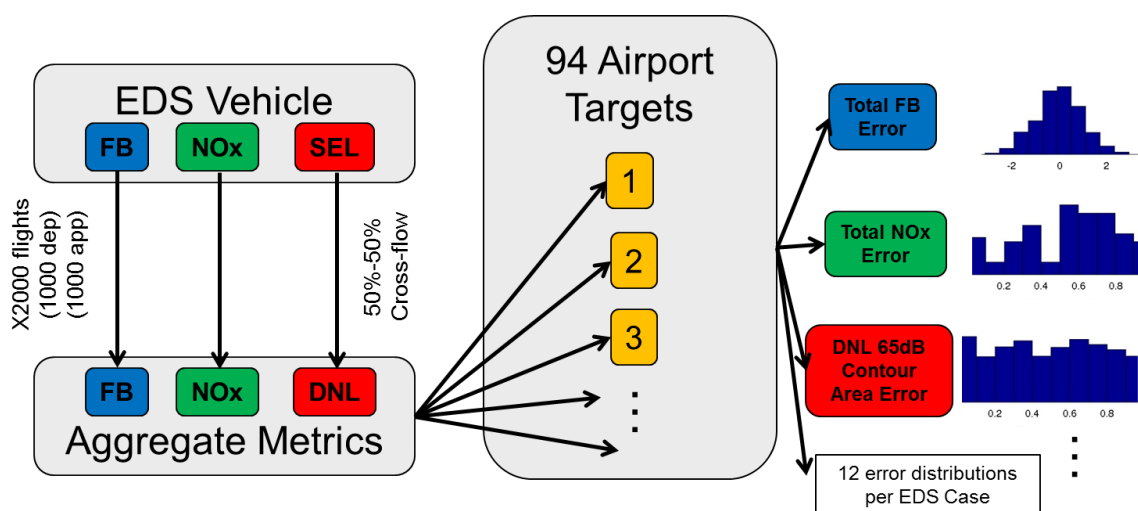

Figure 36: Diagram of Test A Structure

The choice of 2,000 flights ensured observable differences in the DNL contours. This volume of operations is consistent with some of the busiest airports in the

subset. The percentages of flights by each target vehicle were multiplied by the total number of flights (2,000 flights with 1,000 approaches and 1,000 departures) to determine the number of operations by each vehicle at each airport. In this manner, the target metrics were actually weighted by the frequency of operations for each constituent vehicle. Each vehicle was assumed to fly the same representative mission, with this mission determined using the most common stage-length operation per vehicle class in the representative schedule, as listed in Table 16. The seat classes featured a similar breakout of most common stage-lengths per class.

Table 16: Most Common Stage-Lengths per Class

Vehicle Class	Most Common Stage Length	Representative Mission [nmi]
SRJ	1	350
LRJ	1	350
SSA	1	350
LSA	1	350
STA	4	2200
LTA	6	4200
VLA	7	5200

The target airport fuel burn and NO_x metrics were computed by multiplying the vehicle-level performance of each constituent vehicle by the total number of operations at the airport. The target airport DNL contour areas, lengths, and widths (for DNL 55-dB and DNL 65-dB) were computed using ANGIM. The combination of the fuel burn, NO_x emissions, and DNL contour targets establish benchmarks that the generic vehicle model must be able to match.

To make certain that the generic vehicle models would be realistic representations of the constituent vehicles in each class, the design space exploration in EDS needed to be constrained to the feasible space. For the aircraft geometry, these constraints were simple to enforce by bounding the input parameter ranges. Ranges were derived based on subject matter expert feedback. Latin hypercube designs of experiments were

127

employed on the design space, and neural-net-based surrogate models corresponding to each metric were fit to enable surrogate-based optimization for the best generic vehicle models. Simple feed-forward neural-network architectures with between 5 and 10 hidden nodes were sufficient for each metric.

The engine designs were more complicated to constrain due to the iterative nature of the thermodynamic cycle design and engine-sizing tools within the EDS architecture (see Figure 28). Therefore the sea-level static (SLS) uninstalled thrust, overall pressure ratio (OPR), and the bypass ratio (BPR) were each outputs from EDS. These engine metrics were also modeled with feed-forward neural networks such that they could be used in conjunction with the surrogates for the environmental impact metrics.

The neural network surrogate models for each metric were imported into JMP$^{\text{TM}}$, which enabled the prediction-profiler environment. A subset of this prediction profiler environment for the LSA generic vehicle design space exploration is displayed in Figure 37. This environment allows for dynamic exploration of the design space with views of the partial derivative traces for each metric with respect to each input parameter. Figure 37 only shows a subset of the metrics (on the y-axis) and the input parameters (on the x-axis) for the sake of visual clarity. Within the prediction-profiler environment, the desirability functions were defined to give each design a utility score with respect to each metric. The desirabilities for the environmental impact metrics were designed with a nominal-is-best formulation, such that the maximum desirability of a metric corresponds to the mean of the target distributions of the 94 airports for that vehicle or seat class. Initially, the bounds for these desirability curves were set to match the standard deviations of the target distributions as suggested in Figure 25, but some of the bounds had to be relaxed due to existing bias between the actual vehicles and the EDS models. The overall desirability of an alternative is computed as the geometric mean of the desirability score with respect to each metric, as previously
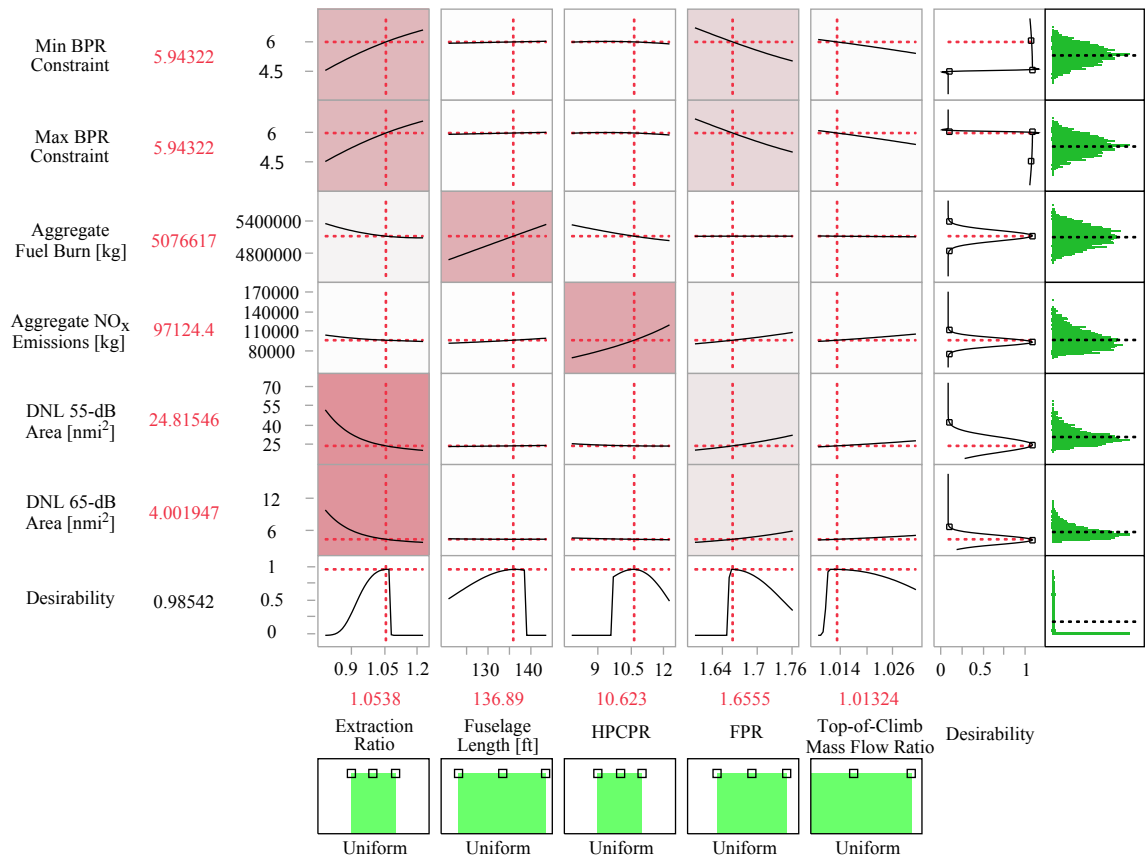
Figure 37: Prediction Profiler for LSA Generic Vehicle

described in Equation (23). The bottom row in Figure 37 shows the partial derivative traces for the overall desirability with respect to each design variable.

To bound the generic vehicle engine design, the ranges shown in Tables 12 and 13 were incorporated with additional desirability functions, effectively bringing the constraints into the objective function. Any EDS vehicle design with an engine falling outside of these ranges was deemed an inferior solution regardless of its performance with respect to the target metrics. Engine designs within these ranges received a desirability score of one for each engine metric, whereas engine designs outside of these bounds received a desirability of zero. This is demonstrated in Figure 37 for BPR. The desirability function for the first row corresponds to the minimum constraint on BPR, whereas the desirability function for the second row corresponds to the maximum constraint, although each maps to the same surrogate model.

The prediction-profiler environment allowed for rapid exploration of the design space through Monte Carlo simulations. Uniform distributions were used for each design variable, although the ranges of the uniform distribution were varied to isolate different portions of the design space. The results of the Monte Carlo samplings were aggregated in the far right column of Figure 37, including the overall desirability scores in the bottom-right cell. In this way, the subset of best generic vehicle models (with the highest overall desirability) were identified from thousands of sample points throughout the design space. While it was anticipated that the best generic vehicle designs within a class would each feature approximately the same input parameter settings, the results of the Monte Carlo simulations yielded highly feasible designs from various different points in the design space. Each of these best designs, however, tended to occur in specific locations of the engine metric space with respect to SLS uninstalled thrust, OPR, and BPR. This is demonstrated for the Large Single Aisle class via the scatterplot matrix in Figure 38.
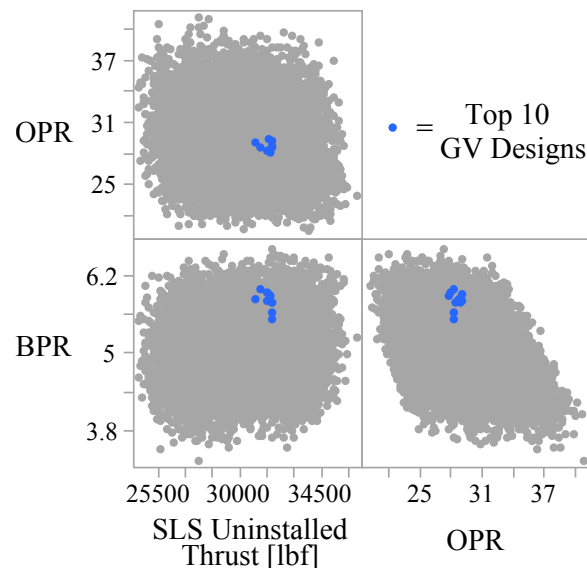

Figure 38: Scatterplot Matrix of LSA GV Engine Metric Space

This indicates the importance of the thermodynamic cycle and the engine sizing

in selecting a generic vehicle model and further validates the engine constraints required for the prediction-profiler environment. These designs were then validated by setting the design variables in EDS and generating the actual performance metrics to confirm the surrogate model results. After confirming the results for each vehicle class (as well as each seat class), it was assumed that other feasible generic vehicle models existed within close proximity of these best alternatives. Thus, to perform a focused design space exploration, the input parameters were perturbed around these best settings. For each of the top five alternatives per class from the Monte Carlo simulations, a 50-case Latin hypercube design of experiments was constructed with the input parameter ranges bound by $\pm 1\%$ deviation around these best alternatives with respect to the original input parameter ranges. This design space perturbation is demonstrated notionally in Figure 39 for a subset of the input parameters for the LTA vehicle class.
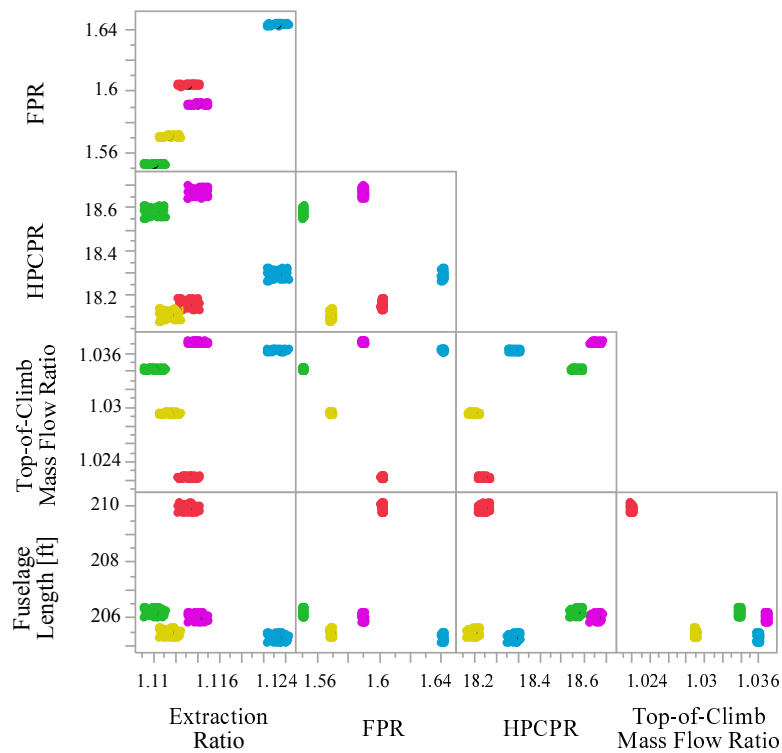

Figure 39: Scatterplot Matrix of LTA Design Space Perturbation

The performance of these designs were then evaluated for the best generic vehicle designs with respect to both Test A and Test B targets using SMAA to calculate descriptive measures for each alternative. Test B added the complexity of trip length variations for each aircraft at each airport. A Matlab-based ANGIM wrapper was designed to run each EDS generic vehicle alternative across the subset of airports using a matching stage-length distribution for each airport as notionally diagrammed in Figure 40.
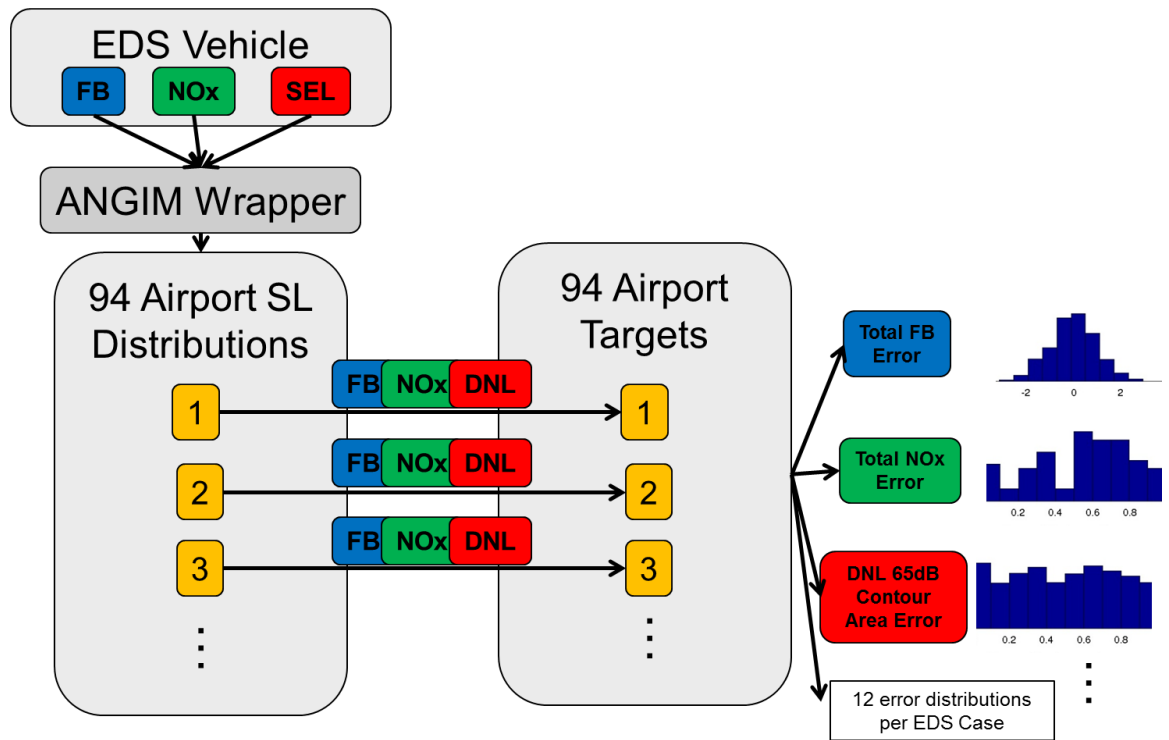

Figure 40: Diagram of Test B Structure

For each class, marginally better generic vehicle alternatives were identified from the focused perturbation design of experiments, but all of the alternatives featured similar accuracy and each were assigned comparable rank-1 acceptability scores. Each alternative also featured central weight vectors that were approximately uniform across the different criteria, suggesting that all of the alternatives featured balanced accuracy for all of the metrics. Examples of these relative error distributions

132

for total fuel burn and terminal area departure are shown in Figure 41. The total mission fuel burn distribution features very small relative error for most of the airports, whereas the terminal area departure fuel burn distribution is multimodal. The shapes of each are characteristic of the different scales for each metric.
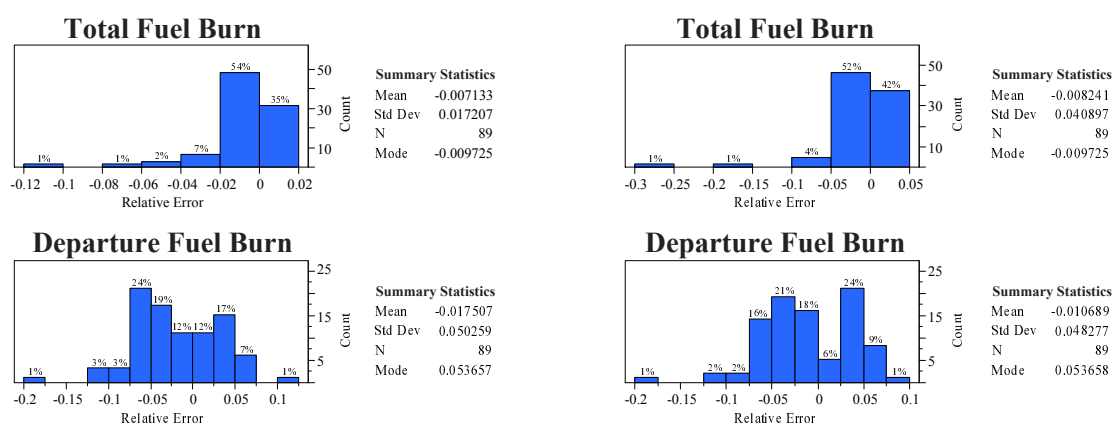

Figure 41: Tests A and B Error Distributions: Fuel Burn

Recall that Test A decouples the variance and the mean of the error distributions such that every generic vehicle alternative has identical variance. As a result, every alternative features an identically shaped distribution, but the distribution is shifted depending on the accuracy of the generic vehicle relative to the mean of the target distribution. The optimization routine attempts to center each metric distribution around zero simultaneously. The Test B formulation adds unique stage length distributions at each airport. This increases the variance of the target distribution, and the generic vehicles adhere to the same trip-length distributions. As a result the error distributions may be differently shaped between different alternatives. A comparison of the Test A and Test B distributions in Figure 41 show that the error distributions are nearly identical, however, and that unique mission lengths did not greatly increase the variance. Similar trends were observed for the NO_x emissions. This suggested that the representative mission length was an effective way to reduce

133

the complexity of the generic vehicle optimization problem.

The error distributions for the noise contour areas were also multimodal and featured much wider variance, as shown in Figure 42. Contour area was measured in square nautical miles, which is a much smaller scale than the mass metrics for fuel burn and NO_x emissions. The distributions are shaped such that there is approximately a 30% difference between the mean and the mode. If the optimizer had targeted the mode instead of the mean, the generic vehicles would consistently over-predict contour areas at most airports.
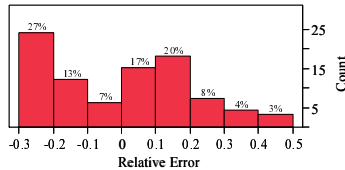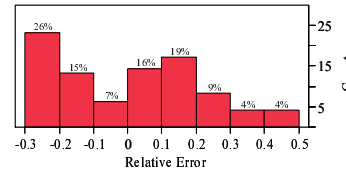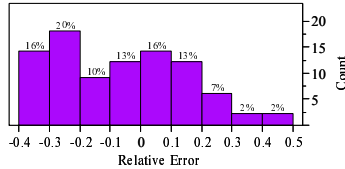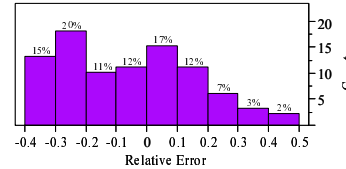
Figure 42: Tests A and B Error Distributions: Contour Area

A comparison between Test A and B once again showed little difference in the shape and variance for the noise contour area error distributions. This was the first evidence that Hypothesis 3 is supported. The subsequent tests combine all of the vehicle classes together, which makes the selection of the best generic fleet a combinatorial problem between the best alternatives in each class. A small subset of the best alternatives in each class were carried forward for the subsequent mixed class tests.

4.4.2   Mixed Class Tests

Tests C-E were each very similar in formulation, as is demonstrated by the notional diagram in Figure 43. If Hypothesis 3 is correct, Test A identified the best generic vehicle alternatives per class such that when these vehicles are mixed together they should accurately predict fleet-level fuel burn, NO_x emissions, and DNL noise contours. Test C was designed to test this assumption by generating target schedules that use the actual distributions of all the in-production vehicles and all of their stage-length operations. Test D was similar, but instead of assuming a fixed number of operations at each airport, the variability of actual average daily operations at each airport were introduced. This test also accounted for the ratio of day flights to night flights (recall that night flights receive a 10-dB penalty). Test E is similar to Test D, but each airport features a unique infrastructure characterized by the number of runways and the airport layout. Both the targets and the generic fleet are assumed to utilize each runway uniformly with cross-flow. The contour length and width netrics were replaced with the Detour Index and Spin Index, given that each airport contour features a unique shape.

For the fleet mixture tests, every generic vehicle family performed well with marginal differences in fleet-level accuracy between each combination. Between Tests C and D, it was observed that the relative error distributions for the fuel burn and NO_x emissions metrics did not change. These metrics are just linear summations of vehicle-level metrics multiplied by the number of operations, as was shown in Equation (16). Thus the target metrics and the generic fleet performance metrics scale together, leading to these identical relative error distributions. The noise metrics, however, do not scale linearly, and thus the error distributions change between these tests. For Test D, the actual volume of operations at some of the airports are relatively small compared to the default of 2,000 operations used for Test C. This can lead to misleading results when considering relative error, as small differences in the

135
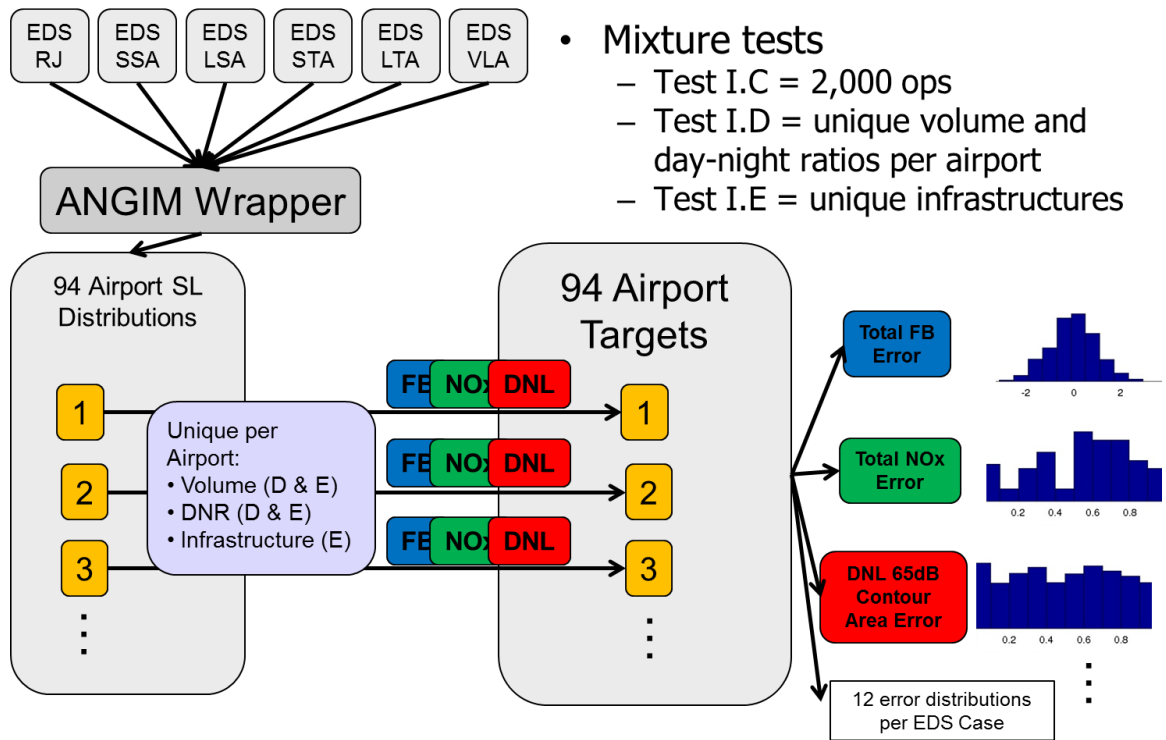
Figure 43: Diagram of Tests C-E Structure

measurements are magnified as large relative errors.

For Test E, the fuel burn and NO_x emissions were identical in formulation to Test D, since these metrics did not depend on the configuration of the airport. The noise metrics were difficult to compare to previous tests due to the introduction of unique shapes and the use of the shape metrics from Figure 16. In order to compare the effectiveness of the best average generic vehicles (as determined by the SMAA analysis) against the traditional approach of using representative vehicles, relative error distributions for each method are shown side-by-side in Figures 44, 45, and 46 for fuel burn, NO_x emissions, and noise, respectively. It should be noted that the errors for the Detour index and Spin index in Figure 46 are presented as absolute error rather than relative error, as these metrics are already scaled between 0 and 1 by normalizing with respect to an equal area circle.

As can be seen in Figure 44, the average generic vehicles for both the vehicle-class

Figure 44: Test E Error Distributions – Fuel Burn

Figure 45: Test E Error Distributions – NO$_x$ Emissions

Figure 46: Test E Error Distributions – DNL 65-dB Contours

and seat-class groupings feature a lower mean error and reduced standard deviations with respect to target total mission and terminal area departure fuel burn compared

137

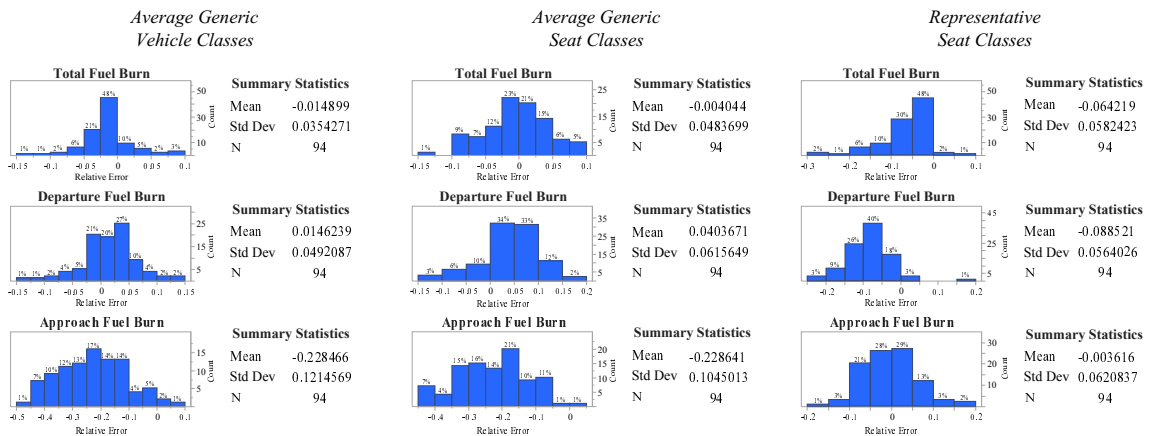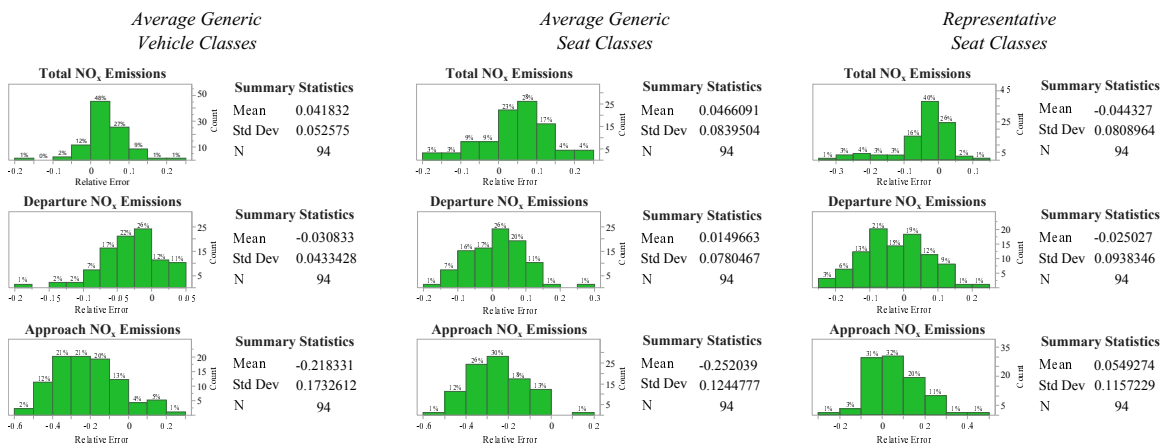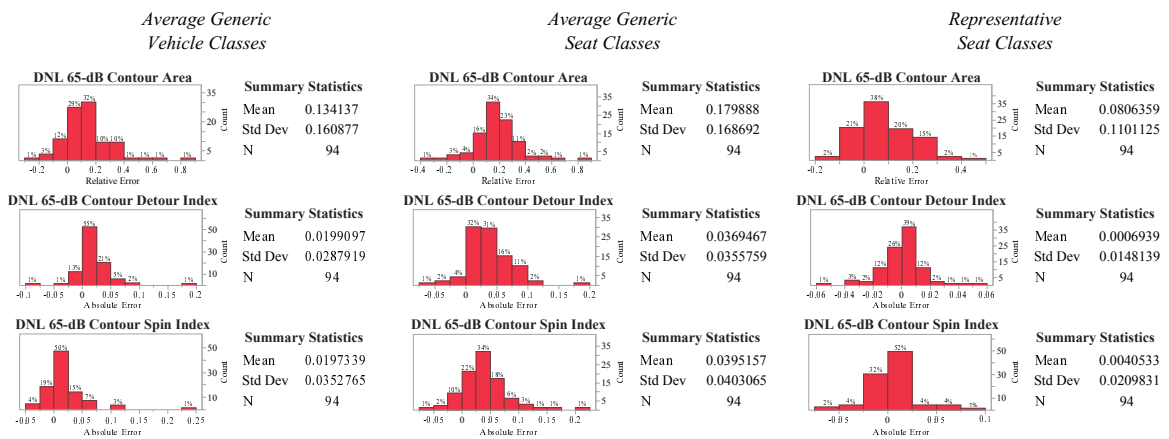to the traditional representative seat-class vehicles. While Figure 45 shows that the representative vehicles have a lower mean error than the generic vehicles for total mission and terminal area departure NO_x, the generic vehicles still feature quality average error and with less variance across the 94 airports.

For the terminal area approach metrics, the representative vehicles are consistently more accurate than the average generic vehicles. The approach metrics were omitted from the SMAA analysis due to the bias introduced by the default Continuous Descent Approach (CDA) procedures performed by all EDS vehicles (see the discussion at the end of Appendix A). The targets generated from the actual vehicles include many aircraft that fly dive-and-drive approaches with pull-up maneuvers at a 3,000-ft altitude, and as a result the average generic vehicles consistently under-predict approach fuel burn and NO_x emissions. Because the representative vehicles are simply a subset of the actual vehicles, many of them include these dive-and-drive procedures, and as a result the representative vehicle method does much better at capturing these terminal area approach metrics. However, CDA is gaining momentum and is expected to be more wide-spread in the future. Given the fact that this thesis is addressing future fleet and technology scenarios, it is anticipated that CDA will be broadly implemented and this assumption is reasonable.

At first glance, the representative vehicles seem to demonstrate more robustness than the average generic vehicles with respect to the noise targets across the subset of airports, as evidenced from lower average error and standard deviations for the contour-area and shape-metric distributions in Figure 46. A closer inspection of the results revealed that the outliers at the tails of the average generic vehicle error distributions corresponded to airports where the operations were dominated by only one constituent vehicle within a class, which typically occurs at airports with a low volume of operations. The noise contours at these airports were very small, which magnified the relative error. For airports with more operations spread across a variety
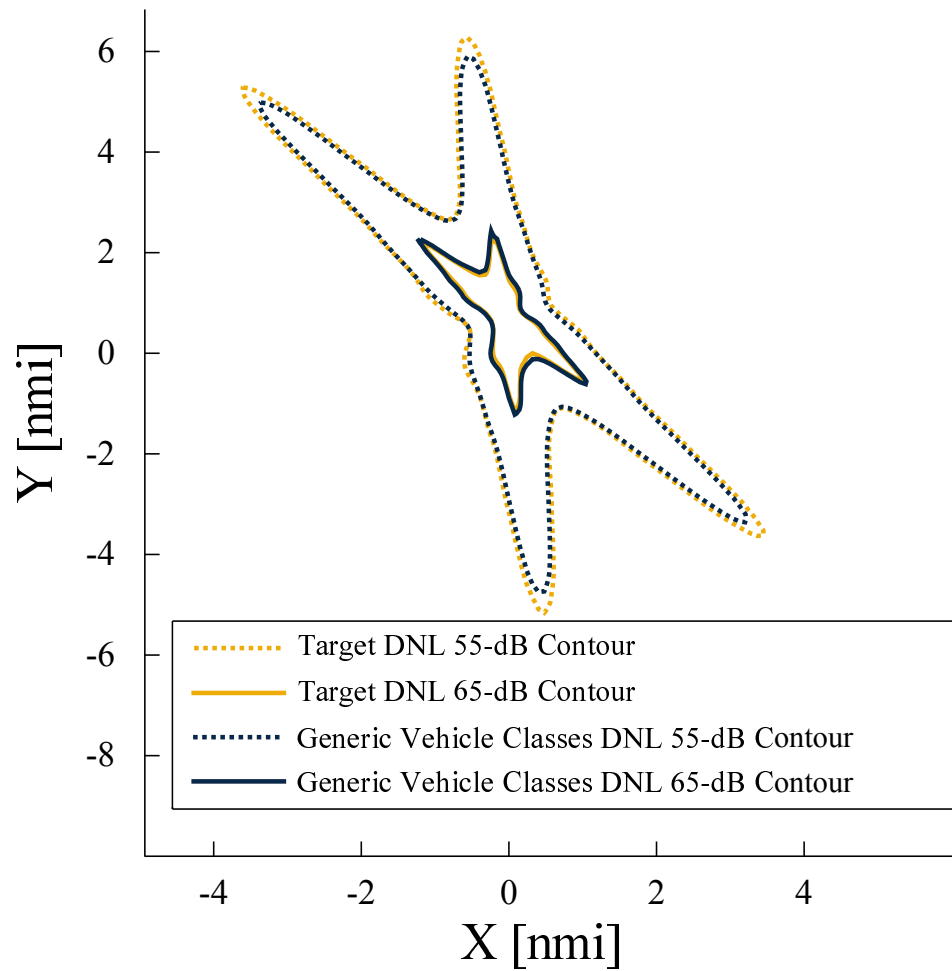
Figure 47: Sample DNL Contour Comparison

of aircraft, such as that shown in Figure 47, the generic vehicles proved to be very accurate. The only observable differences in the contours occur at the closure points of each contour lobe. These lobes are more sensitive to the approach operations, and thus the differences are attributable to the aforementioned bias introduced by differing approach procedures.

For the representative vehicles, the opposite trend was observed with larger errors at airports with more operations and a greater variety of aircraft. The representative vehicles perform well at small airports with less variety of aircraft, particularly if the few aircraft operating at that airport are actually contained within the representative set of vehicles. The relative error can sometimes be misleading because it is

139

Table 17: Relative Error of Cumulative Metrics across 94 Airports

Cumulative Metrics	Average Generic Vehicle Classes	Average Generic Seat Classes	Rep. Seat Classes
Total Fuel Burn	-1.87%	-3.57%	-9.91%
Departure Fuel Burn	0.19%	0.95%	-10.46%
Total NO_x Emissions	2.25%	-3.27%	-12.19%
Departure NO_x Emissions	-3.89%	-2.05%	-9.89%
DNL 65-dB Contour Areas	6.77%	8.28%	11.91%
DNL 55-dB Contour Areas	4.77%	5.95%	12.91%

normalized by the magnitude of the target metric. Thus, minor errors at smaller airports may be magnified as larger relative error. The relative error of the cumulative sums for each metric across the 94 airports provided another point of reference for the performance of the generic vehicles and representative vehicles. The relative errors of these sums are displayed in Table 17. These aggregate errors demonstrate the superior performance of the generic vehicles relative to the representative vehicles, particularly with respect to noise. This analysis is further supported by examining the cumulative results at a smaller subset of 34 airports with significant volume of operations, which is listed in Table 18. As can be seen, the relative error of the representative vehicles increases for most metrics, which is to be expected given the tendency of smaller target metrics to magnify relative errors. On the contrary, the average generic vehicles actually improved in relative error for most metrics for this subset of significant airports, particularly the noise contour areas.

The last major observation from the error distributions was that the vehicle-class-based average generic fleets performed only slightly better across the 94 airports than the seat-class-based average generic vehicles. This result was anticipated in Hypothesis 1, but the relative difference between the performance of these two groupings was less pronounced than expected, suggesting a robustness of the average generic vehicle methodology for various class-grouping techniques.

Table 18: Relative Error of Cumulative Metrics for the Top 34 Airports

Cumulative Metrics	Average Generic Vehicle Classes	Average Generic Seat Classes	Rep. Seat Classes
Total Fuel Burn	-1.95%	-4.12%	-11.03%
Departure Fuel Burn	-0.27%	-0.04%	-11.42%
Total NO_x Emissions	1.82%	-4.69%	-14.10%
Departure NO_x Emissions	-4.56%	-3.55%	-11.99%
DNL 65-dB Contour Areas	4.49%	6.22%	14.84%
DNL 55-dB Contour Areas	5.82%	6.31%	14.38%

4.4.3 Variable Operations Test

The final test explored the robustness of the best generic fleet to changing operational schedules. The volume of operations by each class were independently scaled from a baseline as shown in Equation (25). The scalars for each class were independently scaled from random draws on uniform distributions with a minimum of 1 (no increase in operations by that class) and a maximum of 3 (a threefold increase in operations by that class). Sixty random scenarios were generated and each scenario was applied across the 94 airports. This resulted in many different schedules featuring different volumes of operation and different class distributions.

$$Ops_{Total} = \sum_i k_i \, Ops_i \qquad (25)$$

Where:

Ops_{Total} = Total operations for scaled scenario

Ops_i = Baseline schedule operations for i^{th} vehicle class

k_i = Operations scalar multiplier for i^{th} vehicle class

For this test a new baseline schedule was used, but the performance of the generic fleet with respect to these new baseline targets did not change much from the observations in Test E. The biggest degradation occurred in the Total NO_x emissions, where the increase in error is due to the greater frequency of aircraft with advanced combustor technologies in the baseline fleet compared to the original baseline schedule. These advanced combustors specifically reduce the NO_x emissions indices for a given engine, but do not have any influence on fuel burn or noise. As a result, the average generic vehicles over-predict the total NO_x emissions, but still feature good accuracy for fuel burn and noise. This demonstrates the dependency of the average generic vehicle method on the relative frequency of the constituent vehicles in each class. The means and standard deviations for the error distributions across the scaled scenarios, however, were consistent with the baseline scenarios, as is demonstrated in Figure 48.
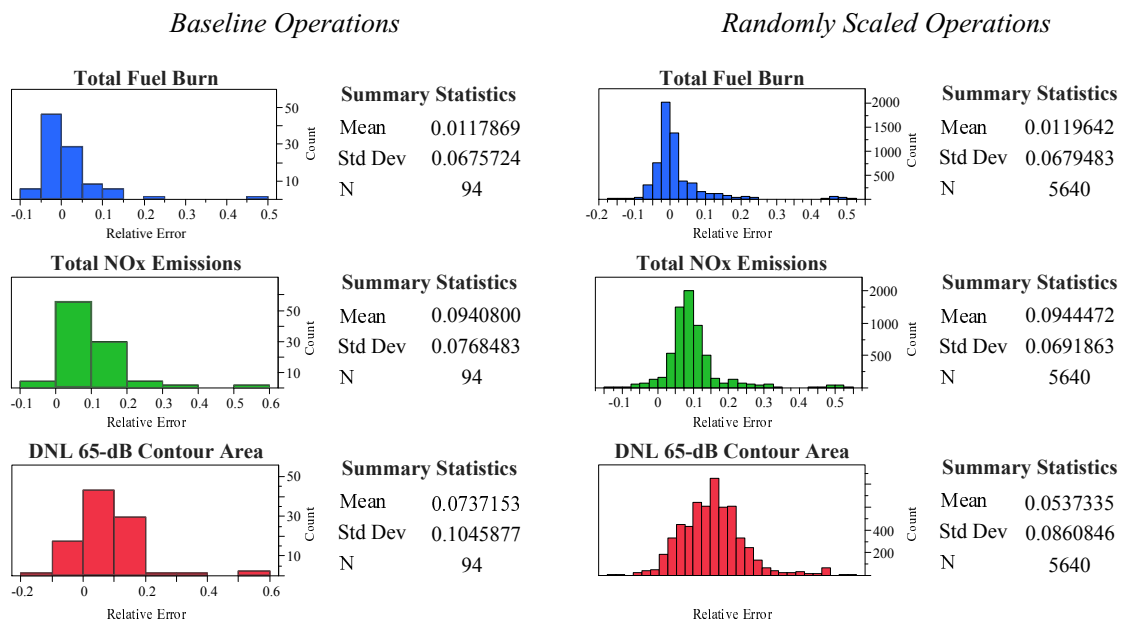

Figure 48: Test F Error Distribution Comparisons

The observations from Test F suggests the GENERICA method demonstrates robustness to changes in total volume of operations as well as changes to the relative

142

frequency of operations by each class.

4.5 Review of Hypothesis Statements

Given the observations from these average generic vehicle tests, the three hypothesis statements can now be addressed. These hypotheses are repeated in this section for the convenience of the reader.

Hypothesis 1: *A per-class average generic fleet of vehicles defined by vehicle-class groupings based on similarities in the environmental performance metrics will feature superior fleet-level accuracy compared to a per-class average generic fleet of vehicles defined by traditional seat-class groupings.*

This hypothesis is weakly supported by the results from Test E. The average generic vehicle class tends to perform better than the average generic seat class, but the differences in the error distributions and cumulative error are marginal, and both formulations outperform the representative seat-class approach. This demonstrates the robustness of the GENERICA method to any vehicle classification scheme, but groupings with less performance variability per class should still yield marginally better fleet-level accuracy. It should be noted that the vehicle-class formulation achieved slightly better accuracy with fewer groups, which is attributable to the minimization of in-class variance through discriminant analysis.

Hypothesis 2: *A fleet of average generic vehicles will more accurately approximate the DNL 65-dB noise contours across a subset of airports as compared to a traditional representative-in-class approach.*

This hypothesis is supported based on the results from Test E, particularly as

demonstrated for the cumulative metric errors listed in Tables 17 and 18. The results suggest that the GENERICA method is actually more critical for noise than for the other metrics, as the generic vehicles were more accurate for busier airports with larger contours and wider varieties of aircraft operations, whereas the representative seat-class vehicles lost accuracy with increasing operational volumes and aircraft variety.

Hypothesis 3: *If the operational distributions of each vehicle class across a subset of airports can be isolated from other operational complexities, the average generic vehicle that minimizes the mean error for the DNL noise contours across the subset of airports will also minimize the error at each airport when all of these operational complexities are reintroduced.*

This hypothesis is supported by the observations from Tests A-F. The best generic vehicle models from Test A continued to perform well as each layer of complexity was sequentially added with each test. This suggests that only Test A is required for the GENERICA method. The power of using this simplified test is that each design can be characterized by single point performance for each metric, whereas Tests B-F featured multiple performance points for the generic vehicles (one per airport for each metric). This enables the use of surrogate-based optimization techniques. Monte Carlo simulations can be used to rapidly and repeatedly sample these surrogate models thousands of time, and desirability scores allow for quick filtering of results to isolate the best average vehicle design. Thus, if the GENERICA method were to be repeated for an updated baseline year, the surrogate model approach would be sufficient. Assuming the vehicle-level modeling tool remains static, the same surrogates can be used and only the desirability functions need to be modified to reflect the change in the baseline targets.

4.6 Implementation of Population Grid Method

The generic vehicles demonstrate accuracy for contour area and shape across the subset of airports, but without measuring the population exposure counts it is difficult to determine how sensitive the true metric is to error introduced by these reduced fidelity models. This required incorporating population data conforming to the grid dimensions in ANGIM. An airport with significant population exposure was selected as a sample problem to compare various population methods, with the previously described Thiessen polygon method proving to be the most appropriate. Population grids were collected for all of the airports in the subset, and the population counts between the actual aircraft and the generic fleet were compared.

4.6.1 Comparison of Population Methods

The goal of the population method was to best approximate the area-weighted approach that typically requires importing contours into ArcGIS® and performing overlay functions on the Census block polygons. Contours for a large hub airport with multiple parallel runways were generated in ANGIM from a 2010 baseline schedule and geospatially referenced to the Latitude and Longitude of one airport runway. The contours were converted to shapefiles and imported into ArcGIS®, and the overlay and area ratio calculations were executed on the 2010 Census block polygons to get targets for the rapid population methods to match. The centroid method was also executed as a point of reference and proved to be the least accurate approach. Four grid-based methods were attempted and compared, with the results shown in Table 19.

The first three methods were each raster-based methods, while the fourth method was the Thiessen polygon grids previously described in Chapter 3. A raster is a regular array of cells, or pixels, containing numeric values [124]. They are commonly

Table 19: Population Method Comparison at Large Hub Airport

Population Method	Population Exposed (% Error)	
	DNL 65-dB	DNL 55-dB
ArcGIS® Overlay	10657 (-)	78714 (-)
Centroid Method	11366 (6.65%)	77369 (-1.71%)
1X Resolution Raster	9977 (-6.38%)	73578 (-6.52%)
15X Resolution Raster	10845 (1.76%)	78582 (-0.17%)
Pycnophylactic Interpolation	10871 (2.01%)	78286 (-0.54%)
Thiessen Polygon Grid	10842 (1.74%)	78576 (-0.18%)

used to represent map data or imagery, but can be used for quantitative data as well. The rasters worked similarly to the Thiessen polygon approach, but at the same resolution the rasters sometimes skipped over very small census blocks and total population counts were not conserved. Increasing the resolution of the raster by a factor of 15 (0.0053-nmi resolution) enabled conservation of total population counts, but at much greater computational expense. Additionally, the high-resolution raster was coupled with a pycnophylactic interpolation technique for smoother spatial gradations, but even after 50 iterations of the smoothing function the population results did not change much, suggesting the grid-resolution was fine enough. The Thiessen polygon grid method matched the 15X resolution raster grid results with much less computational expense, and thus it was selected as the most appropriate method for mapping 2010 Census block data into ANGIM.

4.6.2 Pairing Generic Vehicles with Population Grid Method

The Thiessen polygon method for exporting area-weighted population grids was executed in ArcGIS® for each of the 94 airports within the ANGIM subset, and the resulting population grids became a library of inputs within the ANGIM framework to be called at the end of noise grid calculations. To demonstrate the utility of the generic vehicles, the Thiessen polygons were used in ANGIM with the actual fleet,

the generic vehicle classes, and the representative-in-class aircraft. The cumulative results across the subset of airports are shown in Table 20.

Table 20: Fleet-Level Comparisons across Subset of Airports

Metrics	Actual Fleet	Generic Vehicles (% Error)	Representative (% Error)
DNL 65-dB Contour Area	180.63	183.90 (1.81%)	204.49 (13.21%)
DNL 65-dB Pop Exposure	254352	250146 (-1.65%)	318037 (25.04%)
DNL 55-dB Contour Area	1183.38	1168.82 (-1.23%)	1377.62 (16.41%)
DNL 55-dB Pop Exposure	4551725	4395746 (-3.43%)	5421435 (19.11%)

The contour accuracy for each of the surrogate fleet approaches is reflected in the accuracy for the population counts relative to the actual fleet. The generic vehicles are very accurate relative to the actual fleet, but the representative-in-class feature significant error due to inaccuracy at larger airports with greater population densities in the surrounding communities. To quantify the contour areas and population counts for all 94 airports using the actual fleet, execution time in ANGIM exceeded 80 minutes. The same analysis using the six generic vehicles took only two minutes. While inclusion of more technology vehicle grids will increase ANGIM's execution time, reducing the fleet to these generic vehicles introduces significant computational savings and enables more scenario comparisons.

4.7   Summary of Implementation

Discriminant analysis combined heuristics and statistical classification to assign aircraft to vehicle classes that minimized the variance within each class. Important input parameters to the physics-based vehicle-level model were identified through sensitivity analysis, and designs of experiments were constructed to create surrogate models for each metric. Surrogate-based optimization using desirability functions

147

and Monte Carlo simulations honed in on the best alternatives for each vehicle class and seat class model, and a subset of these alternatives were carried forward for the mixed class tests. The generic vehicles achieved better cumulative accuracy across the airports compared to the traditional representative-in-class approach. The vehicle-class groupings performed slightly better than the seat-class groupings, but the accuracy of both approaches demonstrated the robustness of the GENERICA method to different classification schemes. Pairing these generic vehicles with the Thiessen polygon grid method for population exposure counts demonstrated good accuracy compared to the actual fleet at a significantly reduced execution time. Therefore, the generic vehicle models and the Thiessen polygon grids represent good methods for exchanging fidelity for increased computational speed. The combination of these methods form the critical components of the screening-level framework for assessing aviation's environmental impacts.

CHAPTER V

CAPABILITY DEMONSTRATION

Chapter 4 demonstrated the GENERICA method for optimizing generic vehicle models for use with fleet-level analysis. The generic fleet can now be used as virtual testbeds for projecting fleet-level impacts of vehicle-level technologies. By modeling compatibilities, benefits, and penalties of various technology packages at the subsystem level in a vehicle design tool, bottom-up assessments of projected technological benefits can be conducted. Fleet-level exploratory forecasting requires linking the vehicle level benefits to forecasts of operations in the National Airspace System (NAS). This required some enhancements of the integrated fleet-level environment diagrammed in Figure 29, which was limited to a baseline year schedule of operations discretized into the nine mission lengths listed in Table 11. These enhancements include leveraging existing algorithms for projecting operation counts at each airport and creating technology introduction scenarios for fleet-level comparisons. Incorporating these enhancements completes the proposed framework. A few examples of screening-level capabilities for fleet-level scenario analysis are demonstrated, including fleet-level comparisons of different replacement schedules and an assessment of new runway locations under different technology scenarios.

5.1 System-Wide Fleet-Level Environmental Performance Model

Jimenez et. al extensively reviewed the current state of the art and standard methods for system-wide/fleet-level environmental performance modeling and assessment in their work [30]. They propose a system dynamics model that incorporates available

forecasts from regulatory bodies applied to a reference baseline set of operations tabulated by frequency for origin-destination (OD) pairs for each aircraft type. The Fratar algorithm is applied to converge operations at these OD pairs to a balance of operations (arrivals versus departures), as documented in Ref. [125] and notionally diagrammed in Figure 49. The model includes a scale factor for operations growth to allow for variations from the provided forecasts to allow more parametric scenario analysis.
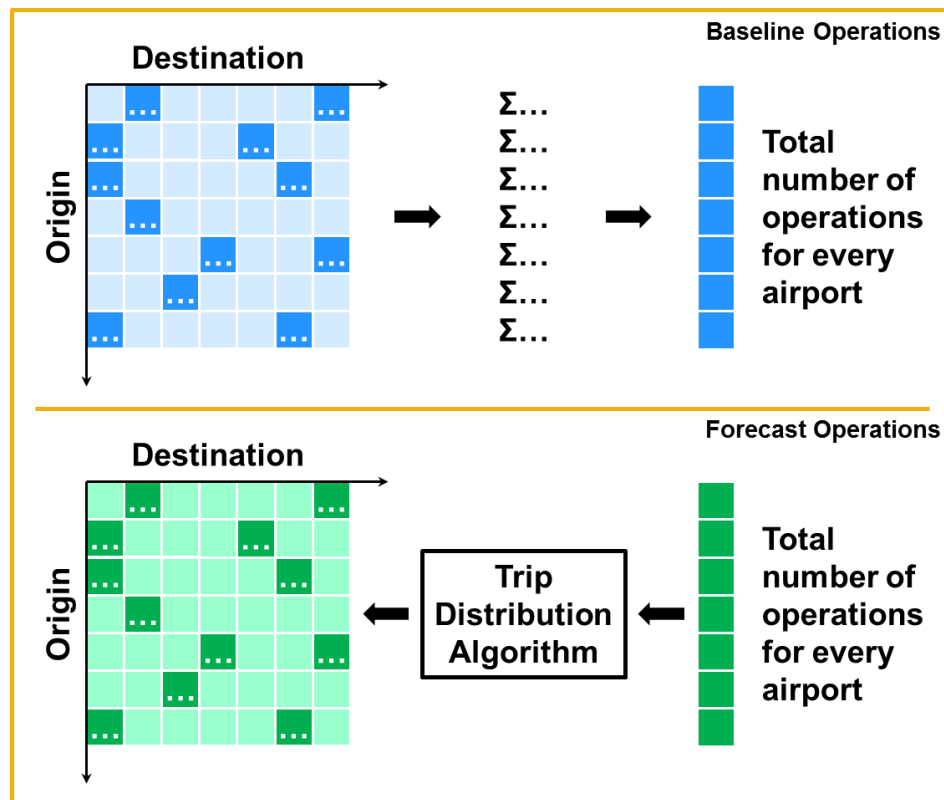
Figure 49: Forecasts and Fratar Algorithm for Origin-Destination Pairs

Fleet-level evolution is formulated by means of a retirement and replacement scheme notionally depicted in Figure 50. Retirements model the removal of aircraft from the operating fleet, whereas replacements capture the introduction of new aircraft. Age of the current aircraft types are tracked, and empirical survival curves based on regulatory standards prescribe the percentage of aircraft that remain in

operation as a function of age [126]. The replacements algorithm implements aircraft type assignments for operations associated with retirements as well as for operations comprising activity growth for a given out year. The replacement formulation is chronological (Out-of-Production, In-Production, and Future), dependent on the mission capabilities (range and payload/seat capacity) of the new fleet as compared to the operations that must be allocated, and assumes that new aircraft have comparable or improved fuel burn relative to the vehicles they replace.
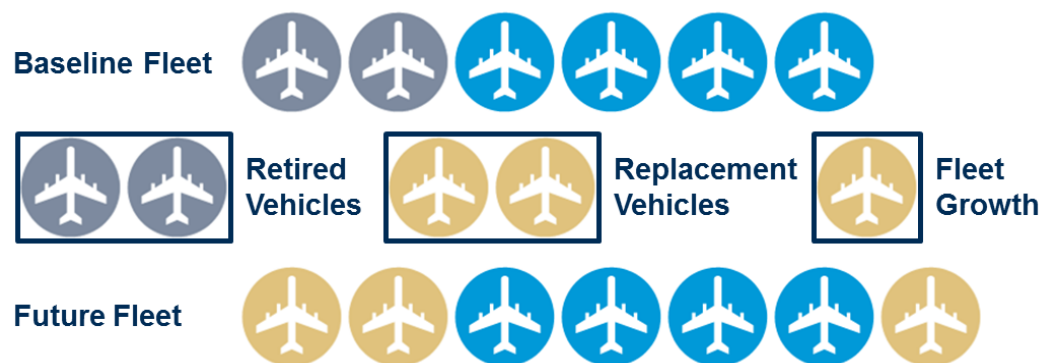
Figure 50: Fleet-Level Evolution via Retirement and Replacement

Once final operational assignments are set, the operational frequencies for each aircraft at each mission range are linked to regressions for fuel burn versus range, as formulated in Equation (16). The regressions are derived from standard least-squares method for each aircraft assuming a quadratic functional form, using operation counts as frequency weights [127]. In this manner, fuel burn and emissions are calculated over time depending on the chosen forecast scenario and the specified vehicle introduction rate. This modeling tool is commonly referred to as the Global and Regional Environmental Aviation Trade-off (GREAT) tool [30, 128]. GREAT, however, was only designed for modeling fuel burn and NO_x emissions. Noise analysis was not included in its formulation because of the additional complexities and computational burdens of calculating noise.

151

By using the GREAT formulation to dynamically create the flight schedule input files required by ANGIM, these two fleet-level modeling tools can link system-wide performance with respect to each of the relevant metrics. The logic for linking these tools is diagrammed in Figure 51. GREAT contains a comprehensive list of airports to capture the OD pair dynamic across the entire NAS, but the noise analysis is only focused on the previously defined subset of airports with community exposure to significant noise. Furthermore, GREAT models operations annually, but the computation run-times of even a rapid noise tool like ANGIM prohibit yearly noise calculations. Instead, the noise analysis filters only the operations at the subset of airports for every tenth year (2010, 2020, 2030, 2040, and 2050).[1] Operations by each vehicle type at each airport are tabulated, and percentages of replacement operations at each airport are also tracked.[2] The baseline schedule of operations are then scaled to match the total operations and percentages per vehicle. These scaled operations are mapped to flight schedule input files for ANGIM, which are then paired with the runway configurations at each airport and executed to generate DNL grids and define DNL contours. In this manner, the changes in these contours can be observed as a function of the GREAT fleet-evolution scenario enabling comparisons between metrics subjected to common operational assumptions.

---

[1]The resolution of noise analysis could be refined to every five years, but as always improved resolution requires a tradeoff in run-times.

[2]Currently the method includes only the baseline average generic vehicles and future technology vehicles. Out-of-production noise grids are not included, although the total volume of operations in the base year are conserved and allocated to the baseline average generic vehicles. This means that the noise analysis may under-predict contour sizes in early years, but the results become more representative in future years as out-of-production aircraft are retired. The method could be enhanced in the future to include noise grids for the out-of-production aircraft, but once again at cost of computation run-time.
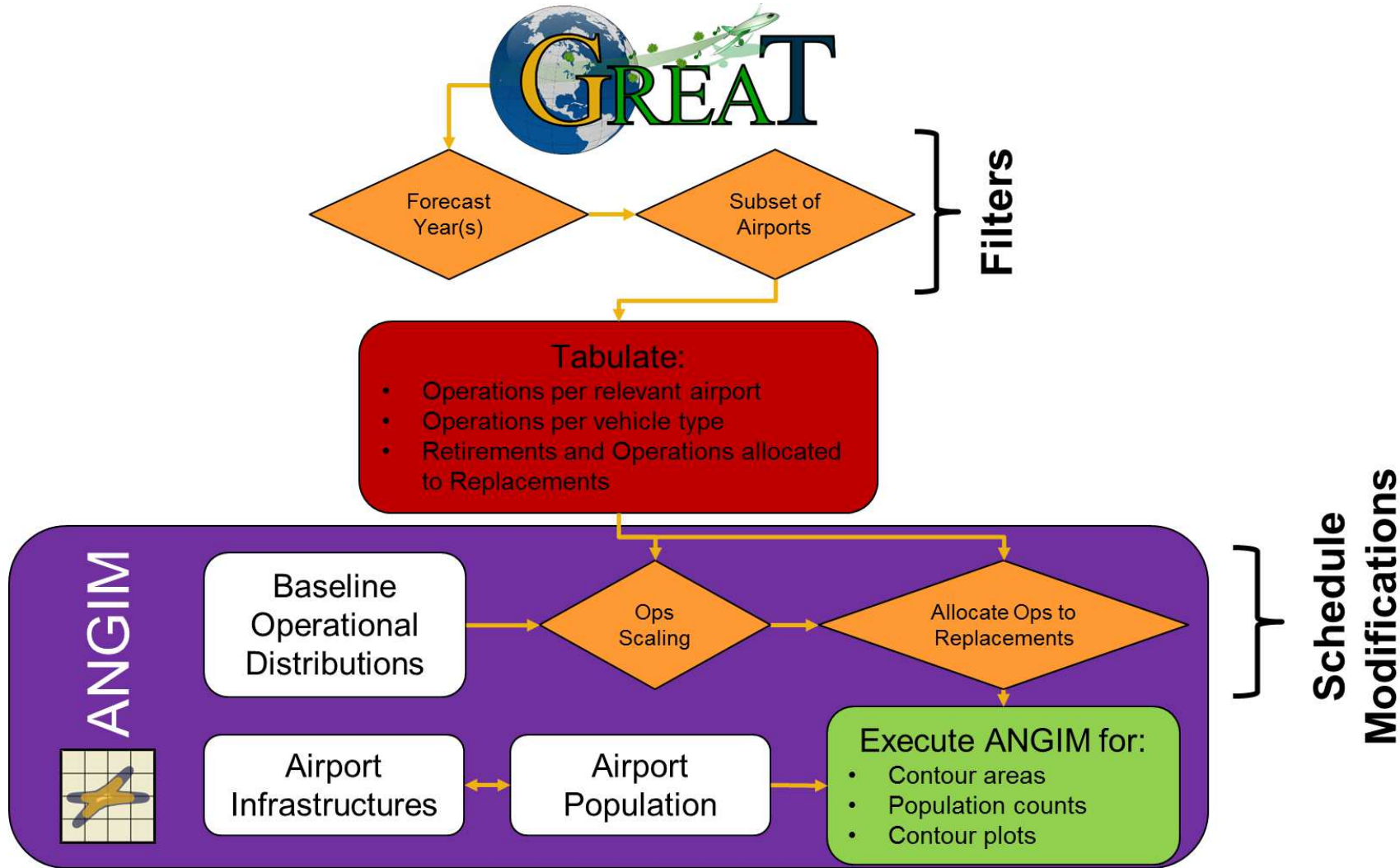
Figure 51: Linking GREAT and ANGIM

5.2 Technology Infusion on Average Generic Vehicles

The average generic vehicles were designed to be used as virtual testbeds. By designing these vehicles in EDS, technology infusion can be modeled at the subsystem level to capture system level benefits or penalties and capture trade-offs between different environmental performance metrics. A library of many different technology models have been developed at Georgia Tech under the CLEEN and ERA programs. These technologies map to changes in the input design variables with respect to the baseline average generic vehicles through a k-factor approach, implemented through a Technology Impact Matrix (TIM) [129]. Technologies considered fall into one of seven categories:

1. 2010 Baseline Technologies

2. Airframe Lightweight Structural and Sub-System Technologies

3. Airframe Aerodynamic Technologies

4. Airframe Noise Technologies

5. Engine Fuel Burn Technologies

6. Engine Noise Technologies

7. Engine Emission Technologies

The amount of change for each input design variable depends on the specific technologies considered, compatibilities between technologies, and interdependencies of simultaneously infused technologies that may mitigate benefits relative to each technology in isolation. In practice many different technology packages may be infused for exploring many different technology scenarios, but for simple demonstration of how these new technology vehicles are used in a fleet-level tool, only two scenarios shall be defined. A Moderate (MOD) investment in technology and an Accelerated

154

(ACC) technology scenario were defined, with each scenario featuring an N+1 and an N+2 generation. The MOD scenario focuses on polymer matrix composite technologies on the engine and advanced engine liners for noise reduction in the N+1 time frame. In the N+2 time frame, the MOD scenario adds to the previous technologies with advances in materials for engine components with advanced powder metallurgy and high temperature erosion/thermal barrier coatings. Damage arresting stitched composites lead to reductions in aircraft structural weight, and other airframe improvements lead to improvement in aerodynamics and a reduction in airframe noise from flaps and landing gear. For the ACC scenario, the N+1 vehicles match the MOD N+2 vehicles, with an optimistic assumption that these technologies advance in TRL faster and are incorporated into the manufacturing process earlier. This allows for additional advancements in the N+2 timeframe, including active flow and clearance control for compressors and turbines, improved airframe aerodynamics through hybrid laminar flow control (HLFC), and reduced structural weight from advanced composite fabrication and structure joining methodologies. The only additional noise technology for the N+2 vehicles are acoustic lines for slat inner surfaces.

The same technology scenarios were applied to each of the baseline generic vehicle models. The resulting changes in the engine specifications and aircraft thrust and weight for each class subject to each technology scenario are listed in Tables 21 and 22. It should be noted that no engine emission technologies were considered for these scenarios. While the CLEEN and ERA project have modeled several advanced combustor technologies that significantly reduce NO_x emissions, most of these technology models were deemed proprietary and thus could not be used in this analysis. As a result, all savings in NO_x emissions are due strictly to corresponding reductions in fuel burn, and at times these emissions even increase due to the fact that many of the engine technologies enable higher overall pressure ratio (OPR) for higher fuel efficiency while mitigating increases in engine weight as listed in Table

21. For this reason, the results presented from this point forward will only focus on fuel burn and noise, with explorations of NO_x emissions reserved for future work.

Table 21: Engine Specifications for Technology Scenarios

Vehicle Class	OPR				BPR			
	GV	MOD N+1	MOD N+2[1]	ACC N+2	GV	MOD N+1	MOD N+2[1]	ACC N+2
RJ	23.08	23.11	23.11	23.10	5.10	5.23	5.24	5.25
SSA	27.38	43.622	47.07	54.78	5.59	8.80	10.85	12.30
LSA	28.25	40.13	43.25	50.35	5.95	9.02	11.01	12.41
STA	33.76	41.10	48.20	61.60	5.15	11.36	12.95	13.49
LTA	36.85	40.81	46.77	59.83	8.41	11.48	13.06	13.76
VLA[2]	29.03	32.70	39.39	50.12	5.14	14.09	16.25	17.31

[1] ACC N+1 aircraft is the same as MOD N+2 aircraft

[2] VLA has 4 engines, all other vehicles have 2 engines

Table 22: Aircraft Static Thrust and MTOW for Technology Scenarios

Vehicle Class	Static Thrust [lbf]				Maximum Takeoff Weight [lb]			
	GV	MOD N+1	MOD N+2[1]	ACC N+2	GV	MOD N+1	MOD N+2[1]	ACC N+2
RJ	14362	13624	13758	14024	84343	68495	69182	70549
SSA	22970	21543	20110	18803	151557	142208	132803	124272
LSA	30634	28651	26626	25087	200057	186624	174369	164975
STA	57090	46883	43925	40279	386710	316278	295892	272560
LTA	100972	80884	74376	67468	675272	539375	496442	450977
VLA[2]	54361	48917	44887	40951	852452	768888	702731	641346

[1] ACC N+1 aircraft is the same as MOD N+2 aircraft

[2] VLA has 4 engines, all other vehicles have 2 engines

Table 21 also shows that the technologies drive the engines towards higher bypass ratios. Historically, this is the best way to reduce engine jet noise, and thus it is anticipated that these high BPR engines should significantly reduce the aircraft noise signature. Table 22 demonstrates how the technologies generally reduce the maximum takeoff weight (MTOW) and the static thrust. The reduction in thrust required is

related to the weight savings, which should lead to significant fuel savings. The weight and thrust reductions have competing effects with respect to noise. The reduction in takeoff thrust required should reduce the noise signature of the aircraft, but reducing thrust may also impact the climb performance with shallower trajectories leading to extended contour lengths.

The resulting fuel burn savings corresponding to each scenario are displayed in Figures 52 and 53, with results broken up into narrow-body (RJ, SSA, LSA) and wide-body (STA, LTA, VLA) aircraft for visual clarity. As can be seen, the fuel savings increase with longer mission ranges, and the savings are much greater for the wide-body aircraft. The fuel savings increase with each technology advancement for all aircraft except the RJ vehicles, which actually feature marginal degradation in fuel savings with technology advancement. The OPR and BPR for the RJ vehicles do not change much between technology scenarios, and while the RJ MOD N+1 does feature some thrust and weight savings, the successive technology generations actually lead to increases in both thrust and weight.
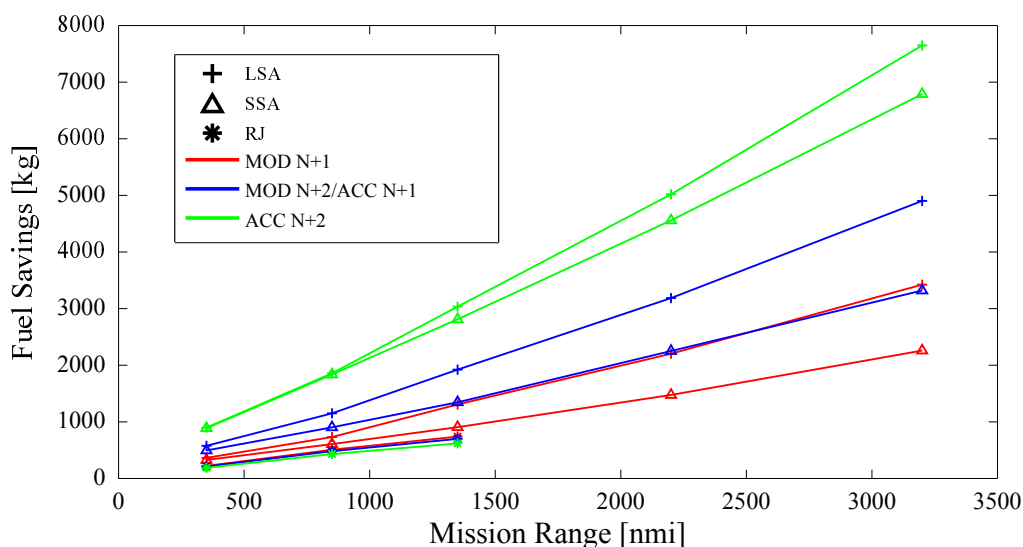

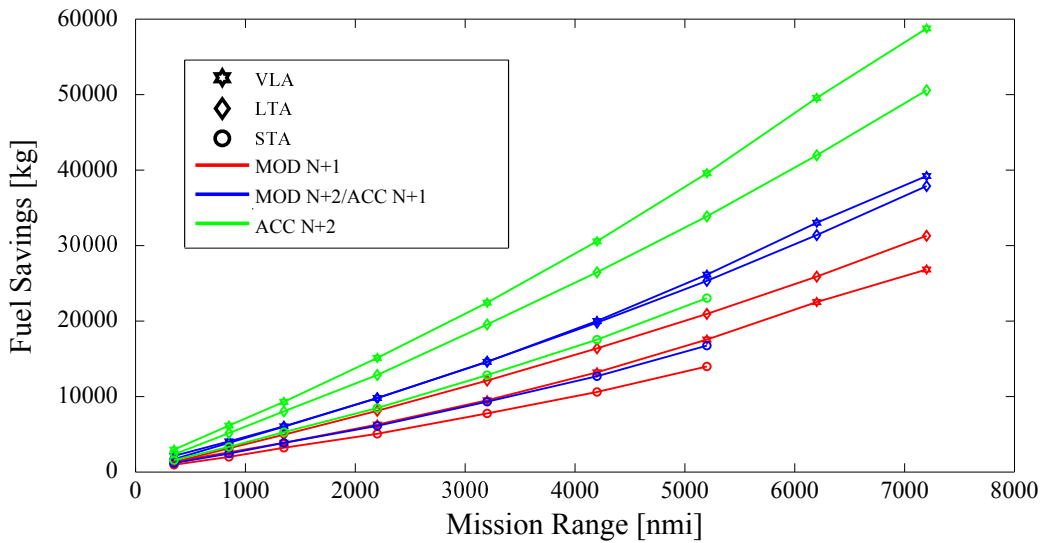Figure 52: Fuel Savings for Narrow-Body Aircraft

Figure 53: Fuel Savings for Wide-Body Aircraft

The noise technologies lead to significant reductions relative to the baseline average generic vehicles, but the relative differences between each technology vehicle are minor. A sample of the SEL 80-dB approach and departure contours for the LSA vehicle are shown in Figures 54 and 55, respectively. The departure contours correspond to a representative stage-length 1 mission. The MOD N+1 technology infusion significantly reduces the noise signature due primarily to a 50% increase in BPR. The more advanced technology portfolios, however, focus more on structural weight reductions which results in only incremental improvements in the noise signature. The ACC N+2 vehicle actually features a slightly longer contour, which is a consequence of the reduced engine thrust and the terminal area trajectories. Similar trends were observed for the other vehicle classes, with the level of improvement varying with size. The LTA and VLA aircraft feature greater reduction in the noise signature. The RJ aircraft already had a small noise signature, and the BPR does not change much with technology integration and thus the reduction in the noise footprint is less pronounced. It should be noted that while the RJ noise contours are small, this vehicle significantly contributes to DNL noise contours at many airports

due to the frequency of operations [130].
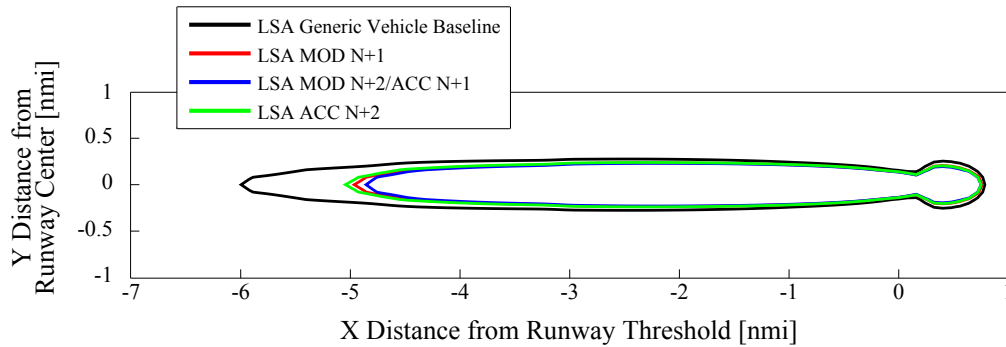
Figure 54: Noise Contour Reductions for LSA: Approach
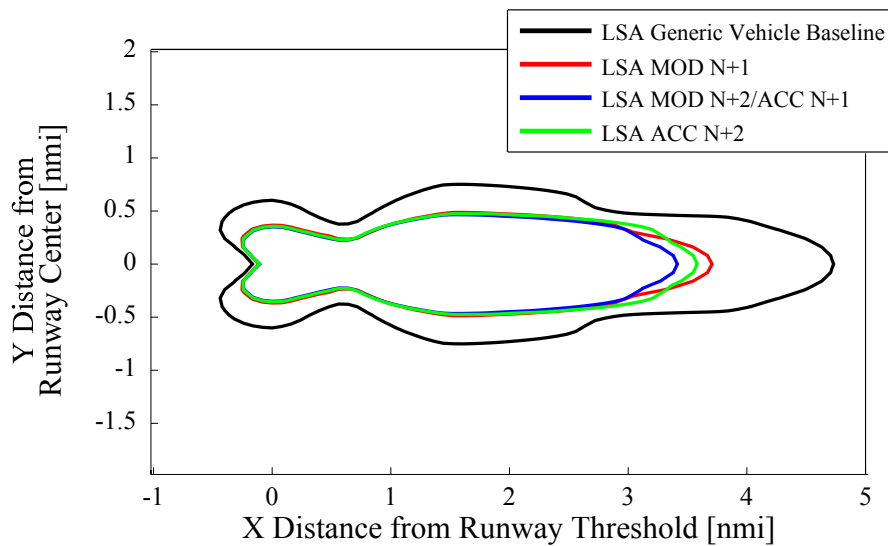
Figure 55: Noise Contour Reductions for LSA: Departure

While the vehicle-level results from technology infusion demonstrate greatly improved performance, the true impact of this technology infusion depends on the relative frequency of operations by each vehicle type. To reduce fleet-level environmental impacts, these new technology vehicles must be introduced to the fleet, and thus fleet-level performance will also depend on the replacement schedules for each vehicle type.

159

5.3   Fleet-Level Scenario Analysis

After including the link between GREAT and ANGIM, the technology infused generic vehicles, and the population grid method introduced in the previous chapter, the final enhanced integrated environmental design tool can be used for fleet-level analysis. This enhanced environment is diagrammed in Figure 56. This enhanced environment is referred to as the GREAT-A method, as it links the previously developed capabilities of GREAT and ANGIM to common and consistent operational schedules.
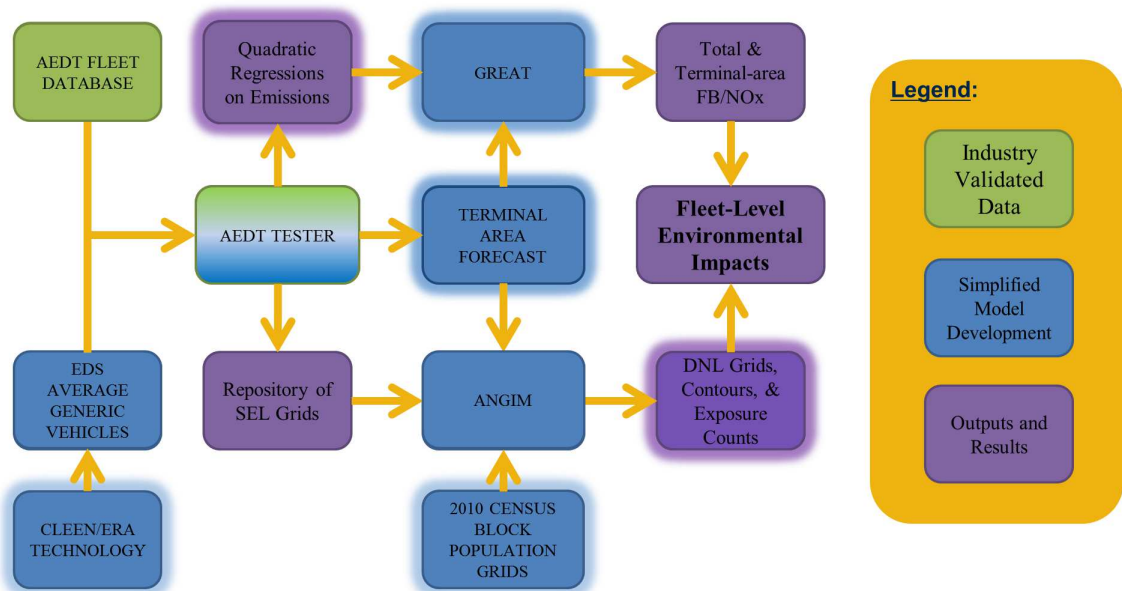
Figure 56: Enhanced Fleet-Level Environment with Specific Tools

5.3.1   Technology Vehicle Replacement Schedules

With these enhancements, various market introduction scenarios can be explored to simultaneously visualize resulting impacts on fuel burn, NO_x emissions, and significant noise exposure. These impacts will vary depending on the forecast used, but the scenarios analyzed in this chapter use the FAA's Terminal Area Forecast (TAF) as a baseline [131]. GREAT includes a capability to parametrically scale a

given forecast to explore different scenarios, but for the purposes of demonstrating the capability no scalings were applied. The forecast of operations by each class are shown in Figures 57 and 58. As can be seen from the scales on each plot, total operations by aircraft in the narrow-body classes (RJ, SSA, LSA) is an order of magnitude greater than total operations by aircraft in the wide-body classes (STA, LTA, VLA). The operations by the existing fleet are represented by the solid lines, while replacement operations are represented by dashed lines. The TAF forecasts a significant increase in demand for RJ, SSA, and STA replacements compared to current day operations by existing aircraft, whereas demand for LSA, LTA, and VLA replacements increase more steadily. It should be noted that GREAT uses an earlier baseline year, which explains why the replacement operations are not zero in 2015.
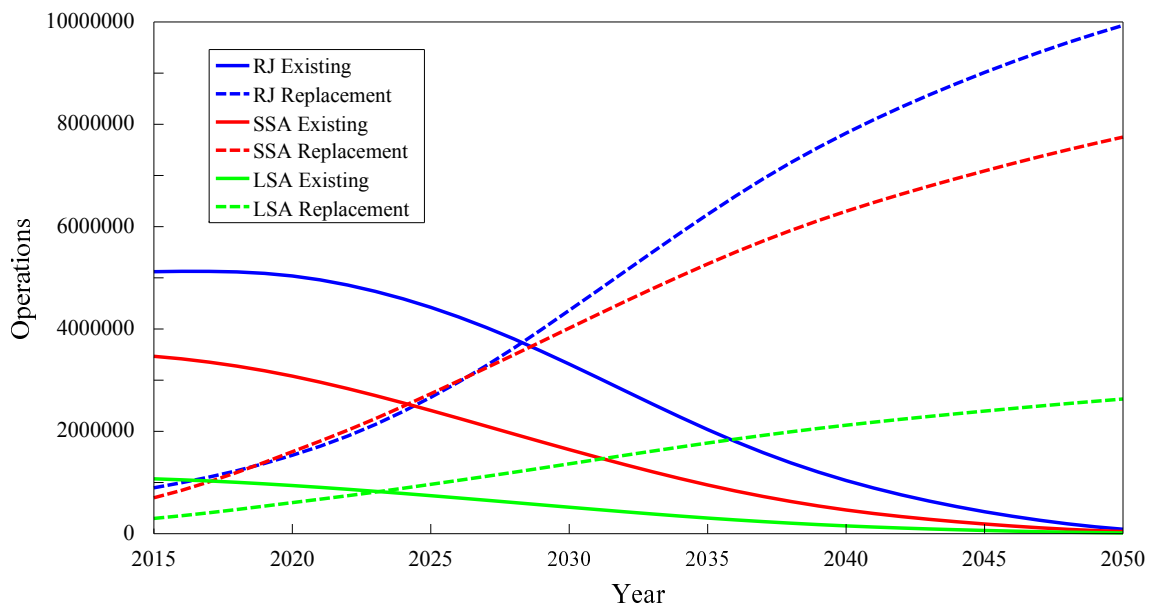
Figure 57: Forecast of Operations for Narrow-Body Aircraft

Aircraft manufacturers typically have limited resources to carry out research and development for multiple programs simultaneously, and thus they must prioritize certain aircraft types depending on customer demand for replacements [89]. As a sample problem, the market introduction schedules from Ref. [89] were used. The

161
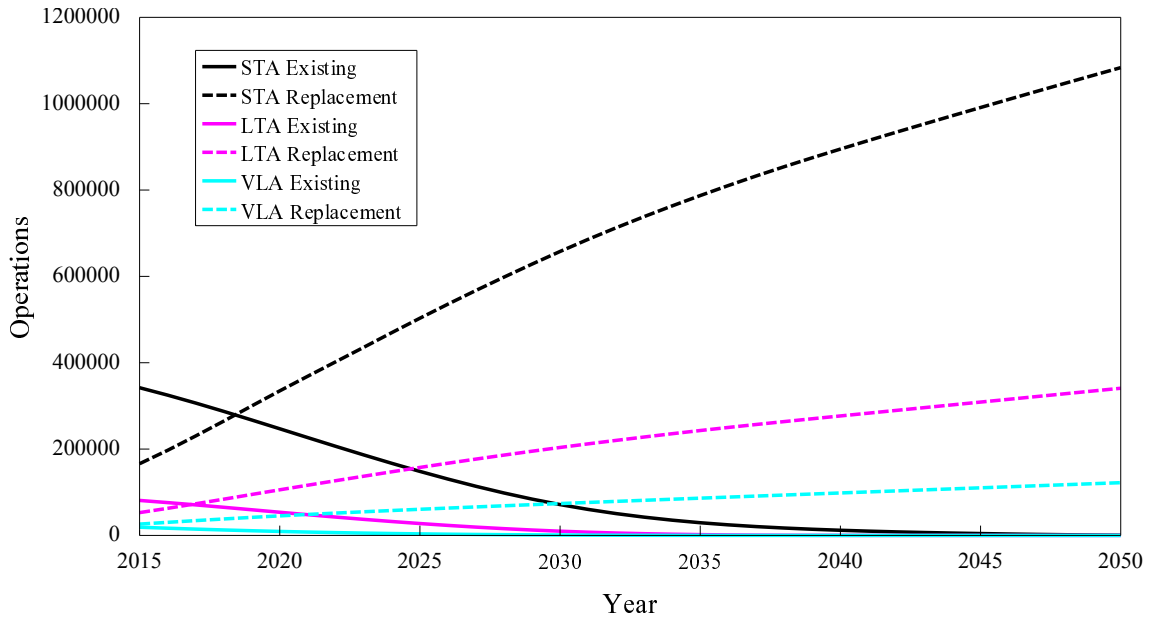
Figure 58: Forecast of Operations for Wide-Body Aircraft

introduction rates for each vehicle class are shown in Figure 59. Note that "SA" refers to the Single Aisle classes (SSA and LSA). Since the vehicles in the LSA class are essentially stretched versions of those in the SSA class, it is assumed that they will share similar future designs which should allow them to be developed in parallel.
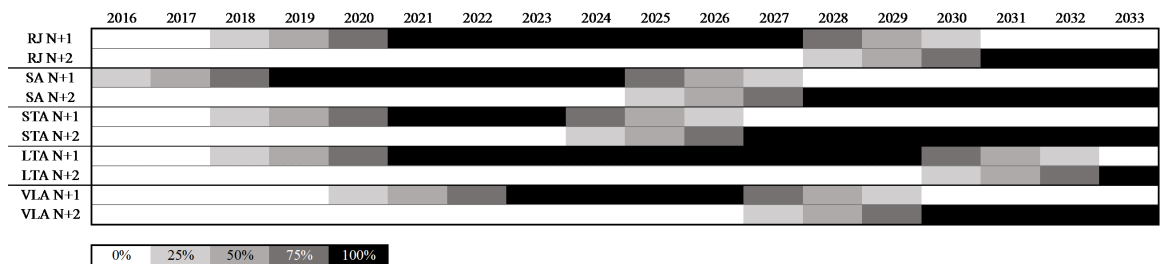
Figure 59: Baseline Technology Vehicle Replacement Schedule

Until the first introduction of N+1 technology vehicles in 2016, all replacement operations due to the combination of retirements and growth are assigned to the baseline average generic vehicles that represent current in-production vehicles. Each N+1 technology vehicle is phased in gradually over four years. In the first year, 25% of replacement vehicles are N+1 technology vehicles, while the other 75% are still

162

average generic vehicles. The following year the replacements are split 50%-50%, and so forth until after four years 100% of replacement operations are allocated to N+1 technology vehicles.

Further in the future, the N+2 vehicles are also phased in over four years while the N+1 vehicles are phased out. This does not mean the N+1 vehicles are retired, but rather that all replacement operations are eventually allocated to the N+2 vehicles. This phase-in structure is common for each vehicle class, but the introduction dates are staggered due to the limitations on R&D investment in parallel vehicle development programs. This schedule was derived from a market study described in Ref. [132].

The baseline replacement schedules were applied to both the MOD and ACC technology scenarios. Since they each use the same market introduction schedule it is difficult to glean any information about the sensitivity of results to the technology introduction rates. In order to demonstrate how critical the vehicle introduction dates are to the projected results, a simple deviation from the baseline market introduction schedule was formulated and run through the integrated environment for comparison. The same technology scenarios were considered, but a new market scenario was created such that the Very Large Aircraft (VLA) technology aircraft are introduced earlier and the Small Single Aisle (SSA) and Large Single Aisle (LSA) programs are delayed. This notional scenario, shown in Figure 60, represents a future where airlines demand advancements in the larger aircraft due to the cumulative fuel savings over large range missions.

In this notional scenario, the aircraft manufacturers prioritize the VLA program at the expense of delays in the SSA and LSA programs. This particular scenario was chosen to exploit previous observations of the area and spatial contributions of the SSA and LSA classes to DNL contours at these airports [130, 133]. The VLA, by comparison, contributes very little to the DNL contours despite having the largest

163
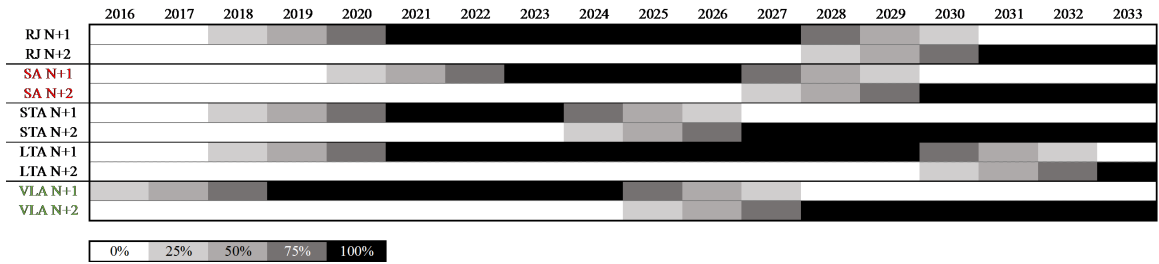
Figure 60: Alternate Technology Vehicle Replacement Schedule

vehicle-level noise footprint because of the relative infrequency of flights compared to other vehicle classes.

5.3.2 Fleet-Level Results

The first analysis isolated the impacts of each technology scenario with respect to a common baseline replacement schedule. Results were compared against a Business-as-Usual (BAU) scenario where all future replacements are allocated to the baseline average generic vehicles. This scenario represents a very conservative worst case, where no new aircraft types or improved technologies ever enter use in the fleet. This means that after all out-of-production aircraft have been retired the entire fleet behaves as a homogeneous mix of current in-production types. The second analysis repeated the technology scenarios under the alternate replacement schedule, once again comparing against the BAU scenario. The results for each were quantified in terms of savings relative to this BAU scenario.

Figure 61 overlays the cumulative fuel savings versus time for each technology and replacement scenario. The cumulative savings relative to the BAU scenario grow in time due to the increasing prevalence of operations by technology vehicles. Additionally, the total volume of operations is steadily increasing over time. For the alternate schedule, it was anticipated that the earlier entry of the VLA technology aircraft would lead to better cumulative savings in time due to the significant
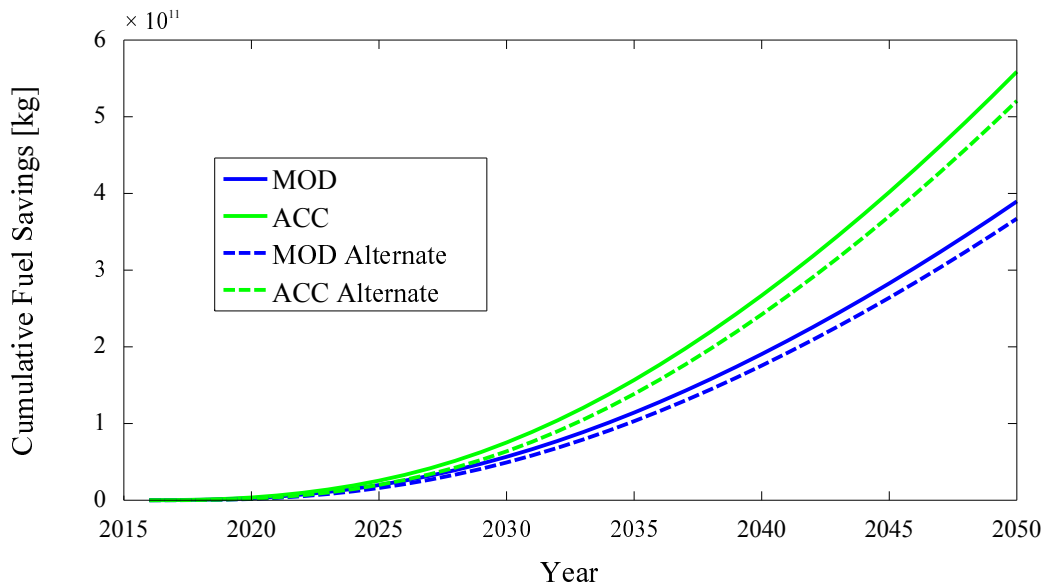
Figure 61: Cumulative Fuel Burn Savings

vehicle-level savings observed in Figure 53, but in fact the cumulative savings lag the baseline schedule. The shift in the cumulative savings curves directly correspond to the delay in the single aisle programs. This highlights the importance of the SSA and LSA classes which account for a majority of the NAS operations.

A better way to measure the fleet-level efficiency of each scenario is to normalize the total fuel burn by the cumulative flown distance by the entire fleet. Figure 62 shows these efficiencies for each technology scenario as well as the BAU scenario. Even the BAU scenario improves in efficiency in the early years, as out-of-production vehicles with poor fuel economy are retired from the fleet and replaced by current in-production aircraft. Over time, however, the fuel efficiency starts to degrade due to changes in the distribution of flights between the classes, particularly due to the sharper increase in demand for SSA flights. The MOD scenario also features a parabolic change in fuel efficiency, but the inflection point is delayed later in time. The ACC scenario repeats the pattern, but with a much shallower parabolic shape and an inflection point occurring much later in time. The alternative schedule scenarios demonstrate the same trends, but at slightly reduced efficiency. In order to

165

avoid the eventual degradation in fuel efficiency in these future years, more advanced vehicles with unconventional configurations must be introduced, but adopting a more aggressive technology scenario in the near term delays the necessity for these advanced configuration vehicles.
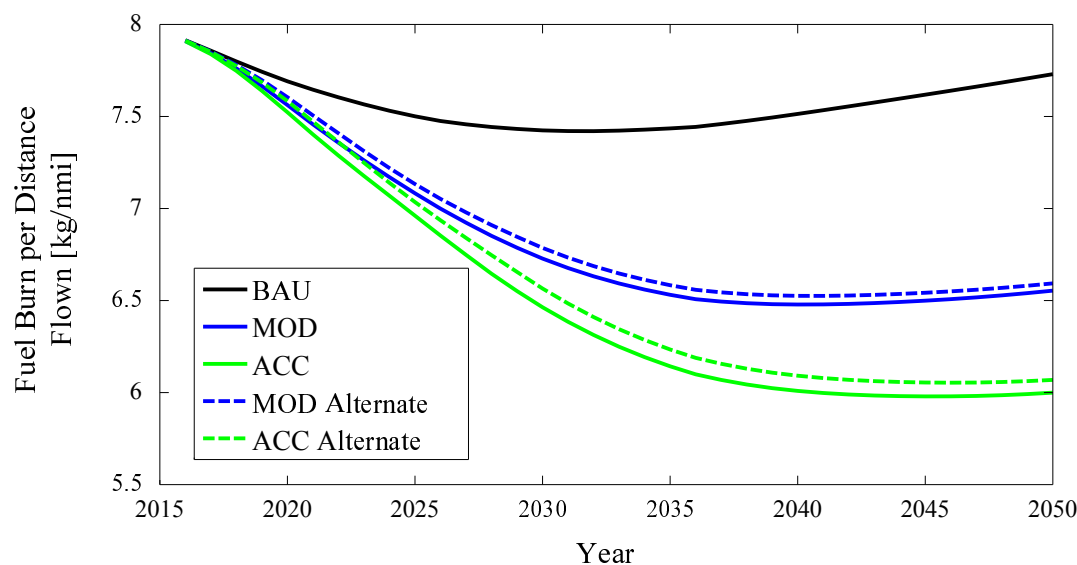
Figure 62: Fuel Burn per Distance Flown

Noise analysis was only conducted every ten years and thus results are presented as stacked bar charts instead of continuous curves. The stacks for the bar charts correspond to the different operational groupings displayed in the parallel plots in Figure 63. Bernardo used hierarchical clustering of operational volumes (Small, Medium, and Large) and distributions by vehicle class to group the subset of airports into eight operational classes [134]. These classes were then paired with calibrated average runway geometries to define a reduced set of generic airports which accurately represent the cumulative sum of contour area across the 94 airports with less computational burden. The analysis in this study does not use Bernardo's generic airports because this would require the definition of a generic population grid for population exposure comparisons. However, organizing results with respect to these operational groupings provide better resolution of the impacts of the different

www.manaraa.com

vehicle classes for different airport types.
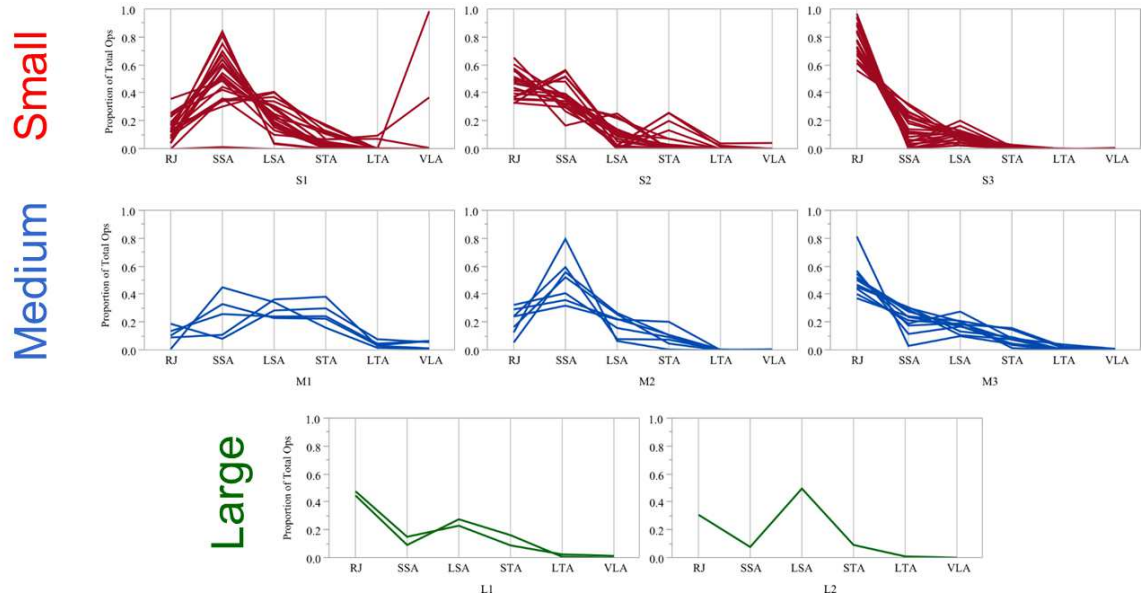
Figure 63: Generic Airport Operational Classes

The reductions in DNL 65-dB contour areas are displayed in Figure 64. It should be noted that these results are not reductions relative to current day noise contour areas, but rather to the worst case BAU scenario. In fact, the noise contour areas for each technology scenario remain relatively static with increasing volume of operations. The extreme contour area reductions in 2040 and 2050 are more demonstrative of potential noise concerns due to operational growth if no advanced vehicles are introduced to the fleet.

The first observation is that there is little difference between the two technology scenarios. The ACC scenario features slightly better noise contour reduction than the MOD scenario, but given that little difference was observed between technology scenarios at the vehicle level (see Figures 54 and 55), it is not surprising that the fleet-level results feature similar behavior. The second observation is that the alternate schedule features the expected noise penalty due to the delay in the critical single aisle program. The offset in noise reductions between the baseline and alternate
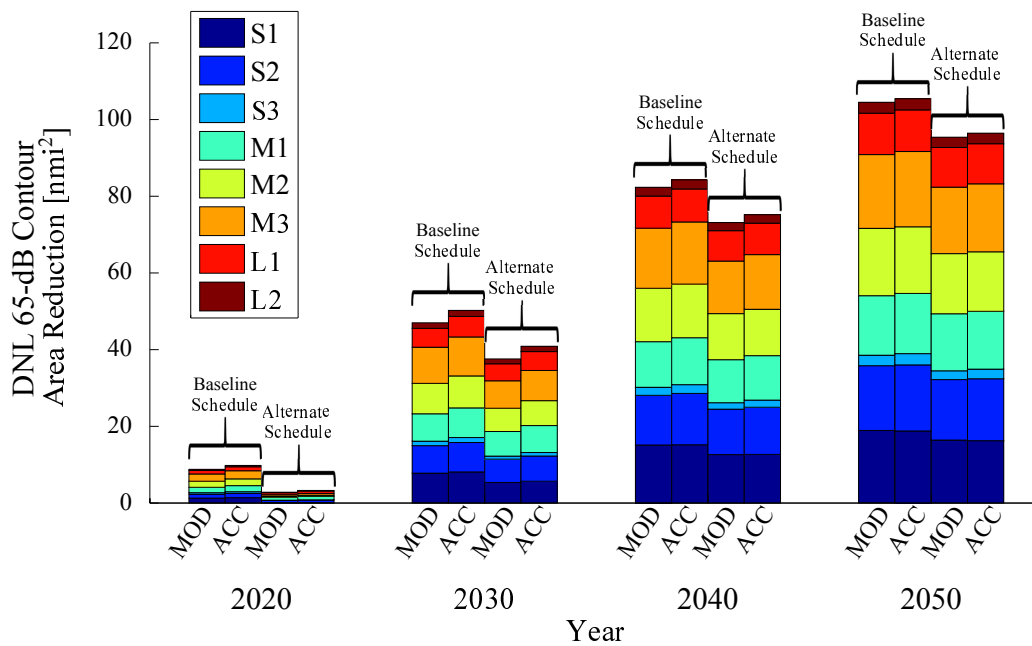
Figure 64: Reductions in DNL 65-dB Contour Areas

schedules seems to be consistent with time, much the same as was observed in the analysis of fuel savings. This offset is most noticeable for the S1 airport class, where the SSA vehicle class comprises as much as 80% of daily operations (see Figure 63).

The reductions in population exposed to significant noise are displayed in Figure 65. The trends between scenarios are relatively similar to those observed for the contour area reduction, although it is interesting to note that by 2050 there is no perceptible difference in population exposure between the MOD and ACC scenarios.

The main takeaway from cross-referencing Figure 65 with Figure 64 is the difference between the relative importance of each airport class. The contour area reductions are fairly evenly distributed between the different airport classes, but some of these classes feature much greater reductions in population exposure. For example, the M1 class shows the greatest savings in population exposure but not much more contour area reduction than the other classes. This class features an approximately even balance of SSA, LSA, and STA operations. The M1 class consists of international airports situated in densely populated areas, with most of
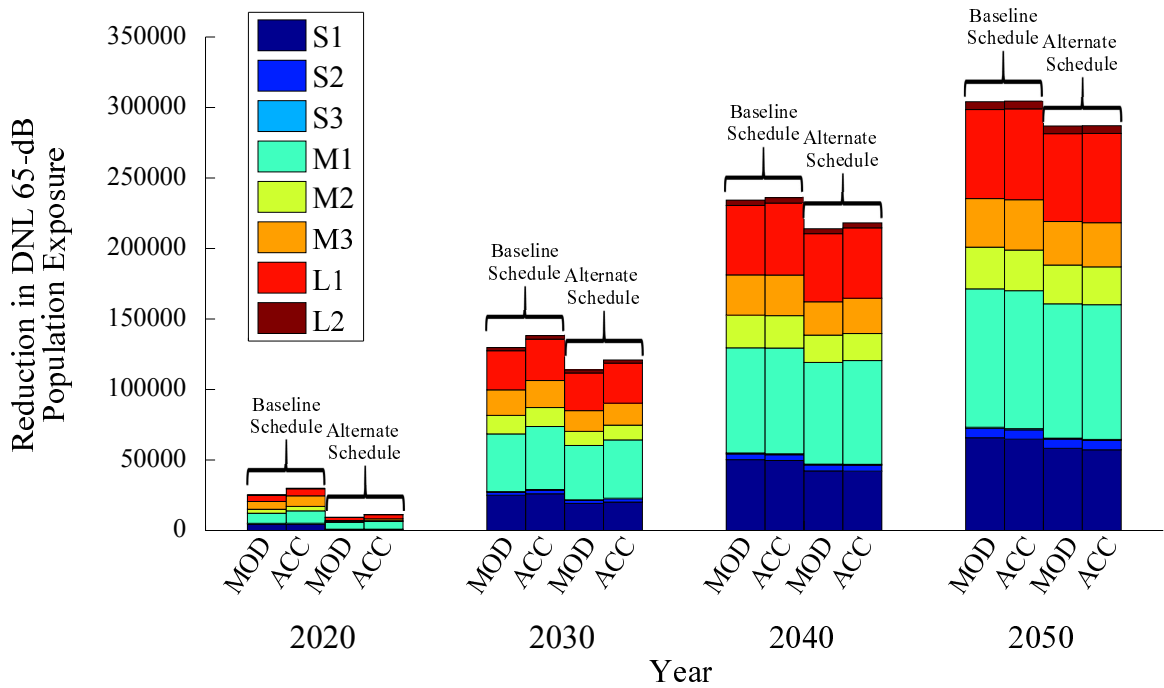
Figure 65: Reductions in DNL 65-dB Population Exposure

these international flights allocated to the STA aircraft. The STA aircraft account for 20-40% of operations at these airports, while they account for less than 20% of operations for most of the other airport classes. With expected increase in demand for international flights, these airports will likely see the most growth relative to present day and much of this demand will be met with replacement STA aircraft. Given the proximity and density of the surrounding population, these airports more critically depend on advanced technology vehicles. On the other hand, the S2 airport class demonstrates sizable reductions in contour area but barely noticeable reductions in population exposure. These airports are not located in population dense areas, and thus the savings in contour areas do not actually contribute much to the goal of reducing population exposed to significant noise.

www.manaraa.com

5.3.3 Summary of Observations

The analysis for each technology scenario showed that the ACC scenario leads to considerably greater cumulative fuel savings, but there was not much difference in the contour area and population exposure reductions between the MOD and ACC scenarios. The noise results particularly demonstrate the importance of technology infusion, as current population exposure counts may double by 2050 under a BAU scenario. The alternate scenario demonstrated how critical the single aisle vehicle class is to fleet-level savings, with a delay in the single aisle program translating to consistent offsets in both cumulative fuel savings and reductions in population exposed to significant noise. Comparisons between contour area and population exposure reductions showed that the M1 class is most critical to the total population exposure, which will benefit most from noise technologies applied to the single aisle and small twin aisle vehicle classes. Focusing only on contour area reduction doesn't provide proper perspective on the relative importance of each airport class. By enabling rapid calculation of community exposure, the relative importance of each airport class can be better understood.

5.4 Placement of New Runways

The previous analysis demonstrated the implementation of the average generic vehicles in an integrated fleet-level environment for exploring forecast scenarios which can introduce vehicles with various technology packages for different market introduction scenarios. This formulation, however, assumes that the airports will be able to increase capacity to handle projected growth in operations. As mentioned in Chapter 1, the evolution of the airports themselves must be considered simultaneously. While there are many ongoing studies for improving airport capacity through advanced NextGen Air Traffic Management (ATM) techniques, the only way for

170

airport capacity to keep up with the projected major increases in demand is to expand airports and build new runways. This led to the third over-arching research question concerning a balanced evaluation of the impacts of these new runways in conjunction with the infusion of new technology. Further questions concerning the placement of new runways and the assessment of the impact to surrounding communities stem from this research question.

ANGIM's simple formulation places no constraints on locations, orientations, or dimensions of runways, and thus the entire design space is theoretically available for exploration. In actuality, choices for new runways are dependent on several other factors beyond just the environmental impact including safety, efficiency, and economics. The weight and degree of concern given to each of these factors depend, in part, on: the Runway Design Code (RDC) which accounts for the types of aircraft operating on the runway, the meteorological conditions, the surrounding environment (including potential wildlife hazards), topography, and the volume of air traffic expected at the airport [135].

Runway orientations are typically chosen to take advantage of the prevailing winds. The most advantageous runway orientation based on wind is the one which provides the greatest wind coverage with the minimum crosswind components. Wind coverage is the percent of time crosswind components are below an acceptable velocity. The desirable wind coverage for an airport is 95%, based on the total numbers of weather observations during the record period, typically 10 consecutive years [135]. Historical wind and weather data can be obtained from the National Oceanic and Atmospheric Administration (NOAA). This analysis is used to determine if additional runways are needed to provide the necessary wind coverage [136]. Given that most of the airports considered in this study have long histories of aviation activities, it is assumed that current airport infrastructures and runway orientations were chosen with all of these issues under consideration. Thus, the orientations of new runways should

likely reflect the current orientations, which suggests that with rare exceptions a capacity-justified runway should be parallel to an existing primary runway [135]. Furthermore, additional primary runways for capacity justification are typically equal in length to the existing primary runway, unless they are intended for smaller aircraft [137]. A new parallel runway should also aim to minimize the number of runway crossings, as this is likely to maximize the airport capacity benefits by reducing the complexity of airfield simulation modeling [36].

Past standards for parallel runways have identified a separation distance of 4,300-ft (0.71-nmi) or greater to maximize efficiency and provide highest hourly capacity [138]. This is because under current FAA regulations, simultaneous landings on parallel runways under low-visibility conditions are only permitted if those runways are 4,300-ft apart. Many airports have parallel runways that are much closer to each other than 4,300-ft, which means those airports' capacity can be cut as much as in half under low-visibility conditions [139]. NextGen driven airspace improvements may enable improved levels of efficiency at closer separation distances even under low-visibility, which will have a substantial effect on development at airports that lack available lands for new runways, such as in dense metropolitan areas [6]. In fact, technical reports on Automatic Dependent Surveillance-Broadcast (ADS-B) along with advanced cockpit displays may make it feasible to reduce runway spacing to as low as 750 feet (0.12-nmi) [139]. This closer separation distance may also have some positive benefits with respect to encroachment of DNL noise contours.

With these potential improvements in mind, three degrees of freedom can constrain potential new runway placements:

1. Choice of primary runway to build parallel runway next to (discrete variable which depends on the number of existing runways)

2. Runway separation distance (Y_2: [750-ft, 4300-ft] or [0.12-nmi, 0.71-nmi])

172

3. Runway endpoint stagger (X_2: range is airport/runway dependent)
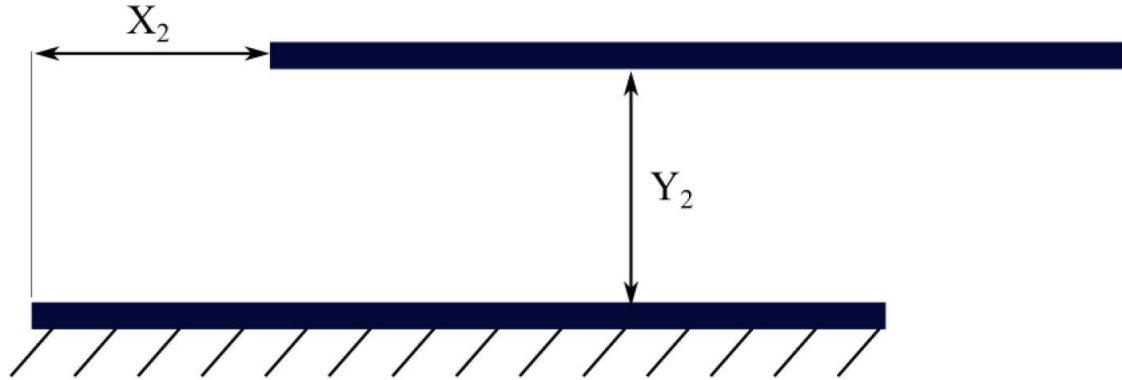
Figure 66: Degrees of Freedom for Parallel Runway Placement

Bernardo showed that the last degree of freedom (runway endpoint stagger) has little influence on overall contour area [79]. However, the stagger does translate the locations of the contours, which may have an impact on population exposure.

5.5   Community Noise Exposure and New Runways

Given the simplifications of the fleet-level tool suite, the terminal-area fuel-burn and NO_x emission calculations were not spatially dependent. This makes it difficult to address the impact of new runways on fuel-burn and emissions without resorting to detailed tools such as AEDT which can include and evaluate fuel-burn and NO_x penalties for various taxiing procedures and flight ground-tracks. However, the structure of ANGIM displayed in Figure 20 enables the inclusion of airport infrastructure and runway configurations to capture the spatial nature of the noise metrics. Furthermore, the population grid method described in Chapter 5 enables this spatial data to capture population exposure counts surrounding the airport. While changes in the fleet-composition, flight ground-tracks, volume of operations, and aircraft technologies will lead to changes in the size and extent of the DNL-contours, changes in airport infrastructure will lead to the most significant changes in the shape

173

of these contours. Given that noise exposure is the most significant environmental concern for communities near airports, ANGIM can be used as a screening-level tool for conducting preliminary Environmental Assessment (EA) studies with regards to new Airport Layout Plans (ALP). Furthermore, ANGIM's formulation and speed allows for the flexibility of exploring several potential locations for new runways.

Combinatorial designs of experiments were formulated to sample the continuous space of new runway locations corresponding to the previously mentioned three degrees of freedom at a subset of ten airports in need of additional capacity. Custom ranges for parallel and lateral spacing of new runway endpoints with respect to each primary runway were derived heuristically by examining airport layout diagrams from FlightAware® as well as satellite maps of the surrounding communities, and thus each airport featured unique designs of experiments. Ranges for each spatial variable were kept as wide as possible, with minimum parallel separation corresponding to the 750-ft separation enabled by ADS-B. Care was taken to avoid new runway locations that intersected interstate highways or clearly occupied residential areas, but bay fill was assumed to be an acceptable option at a few airports. Runway locations were also chosen in an effort to minimize runway crossings and if possible avoid the need for moving existing airport terminals. An example of a runway exploration design of experiments for an airport with two sets of parallel runways is shown in Figure 67. The solid lines represent existing airport runways, and the dashed lines are samples of possible new runways. The rectangles display the spatial area explored for one runway endpoint, with the length of the runway set equal to its parallel existing runway. It should be noted that the size of the runway endpoint design space varies for each runway due to surrounding obstacles including highways, terminals, and other runways. For example, the parallel runway to Runway 4 is very limited in placement due the existence of a terminal, and the runway endpoint design space intersects Runway 1 near the edges. A parallel runway to Runway 2 has much more

174

flexibility in placement and thus the runway endpoint design space is wider. Each design space was sampled with 1000 experiments, with the scale of the resolution varying depending on the size of the design space. For each sample, the DNL contour areas and population exposure counts were computed. This allows for visualization of the continuous space by "heat maps" that show the best and worst locations in the design space depending on which metric is used (contour area or population exposure).
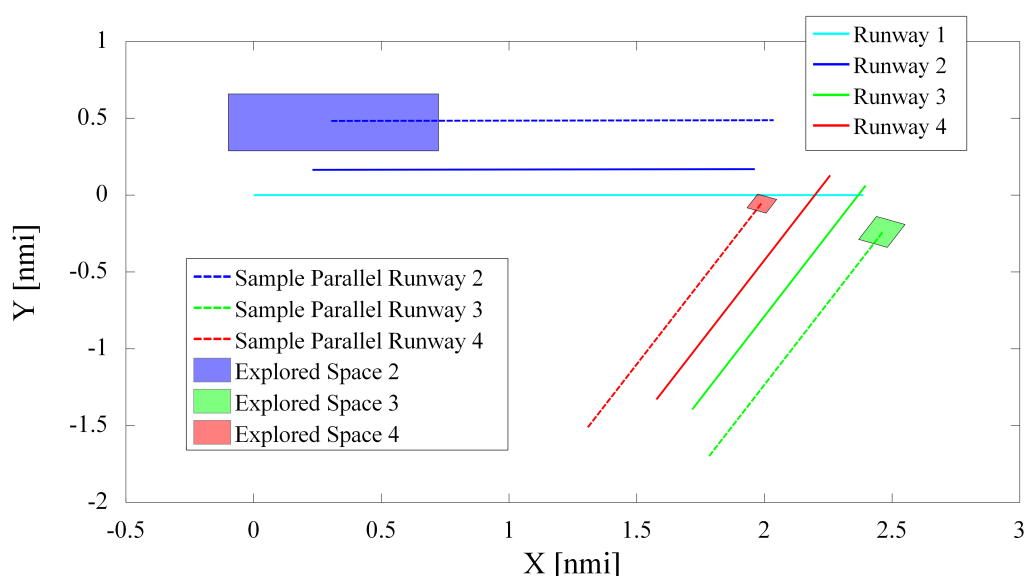
Figure 67: Example of Runway Placement Explorations

Given that new runways take 10-14 years to finish, it was assumed that each runway would be introduced after a decade and be available for use in 2030 [38]. The 2030 flight schedules at each airport from the previous three technology scenarios (BAU, MOD, and ACC) under the baseline market introduction rates were used for analysis. By using average generic vehicles with technology infusion, the combined community impacts of technology integration and new runway locations can be evaluated. Vehicle-level noise technologies may be a key factor for enabling capacity expansions at otherwise capacity constrained airports via increased flexibility for new runway placements. This is justified by the manner that noise is calculated within

ANGIM as described in Chapter 4. ANGIM first calculates the runway-level DNL grids. These grids are strictly a function of the vehicle-level contours for aircraft with operations on that runway, and thus the only way to significantly change the size and extent of the runway-level contour is to infuse vehicle-level noise technologies. After the runway-level DNL grids are calculated, they are translated and rotated to correspond to the specified runway configuration. This determines the spatial reference for the runway-level contours, and the overlap of multiple runway-level grids determines the airport-level noise contours. Assuming that noise technologies are able to reduce the size of the noise contours emanating from each runway axis, more margin may be built into the placement of the new runway before significant encroachment on the surrounding population occurs.

Examples of results for two of the ten airports are included in this chapter. The specific airport names are not listed for sensitivity reasons. Additionally, all results in the heat maps are normalized by the 2030 contour area and population exposure for the BAU scenario, which represents the worst case scenario with no technology vehicle introduction and no new runways. The heat maps and runway layout plots presented in this chapter were repeated for every runway at each of the ten airports. The results for each airport and each potential runway location are unique due to differences in runway configurations and distributions of population in the surrounding communities.

5.5.1 Example Airport: Multiple Parallel Runways

The first example is a large hub airport with multiple parallel runways as shown in Figure 68. This is the most efficient runway configuration for capacity considerations, and with ADS-B allowing for closely spaced runways this airport is an excellent candidate for expansion. The noise analysis quickly determined that each of the three

runway explorations led to comparable noise contour area results, but the exploration of a runway parallel to Runway 1 featured significantly reduced population exposure compared to the other two explorations.
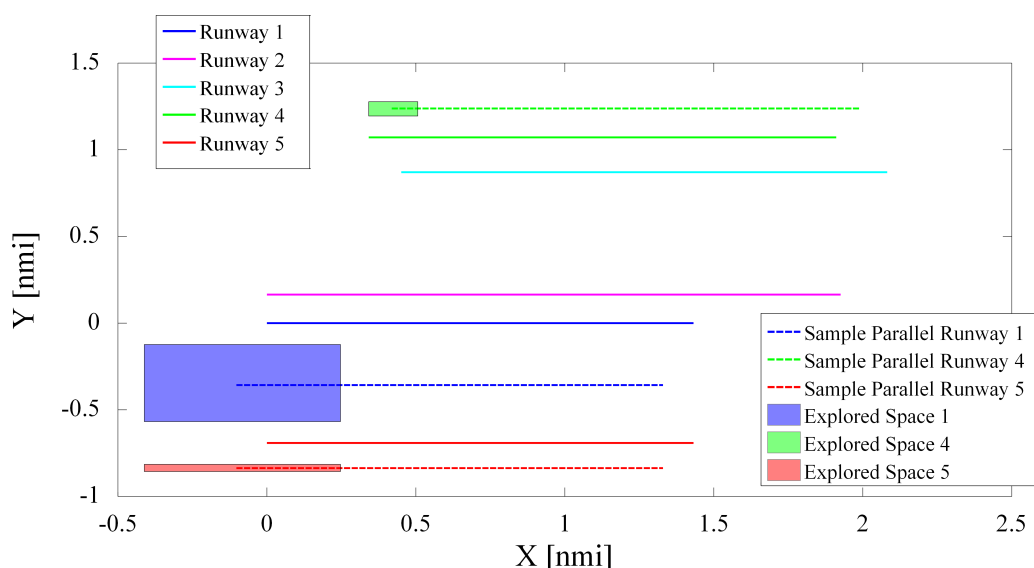
Figure 68: Multiple Parallel Runway Placement Explorations

An example of a heat map for the runway exploration experiment is shown in Figure 69. The filled contours demonstrate the best locations (blue) and worst locations (red) for placement of a new runway with respect to a given metric. It should be noted that the parameters in the design of experiments were referenced to the endpoint of the parallel runway, and thus the results in Figure 69 are actually vertical mirror images with respect to the orientation displayed in Figure 68. The results are presented for the ACC scenario, with contour area (left) and population exposure (right) shown side-by-side for comparison. All of the normalized values are less than one, which is indicative of the noise reductions from the infusion of the advanced technologies.

If choosing a runway location for minimal contour area under this technology scenario, the heat map shows the importance of the parallel spacing. The best
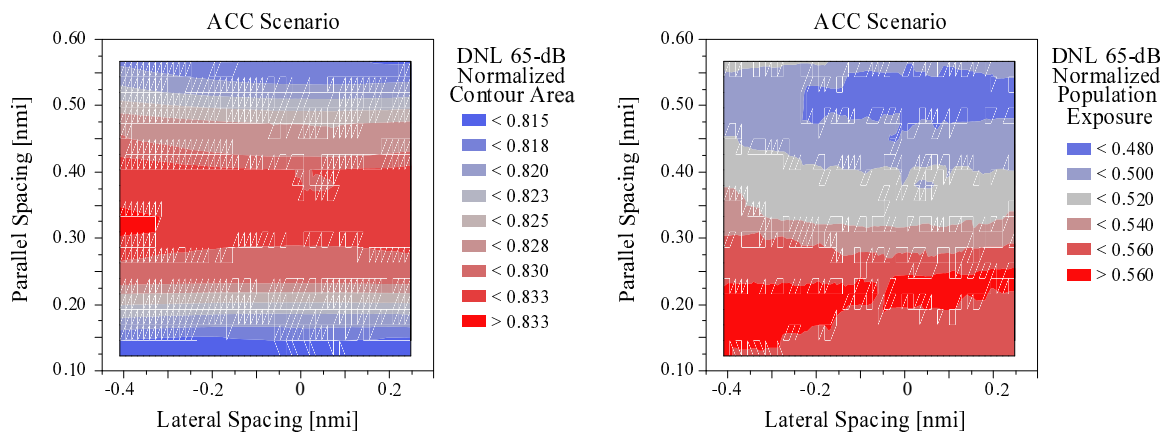
Figure 69: Parallel Runway 1 Heat Maps

locations correspond to the closest and furthest parallel spacings. Given the proximity of Runway 5 to this runway exploration space, the results suggest that area is reduced by placing a new runway as close as possible to an existing runway. This close spacing would not be a feasible solution for alleviating capacity constraints without ADS-B technology. Cross-referencing the contour area heat maps with the population exposure heat maps, it can be seen that wider parallel spacing from Runway 1 (closer to Runway 5) is ideal. Furthermore, population exposure depends on the lateral offset of the new runway whereas contour area showed little dependence on lateral spacing. By including the population exposure counts in the analysis, an airport planner can gain a clearer picture of spatial dependencies and intelligently choose a new runway location. The best runway locations for each metric are shown in Figure 70.

The configurations for minimal contour area versus minimal population exposure show quite different results. An overlay plot of the DNL 65-dB contours for each configuration are shown in Figure 71. Due to the sensitivity of the data, the axes and scales for these contours are purposely omitted. A qualitative comparison of shape suffices to understand the results. Runway 1 and Runway 2 are already very closely spaced, and thus their overlapping runway-level contours lead to lobes that extend further than the lobes from Runways 3, 4, and 5. For minimal area, a runway

178
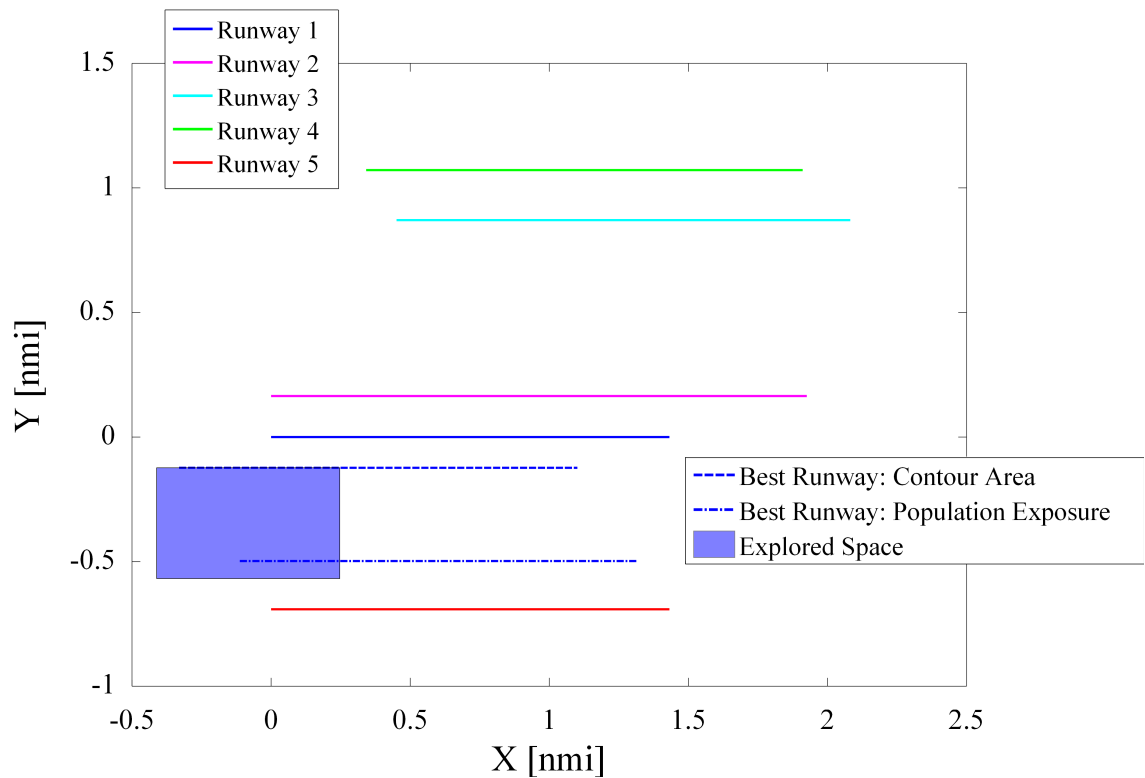
Figure 70: Best Runway Locations from Runway 1 Exploration

placement with minimal parallel spacing further extends these center lobes, but the lobes for the other runways remain small. For minimal population exposure, a new runway placed closer to Runway 5 leads to more balanced lobes. This runway location increases the size of the bottom contour lobes, but this prevents the center lobes from encroaching on the nearby population.

Figure 71: New Runway Contour Comparison: Area v. Population

179

5.5.2 Example Airport: Dual Parallel & Intersecting Runways

The second example is a medium sized airport that is expected to have significant growth in operations in the future. The airport configuration features two sets of parallel runways, with each set perpendicular to the others as shown in Figure 72.
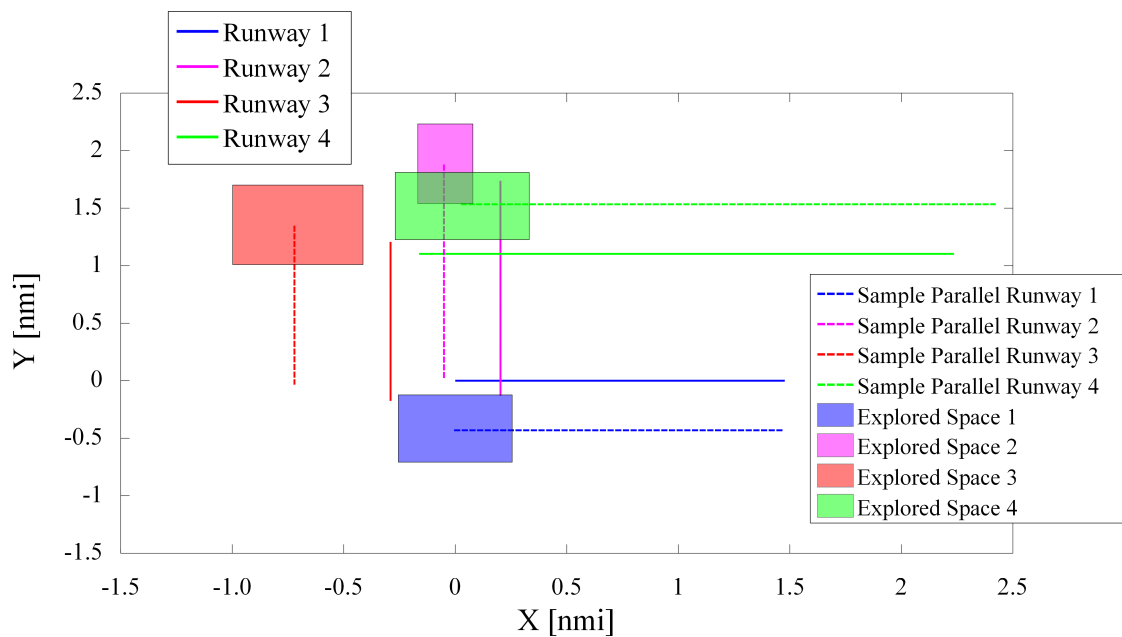
Figure 72: Dual Parallel & Intersecting Runway Placement Explorations

This is an example of an airport on a waterfront. Generally airports on the water try to take advantage of flight tracks over waterways to minimize population exposure. Extending a runway into the water accomplishes much of the same reduction in population, but there are other environmental impacts to filling in a bay for constructing new runways. Ideally these impacts and capacity considerations could be evaluated in conjunction with the noise analysis, but this is beyond the scope of this analysis. In Figure 72, Runway 4 borders the water and a new parallel runway would require some bay fill, but allows for minimal population exposure compared to the other options. The runway exploration parallel to Runway 2 also extends one runway endpoint into the water, but these runways extend onto the land between

Runways 2 and 3. Thus the bay-fill associated with this exploration would not be as significant.

Heat maps for the contour area and population exposure for the runway placement exploration between Runways 2 and 3 are shown in Figure 73, with the parameters referenced to the Runway 2 endpoint. These heat maps include both the BAU (top) and the ACC (bottom) scenarios for comparison. Once again the parameters are referenced to the endpoint of Runway 2, and the results in Figure 73 are actually rotated 90° with respect to the orientation of the exploration space shown in Figure 72.
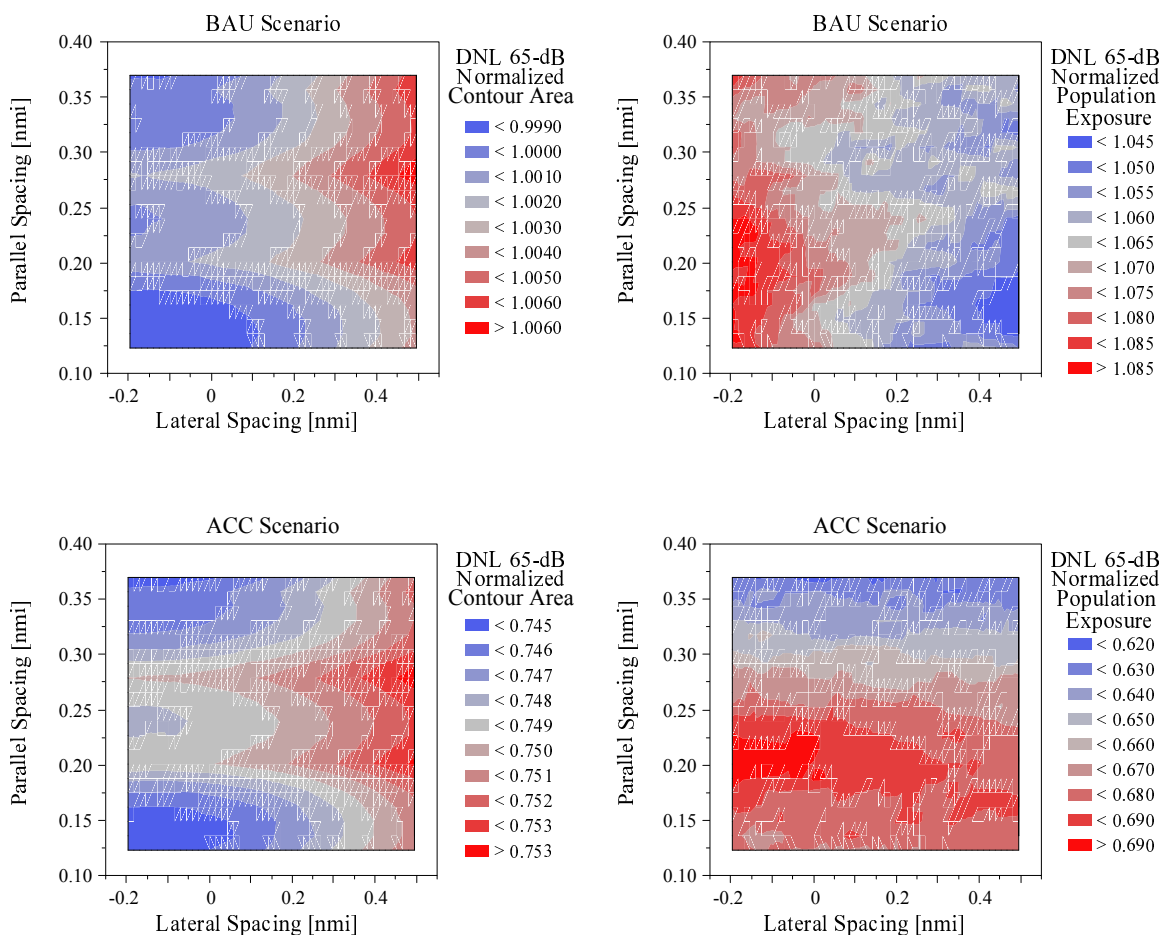
Figure 73: Parallel Runway 2 Heat Maps

Between the two scenarios, the heat maps for minimizing contour area look fairly

similar, with the best locations corresponding to a negative lateral spacing. This lateral spacing translates the new runway location as far inland as possible, which means extending the runway into the water (positive lateral spacing in this case) actually leads to larger contour areas. However, most of the contour growth for a runway that extends into the water would be concentrated over the water where no one lives. This is reflected in the BAU population exposure heat map, which favors new runway locations that extend into the water. The corresponding population exposure heat map for the ACC scenario features very different behavior. All of the locations lead to greatly reduced population exposure relative to the BAU scenario thanks to the advanced technology infusion. However, the best new runway locations for the ACC scenario no longer show as much dependence on the lateral spacing. The heat map suggests the best locations correspond to a runway with wide parallel spacing relative to Runway 2 (closer to Runway 3). Figure 74 shows the best new runway configurations for minimizing population under the BAU and ACC scenarios, respectively.

The vastly different new runway layouts reflect the observations from the heat map. Under the BAU scenario, the corresponding growth in the size of the contour requires a mitigation strategy that pushes the runway endpoint as far into the water as possible, which minimizes the encroachment on the community living on the other side of the airport. For the ACC scenario, technology infusion reduces the vehicle-level noise footprint. This technology infusion actually allows an airport planner to open up the design space for the new runway location. In this scenario, the location that minimizes population exposure also requires less extension into the bay, which would likely reduce other environmental concerns related to construction of new runways.

An overlay plot of the DNL 65-dB contours for each configuration are shown in Figure 75. Once again, the axes and scales for these contours are purposely omitted. A qualitative comparison of shape suffices to understand the results. The
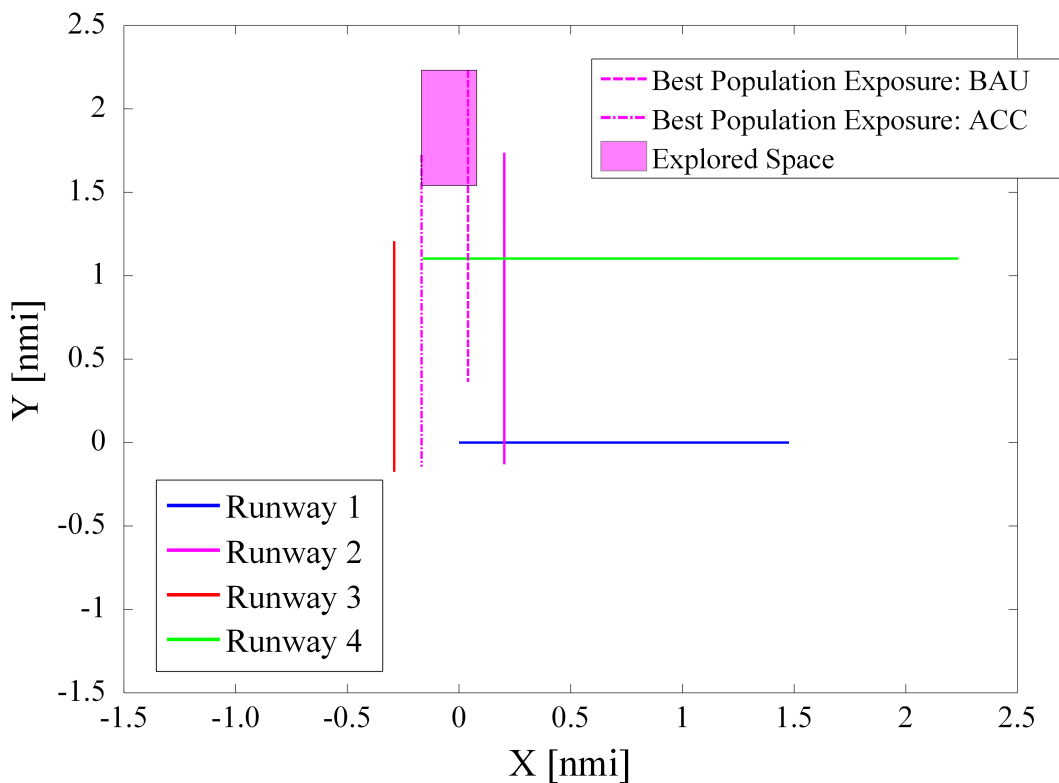
Figure 74: Best Runway Locations from Runway 2 Exploration

first observation is the level of reduction in the contour that results from infusion of technologies. This is most evident from the recession at the lobe closure points. In the BAU scenario, adding a new runway between Runways 2 and 3 leads to overlap of their runway-level contours and a corresponding encroachment at the contour ends. Under the ACC technology scenario, the new runway is placed close to Runway 3, and significant recession in the contour closure point corresponding to Runway 2 is observed. The reduction in the closure point for Runway 2 explains the reduction in population exposure.
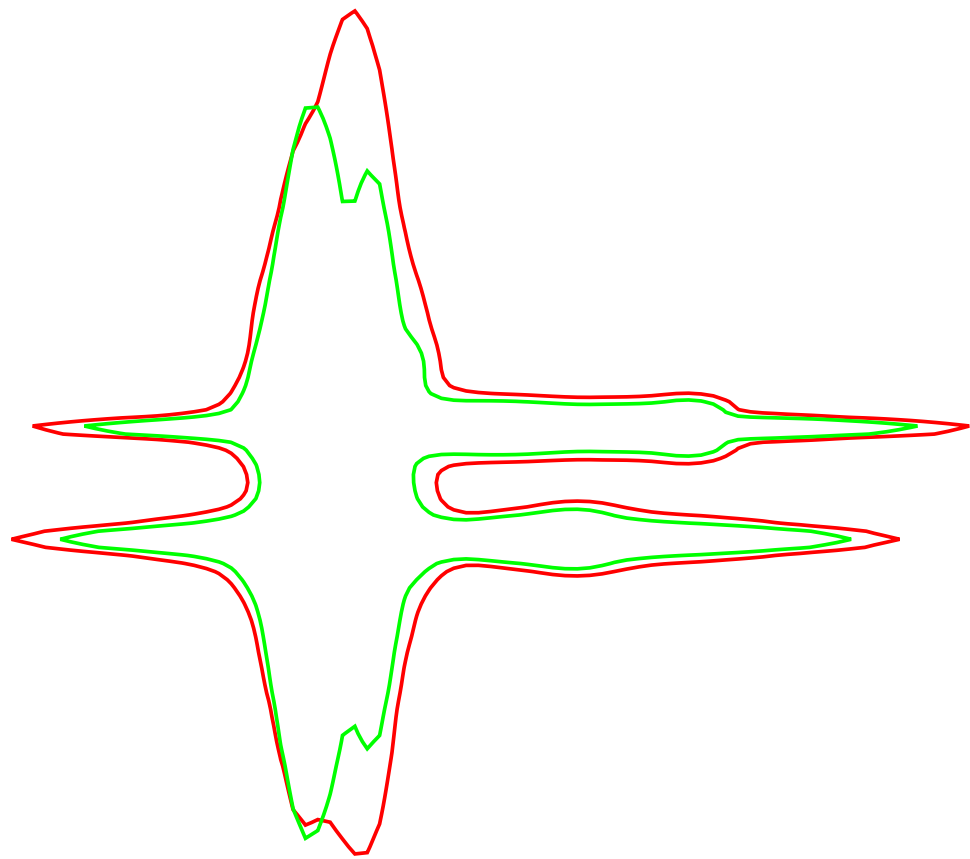
BAU Scenario Best New Runway for Population Exposure
ACC Scenario Best New Runway for Population Exposure

Figure 75: New Runway Contour Comparison: BAU v. ACC

5.5.3   Fleet-Level Integration of New Runways

The runway exploration experiments were unique for each airport, but the two examples included are representative of general observations. The explorations enabled quick identification of the best locations for new runway placement, and the heat maps provided visual feedback on spatial trends. Very rarely did the new runway location for minimal contour area correspond to the location for minimal population exposure. The locations for minimal contour area did not typically change much between technology scenarios, although the sizes of the contours were considerably reduced with technology infusion regardless of runway placement. The locations for minimal population exposure sometimes changed between the BAU scenario and the MOD or ACC scenarios as was observed in Figures 73 and 74. This wasnt true for every experiment because each airport and surrounding community is unique, but reductions in vehicle noise signatures prevent encroachment of contours into densely populated areas and allow airport planners more flexibility with new runway placements. This implies that an airport planner must consider the future composition of the fleet when choosing a location for a new runway for best allocation of noise.

While the runway placement experiments were designed to mitigate expected increases in population exposure, the analysis revealed that addition of a new runway can actually reduce population exposure counts at many of the airports. Most of these experiments found new runway locations that led to less population exposure than the baseline configuration, even for the BAU fleet scenario. These experiments, however, were performed only for a single year (2030). By integrating these new runway configurations into the fleet-level analysis, total population exposure counts over time were directly compared to the same scenarios without new runways to quantify the savings introduced by these new runway locations. The results from this final analysis are shown in Figure 76. Only a few of the airport classes from Figure

185

63 were included in the new runway study, and thus only this subset of airport classes is included in Figure 76.
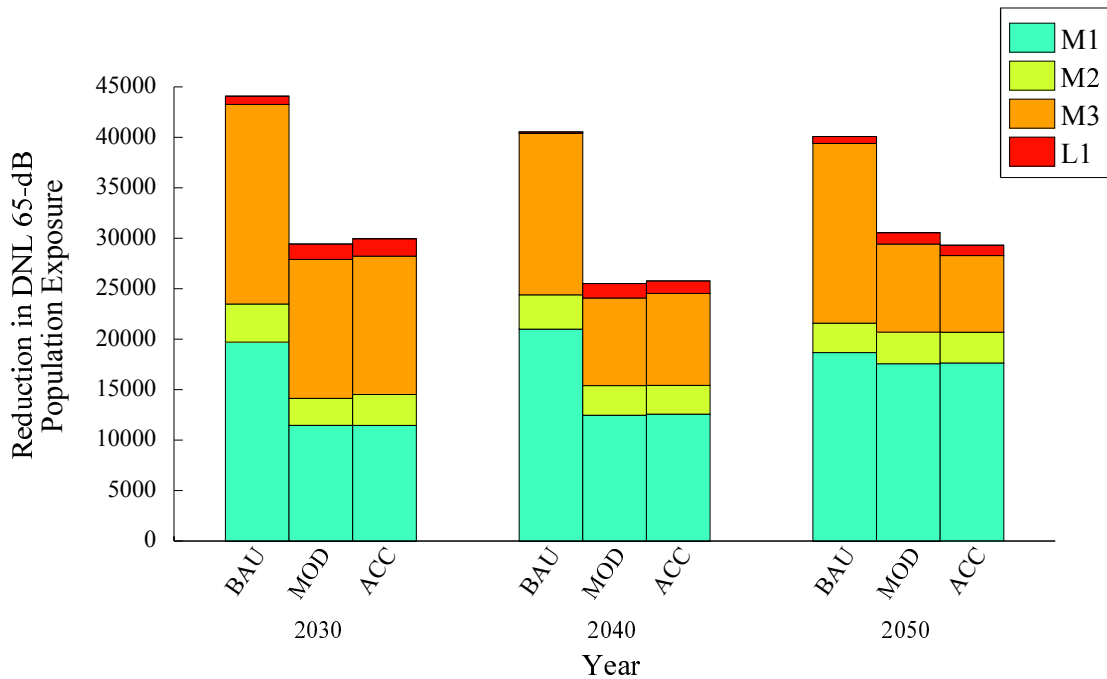
Figure 76: Reductions in Population Exposure with New Runways

These results are referenced to the previous fleet-level scenarios that did not include new runways. For the BAU scenario, the results show significant savings which are strictly due to intelligent placement of runways. In this case, no technology vehicles were introduced and yet population exposure reductions were still achievable. For the MOD and the ACC scenarios, the results are additional savings relative to the scenarios shown in Figure 65. The savings are less than the BAU scenario because reduction of aircraft noise signatures of the aircraft already introduces significant reductions in population exposure, but the results show that intelligent selection of new runway placement enables airport capacity expansion without additional encroachment on the surrounding community. Often this selection of new runways leads to an increase in the contour area, as demonstrated in Figure 77.
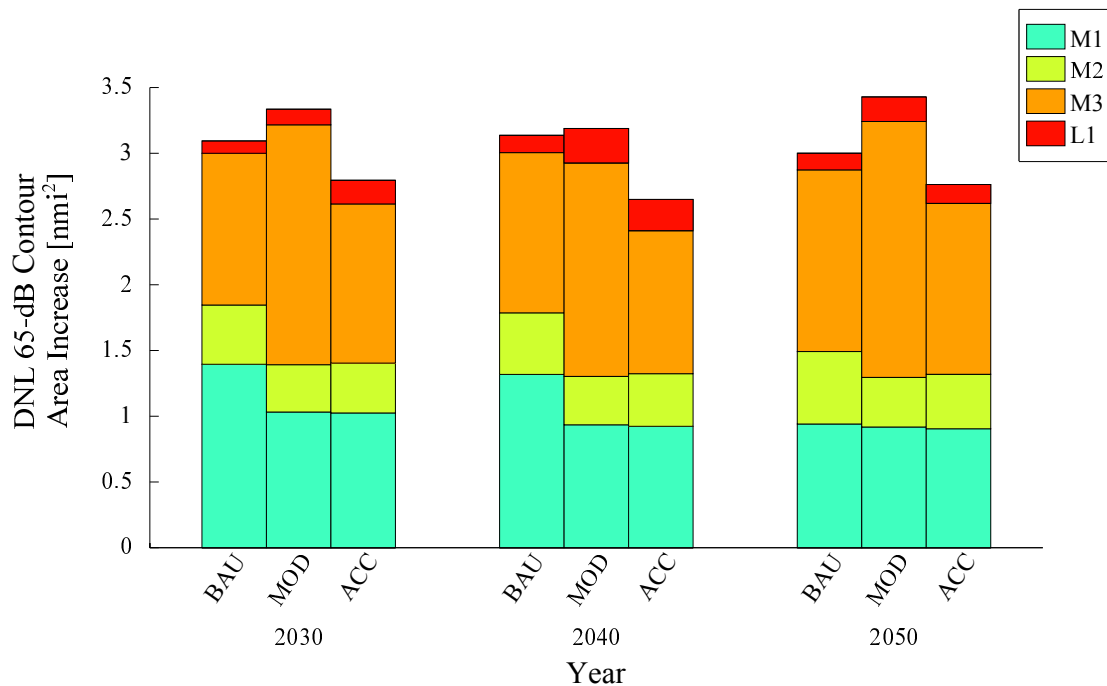
Figure 77: Increases in DNL 65-dB Contour Area with New Runways

The results in Figure 77 demonstrate that simply measuring DNL 65-dB contour area without considering the distribution of population around an airport may lead to misleading analysis. While at the vehicle-level decreasing the aircraft noise foot print is always recommended, the true metric of interest is the population exposure to significant noise. For this reason the spatial distribution of noise is much more important than the geometric size of the DNL contours. For all three technology scenarios, the new runways that reduce population exposure simultaneously increase in the net contour area across the subset of airports.

5.6 Summary of Capability Demonstrations

The generic vehicles and the Thiessen polygon population grids were incorporated into an enhanced fleet-level environment to perform scenario analysis. A system dynamics model that uses existing forecasts to generate future operational schedules at each airport was linked to the rapid noise computation model in an automated

187

fashion. Technologies were infused on the generic vehicle models in the physics-based vehicle-level tool demonstrating improvements in fuel burn and reductions in aircraft noise signatures. Various technology scenarios were defined, and these technology vehicles were used as replacement aircraft for two replacement scenarios. Each scenario was compared to observe trends in cumulative fuel savings as well as reductions in contour area and population exposure for different airport types. Finally, an exploration of new runway locations was conducted at ten capacity constrained airports for each technology scenario.

Fleet-level analysis showed the critical importance of technology improvements specifically for the single aisle vehicles for both fuel savings and reduction in population exposure to significant noise. Infusion of noise technologies for the small twin aisle class is also critical, as these aircraft are allocated a significant share of operations at international airports. These airports are expected to see the largest growth in demand, with much of this demand leading to more flights by the small twin aisle vehicle class. The runway explorations demonstrated the difference between airport planning for contour reduction versus planning for reduced population exposure. Best locations for new runways sometimes changed when considering the infusion of advanced technology vehicles. Fleet-level integration of new runways for each of the ten airports showed that it is possible to increase airport capacity and simultaneously reduce population exposure to significant noise, even for a scenario with no technology vehicles. These locations for minimizing population exposure corresponded to increases in contour area, which suggests that the latter is not the appropriate metric to consider when planning for airport expansion with new runways.

CHAPTER VI

CONCLUSION

All of the capabilities and analyses presented in this dissertation address the overarching research objective as presented in Chapter 1:

Research Objective: *To develop a framework for modeling relevant environmental performance metrics and objectively simulating the future environmental impacts of aviation given the evolution of the fleet, the development of new technologies, and the expansion of airports.*

This objective was motivated by recent international focus on the environmental impacts of aviation, specifically the ICAO goals concerning GHGs, terminal-area air quality, and community exposure to significant noise. The framework was formulated for flexible exploration of different technology scenarios, and hinges on modeling and simulation. This led to the following overarching hypothesis:

Overarching Hypothesis: *By exchanging fidelity for computational speed, a screening-level framework for assessing aviation's environmental impacts can be developed to observe new insights on fleet-level trends and inform environmental mitigation strategies.*

The reduction of the fleet to a handful of generic vehicles represents an exchange of fidelity for computational speed. Mapping Census block population data to a grid conforming to the dimensions of a rapid noise computation model is another

example of exchanging fidelity for speed. These methods enabled the framework for assessing aviation's environmental impacts. This was accomplished through modeling and simulation of performance improvements and technology compatibilities at the subsystem level for the generic vehicle models and propagating these results to aircraft-level environmental performance. The aircraft-level results are linked to forecast schedules of operations to project the fleet-level results with respect to assumptions of growth rates and replacement schedules. The modularity of the methodology also allowed for exploration of new runway configurations to account for potential evolution of airport infrastructures, which has implications for capacity constraints as well as community noise exposure around airports.

The capability demonstration and analysis included in Chapter 5 led to a few insights on fleet-level trends that can inform environmental mitigation strategies. A few examples of fleet-level trends observed are listed below:

- Technology improvements for the Single Aisle vehicle class are most critical due to the projected increase in demand for replacement aircraft from this class, and thus Single Aisle aircraft technology programs should be prioritized.

- International hub airports contribute to a large percentage of the total population exposure counts across the subset of major US airports. These airports feature more operations by Small Twin Aisle aircraft than other airport classes, and these operations may increase dramatically with the anticipated growth in demand for international travel. Noise technology programs should prioritize these Small Twin Aisle aircraft (along with the Single Aisle aircraft).

- Increases in airport capacity by construction of new runways can be accomplished without increasing population exposure counts, particularly when paired with noise technologies applied to aircraft. This requires intelligent placement of runways with knowledge of population densities in communities

190

surrounding the airport. Often a solution for reducing population exposure also corresponds to an *increase* in contour area.

The analysis conducted and this list of observations is by no means exhaustive, but they demonstrate the utility of this framework to inform environmental mitigation strategies. This supports the overarching hypothesis, and presumably more specific strategies can be derived by exploring more technology and replacement scenarios. By reducing the computational expense associated with this type of analysis, the framework demonstrates more flexibility to enumerate and compare more scenarios and provide policy-makers with better perspective on the future environmental impact of aviation.

6.1 Summary of Contributions

The GENERICA method for optimizing generic vehicles, the enhancements of existing airport-level (ANGIM) and fleet-level (GREAT) tools, and the exploration of new runway locations each represent major contributions introduced in this work. The techniques and lessons learned for each are briefly summarized.

6.1.1 Average Generic Vehicles with Noise

Chapter 2 reviewed the average generic vehicle methodology introduced by Becker in his dissertation, but this approach was limited to evaluation of fuel burn and NO_x emissions. Because DNL noise is an airport-level metric, Becker's test structure was insufficient for optimizing generic vehicles that can also approximate fleet-level noise performance. In response to this capability gap, the method for Generating Emissions and Noise, Evaluating Residuals, and using Inverse methods for Choosing the best Alternatives (GENERICA) was developed. The primary difference between

191

Becker's method and GENERICA was the characterization of fleet-level performance at each airport in addition to the cumulative fleet-level metrics. Instead of just minimizing cumulative error, GENERICA attempts to minimize the mean error and variance of the relative error distributions for each metric across the subset of airports. Becker showed in his work that the generic vehicle method was more effective at representing aggregate fleet-level fuel burn and NO_x emissions than a traditional representative-in-class approach, and it was hypothesized that the enhancements enabled by GENERICA would show that this also holds for DNL 65-dB noise contours as well.

An alternative vehicle classification scheme was introduced that used discriminant analysis to bin aircraft according to common vehicle-level performance with respect to the collection of environmental metrics. These "vehicle classes" were expected to reduce performance variance within each class compared to traditional seat-class-based groupings, and it was hypothesized that this would enable individual generic vehicles to better represent the aggregate performance of each group. To test this hypothesis, the GENERICA method was repeated using both classification schemes. A test structure of sequentially increasing complexity was designed for traceability of generic vehicle performance with respect to different operational variations across the subset of airports. It was shown that by isolating the operational distributions of each vehicle class from other operational complexities, rapid design space exploration and exploitation was possible using design of experiments, surrogate modeling, Monte Carlo simulation, and "desirability" scores for multi-criteria decision making, as formulated in Chapter 3 and implemented in Chapter 4. It was hypothesized that the surrogate models would identify the best locations in the vehicle-level design space for matching fleet-level results, and that these models would continue to demonstrate accurate performance across the subset of airports as other sources of variability (trip-length distributions, volumes of operation, airport

infrastructure, etc.) were re-introduced.

The results showed that the generic vehicle models depend mostly on the thermodynamic cycle design and the sizing of the engine. The top ranked vehicles for each test were widely distributed with respect to many of the vehicle-level input parameters, but the best models featured similar engine OPR, BPR, and sea-level static thrust. These best designs continued to perform well as the operational complexity of the target metrics were increased. The final tests showed that the generic vehicle method demonstrated better accuracy than traditional representative-in-class vehicles. This method proved even more critical for the cumulative DNL 65-dB contour areas. The representative vehicles performed well for noise at smaller airports with less operational variability, particularly if the representative vehicles were allocated the majority of the operations per class at these airports. For larger airports with more variability and greater volumes of operations, the generic vehicles performed better. Since the large airports contribute more to the cumulative contour areas, the generic vehicle models featured superior accuracy for cumulative noise. All hypotheses were supported, but the generic vehicle classes only demonstrated marginal improvement relative to generic seat classes. The hypothesis concerning the aircraft classification schemes was weakly supported, but this served as a testament to the flexibility of the GENERICA method to optimize generic vehicles with respect to any vehicle classification technique.

As baseline schedules and the composition of the current fleet change over time, the GENERICA method can be repeated and the generic fleet can be updated to reflect these changes. The surrogate modeling approach used for Test A would be sufficient, which significantly reduces the amount of data preparation and computational burden required to repeat the generic vehicle optimization. In this manner, the GENERICA method can serve as a standard for reducing the complexity of the fleet regardless of the specific modeling tools used provided these tools meet

the requirements enumerated in Chapter 2. The resulting generic vehicles can serve as virtual testbeds for technology infusion that can be used for fleet-level analysis.

6.1.2   Fleet Analysis with Average Generic Vehicles

Chapter 5 focused on the enhancement of the integrated fleet-level environment for the purpose of meaningful analysis. The goal of these enhancements were to leverage the generic vehicles and link them to existing forecasts of operational schedules. The first enhancement required logic to filter and export flight schedules for each of the airports from an existing system-wide fleet-level environmental performance model to the rapid noise tool. This allowed for simultaneous evaluation of each performance metric with respect to a common set of operations, forecast assumptions, and vehicle replacement schedules. In this manner, bottom-up analysis that was previously only possible for fuel burn and NO_x emission evaluations can now be linked to noise projections.

The rapid noise tool only featured a capability for calculating DNL grids and noise contours, but the true metric of interest is the population exposure to significant noise. Importing the noise contours into a Geographical Information System such as ArcGIS® is possible given proper geospatial referencing of runway endpoints, but this approach is computationally expensive and requires complicated setup. Furthermore, this doesn't take advantage of the existing architecture of the rapid noise tool. Instead, a method was created that exported population data into discretized grids that matched the dimensions and resolution already used for the rapid noise tool's DNL grids. This population data was collected for each airport through one time pre-processing of 2010 Census blocks in ArcGIS® through the area-weighted method described in Chapter 3. The end result was a library of population grids that can be called by the rapid noise tool and link noise analysis to the distribution of population surrounding an airport. By cross-referencing the DNL grids with the corresponding

population grids, community noise exposure may be rapidly calculated simply by summing the population counts for grid points with DNL decibel levels above a given threshold (typically DNL 65-dB). In this manner, community noise exposure is integrated into the noise tool with almost no increase in runtime, thus leveraging the speed of the existing tool.

The final enhancement was the infusion of technology on the average generic vehicle baselines. In the near term, replacement operations are allocated to the baseline generic vehicles, but the main goal of the integrated analysis is to quantify the level of improvement due to various technology packages and the dependence of these results on the forecast and replacement assumptions. To demonstrate this capability, a Moderate (MOD) and an Accelerated (ACC) technology scenario were each defined and savings with respect to a Business-as-Usual (BAU) scenario were quantified. A baseline and an alternate replacement schedule were each implemented to demonstrate the criticality of first integrating advanced technologies on the Small Single Aisle (SSA) and Large Single Aisle (LSA) classes.

Results from fleet-level fuel burn analysis showed various levels of cumulative fuel savings. By normalizing the results with respect to distance flown, it was observed that for each scenario there was an inflection point in fuel burn efficiency. These inflection points occur at different points of time for each scenario, with more accelerated technology infusion pushing this inflection point far into the future. The takeaway from this analysis is that accelerating these technology programs in the N+1 and N+2 time frames buys more time for the development of unconventional designs with revolutionary fuel burn savings as is targeted in the N+3 time frame.

Results from fleet-level noise analysis showed significant savings in contour area and population exposure relative to the BAU scenario. The savings were comparable between the MOD and ACC technology scenarios, as the vehicle-level improvements in noise were significant compared to the baseline vehicle contours but did not vary

195

greatly between scenarios. The noise savings were more reflective of the problem in the BAU scenario than a decrease in the DNL contours across the subset of airports. In fact, the contour areas for the MOD and ACC scenarios remained relatively static over each decade while the volumes of operation increased significantly at each airport. Comparisons between contour area savings and population exposure savings showed that the relative importance of each airport class differed depending on the metric of choice. The savings at the M1 class if airports, for instance, represented a greater proportion of the population savings than the contour area savings. The savings at the S3 class of airports represented a greater proportion of the contour area savings than the population savings.

6.1.3   Exploration of New Runway Locations

Chapter 5 explored potential options for placement of new runways to increase airport capacity. This was accomplished through spatial designs of experiments conducted for a set of ten airports in need of capacity enhancement by 2030. These experimental designs were derived heuristically by examining airport layout diagrams and attempting to constrain new runway locations based on existing obstacles. For each airport and each potential new runway, "heat maps" were generated that show the continuous dependence of contour area and population exposure on the location of the new runway endpoint. Visualization of results through these heat maps was made possible by the inexpensive computation times associated with the rapid noise tool coupled with average generic vehicle classes and the previously developed population grid method.

The designs of experiments were repeated across the ten airports for the 2030 flight schedules corresponding to the three technology scenarios (BAU, MOD, and ACC), and the heat maps were normalized by the results for the BAU scenario

with baseline runway configurations (no new runways). A few general trends were observed, although results were unique for each airport due to different layouts and population distributions. The locations of new runways for minimum contour areas were often very different from the locations for minimum population exposure, as the latter attempted to balance the encroachment of the contour lobes into population centers while the former focused on the overall size of the contours. The locations for minimizing population exposure sometimes changed between the BAU and the two technology scenarios, demonstrating the increased flexibility of runway placements enabled by reduced vehicle-level noise footprints. Most importantly, integration of the best new runway locations for minimizing population exposure showed that intelligent runway design can identify future airport configurations with new runways and simultaneous *decrease* in population exposure, even in the BAU scenario. The results from this fleet-level integration showed that these new runway locations typically lead to increase in cumulative contour areas, which suggests that airport-level noise analysis must not focus on contour area alone.

6.2 Future Work

Many simplifying assumptions were necessary to scope this research, and future work can be derived by exploring these assumptions in greater detail. Some future work items are discussed with respect to each of the major contributions, but the list is not exhaustive.

6.2.1 Incorporate Stochastic Parameters in GENERICA Method

The test structure for the GENERICA method identified several sources of operational complexity, but the weighted frequency of each of the unique constituent vehicles proved to be the most important factor. A few complexities were not

197

included, however, including the unique atmospheric conditions and flight tracks associated with each airport. While these represent stochastic parameters associated with the airports, it is not certain how including these parameters when generating the target metric distributions may change the input parameter settings of the best generic vehicles. Furthermore, surrogate models could be developed that map variations in vehicle-level performance to deviations from standard day sea-level atmospheric conditions or alternatives to the currently used straight-in straight-out ground tracks. Some of these methods have been explored in Refs. [140], [141], and [142]. Enabling average generic vehicles to capture these deviations would broaden the scope of scenario-analysis capabilities for the integrated fleet-level environment.

6.2.2   Additional Analysis with GREAT-A

The fleet-level analysis was scoped considerably for this work, but there are several areas for potential improvement. Many more technology scenarios may be enumerated, including novel engine architectures (such as geared turbofan engines) and unconventional configurations (such as hybrid-wing body and box-wing concepts). These designs would not require a generic vehicle approach given the fact that the current fleet does not include these vehicles, although efforts should be made to match baseline concepts to publicly available data on projected performance of these aircraft. Sensitivities of fleet-level performance to market penetrations of these advanced concepts could then be weighed against advanced tube-and-wing technology vehicles.

The analysis did not take advantage of many of the parametric formulations for operational schedules available in the system-wide fleet-level environmental performance model. Options for scaling the growth of operations and adjusting retirement curves were set to default values for all analysis in this work. Future work

may take advantage of these additional parameters for broader scenario analysis. More alternate replacement schedules could also be explored. Furthermore, the noise analysis did not include vehicle-level noise grids for out-of-production vehicles. Volume of operations were conserved at each airport, but the out-of-production operations were allocated to baseline generic vehicles. Including the actual out-of-production vehicle grids or at least a representative set of these vehicles would allow for benefits analysis of policies that accelerate the retirement of these older, noisier aircraft. It should be noted that the fuel burn analysis did include out-of-production aircraft.

The analysis of terminal-area NO_x emissions was scoped from the final analysis, primarily because engine combustor technologies were not included in the technology packages for the MOD and ACC scenarios. NO_x evaluations should be included in the future, but terminal-area NO_x evaluations require a surrogate modeling approach that links changes in baseline emissions to deviations from standard day sea-level atmospheric conditions. Preliminary observations of advanced combustor technology models have demonstrated significant reductions in NO_x emissions. These technologies will be key enablers for higher OPR engines by mitigating the corresponding increases in NO_x.

The noise analysis assumed uniform utilization of runways with cross-flow, but in fact many airports feature dedicated runways for departure or approach operations. While runway utilization at these airports are not publicly available, access to existing inventories would allow for more accurate representations of airport usage which could lead to significant changes in the DNL contour shapes. The impact of the uniform utilization should be investigated in more detail, and if possible these utilization factors and constraints should be incorporated into the rapid noise formulation.

In addition, all analysis was performed using static population data from the 2010 Census blocks. Including population dynamics to simulate potential growth

or decay in population counts around airports would be more representative of reality, although much uncertainty is associated with projecting future population distributions at this level of resolution. These population growth models could possibly be calibrated by repeating the population grid exporting procedure at Census blocks from 1990 and 2000 and observing the population dynamics per grid point over time.

6.2.3 Evaluating New Runways for Capacity Improvements

The new runway explorations limited the analysis to noise with the assumption that these runways would create the necessary increase in capacity. Future work should link these explorations to capacity models to show the tradeoffs between capacity enhancement and noise exposure. The costs associated with bay-fill should also be investigated in more detail, and fleet-level integration of new runways should be adjusted if bay-fill is not a feasible option.

The runway explorations would also be improved by actual runway utilization information. Future scenario analysis could explore not only new runway locations but also optimal utilization for best spatial allocation of noise. Further population exposure reductions may be possible through curved ground tracks or steeper continuous descent approaches, and thus these tracks should be considered in conjunction with the runway placements.

APPENDIX A

STOCHASTIC MULTI-CRITERIA ACCEPTABILITY ANALYSIS (SMAA)

Many traditional Multi-Criteria Decision Analysis (MCDA) methods exist today and can be applied to a variety of problems. Several of these require the decision-maker to provide preference information, often in the form of weights. Complications associated with these methods arise because the solutions to these problems are highly dependent on the preference information. The preference information is subjective and dependent on the different stakeholders involved in the problem. In some situations, the preference information can be incomplete, and in other situations involving multiple decision-makers, inconsistent preference information may result due to the differences in opinions [149, 164].

One of the oldest MCDA methods is the utility function-based approach. This approach uses a utility function to calculate a utility score for each alternative, given the evaluations of the alternative's criteria. The utility function expresses the decision-makers' preferences in the form of numeric values, the utility score, where larger values are favorable. This method has been intensively researched and applied in various applications, however it has become apparent that the exact parameter values required from earlier methods are not sufficient in all decision-making situations.

Assigning exact values to parameters disregards the ignorance in a problem, where ignorance is classified by three subcategories: incompleteness, imprecision, and uncertainty. Assigning exact parameter values may also be difficult when the problem involves multiple decision-makers whom possess differences in opinions. By

assigning these exact values, the solution found for the problem becomes difficult to justify. Alternatively, an inverse method should be applied. Instead of inputting exact parameter values and finding one solution, the parameter values are described as a result from analyzing different sets of outcomes. In 1973, Charnetski introduced the comparative hypervolume criterion, with further study in 1978 by Charnetski and Soland. This criterion is based on calculating the volume of the multi-dimensional weight space for each alternative which make that alternative the preferred one. The method uses preference information in the form of linear constraints for weights, but it is limited to deterministic values for criteria measurements, only allowing the use of additive utility functions [145, 146]. The overall compromise criterion was introduced in 1986 by Bana e Costa. The objective of this method is to identify a set of weights which results in the least amount of conflict between various decision-makers. Each decision-makers preferences are taken into consideration in defining the joint probability density function for the weight space. Each point in the weight space corresponds to an acceptability index, a measure of the degree of acceptability. The aggregation of the acceptability indices leads to the overall compromise criterion, the parameter used for finding the set of weights with the least conflict [147]. In theory, the method is very useful; however in practice, it is limited to only handle three criteria [164].

The latter methods significantly influenced the development of the Stochastic Multicriteria Acceptability Analysis (SMAA) by Lahdelma et al. in 1998 [155]. SMAA is an inverse MCDA method, which explores the feasible parameter spaces with multidimensional integrals. SMAA calculates descriptive measures which provide information to assist the decision making process. This allows the ignorance within a parameter and the inconsistent preferences to be defined and become beneficial in finding a solution instead of being detrimental to the justification of a solution.

SMAA is a utility function-based MCDA technique, which allows decision-makers

the ability to explore the weight space as an alternative to pre-defining subjective and possibly inconsistent preferences or weights. The fundamental idea behind SMAA is to support decision-makers by calculating descriptive measures, which help describe the potential weights and the corresponding outcomes. SMAA describes the set of weighting combinations, which make each alternative the preferred alternative.

A.1   SMAA [164, 155]

In a discrete multi-objective problem, there are m alternatives $x = \{x_1, x_2, \ldots, x_i, \ldots, x_m\}$ which are evaluated by n criterion, $\{g_1, g_2, \ldots, g_j, \ldots, g_n\}$, where $g_j(x_i)$ represents the evaluation of x_i by criterion g_j. The method allows multiple decision-makers the ability to express their preferences by an individual weight vector, w and any type of utility function $u(x_i, w)$ which is jointly accepted by all the decision-makers. The additive linear utility function is the most commonly used and given by the following:

$$u(x_i, w) = \sum_{j=1}^{n} w_j g_j(x_i) \tag{26}$$

The weight vectors are comprised of individual weights, w_j for each criterion. Each weight value is positive and normalized acting as a scaling factor. The set of feasible weight vectors define the weight space, W as shown below:

$$W = \left\{ w \in R^n : w \geq 0, \sum_{j=1}^{n} w_j = 1 \right\} \tag{27}$$

Unlike many traditional utility function-based methods, SMAA allows decision-makers to define the ignorance in a problem such as in the criteria and in the weights. Ignorance includes the imprecision, incompleteness and uncertainty as previously mentioned. The criteria's ignorance is represented by stochastic

203

parameters (ξ_{ij}) corresponding to the evaluation of $g_j(x_i)$ with the density function, $f_\chi(\xi)$, where the density function is defined in the space $\chi \subseteq R^{m \times n}$. Similarly the ignorance in the weights is represented by weight distributions with joint density function $f_w(w)$ defined in the weight space, W. In certain problems, where a complete lack of weight information exists, the density function is represented by a uniform distribution in W.

$$f_w(w) = \frac{1}{volume(W)} \tag{28}$$

For each alternative, x_i the set of favorable weights, $W_i(\xi)$ is determined. The set of favorable weights is defined as the set of weight vectors which make the utility score of alternative x_i larger than or equal to any of the other alternative's utility score $u(\xi_k, w)$, making the alternative x_i the most preferred alternative.

$$W_i(\xi) = \{w \in W : u(\xi_i, w) \geq u(\xi_k, w), \forall k = 1, ..., m\} \tag{29}$$

The original SMAA method calculates three descriptive measures including the acceptability index, the central weight vector, and the confidence factor. The descriptive measures are computed using Monte Carlo simulations and therefore may contain errors, which are usually small enough where they do not need to be accounted for. The number of simulations drives the accuracy of the computations and can be determined to maintain a specified error limit.

The first of the descriptive measures is the acceptability index, a_i. The acceptability index measures the probability that an alternative is the preferred one for the assumed weight distributions used in the computations. It describes the variety of different weight combinations which make an alternative the most preferred alternative. It is computed as a multidimensional integral over the criteria distributions and favorable weight space.

$$a_i = \int_{\xi \in \chi} f_\chi(\xi) \int_{w \in W_i(\xi)} f_w(w) \mathrm{d}w \mathrm{d}\xi \qquad (30)$$

A high acceptability index suggests that the corresponding alternative is highly acceptable as the preferred alternative, whereas an acceptability index of zero indicates that the corresponding alternative is never the preferred alternative for the given preference model.

The central weight vector, w_i^c gives the expected center of gravity of the favorable weight space. It is computed as the multidimensional integral over the criteria distributions and the favorable weights.

$$w_i^c = \frac{1}{a_i} \int_{\xi \in \chi} f_\chi(\xi) \int_{w \in W_i(\xi)} f_w(w) w \mathrm{d}w \mathrm{d}\xi \qquad (31)$$

The central weight vector describes the weights which a hypothetical decision-maker supporting the alternative would most likely select. However, in application, deviations between the actual preferences and the central weight vector may exist. Nonetheless, presenting the central weight vectors provides decision-makers an inverse approach to collect information about the outcomes of different preferences, providing decision-makers insight on how different sets of weightings lead to specific outcomes.

The confidence factor, p_i^c calculates the probability that an alternative is the preferred one for the given central weight vector. It is computed as a multidimensional integral over the criteria distributions.

$$p_i^c = \int_{\xi \in \chi : u(\xi_i, w_i^c) \geq u(\xi_k, w_i^c), \forall k = 1, \dots, m} f_\chi(\xi) \mathrm{d}\xi \qquad (32)$$

The confidence factor measures whether the criteria measurements are sufficient in accuracy to discern between the alternatives when the weight vector is fixed. A high confidence factor suggests that the corresponding alternative is likely to be the

preferred alternative, whereas a low confidence factor suggests that the alternative is unlikely to become the preferred alternative with the given central weight vector.

A.2 SMAA-2 [164, 156]

SMAA-2 was introduced in 2001 by Lahdelma and Salminen. It builds on the original SMAA method by incorporating ranks among the alternatives and by generalizing the utility function, made possible by allowing additional types of preference information. Additional descriptive measures are computed with SMAA-2, providing decision-makers with more insight to the multi-objective problem. The new descriptive measures include the rank acceptability index, the best rank-type measures, and the holistic acceptability index. In order to define the new measures, rank must first be established. Rank is defined by the following:

$$rank(i, \xi, w) = 1 + \sum_{k \neq i} \rho \left(u(\xi_k, w) > u(\xi_i, w) \right) \tag{33}$$

where the function ρ outputs "1" if the inequality holds true and outputs "0" if the inequality is false. The rank is defined by an integer, where a lower integer indicates a higher rank. Rank "1" identifies the most preferred alternative and rank "m" identifies the worst alternative. Once the rank is established, the sets of favorable rank weights, W_i^r are determined by the following:

$$W_i^r(\xi) = \{w \in W \mid rank(i, \xi, w) = r\} \tag{34}$$

A set of favorable rank weights contains all the weight vectors which results in the corresponding alternative achieving the specified rank, r. SMAA-2 analyzes these spaces in order to determine the rank descriptive measures. The rank acceptability index, b_i^r, is similar to the acceptability index in the original SMAA method, the

206

difference being the measure now considers the acceptability for a certain rank. It measures the probability that an alternative is of rank r for the assumed weight distributions used in the computations. It describes the variety of different weight combinations, which results in the alternative obtaining rank r. It is computed as the multidimensional integral over the criteria distribution and the favorable rank weights.

$$b_i^r = \int_{\xi \in \chi} f_\chi(\xi) \int_{w \in W_i^r(\xi)} f_w(w) \mathrm{d}w \mathrm{d}\xi \tag{35}$$

A rank acceptability index of "1" indicates that the corresponding alternative will always obtain rank r for any given set of weights, whereas a rank acceptability of "0" indicates that the alternative will never obtain the specified rank r. In an ideal case, the preferred alternative will result in a rank acceptability index of 1 for the first rank. For the purposes of this study the focus will be limited to the rank-1 acceptability index, the central-weight vectors, and the confidence factors. Figure 78 below demonstrates how the SMAA algorithm works for a notional problem featuring three criteria. The "weight-space" is depicted as a triangle because the weights must add up to one, and thus they are dependent on each other. Each point in the weight-space represents a single weighting scenario. Every alternative is evaluated and ranked with respect to that weighting scenario, and the process is repeated for a number of different sampled weighting scenarios. The ranks are then accumulated for all of these scenarios and used to calculate the rank-1 acceptability indices, the central weight vectors for each alternative, and a confidence factor associated with each central weight vector.
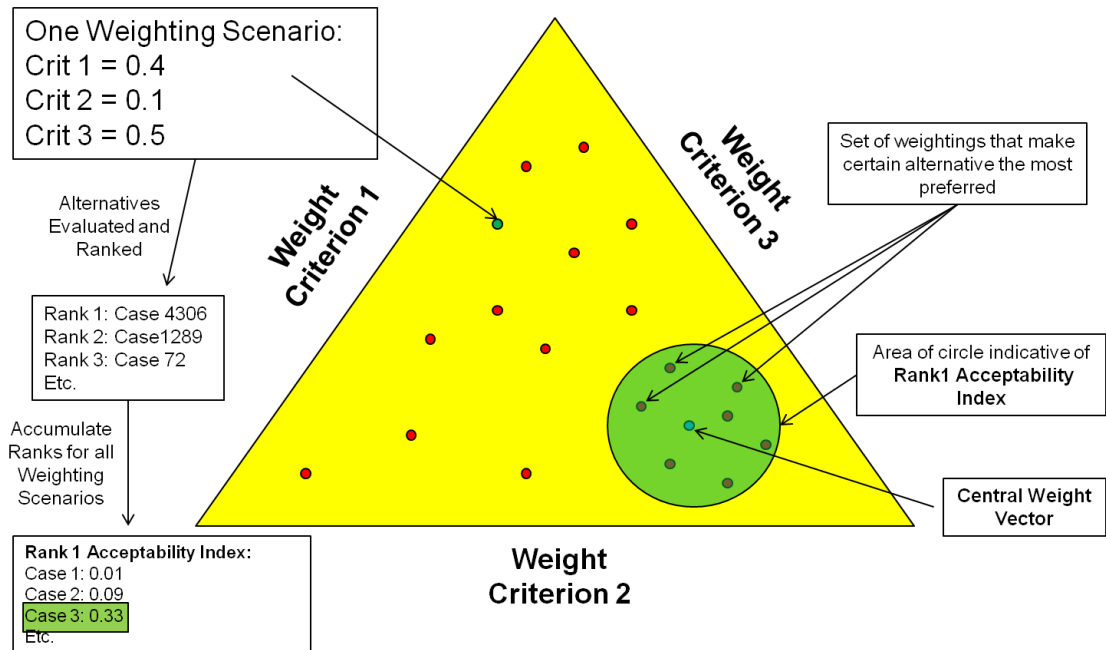
Figure 78: Notional Diagram of Weight Space and SMAA Method

A.3 Simulations

In order to calculate the descriptive measures of SMAA, multidimensional integrations are required. The high dimensionality and the various distributions involved in a problem introduce a high level of complexity in calculating the integrals. Numerical integration techniques are computationally expensive and infeasible as the required effort increases exponentially with the number of dimensions. Instead, Monte Carlo simulations are conducted to handle the complexity. In the Monte Carlo simulations, values for the parameters (weights, criteria, etc.) are selected from their joint probability distributions. The set of parameter values are then used in calculations to determine the rank for the parameter values. Numerous iterations are executed and the aggregation of the results approximates the descriptive measures. The accuracy of these approximations can be set by executing a certain number of simulations. To obtain a 95% confidence accuracy level, A, for the acceptability indices, the number of simulations required, K, is determined by the following [99]:

$$K = \frac{1.96^2}{4A^2} \tag{36}$$

Similarly, a 95% confidence accuracy level for central weight vectors can be achieved with the following number of simulations:

$$K = \frac{1.96^2}{4a_i A^2} \tag{37}$$

where a_i is the acceptability index. In most cases, 10,000 simulations provide sufficient accuracy [163].

There have been several applications of SMAA ranging from drug benefit-risk analysis to ranking potential locations for a university kindergarten. Furthermore, many applications have dealt with supporting, planning and development programs such as cleaning polluted soil, ecosystem management, and centralizing cargo at an airport hub. This wide range of applications demonstrates the versatility of the SMAA algorithm. The ability to explore preference (weight) and parameter (criteria) spaces without preference information allows the algorithm to maintain as much objectivity as possible.

A.4 Generic Vehicle Error-Distributions as Stochastic Criteria Measures

The SMAA method was implemented using open source software called JSMAA [162]. The method allows for defining a set of alternatives (in this case the potential generic vehicle designs), a set of criteria to evaluate the alternatives (in this case the 12 metrics that follow), and measurements of these criteria associated with each alternative. The software allows for the measurements to be defined by exact values or by distributions to capture uncertainty in the metrics, which can be used to evaluate the confidence

factors mentioned in Section A.1. There are several options for distributions, but the nature of the error distributions for the generic vehicle problem have very irregular shapes depending on the metric. Thus, instead of assuming a functional form for these error distributions, the discrete observations of error for the subset of airports were used for the stochastic sampling with each observation having equal probability of being sampled. The metrics of interest are as follows:

1. Total mission fuel burn [kg]

2. Terminal area departure fuel burn (below 3,000-ft) [kg]

3. Terminal area approach fuel burn (below 3,000-ft) [kg]

4. Total mission NO_x emissions [g]

5. Terminal area departure NO_x emissions (below 3,000-ft) [g]

6. Terminal area approach NO_x emissions (below 3,000-ft) [g]

7. DNL 55-dB contour area [nmi^2]

8. DNL 55-dB contour maximum width [nmi]

9. DNL 55-dB contour maximum length [nmi]

10. DNL 65-dB contour area [nmi^2]

11. DNL 65-dB contour maximum width [nmi]

12. DNL 65-dB contour maximum length [nmi]

One issue concerning the use of the JSMAA software for this problem is that the value functions associated with each criteria can only be ascending or descending, whereas the nominal is best formulation for these metrics would require a value function that peaks at zero, and decreases for values less than or greater than zero.

Since no preference is placed on under-predicting versus over-predicting, this problem can be avoided by instead using the distribution of the absolute value of the relative error. This essentially folds the distribution over the zero-relative error point and turns the problem into a minimum is best formulation.

One advantage of this approach is that the ranges for these error distributions can be used to quickly gauge the existence of a design that captures zero-error. The absolute value of the relative error distribution folds the distribution over the zero-error axis, as is demonstrated in Figure 79. If the design fails to capture zero-error, however, then the relative error distribution and the absolute value of the relative error distribution will have similar shapes, as is demonstrated in Figure 80. In this example, the terminal area approach fuel-burn for the potential Generic Vehicle is under-predicting the target metrics at every airport. As a result, the relative error distribution does not capture zero error, and thus the absolute relative error distribution is purely a reflection of the relative error distribution with a similar shape. If the Generic Vehicle alternative had over-predicted terminal area approach fuel-burn at every airport, then the distribution of the absolute value of the relative error will be exactly identical to the distribution of the relative error.
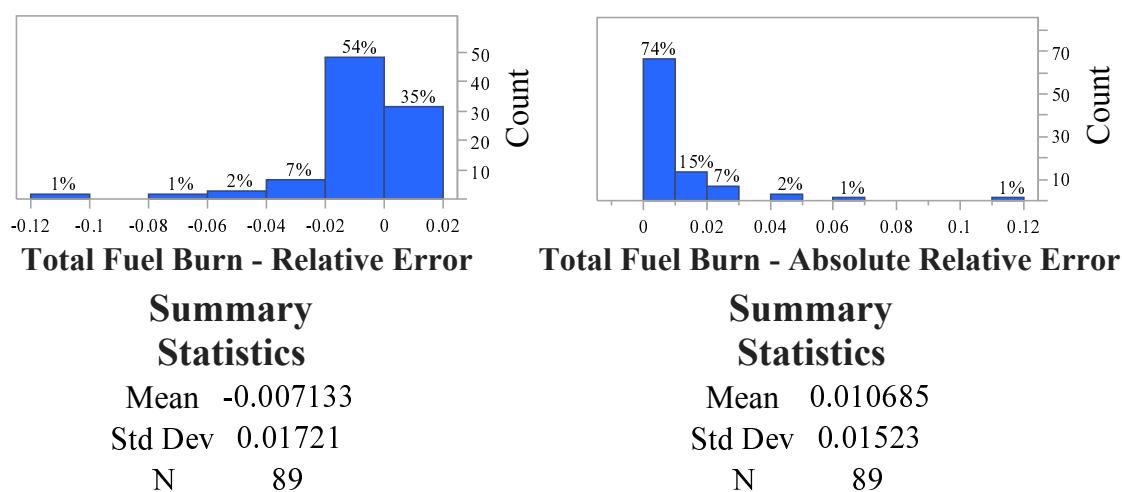

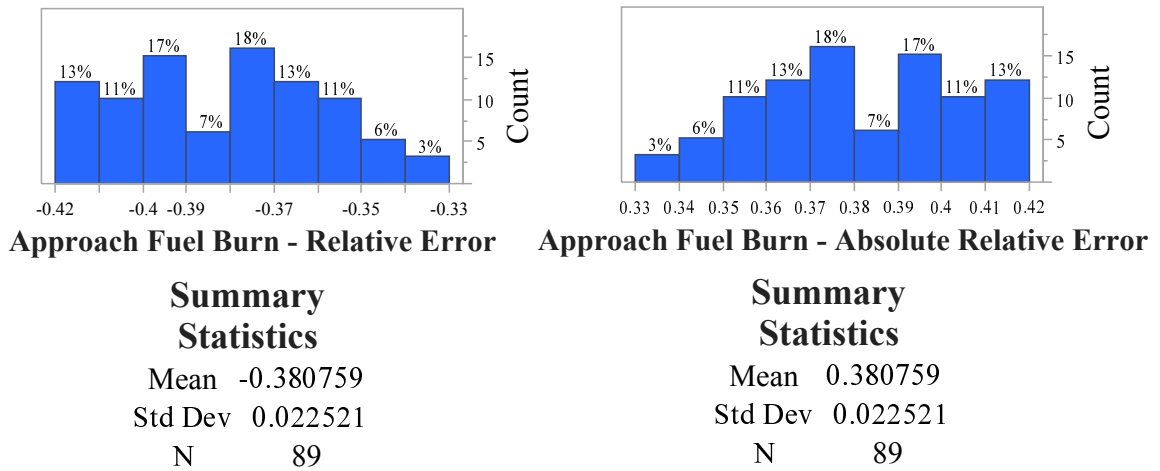Figure 79: Different Relative and Absolute Relative Error Distributions

Summary Statistics

Mean	-0.380759
Std Dev	0.022521
N	89

Summary Statistics

Mean	0.380759
Std Dev	0.022521
N	89

Figure 80: Similar Relative and Absolute Relative Error Distributions

In the latter example, it was determined that a bias existed between the EDS vehicle approach fuel-burn and NO_x emissions and the targets generated from the constituent database vehicles. Upon closer examination, this bias exists because the EDS vehicles assume Continuous Descent Approaches (CDAs) whereas many of the database vehicles feature traditional dive-and-drive approaches with a level-off at approximately 3,000-ft altitude, as is demonstrated in Figure 81. Until CDA procedures are developed for all of the actual vehicles or dive-and-drive approach procedures are designed within the EDS-AEDT mapping, this bias remains irreducible. As a result, every potential Generic Vehicle from EDS features this bias. Given that these differences are due to different operational assumptions rather than vehicle characteristics, this observation indicated that terminal-area approach metrics should be left out of the SMAA analysis. This difference in approach procedures also manifested itself in the form of the DNL contour maximum lengths, and thus contour length was also removed from the SMAA analysis. This effectively reduced the number of metrics included in the SMAA analysis from 12 to 8.

It should be noted that the setup for the SMAA analysis is the same for each of the validation Tests A-F. The only change that occurred is for Test E and F, the DNL
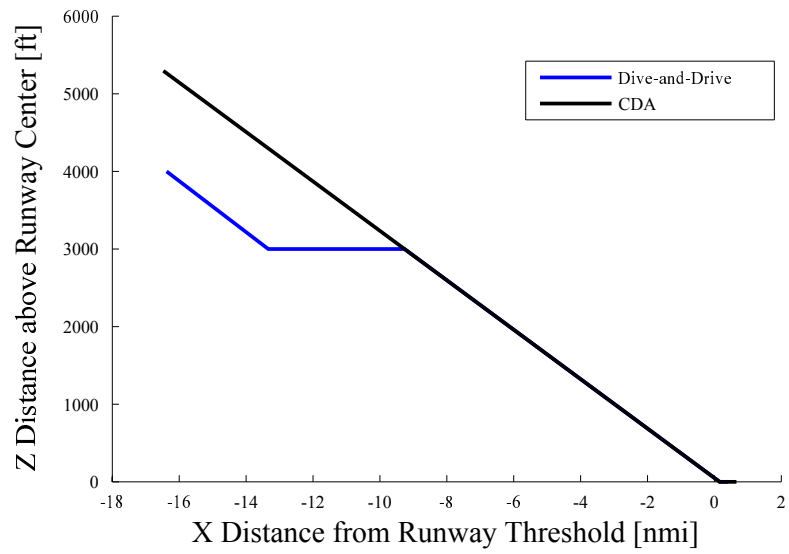
Figure 81: Approach Trajectory Comparison

contour widths were removed and replaced by the Detour index and the Spin index described in Figure 16. This increased the number of metrics from 8 to 10.

REFERENCES

[1] Black, T. and Johnsson, J., "Boeing Raises 20-Year Jet Demand Forecast by 3.8%," *Bloomberg News*, June 11, 2013.

[2] Clark, N., "Big-Ticket Orders at Paris Air Show," *New York Times*, June 20, 2013.

[3] Mayerowitz, S., "Airlines Go on a Record New Jet Shopping Spree," *The Associated Press*, January 2014.

[4] "Terminal Area Forecast Summary, Fiscal Years 2012-2040," Technical Report, Federal Aviation Administration, 2012.

[5] "Aviation and the Environment: Results from a Survey of the Nation's 50 Busiest Commercial Service Airports," Technical Report GAO/RCED-00-222, United States General Accounting Office, August 2000.

[6] "Concept of Operations for the Next Generation Air Transportation System," Technical Report, Joint Planning and Development Office, June 13 2007.

[7] "IATA Technology Roadmap," Technical Report, International Air Transport Association, June 2013.

[8] "The Postal History of ICAO: Annex 16 - Environmental Protection," International Civil Aviation Organization, 2013, `http://www.icao.int/secretariat/PostalHistory/annex_16_environmental_protection.htm`.

[9] "Consolidated statement of continuing ICAO policies and practices related to environmental protection," International Civil Aviation Organization, Resolution A37-18, 2010, `http://www.icao.int/environmental-protection/Documents/A37-Env-Resos-9958.pdf`.

[10] "Aviation Environmental Design Tool (AEDT) Progress," Information Paper CAEP/7-IP/24, International Civil Aviation Organization (ICAO): Committee on Aviation Environmental Protection (CAEP), Montreal, February 2004.

[11] Koopmann, J., Ahearn, M., Boeker, E., Hansen, A., Hwang, S., Malwitz, A., Senzig, D., Solman, G. B., Dinges, E., Yaworski, M., Soucacos, P., and Moore, J., *Aviation Environmental Design Tool (AEDT) Technical Manual Version 2a*, U.S. Department of Transportation (USDOT) Volpe National Transportation Systems Center, Federal Aviation Administration Office of Environment and Energy, 55 Broadway, Cambridge, MA 02142, November 2012, DOT-WNTSC-FAA-12-09.

[12] "National Environmental Policy Act (NEPA) Implementing Instructions for Airport Actions," U.S. Department of Transportation (DOT), Federal Aviation Administration (FAA), ARP Order 5050.4B, April 2006.

[13] "Aircraft Contrails Factsheet," Factsheet EPA 430-F-00-005, Environmental Protection Agency, September 2000.

[14] "Clean Air Act of 1970," Code of Federal Regulations 42 U.S.C. §7409; 40 C.F.R. Part 50, 1972.

[15] Falzone, K. L., "Airport Noise Pollution: Is There a Solution in Sight?" *Boston College Environmental Affairs Law Review*, Vol. 26, No. 4, 1999, pp. 769, `http://lawdigitalcommons.bc.edu/ealr/vol26/iss4/8`.

[16] "Noise Control Act of 1972," Public Law P.L. 92-574, 86 Stat. 1234, 42 U.S.C. §4901 - 42 U.S.C. §4918., 1972.

[17] "Technology for a Quieter America," National Academy of Engineering of the National Academies, The National Academies Press, Washington, D.C., 2010, pp. 5–87.

[18] Truax, B., *The Handbook For Acoustic Ecology*, No. 5 in The World Soundscape Project: The Music of the Environment Series, Simon Fraser University, ARC Publications, 2nd ed., 1978.

[19] "CleanSky: Innovating together, flying greener," CleanSky, `http://www.cleansky.eu/`.

[20] "Strategic Research Agenda," Technical Report Volume 1, Advisory Council for Aeronautical Research in Europe (ACARE), Brussels, October 2002, `http://www.acare4europe.org/sites/acare4europe.org/files/document/ASD-volume1-2nd-final-ss%20illus-171104-out-asd.pdf`.

[21] "Strategic Research Agenda," Technical Report Volume 2, Advisory Council for Aeronautical Research in Europe (ACARE), Brussels, October 2004, `http://www.acare4europe.org/sites/acare4europe.org/files/document/ASD-Annex-final-211004-out-asd.pdf`.

[22] "Strategic Research and Innovation Agenda (SRIA)," Technical Report Volume 2, Advisory Council for Aeronautical Research in Europe (ACARE), Brussels, September 2012, `http://www.acare4europe.org/sites/acare4europe.org/files/attachment/SRIA%20Volume%202.pdf`.

[23] "Flightpath 2050 - Europe's Vision for Aviation," Technical Report, Advisory Council for Aeronautical Research in Europe (ACARE), Luxembourg, 2011, `http://ec.europa.eu/transport/modes/air/doc/flightpath2050.pdf`.

[24] Kryter, K., "Concepts of perceived noisiness, their implementation and application," *The Journal of the Acoustical Society of America*, Vol. 43, No. 2, October 1967, pp. 344–361.

[25] Collier, F., "NASA: Environmentally Responsible Aviation Project - Real Solutions for Environmental Challenges Facing Aviation," 50th Aerospace Sciences Meeting (ASM), National Aeronautics and Space Administration (NASA), American Institute of Aeronautics and Astronautics (AIAA), Nashville, Tennessee, January 2012.

[26] "Part 36 - Noise Standards: Aircraft Type and Airworthiness Certification," United States Department of Transportation (USDOT), Federal Aviation Administration (FAA), Code of Federal Regulations, Federal Aviation Regulation 14 CFR F.A.R. Part 36, October 2012.

[27] "Environmental Protection: Aircraft Engine Emissions," International Civil Aviation Organization (ICAO), International Standards and Recommended Practices Annex 16, Volume II, 1993.

[28] "Continuous Lower Emissions, Energy, and Noise (CLEEN) Program," Federal Aviation Administration (FAA), `http://www.faa.gov/about/office_org/headquarters_offices/apl/research/aircraft_technology/cleen/`.

[29] "Environmentally Responsible Aviation (ERA) Project: Integrated Systems Research Program," National Aeronautics and Space Administration (NASA), `http://www.aeronautics.nasa.gov/isrp/era/`.

[30] Jimenez, H., Pfaender, H., and Mavris, D., "Fuel Burn and CO2 System-Wide Assessment of Environmentally Responsible Aviation Technologies," *AIAA Journal of Aircraft*, Vol. 49, No. 6, November-December 2012, pp. 1913–1930.

[31] Collier, F., Zavala, E., and Huff, D., "Subsonic Fixed Wing Project Reference Document," National Aeronautics and Space Administration (NASA), `http://www.aeronautics.nasa.gov/nra_pdf/sfw_proposal_c1.pdf`.

[32] Mankins, J. C., "Technology Readiness Levels," White Paper, National Aeronautics and Space Administration (NASA), April 1995.

[33] "Technology Readiness Levels Introduction," National Aeronautics and Space Administration (NASA), `http://web.archive.org/web/20051206035043/http://as.nasa.gov/aboutus/trl-introduction.html`.

[34] Collier, F., Mangelsdorf, M., and Yokum, S., "NASA Environmentally Responsible Aviation Project: N+2 Advanced Vehicle Concepts NASA Research Announcement (NRA) Draft Solicitation," Technical Report, National Aeronautics and Space Administration (NASA), 2010.

[35] Fleming, G. G., Balasubramanian, S., and Malwitz, A., "Global Fuel Burn and Emissions to 2050," *Transportation Research Board 2014 Annual Meeting*, U.S. Department of Transportation, John A. Volpe National Transportation Systems Center, 2014.

[36] Jenks, C. W., Jencks, C. F., Salamone, M. R., Schatz, T. H., Baker, T., Delaney, E. P., and Lamberton, S. C., "Evaluating Airport Capacity," ACRP Report 79, Airport Cooperative Research Program (ACRP), 2012, Sponsored by the Federal Aviation Administration (FAA).

[37] "Aviation Infrastructure: Challenges Related to Building Runways and Actions to Address Them," Technical Report GAO-03-164, United States General Accounting Office, January 2003.

[38] "Aviation and the Environment: Impact of Aviation Noise on Communities Presents Challenges for Airport Operations and Future Growth of the National Airspace System," Technical Report GAO-08-216T, United States General Accounting Office, October 2007.

[39] "Aviation and the Environment: Systematically Addressing Environmental Impacts and Community Concerns Can Help Airport Reduce Project Delays," Report to Congressional Requesters GAO-10-50, United States General Accounting Office, September 2010.

[40] Waitz, I., Townsend, J., Cutcher-Gershenfeld, J., Greitzer, E., and Kerrebrock, J., "AVIATION AND THE ENVIRONMENT: A National Vision Statement, Framework for Goals and Recommended Actions," Report to the United States Congress, Partnership for AiR Transportation Noise and Emissions Reduction (PARTNER), December 2004, An FAA/NASA/Transport Canada-sponsored Center of Excellence.

[41] "Aviation and the Environment: Strategic Framework Needed to Address Challenges Posed by Aircraft Emissions," Report to the Chairman, Subcommittee on Aviation, Committee on Transportation and Infrastructure, House of Representatives GAO-03-252, United States General Accounting Office, February, 2003.

[42] "Capacity Needs in the National Airspace System 2007-2025," Technical Report, The MITRE Corporation Center for Advanced Aviation System Development, May 2007.

[43] "Capacity Needs in the National Airspace System 2007-2025," Technical Report, The MITRE Corporation Center for Advanced Aviation System Development, May 2015.

[44] Becker, K. F., *A Methodology to Enable Rapid Evaluation of Aviation Environmental Impacts and Aircraft Technologies*, Doctoral Thesis, Georgia Institute of Technology, North Ave NW, Atlanta, GA 30332, August 2011.

[45] "The Science of Climate Change," Technical Report, Intergovernmental Panel on Climate Change (IPCC) Working Group I, 1996.

[46] Stocker, T. F., Qin, D., Plattner, G.-K., Tignor, M. M., Allen, S. K., Boschung, J., Nauels, A., Xia, Y., Bex, V., and Midgley, P. M., "Climate Change 2013: The Physical Science Basis," Summary for Policymakers, Intergovernmental Panel on Climate Change (IPCC) Working Group I, October 2013.

[47] "Overview of Greenhouse Gases," United States Environmental Protection Agency (EPA), 2013, http://epa.gov/climatechange/ghgemissions/gases.html.

[48] Solomon, S., Qin, D., Manning, M., Alley, R., Berntsen, T., Bindoff, N., Chen, Z., Chidthaisong, A., Gregory, J., Hegerl, G., Heimann, M., Hewitson, B., Hoskins, B., Joos, F., Jouzel, J., Kattsov, V., Lohmann, U., Matsuno, T., Molina, M., Nicholls, N., Overpeck, J., Raga, G., Ramaswamy, V., Ren, J., Rusticucci, M., Somerville, R., Stocker, T., Whetton, P., Wood, R., and Wratt, D., "Climate Change 2007: The Physical Science Basis. Contribution of Working Group I to the Fourth Assessment Report of the Intergovernmental Panel on Climate Change," Technical Summary, Intergovernmental Panel on Climate Change (IPCC) Working Group I, Cambridge University Press, Cambridge, United Kingdom and New York, NY, USA, 2007.

[49] Shindell, D. and et al, "Improved Attribution of Climate Forcing to Emissions," *Science*, Vol. 326, No. 5935, October 2009, pp. 716–718.

[50] Turns, S. R., *An Introduction to Combustion Concepts and Applications*, McGraw Hill, 2012.

[51] Oates, G. C., editor, *Aircraft Propulsion Systems Technology and Design*, American Institute of Aeronautics and Astronautics (AIAA), Inc., Washington, DC, 3rd ed., 1989, Third Printing.

[52] Stern, A. C., Boubel, R. W., Turner, D. B., and Fox, D. L., *Fundamentals of Air Pollution*, Academic Press, Inc., Orlando, FL, 2nd ed., 1984.

[53] Federal Aviation Administration Office of Environment and Energy, *Aviation & Emissions: A Primer*, January 2005.

[54] Reeves, C. E., Penkett, S. A., Bauguitte, S., Law, K. S., Evans, M. J., Bandy, B. J., Monks, P. S., Edwards, G. D., Phillips, G., Barjat, H., Kent, J., Dewey, K., Schmitgen, S., and Kley, D., "Potential for photochemical ozone formation in the troposphere over the North Atlantic as derived from aircraft observations during ACSOE," *Journal of Geophysical Research*, Vol. 107, No. D23: 4707, 2002.

[55] Gierczak, T., Talukdar, R. K., Herndon, S. C., Vaghjiani, G. L., and Ravishankara, A. R., "Rate Coefficients for the Reactions of Hydroxyl Radicals

with Methane and Deuterated Methanes," *The Journal of Physical Chemistry*, Vol. 101, No. 17, 1997, pp. 3125–3134.

[56] Lary, D., "Catalytic destruction of stratospheric ozone," *Journal of Geophysical Research*, Vol. 102, No. D17, September 1997, pp. 21515–26.

[57] Generalic, E., "Atmosphere," Croatian-English Chemistry Dictionary & Glossary, http://glossary.periodni.com/glossary.php?en=atmosphere.

[58] Burkhardt, U. and Krcher, B., "Global radiative forcing from contrail cirrus," *Nature Climate Change*, Vol. 1, March 2011, pp. 54–58.

[59] Heymsfield, A., Baumgardner, D., Demott, P., Forster, P., Gierens, K., and Krcher, B., "Contrail Microphysics," *Bulletin of the American Meteorological Society*, Vol. 91, No. 4, April 2010, pp. 465–472.

[60] Bernardo, J., Boling, B., Bonnefoy, P., Burdette, G., Hansman, J., Kirby, M., Lim, D., Mavris, D., Mozdzanowska, A., Nam, T., Pfaender, H., Waitz, I., and Yutko, B., "CO2 Emission Metrics for Commercial Aircraft Certification: A National Airspace System Perspective," Project 30 Findings Report PARTNER-COE-2012-002, Partnership for AiR Transportation Noise and Emissions Reduction (PARTNER), March 2012.

[61] "CAEP/9 Agreed Certification Requirement for the Aeroplane CO2 Emissions Standard," International Civil Aviation Organization, Tech. Rep. ICAO CIR 337, 2013.

[62] "Control of Air Pollution From Aircraft and Aircraft Engines," Environmental Protection Agency (EPA), Proposed Emission Standards and Test Procedures, Federal Register: The Daily Journal of the United States Government, 2011.

[63] Janić, M., *The Sustainability of Air Transportation: A Quantitative Analysis and Assessment*, Ashgate Publishing Limited, 2007.

[64] Holmes, C., Tang, Q., and Prather, M., "Uncertainties in Climate Assessment for the Case of Aviation NO," *Proceedings of the National Academy of Sciences of the United States of America*, Vol. 108 (27), July 2011, pp. 10997–1002, PMID: 21690364.

[65] Rypdal, K., "Aircraft Emissions," *Good Practice Guidance and Uncertainty Management in National Greenhouse Gas Inventories*.

[66] "Health and Environmental Impacts of NO_x," Technical Report, United States Environmental Protection Agency (EPA), February 2013.

[67] Singh, A. and Agrawal, M., "Acid rain and its ecological consequences," *Journal of Environmental Biology*, Vol. 29, No. 1, 2008, pp. 15–24.

[68] More, S. R., *Aircraft Noise Characteristics and Metrics*, Doctoral Thesis, Purdue University, West Lafayette, Indiana, December 2010.

[69] "Noise Standards: Aircraft Type and Airworthiness Certification, Calculation of Effective Perceived Noise Level from Measured Data," United States Department of Transportation (USDOT), Federal Aviation Administration (FAA), Federal Aviation Regulation F.A.R. Part 36, Appendix A2 to Part 36 - §A36.4, 2002.

[70] "Tutorial: Aircraft Noise and its Prediction," National Aeronautics and Space Administration (NASA), June 2013, `https://mdao.grc.nasa.gov/reengine/noise_primer.html`.

[71] "Procedure for the Calculation of Airplane Noise in the Vicinity of Airports," Society of Automotive Engineers (SAE), Committee A-21, Aircraft Noise, Aerospace Information Report SAE-AIR-1845, March 1986.

[72] Boeker, E. R., Dinges, E., He, B., Fleming, G., Roof, C. J., Gerbi, P. J., Rapoza, A. S., and Hemann, J., *Integrated Noise Model (INM) Version 7.0 Technical Manual*, U.S. Department of Transportation (USDOT) Federal Aviation Administration (FAA) Office of Environment and Energy, 800 Independence Avenue, S.W., Washington, DC 20591, January 2008.

[73] "Report on Standard Method of Computing Noise Contours around Civil Airports," European Civil Aviation Conference, Tech. Rep. 29, 1997.

[74] Schomer, P. D., "Criteria for Assessment of Noise Annoyance," *Noise Control Engineering Journal*, Vol. 53, No. 4, July-August 2005, pp. 125–137.

[75] Schultz, T. J., "Synthesis of Social Surveys on Noise Annoyance," *Journal of the Acoustical Society of America*, Vol. 64, No. 2, 1978, pp. 377–405.

[76] "Portfolio of Goals, FY 2012," Technical Report, Federal Aviation Administration, 2012.

[77] "Noise Exposure Map and Noise Compatibility Program, Executive Summary," Code of Federal Regulations 14 CFR Part 150 Study, Bradley International Airport, October 2003.

[78] "Airport Noise and Emissions Regulations: Cleveland-Hopkins International," The Boeing Company, 2011, `http://www.boeing.com/commercial/noise/cleveland_hopkins.html`.

[79] Bernardo, J. E., *Formulating and Implementing a Generic Fleet-Level Noise Methodology*, Doctoral Thesis, Georgia Institute of Technology, North Ave NW, Atlanta, GA 30332, May 2013.

[80] Angel, S., Parent, J., and Civco, D., "Ten Compactness Properties of Circles: Measuring Shape in Geography," *Canadian Geographer*, Vol. 54, No. 4, 2010, pp. 441–461.

[81] "TECHNICAL DOCUMENTATION: 2010 Census Summary File 1," 2010 Census of Population and Housing Units SF1/10-4 (RV), U.S. Census Bureau, September 2012.

[82] "TIGER Products," United States Census Bureau, 2014, `https://www.census.gov/geo/maps-data/data/tiger.html`.

[83] Kish, C., *An Estimate of the Global Impact of Commercial Aviation Noise*, Master's thesis, Massachusetts Institute of Technology, 2008.

[84] Moolchandani, K. A., Agusdinata, D. B., DeLaurentis, D. A., and Crossley, W. A., "Assessment of the Effect of Aircraft Technological Advancement on Aviation Environmental Impacts," *51st AIAA Aerospace Sciences Meeting including the New Horizons Forum and Aerospace Exposition*, No. AIAA 2013-0652, Purdue University, January 2013.

[85] `http://www.seatguru.com/`.

[86] Hahn, R. W., "An Economic Analysis of Scrappage," *RAND Journal of Economics*, Vol. 26, No. 2, 1995, pp. 222–242.

[87] Dikshit, P. N. and Crossley, W. A., "Airport Noise Model Suitable for Fleet-Level Studies," *9th AIAA Aviation Technology, Integration, and Operations Conference (ATIO)*, No. AIAA 2009-6937, Purdue University, September 2009.

[88] Hogg, R. and Tanis, E., *Probability and Statistical Inference*, Pearson, 8th ed., 2010.

[89] Pfaender, H., Jimenez, H., and Mavris, D., "Effects of Technology R&D Investments on System Level Performance," *Aviation Technology, Integration, and Operations Conference at AIAA Aviation*, No. AIAA 2013-4284, Georgia Institute of Technology, Los Angeles, CA, August 2013.

[90] Aly, M., "Survey on Multiclass Classification Methods," .

[91] Branke, J., Deb, K., Miettinen, K., and Slowinski, R., editors, *Multiobjective Optimization: Interactive and Evolutionary Approaches*, Springer Science+Business Media, LLC, 2008.

[92] Bhaduri, B., Bright, E., and Coleman, P., "Development of High Resolution Population Distribution Data to Enhance Cancer Prevention and Control Research," SEER Special Project 08 RFP No. NCI-PC-25014-20, Geographic Information Science & Technology: Oak Ridge National Laboratory, Oak Ridge, TN 37831-6017, 2004.

[93] Wu, S., Qiu, X., and Wang, L., "Population Estimation Methods in GIS and Remote Sensing: A Review," *GIScience & Remote Sensing*, Vol. 42, No. 1, 2005, pp. 80–96.

[94] Koziel, S. and Leifsson, L., editors, *Surrogate-Based Modeling and Optimization: Applications in Engineering*, Springer Science+Business Media, 2013.

[95] Bandler, J., Cheng, Q., Dakroury, S., Mohamed, A., Bakr, M., Madsen, K., and Sndergaard, J., "Space mapping: the state of the art," *IEEE Transactions on Microwave Theory and Techniques*, Vol. 52, No. 1, January 2004, pp. 337–361.

[96] Anderson, M. and Robinson, J., "Generalized Discriminant Analysis Based on Distances," *Australian & New Zealand Journal of Statistics*, Vol. 45, Issue 3, No. DOI: 10.1111/1467-842X.00285, September 2003, pp. 301–318.

[97] Rencher, A. C., *Methods of Multivariate Analysis*, JJohn Wiley & Sons, Inc., 2002.

[98] Hastie, T., Tibshirani, R., and Friedman, J., editors, *The Elements of Statistical Learning: Data Mining, Inference, and Prediction*, Springer Science+Business Media, LLC, 2nd ed., 2009.

[99] Milton, J. and Arnold, J., *Introduction to Probability and Statistics*, McGraw-Hill International, New York, NY, 3rd ed., 1995.

[100] Hyndman, R. J. and Koehler, A. B., "Another look at measures of forecast accuracy," *International Journal of Forecasting*, Vol. 22, No. 4, 2006, pp. 679–688.

[101] Okabe, A., Boots, B., Sugihara, K., and Chiu, S. N., *Spatial Tessellations Concepts and Applications of Voronoi Diagrams*, No. ISBN 0-471-98635-6, John Wiley, 2nd ed., 2000.

[102] Ertl, B., "Euclidean Voronoi diagram," `https://commons.wikimedia.org/wiki/File:Euclidean_Voronoi_diagram.svg`.

[103] Kirby, M., "Environmental Design Space (EDS)," Presentation for Aviation Environmental Tools Colloquium COE Project 14, Federal Aviation Administration, December 2010.

[104] Kirby, M. and Mavris, D., "The Environmental Design Space," *26th International Congress of the Aeronautical Sciences*, Vol. 26th International Congress of the Aeronautical Sciences, Georgia Institute of Technology, 2008.

[105] Kestner, B. K., Schutte, J. S., Gladin, J. C., and Mavris, D. N., "Ultra High Bypass Ratio Engine Sizing and Cycle Selection Study for a Subsonic Commercial Aircraft in the N+2 Timeframe," *Proceedings of ASME Turbo Expo 2011*, No. GT2011-45370, Aerospace Systems Design Laboratory (ASDL), Vancouver, Canada, June 2011.

[106] Converse, G. and Giffin, R., "Extended Parametric Representation of Compressors Fans and Turbines, Vol. I - CMPGEN Users Manual," Contractor Report NASA CR-174645, March 1984.

[107] Glassman, A., "Design Geometry and Design/Off-Design Performance Computer Codes for Compressors and Turbines," Contractor Report NASA CR 198433, University of Toledo, Toledo, Ohio, 1995.

[108] Lytle, J., "The Numerical Propulsion System Simulation: A Multidisciplinary Design for Aerospace Vehicles," Technical Memorandum NASA TM-1999-209194, NASA Glenn Research Center, Cleveland, Ohio, September 1999.

[109] Lytle, J., "The Numerical Propulsion System Simulation: An Overview," Technical Memorandum NASA TM-2000-209915, NASA Glenn Research Center, Cleveland, Ohio, June 2000.

[110] Onat, E. and Klees, G., "A Method to Estimate Weight and Dimensions of Large and Small Gas Turbine Engines," Contractor Report NASA-CR-159481, Boeing Aerospace Company, January 1979.

[111] Tong, M., Halliwell, I., and Ghosn, L., "A Computer Code for Gas Turbine Engine Weight and Disk Life Estimation," *ASME Turbo Expo*, No. GT-2002-30500, 2002.

[112] Schutte, J., *Simultaneous Multi-Design Point Approach to Gas Turbine On-Design Cycle Analysis for Aircraft Engines*, Doctoral Thesis, Georgia Institute of Technology, Atlanta, Georgia, May 2009.

[113] McCullers, L., "Flight Optimization System," Users Guide Release 6.12, Swales Aerospace, October 2004.

[114] Norman, P. D., Lister, D. H., Lecht, M., Madden, P., Park, K., Penanhoat, O., Plaisance, C., and Renger, K., "Development of the Technical Basis for a New Emission Parameter Covering the Whole AIRcraft Operation (NEPAIR)," Final Technical Report G4RD-CT-2000-00182, European Commission, September 2003.

[115] Zorumski, W., "Aircraft Noise Prediction Program Theoretical Manual, Part 1," Technical Memorandum NASA TM-83199-Pt-1, NASA Langley Research Center, Hampton, Virginia, February 1982.

[116] Zorumski, W., "Aircraft Noise Prediction Program Theoretical Manual, Part 2," Technical Memorandum NASA TM-83199-Pt-2, NASA Langley Research Center, Hampton, Virginia, February 1982.

[117] de Luis, J., *A Process for the Quantification of Aircraft Noise and Emissions Interdependencies*, Doctoral Thesis, Georgia Institute of Technology, North Ave NW, Atlanta, GA 30332, August 2008.

223

[118] Kestner, B. K., Schutte, J. S., Tai, J. C., Perullo, C. A., and Mavris, D. N., "Surrogate Modeling for Simultaneous Engine Cycle and Technology Optimization for Next Generation Subsonic Aircraft," *Proceedings of ASME Turbo Expo 2012*, No. GT2012-68724, Aerospace Systems Design Laboratory (ASDL), Copenhagen, Denmark, June 2012.

[119] McNamara, S., "The case for investing in the regional airline industry," Tech. rep., European Regions Airline Association (Limited), 2014.

[120] de Souza e Silva, P. C., "Market Outlook 2015 - 2034," Tech. rep., Embraer, June 2015, www.embraermarketoutlook.com.

[121] "Market Forecast 2015 - 2034," Tech. rep., Bomabardier Commercial Aircraft, 2015.

[122] Hulst, D., "Current Market Outlook 2014-2033," Tech. rep., Boeing Commercial Airplanes Market Analysis, 2014.

[123] LeVine, M., Kirby, M., and Mavris, D., "Noise-Sensitivity to Vehicle-Level Design Variables," *12th AIAA Aviation, Technology, Integration, and Operations (ATIO) Conference and 14th AIAA/ISSM*, 12th AIAA Aviation, Technology, Integration, and Operations (ATIO) Conference and 14th AIAA/ISSM, Georgia Institute of Technology, Indianapolis, IN, September 2012.

[124] Price, M., editor, *MasMaster ArcGIS®*, McGraw-Hill, sixth ed., 2014.

[125] Long, D., Lee, D., Johnson, J., Gaier, E., and Kostiuk, P., "Modeling Air Traffic Management Technologies With a Queuing Network Model of the National Airspace System," NASA Contractor Report NASA / CR- 1999- 208988, Logistics Management Institute, McLean, Virginia, January 1999.

[126] "FESG CAEP/8 Traffic and Fleet Forecasts Information Paper 2," Environmental Protection Technical Report TR CAEP/8-IP/2, International Civil Aviation Organization Committee on Aviation, 2008.

[127] Hollingsworth, P., Pfaender, H., and Jimenez, H., "A Method for Assessing the Environmental Benefit of FutureAviation Technologies," *Proceedings of the 26th International Congress of the Aeronautical Sciences ICAS 2008*, Optimage Ltd., Edinburg, UK, Anchorage, AK, Sept. 2008.

[128] Pfaender, H., Jimenez, H., and Mavris, D., "Effects of Technology R&D Investments on System Level Performance," *Aviation Technology, Integration, and Operations Conference at AIAA Aviation*, 2013.

[129] Schutte, J. and Mavris, D., "FY2011 Environmentally Responsible Aviation Systems Analysis Report: Technology Portfolio and Advanced Configurations," Tech. rep., Georgia Institute of Technology, January 2011.

[130] Bernardo, J. E., Kirby, M. R., and Mavris, D., "DNL Contour Area Sensitivity to Fleet-Level Operational Characteristics," *AIAA/3AF Aircraft Noise and Emissions Reduction Symposium at AIAA Aviation*, No. AIAA 2014-2877, Georgia Institute of Technology, Atlanta, GA, June 2014.

[131] "Terminal Area Forecast Summary, Fiscal Years 2013-2040," Technical Report, Federal Aviation Administration, 2013.

[132] Jimenez, H., F. C. P. H. M. D., "Development of fleet scenarios for next decadal technologies and concepts," *Proceedings of the 13th AIAA Aviation Technology, Integration, and Operations (ATIO) Conference at AIAA Aviation*, Georgia Institute of Technology, AIAA, August 2013.

[133] Bernardo, J. E., Kiehl, O., Kirby, M. R., and Mavris, D., "Analysis of Vehicle Class Contributions to Total DNL Response," *AIAA/3AF Aircraft Noise and Emissions Reduction Symposium at AIAA Aviation*, No. AIAA 2014-2876, Georgia Institute of Technology, Atlanta, GA, June 2014.

[134] Bernardo, J. E., Kirby, M., and Mavris, D., "Development of generic airport categories for rapid fleet-level noise modeling," *Journal of Aerospace Operations*, , No. 2, June 2015, pp. 91–119.

[135] "Airport Design," U.S. Department of Transportation (USDOT), Federal Aviation Administration (FAA), Advisory Circular AC 150/5300-13A CHG 1, February 2014.

[136] "Airport Master Plans," US Department of Transportation (USDOT), Federal Aviation Administration (FAA), Advisory Circular AC 150/5070-6B Change 1, May 2001.

[137] "Runway Length Requirements for Airport Design," US Department of Transportation (USDOT), Federal Aviation Administration (FAA), Advisory Circular AC 150/5325-4B, July 2005.

[138] Yim, W. F., "An Analysis of Airport Runway Designs to Maximize New Airport Throughput to meet Chinas Long-Term Air Travel Demand," *American Society of Civil Engineers (ASCE): Sustainable Transportation Systems*, , No. 10.1061/9780784412299.0011, 2012, pp. 77–84.

[139] Butler, V., "Increasing Airport Capacity Without Increasing Airport Size," Public Policy Research, Reason Foundation, 3415 S. Sepulveda Blvd., Suite 400, Los Angeles, CA 90034, March 2008.

[140] LeVine, M., Kaul, A., Bernardo, J., Kirby, M., and Mavris, D., "Methodology for Calibration of ANGIM Subjected to Atmospheric Uncertainties," *Aviation Technology, Integration, and Operations Conference at AIAA Aviation*, No. AIAA 2013-4321 in 2013 Aviation Technology, Integration, and Operations Conference (ATIO), Georgia Institute of Technology, Los Angeles, CA, August 2013.

[141] LeVine, M. J., Moss, R., Kirby, M., and Mavris, D., "Methodology for Runway-Level DNL Contour Calibration in ANGIM to Capture Impacts of Deviation from Standard Day Sea-Level Atmosphere," *AIAA Modeling and Simulation Technologies Conference at AIAA Aviation*, No. AIAA 2014-2348, Georgia Institute of Technology, Atlanta, GA, June 2014.

[142] Wilson, A. J., LeVine, M. J., Bernardo, J. E., Kirby, M., and Mavris, D., "Development of Generic Ground Tracks of Performance Based Navigation Operations for Fleet-Level Airport Noise Analysis," *15th AIAA Aviation Technology, Integration, and Operations Conference at AIAA Aviation*, No. AIAA 2015-3029, Georgia Institute of Technology, Dallas, TX, 2015.

[143] Antoine, N. E. and Kroo, I. M., "Framework for Aircraft Conceptual Design and Environmental Performance Studies," *AIAA Journal*, Vol. 43, No. 10, October 2005.

[144] Bernardo, J., Kirby, M., and Mavris, D., "Development of a Generic Fleet-Level Noise Methodology," 50th AIAA Aerospace Sciences Meeting including the New Horizons Forum and Aerospace Exposition, Georgia Institute of Technology, Nashville, TN, January 2012.

[145] Charnetski, J. R., *The Multiple Attribute Problem with Partial Information: The Expected Value and Comparative Hypervolume Methods*, Doctoral Thesis, University of Texas at Austin, Austin, TX, 1973.

[146] Charnetski, J. R. and Soland, M. R., "Multiple-Attribute Decision Making with Partial Information: The Comparative Hypervolume Criterion," *Naval Research Logistics, Quarterly*, Vol. 25, 1978, pp. 279–288.

[147] e Costa, B., "A Multicriteria Decision Aid Methodology to Deal with Conflicting Situations on the Weights," *European Journal of Operational Research*, Vol. 26, 1986, pp. 22–34.

[148] DuBois, D. and Paynter, G. C., "Fuel Flow Method 2 for Estimating Aicraft Emissions," SAE Technical Paper 2006-01-1987, The Boeing Co., Warrendale, PA, 2006.

[149] Figueira, J., Greco, S., and Ehrgott, M., *Multiple Criteria Decision Analysis: State of the Art Surveys*, Vol. 78 of *International Series in Operations Research & Management Science*, Springer Science+Business Media, Inc., New York, 2005.

[150] Greitzer, E. M., "Volume 2: Appendices Design Methodologies for Aerodynamics, Structures, Weight, and Thermodynamic Cycles," FINAL REPORT Cooperative Agreement Number NNX08AW63A, Massachusetts Institute of Technology, Aurora Flight Sciences, and Pratt & Whitney Team, March 2010.

[151] Inselberg, A., *Parallel Coordinates: Visual Multidimensional Geometry and its Applications*, No. DOI: 10.1007/978-0-387-68628-8, Springer New York, Tel Aviv University, Israel, 2009.

[152] Kanter, J., "U.N. Group Moves to Develop Global Airline Emission Rules," *New York Times*, October 2013.

[153] Kingsland, S., *Modeling nature: episodes in the history of population ecology*, University of Chicago Press, Chicago, IL, 1995.

[154] Kroo, I. M., "An Interactive System for Aircraft Design and Optimization," *Aerospace Design Conference*, , No. AlAA 92-1190, February 1992.

[155] Lahdelma, R., Hokkanen, J., and Salminen, P., "SMAA-Stochastic Multiobjective Acceptability Analysis," *European Journal of Operational Research*, Vol. 106, 1998, pp. 137–143.

[156] Lahdelma, R. and Salminen, P., "SMAA-2: Stochastic Multicriteria Acceptability Analysis for Group Decision Making," *Operations Research*, Vol. 49, No. 3, 2001, pp. 444–454.

[157] Malthus, T., *An Essay on the Principle of Population*, Oxford World's Classics (reprint), 1798.

[158] McIntosh, R., *The Background of Ecology*, Cambridge University Press, 1985.

[159] Nuic, A., *User Manual for the Base of Aircraft Data (BADA)*, EUROCONTROL Experimental Centre, Centre de Bois des Bordes, B.P.15, F - 91222 Brétigny-sur-Orge, Cedex, France, Revision 3.10 ed., April 2012.

[160] Renshaw, E., *Modeling Biological Populations in Space and Time*, Cambridge University Press, 1991.

[161] Senzig, D. A., Fleming, G. G., and Iovinelli, R. J., "Modeling of Terminal-Area Airplane Fuel Consumption," *AIAA Journal of Aircraft*, Vol. 46, No. 4, July-August 2009.

[162] Tervonen, T., "JSMAA: Open Source Software for SMAA Computations Version 1.0.2," *International Journal of Systems Science*, 2012.

[163] Tervonen, T., "Stochastic Multicriteria Acceptability Analysis - Theory, Applications, and Software," *ALIO/INFORMS Joint International Meeting*, Buenos Aires, June 2010, `http://drugis.org/files/tervonen-pres-alioinforms2010.pdf` [cited April 2013].

[164] Tervonen, T. and Figueira, J., "A Survey on Stochastic Multicriteria Acceptability Analysis Methods," *Journal of Multi-Criteria Decision Analysis*, Vol. 15, No. 1/2, January 2008, pp. 1–14.

[165] Tobler, W., "A computer movie simulating urban growth in Detroit region," *Economic Geography*, Vol. 46, 1970, pp. 230–240.

[166] Tobler, W. R., "Smooth Pyncophylactic Interpolation for Geographical Regions," *Journal of the American Statistical Association*, Vol. 74 (367), 1979, pp. 519–530.

[167] Willcox, K., "Development of a Distributed Approach to System Level Uncertainty Quantification," Partnership for Air Transportation Noise and Emissons Reduction (PARTNER), 2014, `http://partner.mit.edu/projects`.

[168] Zhan, F. B., Tapia-Silva, F., and Santillana, M., "Estimating small-area population growth using geographic-knowledge-guided cellular automata," *Journal of Remote Sensing*, Vol. 31, No. 21, November 2010, pp. 56895707.

[169] "T-100 Database," Research and Innovative Technology Administration (RITA), Bureau of Transportation Statistics (BTS), `transtats.bts.gov`.

[170] "International Civil Aviation Organization (ICAO) Engine Emissions Databank (EEDB)," European Aviation Safety Administration (EASA), April 2013, `http://www.easa.europa.eu/environment/edb/aircraft-engine-emissions.php`.

[171] "International Civil Aviation Organization (ICAO) Aircraft Noise and Performance (ANP) Database," Eurocontrol, December 2012, `http://www.aircraftnoisemodel.org/`.

VITA

Matthew J. LeVine was born and raised in St. Petersburg, Florida. After graduating from an International Baccalaureate program at St. Petersburg High School, Matthew enrolled in a dual undergraduate degree program between Emory University and the Georgia Institute of Technology. At Emory University, Matthew focused on music theory, trombone, and music composition. The program culminated in an undergraduate Honors Thesis in music composition, for which he composed and arranged a performance of a fifty-minute oratorio entitled *Thar She Blows!* Matthew graduated magna cum laude with a Bachelor of Arts in Music from Emory University in 2007.

The same year, Matthew began an undergraduate program in aerospace engineering at Georgia Tech. This program culminated in a senior design project entitled the Space Weather Experimental PlaTform (SWEPT), which was a design of a constellation of satellites for measuring and characterizing the extent of Earth's magnetotail around the Sun-Earth L2 Lagrange point. The SWEPT design earned first place in the 2009-2010 AIAA Undergraduate Team Space Design competition, and as project manager Matthew presented a poster of the design at the AIAA Space 2010 Conference and Exposition. Matthew graduated with Highest Honors with a Bachelor of Science in Aerospace Engineering from the Georgia Institute of Technology in 2010.

Immediately following graduation, Matthew began his graduate degree at Georgia Tech under Dr. Dimitri Mavris in the Aerospace Systems Design Laboratory. Matthew earned his Masters in Aerospace Engineering in the Spring of 2012, and was promoted to Senior Graduate Researcher due to his initiative and leadership

within the Civil Aviation Division. Matthew also has focused on teaching, earning an Advanced Level Teaching Certificate as part of the Tech to Teaching Higher Education Pathway through the Center for the Enhancement of Teaching and Learning. After graduation, Matthew will serve as a lecturer in Aerospace Engineering at Georgia Tech Lorraine in Metz, France for the 2016 spring semester. In the future, he plans on pursuing a faculty position at a research university.